Université de Liège
Faculté des Sciences Appliquées
Département ArGEnCo
Architecture, Géologie, Environnement et constructions
Secteur GEO³
Géotechnologies, Hydrogéologie, Prospection Géophysique

Solute transport modelling at the groundwater body scale: Nitrate trends assessment in the Geer basin (Belgium)

Thèse de doctorat
présentée par Philippe ORBAN
en vue de l'obtention du grade de Docteur en Sciences de l'Ingénieur

Soutenue devant le jury composé de :

R. CHARLIER, Université de Liège (Belgique) – Président
A. DASSARGUES, Université de Liège (Belgique) – Promoteur
S. BROUYERE, Université de Liège – Co-promoteur
E. DELHEZ, Université de Liège (Belgique)
M. PIROTTON, Université de Liège (Belgique)
V. HALLET, Facultés Universitaires Notre-Dame de la Paix, Namur (Belgique)
R. THERRIEN, Université Laval (Canada)
J.-M. LEMIEUX Eidgenössische Technische Hochschule Zürich (Suisse)
J. BARTH, GeoZentrum Nordbayern, Erlangen-Nürnberg (Allemagne)

Novembre 2008

ABSTRACT

Water resources management is now recognized as a multidisciplinary task that has to be performed in an integrated way, within the natural boundaries of the hydrological basin or of the aquifers. Policy makers and water managers express a need to have tools able at this regional scale to help in the management of the water resources. Until now, few methodologies and tools were available to assess and model the fate of diffuse contaminants in groundwater at the regional scale.

In this context, the objective of this research was to develop a pragmatic tool to assess and to model groundwater flow and solute transport at the regional scale. A general methodology including the acquisition and the management of data and a new flexible numerical approach was developed. This numerical approach called Hybrid Finite Element Mixing Cell (HFEMC) was implemented in the SUFT3D simulator developed by the Hydrogeology Group of the University of Liège.

A first application of this methodology was performed on the Geer basin. The chalk aquifer of the Geer basin is an important resource of groundwater for the city of Liège and its suburbs. The quality of this groundwater resource is threatened by diffuse nitrate contamination mostly resulting from agricultural practices.

New field investigations were performed in the basin to better understand the spatial distribution of the nitrate contamination. Samples were taken for environmental tracers (tritium, CFC's and SF_6) analysis. The spatial distribution of environmental tracers concentrations is in concordance with the spatial distribution of nitrates. This allows proposing a coherent interpretative schema of the groundwater flow and solute transport at the regional scale.

These new data and the results of a statistical nitrate trend analysis were used to calibrate the groundwater model developed with the HFEMC approach. This groundwater flow and solute transport model was used to forecast the evolution of nitrate concentrations in groundwater under a realistic scenario of nitrate input for the period 2008-2058. According to the modelling results, upward nitrate trends observed in the basin will not be reversed for 2015 as prescribed by the EU Water Framework Directive.

The regional scale groundwater solute transport model was subsequently used to compute nitrate concentrations in groundwater under different scenarios of nitrate input to feed a socio-economic analysis performed by BRGM. These computed concentrations were used to assess the benefit, for the users, linked to the reduction of contamination resulting from the changes in nitrate input. These benefits were compared to the costs associated to the implementation of the considered agri-environmental schemes that allow reducing the nitrate input to groundwater.

RESUME

La gestion des ressources en eaux souterraines est actuellement reconnue comme une tâche multidisciplinaire devant être réalisée, de manière intégrée, au sein des frontières naturelles des bassins hydrologiques ou des aquifères. Les politiciens et gestionnaires des ressources en eaux requièrent des outils capables, à cette échelle, d'aide à la gestion des ressources en eaux. A ce jour, peu de méthodologies et d'outils sont disponibles pour évaluer et modéliser le devenir de pollutions diffuses dans les eaux souterraines à l'échelle régionale.

Dans ce contexte, l'objectif de cette recherche est de développer un outil pragmatique pour évaluer et modéliser les écoulements et le transport de solutés dans les eaux souterraines à l'échelle régionale. Une approche générale a été développée qui inclut l'acquisition, le traitement de données et une nouvelle approche numérique flexible. Cette approche, appelée « Hybrid Finite Element Mixing Cell » (HFEMC), a été implémentée dans le code SUFT3D développé par le Groupe d'Hydrogéologie de l'Université de Liège.

Une première application de cette méthodologie a été réalisée pour le bassin du Geer (480 Km^2). L'aquifère crayeux de ce bassin est une ressource importante en eaux souterraines pour la ville de Liège et ses faubourgs. La qualité de cette eau souterraine est menacée par une contamination diffuse en nitrate résultant principalement des pratiques agricoles.

De nouvelles investigations de terrain ont été réalisées dans le bassin afin de mieux comprendre la distribution spatiale de la pollution en nitrate. Des échantillons ont été prélevés pour analyse des concentrations en traceurs environnementaux (tritium, CFCs et SF_6). La distribution spatiale des concentrations en traceurs environnementaux est en concordance avec la distribution spatiale des nitrates. Cela permet de proposer un schéma cohérent d'interprétation des écoulements d'eaux souterraines et de transport de solutés à l'échelle de l'aquifère.

Ces nouvelles données ainsi que les résultats d'une étude statistique des tendances des nitrates ont été utilisés pour calibrer le modèle eau souterraine développé à l'aide de l'approche HFEMC. Ce modèle d'écoulement des eaux souterraines et de transport de soluté a été employé pour prédire l'évolution, pour la période 2008-2058, des concentrations en nitrate dans les eaux souterraines pour un scénario réaliste d'apport de nitrate. Au regard des résultats de modélisation, les tendances à la hausse observées dans le bassin ne seront pas

inversées pour 2015 comme requis par la Directive Cadre sur l'Eau de la Commission Européenne.

Le modèle de transport de soluté dans les eaux souterraines à l'échelle régionale a été utilisé pour calculer les concentrations en nitrate dans les eaux souterraines pour différents scénarios d'apport en nitrate afin d'alimenter une analyse socio-économique réalisée par le BRGM. Ces concentrations calculées ont été utilisées afin d'évaluer les bénéfices, pour les utilisateurs, liés à la réduction de la contamination résultant des changements dans l'input nitrate. Ces bénéfices ont été comparés aux coûts associés à l'implémentation des mesures agro-environnementales qui permettent de réduire l'input nitrate vers les eaux souterraines..

ACKNOWLEDGMENTS

At the end of my Master study, when Professor Dassargues asked me to work in his team first as a PhD student and later as an assistant, I never thought to finalise a PhD thesis. During seven years, I have been confronted to various tasks, sometimes very different of my PhD thesis works. Nevertheless, this manuscript is the proof that this research has succeeded. This study is integrated with the works developed by the Hydrogeology Group of the University of Liège for years now as well in the domain of regional scale modelling as in the domain of the study of the hydrogeology of the Geer basin.

This thesis was supervised by Alain Dassargues and Serge Brouyère. First of all, I would like to thank them for supporting me and for their guidance during these years. I'm also grateful for the anticipating reading of the work they have done, as well as for proposals and suggestions to improve its quality. I would also thank Alain Dassargues for giving me the opportunity to work with him as an assistant. He always trusted me during these years both for pedagogical tasks and for research works. It is a chance and a pleasure to work with Serge Brouyère. Thank you Serge, you introduced me to research and encouraged me to go further in my works.

I would like to thank Robert Charlier, Michel Pirotton, Eric Delhez, Vincent Hallet, René Therrien, Jean-Michel Lemieux and Johannnes Barth who accepted to devote a piece of their time to read this manuscript and to be members of this jury.

The Hydrogeology Group is really a pleasant working environment thanks to the people there. Thanks to all my colleagues Jordi, Ingrid, Horatiu, Marie, Cristina, Nicolas, Julie G., Laurent P., Laurent T., Julie C., Angaman, Gaëlle, Tanguy, Jean, David, Pierre ad Fred for all these good times, for their help and their interesting hydrogeological or non-hydrogeological discussions. I would like particularly to thank Jordi and Ingrid. Thank you Ingrid for supporting me during all these years and for your sound advices as well concerning database or mapping techniques. And thank you Jordi for all these good times we have shared in our office, along the Mediterranean Sea or in a yellow caravan. This last year of work has been, for some aspect, difficult but you have always been there for an advice or talk.

Thank to Bernard Belot for the chemical analysis of major ions and to Professor Malozewski and his team for the tritium analysis. Thanks are also due to Annick Anceau and the team of the Earth Science library for helping me in my research of unobtainable papers.

A particular thanks to Cécile Hérivaux from the BRGM team for our fruitful collaboration regarding the socio-economic study performed on the Geer basin in the framework of the AquaTerra project.

Many thanks to Martine, Nadia and Christiane the secretary staff who are always present and available.

When developing model at the regional scale, lots of data have to be collected. I would like to thank the team of the CILE, SWDE and VMW companies and the team of the DGRNE for their warm welcomes, the data they have provided and their enthusiasm regarding my work.

Thanks to the University of Liège for giving me the opportunity through its funding to performed this work. Many thanks to the Administration of the Walloon Region for funding parts of this work through the PIRENE project or the environmental tracer surveys. Conceptual and numerical developments of the HFEMC method have also been performed in the framework of the Interuniversity Attraction Pole TIMOTHY (IAP Research Project P6/13) funded by the Belgian Federal Science Policy Office (BELSPO) and the European Integrated Project AquaTerra (GOCE 505428) funded by the Community's Sixth Framework Programme..

Finally, I am very grateful to all my family for continuously supporting all along my studies. During these seven years, I have had the happiness to marry you Delphine and then to welcome Chloé and Nathan who have extended our family. Thanks to you for your help and your patience.

KNOWLEDGE DISSEMINATION

List of publications

- Barth, J. A. C., P. Grathwohl, H. J. Fowler, A. Bellin, M. H. Gerzabek, G. J. Lair, D. Barcelo, M. Petrovic, A. Navarro, P. Négrel, E. Petelet-Giraud, D. Darmendrail, H. Rijnaarts, A. Langenhoff, J. de Weert, A. Slob, B. M. van der Zaan, J. Gerritse, E. Frank, A. Gutierrez, R. Kretzschmar, T. Gocht, D. Steidle, F. Garrido, K. C. Jones, S. Meijer, C. Moeckel, A. Marsman, G. Klaver, T. Vogel, C. Bürger, O. Kolditz, H. P. Broers, N. Baran, J. Joziasse, W. Von Tümpling, P. Van Gaans, C. Merly, A. Chapman, S. Brouyère, J. Batlle Aguilar, **Ph. Orban**, N. Tas and H. Smidt (2008). "Mobility, turnover and storage of pollutants in soils, sediments and waters: achievements and results of the EU project AquaTerra. A review." *Agronomy for sustainable development* **28**. DOI: 10.1051/agro.2007060.

- Barth, J. A. C., E. Kalbus, C. Schmidt, M. Bayer-Raich, F. Reinstorf, M. Schirmer, D. Thiéry, I. G. Dubus, A. Gutierrez, N. Baran, C. Mouvet, E. Petelet-Giraud, P. Négrel, O. Banton, J. Batlle Aguilar, S. Brouyère, P. Goderniaux, **Ph. Orban**, J. C. Rozemeijer, A. Visser, M. F. P. Bierkens, B. Van der Grift, H. P. Broers, A. Marsman, G. Klaver, J. Slobodnik and P. Grathwohl (2007). "Selected groundwater studies of EU project AquaTerra leading to large-scale basin considerations." *Water Practice & Technology* **2**(3). DOI: 10.2166/WPT.2007062.

- Batlle-Aguilar, J., **Ph. Orban**, A. Dassargues and S. Brouyère (2007). "Identification of groundwater quality trends in a chalk aquifer threatened by intensive agriculture in Belgium." *Hydrogeology Journal* **15**: 1615-1627.

- Brouyère, S., **Ph. Orban**, S. Wildemeersch, J. Couturier, N. Gardin and A. Dassargues. "The hybrid finite element mixing cell method: a new flexible method for modelling mine water problems." *Mine Water and the Environment*: In press.

- Hérivaux, C., **Ph. Orban**, J. Batlle-Aguilar, P. Goderniaux and S. Brouyère. "Socio-economic analysis integrating soil-water system modelling for the Geer catchment (Meuse, Walloon region) - diffuse nitrate pollution in groundwater." Manuscript in preparation.

- **Orban, Ph**., S. Brouyère, J. Couturier, P. Goderniaux, J. Batlle-Aguilar and A. Dassargues. "Modelling nitrate trends in groundwater at the regional scale using the HFEMC approach: Application to the chalk aquifer of the Geer basin (Belgium)." Manuscript in preparation for submission to *the Journal of Contaminant Hydrology.*

- **Orban, Ph**., C. Popescu, I. Ruthy and S. Brouyère (2004). "Database and general modelling concepts for groundwater modelling in the Squash project." *Hidrotehnica* **49**(9-10): 51-57.

- Visser, A., M. F. P. Bierkens, I. G. Dubus, J.-L. Pinault, N. Surdyk, D. Guyonnet, J. Batlle-Aguilar, S. Brouyère, P. Goderniaux, **Ph. Orban**, M. Korcz, J. Bronder, J. Dlugosz and M. Odrzywolek. "Comparison of methods for the detection and extrapolation of trends in groundwater quality." Manuscript in preparation.

Conference proceedings

- Batlle-Aguilar, J., **Ph. Orban**, A. Dassargues and S. Brouyère (2006). Identification of groundwater quality trends in a chalky aquifer threatened by intensive agriculture. International Association for Mathematical Geology, XIth Congress, Liège (Belgium).

- Batlle-Aguilar, J., **Ph. Orban**, A. Dassargues and S. Brouyère (2007). Identification of groundwater quality trends in a chalky aquifer threatened by intensive agriculture. Diffuse inputs into the groundwater: Monitoring - Modelling - Management, Graz (Austria).

- Brouyère, S., **Ph. Orban**, S. Wildemeersch, J. Couturier, N. Gardin and A. Dassargues (2008). The Hybrid Finite Element Mixing Cell method: a new flexible method for modelling mine water problems. Mine Water and the Environment: 10th International MineWater Association Congress, Karlovy Vary (Czech Republic).

- **Orban, Ph**., J. Batlle-Aguilar, A. Dassargues and S. Brouyère (2006). Large-scale groundwater flow and transport modeling: Methodology and application to the Geer basin, Belgium. International Association for Mathematical Geology, XIth Congress, Liège (Belgium).

- **Orban, Ph**., S. Brouyère, H. Corbeanu and A. Dassargues (2005). Large-scale groundwater flow and transport modelling: methodology and application to the Meuse Basin, Belgium. Bringing Groundwater Quality Research to the Watershed Scale, 4th International Groundwater Quality conference, IAHS, Waterloo, Canada.

Scientific report

PIRENE project

- Brouyère, S., H. Corbeanu, M. Dachy, N. Gardin, **Ph. Orban** and A. Dassargues (2004). Projet de recherche PIRENE: Rapport final, DGRNE**:** 105.

- Brouyère, S., **Ph. Orban**, H. Corbeanu and A. Dassargues (2003). Projet de recherche PIRENE: 3ème Rapport annuel DGRNE**:** 77.

- Brouyère, S., **Ph. Orban**, A. Dassargues and A. Monjoie (2001). Projet de recherche PIRENE: 1er Rapport annuel DGRNE**:** 43.

- Brouyère, S., **Ph. Orban**, A. Dassargues and A. Monjoie (2002). Projet de recherche PIRENE: 2ème Rapport annuel, DGRNE**:** 50.

AquaTerra project

- Broers, H. P., A. Visser, M. F. P. Bierkens, I. G. Dubus, J.-L. Pinault, N. Surdyk, D. Guyonnet, J. Batlle-Aguilar, S. Brouyère, P. Goderniaux, **Ph. Orban**, M. Korcz, J. Bronder, J. Dlugosz and M. Odrzywolek (2008). Draft overview paper on trend analysis in groundwater summarizing the main results of TREND2 in relation to the new Groundwater Directive. Deliverable T2.12, AquaTerra (Integrated Project FP6 no. 505428)**:** 46.

- Broers, H. P., A. Visser, I. G. Dubus, N. Baran, X. Morvan, M. Normand, A. Gutiérrez, C. Mouvet, J. Batlle Aguilar, S. Brouyère, **Ph. Orban**, S. Dautrebande, C. Sohier, M. Korcz, J. Bronder, J. Dlugosz and M. Odrzywolek (2005). Report with documentation of reconstructed land use around test sites. Deliverable T2.2, AquaTerra (Integrated Project FP6 no. 505428)**:** 64.

- Broers, H. P., A. Visser, R. Heerdink, B. Van der Grift, N. Surdyk, I. G. Dubus, N. Amaoui, **Ph. Orban**, J. Batlle-Aguilar, P. Goderniaux and S. Brouyère (2008). Report which describes the physically determinstic determination and extrapolation of time trends at selected test locations in Dutch part of the Meuse Basin, the Brévilles catchment and the Geer catchment. Deliverable T2.10, AquaTerra (Integrated Project FP6 no. 505428)**:** 47.

- Broers, H. P., A. Visser, R. Heerdink, B. Van der Grift, N. Surdyk, I. G. Dubus, A. Gutierrez, **Ph. Orban** and S. Brouyère (2007). Report with results of groundwater flow and reactive transport modelling at selected test locations in Dutch part of the Meuse basin, the Brévilles catchment and the Geer catchment. Deliverable T2.8, AquaTerra (Integrated Project FP6 no. 505428)**:** 26.

- Broers, H. P., A. Visser, R. Heerdink, B. Van der Grift, N. Surdyk, I. G. Dubus, A. Gutierrez, **Ph. Orban** and S. Brouyère (2007). Short report describing the progress of the groundwater flow and reactive transport modelling and elucidating interactions with COMPUTE and HYDRO and FLUX workpackages. Deliverable T2.7, AquaTerra (Integrated Project FP6 no. 505428): 35.

- Broers, H. P., A. Visser, J.-L. Pinault, D. Guyonnet, I. G. Dubus, N. Baran, A. Gutierrez, C. Mouvet, J. Batlle-Aguilar, **Ph. Orban** and S. Brouyère (2005). Report on extrapolated time trends at test sites, Deliverable T2.4, AquaTerra (Integrated Project FP6 no. 505428)**:** 81.

- Broers, H. P., A. Visser, B. Van der Grift, I. G. Dubus, Guttierrez, C. Mouvet, N. Baran, **Ph. Orban**, J. Batlle-Aguilar and S. Brouyère (2006). Input data sets and short report describing the subsoil input data for groundwater and reactive transport modelling at test locations in Dutch part of the Meuse basin, the Brévilles catchment and the Geer catchment. Deliverable T2.5, AquaTerra (Integrated Project FP6 no. 505428)**:** 23.

- Dubus, I. G., J.-L. Pinault, N. Surdyk, D. Guyonnet, H. P. Broers, A. Visser, **Ph. Orban**, J. Batlle-Aguilar, P. Goderniaux and S. Brouyère (2008). Report with comparison of statistical and physically deterministic methods of trend assessment and

extrapolation in terms of data requirements, costs and accuracy. Deliverable T2.11, AquaTerra (Integrated Project FP6 no. 505428): 33.

- Hérivaux, C., **Ph. Orban**, J. Batlle-Aguilar, S. Brouyère and P. Goderniaux (2008). Socio-economic analysis integrating soil-water system modelling for the Geer catchment (Meuse, Walloon region) - diffuse nitrate pollution in groundwater. Deliverable I3.8, AquaTerra (Integrated Project FP6 no. 505428)**:** 45.

- **Orban, Ph**., J. Batlle-Aguilar, P. Goderniaux, A. Dassargues and S. Brouyère (2006). Description of hydrogeological conditions in the Geer sub-catchment and synthesis of available data for groundwater modelling. Deliverable R3.16, AquaTerra (Integrated Project FP6 no 505428)**:** 20.

- **Orban, Ph.** and S. Brouyère (2006). Groundwater flow and transport delivered for groundwater quality trend forecasting by TREND T2. Deliverable R3.18, AquaTerra (Integrated Project FP6 no 505428)**:** 20.

Synclin'Eau Project

- Lorenzini, G., **Ph. Orban**, S. Brouyère and A. Dassargues (2008). Note méthodologique relative à la modélisation hydrogéologiques des masses d'eau souterraine RWM011, RWM012 et RWM021 (aspects quantitatifs et qualitatifs) Synclin'Eau. Convention RW et SPGE - Aquapôle**:** 26.

TABLE OF CONTENTS

LIST OF THE MAIN SYMBOLS

Symbol	Definition	Dimension
A	Exchange area	$[L^2]$
A_{LR}	Surface area of the linear reservoir	$[L^2]$
$A_{LR,i}$	Surface area of the linear reservoir i	$[L^2]$
b	Mean saturated thickness of the aquifer	[L]
b	Sen's slope estimator	$[ML^{-3}T^{-1}]$
C	Solute concentration	$[ML^{-3}]$
C'	Solute concentration associated to source	$[ML^{-3}]$
$\overline{C}$	Average concentration	$[ML^{-3}]$
C_{ij}	Solute concentration associated to the flux between cells i and j	$[ML^{-3}]$
C_{im}	Solute concentration in the immobile water	$[ML^{-3}]$
C_m	Solute concentration in the mobile water	$[ML^{-3}]$
C_{sorb}	Sorbed concentration on the subsurface solids	$[MM^{-1}]$
$C_{in}(t)$	Temporal evolution of the concentration at the entry of the system	
$C_{out}(t)$	Temporal evolution of the concentration at the outlet of the system	
C_r	Courant number	[-]
D	Mean annual river discharge	[L]
$\underline{\underline{D}}$	Mechanical dispersion	$[L^2T^{-1}]$
$\underline{\underline{D_h}}$	Hydrodynamic dispersion	$[L^2T^{-1}]$
D_m	Diffusion coefficient	$[L^2T^{-1}]$
E	Mean annual true evapotranspiration	[L]
$\underline{f_c}$	Advective flux	$[ML^{-2}T^{-1}]$
$\underline{f_D}$	Hydrodispersive flux	$[ML^{-2}T^{-1}]$
F	Generalised specific storage coefficient	$[L^{-1}]$
$F(t)$	Transfer function	
$g(\tau)$	Impulse response	
h	Pressure potential	[L]
H_i	Water level in reservoir I or water level at node i	[L]
$\overline{H}_{LR}$	Mean water level in the linear reservoir	[L]
H_{ref}	Drainage level of the linear reservoir	[L]
I	Infiltration rate	[L]
$\underline{\underline{K}}$	Hydraulic conductivity	$[LT^{-1}]$
K_d	Distribution coefficient	$[L^3M^{-1}]$
K_r	Hydraulic conductivity of the river sediments	$[LT^{-1}]$
L	Losses	[L]
L	Length of the segment of river	[L]
P	Mean annual precipitation	[L]
P_D	Dispersion parameter	[-]
P_e	Peclet number	[-]
q	Volumetric flux	$[T^{-1}]$

q_{nj}	Flux from cell n to cell j	$[L^3T^{-1}]$
Q	Source and sink term	$[L^3T^{-1}]$
$Q_{i,j}$	Flow rates exchanged between cells i and j	$[L^3T^{-1}]$
Q_i	Source and sink term in reservoir i	$[L^3T^{-1}]$
Q_n	Source term in cell n	$[L^3T^{-1}]$
Q_{riv}^{GW}	Flux echanged between the river and the groundwater	$[L^3T^{-1}]$
r	Correlation coefficient	[-]
R	Retardation factor	[-]
S_{LR}	Storage of the linear reservoir	[-]
$S_{LR,i}$	Storage of the linear reservoir i	[-]
t	Time	[T]
$\bar{t}$	Average time	[T]
T	Mean transit time	[T]
T	Mann-Kendall estimator	[-]
T^*	Apparent mean transit time	[T]
$\underline{v}$	Advective velocity	$[LT^{-1}]$
$\underline{v_D}$	Darcy flux	$[LT^{-1}]$
$V_{eff,\,res}$	Effective mixing volume of the reservoir	$[L^3]$
V_i	Control volume associated to node i	$[L^3]$
w	Width of the river	[L]
W	Sink term	$[L^3T^{-1}]$
$X(t)$	Input function or solicitation of the system	
$Y(t)$	Output function or response of the system	
z	Gravity potential	[L]
α	First-order transfer coefficient between mobile and immobile water	$[T^{-1}]$
α_L	Longitudinal dispersivity	[L]
α_T	Transversal dispersivity	[L]
$\alpha_{i,j}$	First order exchange coefficient between reservoirs i and j	$[L^2T^{-1}]$
$\alpha_{SD,i\text{-}SD,j}$ or $\alpha_{interface}$	First order exchange coefficient between subdomains i and j	$[T^{-1}]$
α_{LR}	First order exchange coefficient of the linear reservoir	$[L^2T^{-1}]$
α_r	Conductance coefficient of the river	$[L^2T^{-1}]$
Δt	Time step	[T]
ΔS	Variation in groundwater storage	[L]
η	Mixing efficiency	[-]
λ	First order linear degradation coefficient	$[T^{-1}]$
θ	Total porosity	[-]
θi_m	Porosity of immobile water	[-]
θ_m	Effective porosity or porosity of mobile water	[-]

LIST OF THE MAIN ACRONYMS

Acronym	Definition
a.s.l.	Above sea level
BRGM	Bureau de Recherches Géologiques et Minières (France)
CEA	Cost-Effectiveness analysis
CFC	Chlorofluorocarbons
CILE	Compagnie Intercommunale Liégeoise des Eaux
CVFE	Control Volume Finite Element
DGRNE	Division Générale des Ressources Naturelles et de l'Environnement (Administration of the Walloon region)
DOC	Dissolved Organic Carbon
EPIC	Erosion Productivity Impact Calculator
EU	European Union
GIS	Geographical Information System
GMS	Groundwater Modeling System
HFEMC	Hybrid Finite Element Mixing Cell
MODFLOW	Modular finite difference groundwater flow model
MT3DMS	Modular three-dimensional multi-species transport model
PIRENE	Programme Intégré de REcherche ENvironnement-Eau
REV	Representative Elementary Volume
RMSE	Root Mean Squared Error
RTD	Research and Technological Development
SGB	Service Géologique de Belgique (Belgian Geological Survey)
SPGE	Société Publique de Gestion de l'Eau
SUFT3D	Saturated Unsaturated Flow and Transport in 3 Dimension
SUPG	Streamline Upwind Petrov-Galerkin
SWDE	Société Wallonne des Eaux
TU	Tritium Unit
TVD	Total Variation Diminishing
VMW	Vlaamse Maatschappij voor Watervoorziening
WFD	Water Framework Directive
WHO	World Health Organisation

1 INTRODUCTION

1.1 Context of the research

Interest of end-users and policy makers for understanding and managing groundwater systems at the regional scale has increased for years. It appears clearly that water can not be managed internally within administrative local, regional or national boundaries but rather taking into account the physical boundaries of hydrological systems, such as hydrogeological limits for groundwater. This concern has been translated in the European Water Framework Directive (2000/60/EC) that states that water has to be managed at the scale of the Hydrographic District. This Directive introduces also the concept of “groundwater body” as the basic unit for groundwater management. The Directive states that a “good quantitative and qualitative status” has to be achieved for the year 2015. Moreover, upward trends of anthropogenic pollution have to be identified and reversed.

Modelling tools simulating groundwater processes at the groundwater body scale are useful tools to help managers to implement the Directive. Such models can be used to improve the understanding of the functioning of groundwater systems and for predictions about the state of the system under defined pressures such as for example, climate changes and/or diffuse pollutions, among which nitrate has been identified as one of the most problematic and widespread diffuse contaminants of groundwater. Efforts are thus needed to develop regional scale groundwater models to assess with reliability the impact of land-use and related pollution on groundwater or to define appropriate long term management scenarios assessing the costs of such scenarios.

At regional scale, groundwater models of different complexity, ranging from black-box models to physically-based and spatially-distributed models, have been used in various hydrogeological conditions. Black-box models, such as transfer functions, have been applied for example to model groundwater in large scale hydrological models, to model karstic systems, in particular for the interpretation of isotopic data. Their concepts are simple and attractive because they require relatively few data. The main drawbacks are however that modelling results are not spatially-distributed and their predictive capability is questionable, due to the semi-empirical nature of process descriptions. On the contrary, due to a more advanced description of ongoing processes, physically-based distributed models are expected to have better predictive capabilities than black-box models. However, because such models require more data, they are generally applied in case studies that are better characterised from

a hydrogeological point of view, for which the distribution of groundwater levels or solute concentrations in the groundwater systems are needed.

The Hydrogeology Group of the University of Liège develops, for years now, regional groundwater models that were mainly focused until the beginning of this century on groundwater flow modelling. To face problems caused by the development of large scale groundwater model, a new flexible modelling approach, the Hybrid Finite-Element Mixing-Cell method (HFEMC), has been developed in the framework of this thesis by the Hydrogeology Group of the University of Liège. This approach has been used in the framework of the research projects PIRENE and AquaTerra.

1.2 The PIRENE and AquaTerra projects

This research has been performed in the scope of two projects, the PIRENE and the AquaTerra projects which both aim to provide tools for integrated water management at the basin scale.

In 2001, the Government of the Walloon Region (Belgium) initiated the PIRENE project to develop tools for integrated water quantity/quality management in the Walloon region. As a partner of this project, the Hydrogeology Group of the University of Liège had to develop a physically based, transient groundwater flow and transport model for the Walloon part of the Meuse Basin (approximately 18.000 km²). A methodology (the Hybrid Finite Element Mixing Cell Approach) and a numerical code grouping together different approaches (non-distributed or distributed mixing cells, advection-dispersion equation…) and allowing the transition from a simplified approach to a deterministic model were developed. This new methodology was tested on the Walloon part of the Meuse basin for which a groundwater flow model was developed.

AquaTerra is an integrated project of the 6th EU RTD Framework Program grouping together scientists from 45 European (including Swiss and Serbian) organisations. It aims to provide a better understanding of the river-sediments-soil-groundwater system as a whole by identifying relevant processes, quantifying the associated parameters and developing numerical models to identify adverse trends in soil functioning, water quantity and quality. In this project, the Geer basin was used as a case study to test tools for groundwater trends analysis and to compare regional scale modelling approaches developed among other by the Hydrogeology Group of the University of Liège.

1.3 Objectives of the research

The two main objectives of this work are:

- to develop a general methodology for groundwater flow and solute transport assessment and modelling at the regional scale, in the framework of the European Water Framework Directive;
- to perform, as a first test, an application of this methodology to assess and predict spatially-distributed nitrate trends in the Geer basin.

To reach the first objective of this research, a new flexible modelling approach, the Hybrid Finite Element Mixing Cell approach (HFEMC) has been developed. This approach allows combining in a single model, and in a fully integrated way, different mathematical approaches of various complexities for groundwater modelling in complex and large scale environments. This method has been implemented in the groundwater flow and solute transport numerical code SUFT3D.

To reach the second objective, new field surveys, consisting in groundwater sampling for environmental tracer analysis, were performed to better understand the spatial distribution of the nitrate contamination before modelling.

This document is structured as follow:

In the second chapter, existing regional approaches to model groundwater are reviewed with their main advantages and drawbacks highlighted. Information about nitrate, environmental tracers and statistical trend analysis are also provided.

The third chapter presents the HFEMC approach and the basic concepts underlying its implementation in the SUFT3D simulator. Synthetic tests developed to validate the approach and the implementation are exposed.

In the fourth chapter, the Geer basin case study is presented. Main results of previous studies are synthesised. A recent study focusing on the link between nitrate contamination and the age of groundwater is also presented. Main results are presented and explanations concerning the spatial distribution of the nitrate contamination are proposed. The groundwater model developed for nitrate trends prediction is presented. Results of this model are discussed. A

socio-economic study of the impact of the nitrate contamination in the Geer basin in which the results of the model have been used is described as an example of use of regional scale groundwater model.

Chapter 5 summarises the main conclusions of this work and presents future perspectives.

2 REVIEW OF THE LITERATURE

2.1 Representative Elementary Volume

The development of hydrogeologic models is based on a continuum assumption (Bear 1972; Eaton 2006 among others), flow and transport are considered on a volumetric averaged basis at a macroscopic scale assumed to be equivalent to an ideal porous media.

The parameters governing flow and transport equations are defined at a scale larger than that of the microscopic pores. The minimum volume over which the governing equations of flow and transport apply is commonly referred to as a Representative Elementary Volume (REV) (de Marsily 1986; Bear and Verruijt 1987). The dimensions of such a REV are defined according the purpose of the investigation, but it must be of a size range within which values of parameters are statistically significant, more or less constant, continuous and large enough for parameters to be quantified experimentally.

Representative Elementary Volumes used for groundwater flow problems are generally larger than those that should be used for the transport problem. Heterogeneities that are generally averaged in the flow problems have much more impacts when considering the solute transport problem (de Marsily *et al.* 2005).

2.2 Migration of solutes in groundwater

In the framework of this thesis, contaminants that will be considered are solutes only, defined here as a substance present in the water phase at a concentration below the solubility constant of that product in water. Pollutants present as a pure product or in a gaseous phase will not be considered in this study. Moreover, the considered solute is assumed to be at a concentration low enough to have a negligible impact on the density and viscosity of water.

Processes considered in hydrogeology to model the transport of dissolved contaminants are (1) advection, (2) dispersion, (3) degradation and (4) retardation and trapping.

2.2.1 Advection

Advection is the mechanism carrying contaminants in the porous media at the mean effective velocity of groundwater. The advective flux can be expressed by:

$$\underline{f_c} = C\underline{v} = C\underline{v_D} / \theta_m = -C\underline{\underline{K}}\,\underline{\nabla h} / \theta_m \qquad \textbf{(2.1)}$$

where $\underline{f_c}$ is the advective flux [$ML^{-2}T^{-1}$]; C is the volumic concentration of contaminant [ML^{-3}]; $\underline{v}$ is the mean velocity of solute migration, often called advective velocity or effective velocity [LT^{-1}]; $\underline{v_D}$ is the Darcy flux [LT^{-1}]; θ_m is the effective porosity, the proportion of the media accessible to the groundwater flow [-]; $\underline{\underline{K}}$ is the hydraulic conductivity [LT^{-1}]; h is the pressure potential [L].

The evaluation of the advective component of the solute transport requires determining the value of the hydraulic conductivity and of the effective porosity of the medium at the appropriate scale.

Numerous authors have highlighted the scale dependence of the hydraulic conductivity values (Clauser 1992; Neuman 1994; Sánchez-Vila *et al.* 1995; Sánchez-Vila *et al.* 1996 among others). For example, Clauser (1992) synthesised values of permeability measured at different scales ranging from laboratory data to packer tests, Lugeon tests and calibration of models in crystalline rocks (Figure 2.1). An increase in average permeability of around three orders of magnitude from the laboratory to the borehole scale is clearly observable. Such an increase is not as well observable when going from the borehole to the regional scale. Permeabilities and thus hydraulic conductivities tend to increase with the characteristic scale of their measurement.

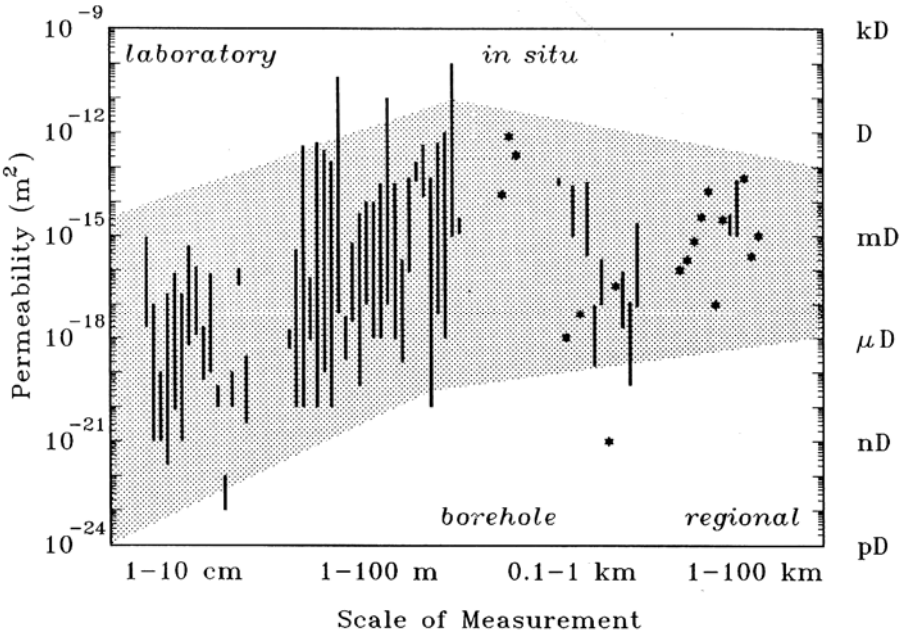

Figure 2.1. Permeability of crystalline rocks and characteristic scale of measurements: bar marks the maximum permeability range when several individual values are reported; stars represent single values (from Clauser 1992)

Renard (1996) proposed a synthesis of terminology used to define the scale of work in hydrogeology and the types of measurement used at these different scales. As shown in Figure 2.2, pumping tests which are one of the main tools used to determine hydraulic conductivities in subsurface hydrogeology are generally representative at a scale of maximum several hundreds of meters. Value of hydraulic conductivities determined by pumping tests can thus be considered as representative of REV of such a size.

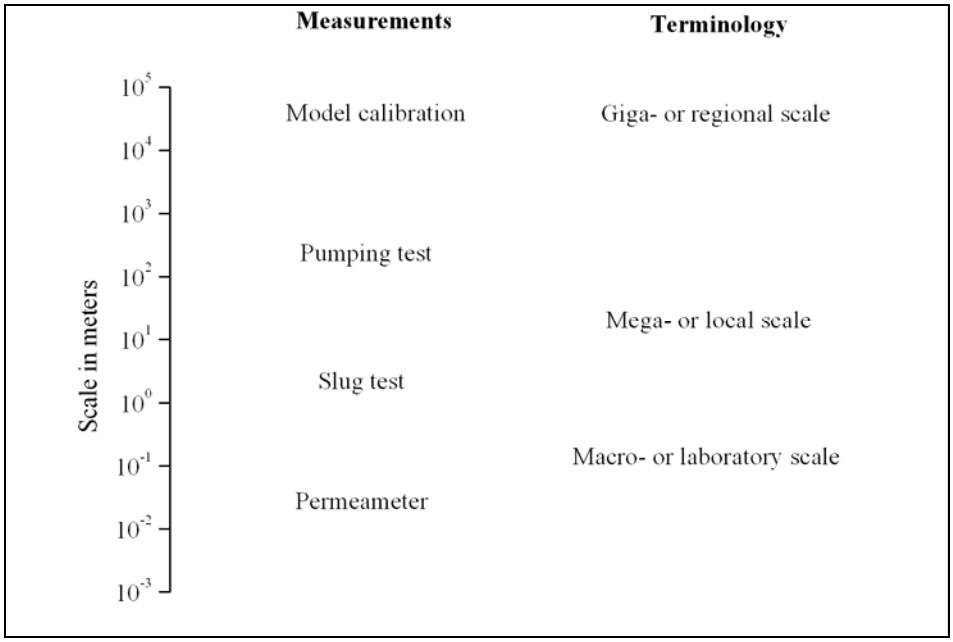

Figure 2.2. Different scales and measurement techniques for studying porous media (modified from Renard 1996)

The amplitude and physical meaning attributed to the effective porosity are function of the size of the REV. For example, in fractured media, if a REV of the size of the fracture is considered, a very high value for the porosity and the hydraulic conductivity will be obtained in the fissures. On the contrary if the fissures are not represented explicitly but assumed to be integrated in the properties of a REV of bigger size, the effective porosity will be smaller. The hydraulic conductivity obtained for this REV will also be smaller as it integrates the permeability of the fissures but also of the matrix. Hallet (1998) proposed the notion of REV porosity as being the mean effective porosity for the considered REV in fractured media.

Brouyère (2001) noticed that values of the effective porosity deduced from tracer tests performed at Hermalle-sous-Argenteau in the alluvial aquifer of the Meuse river (Belgium) seem to increase slightly with the tracing distance and the modal travel time of tracers in the underground. Guimerà and Carrera (2000) synthesised data from different tracer tests in different fractured media (Figure 2.3). They noticed a significant correlation between peak arrival times and porosity values deduced from the interpretation of tracer tests. They assume that the portion of voids actually accessed by the tracer increases with time as a result of tracer diffusion into both the rock matrix and stagnant groundwater.

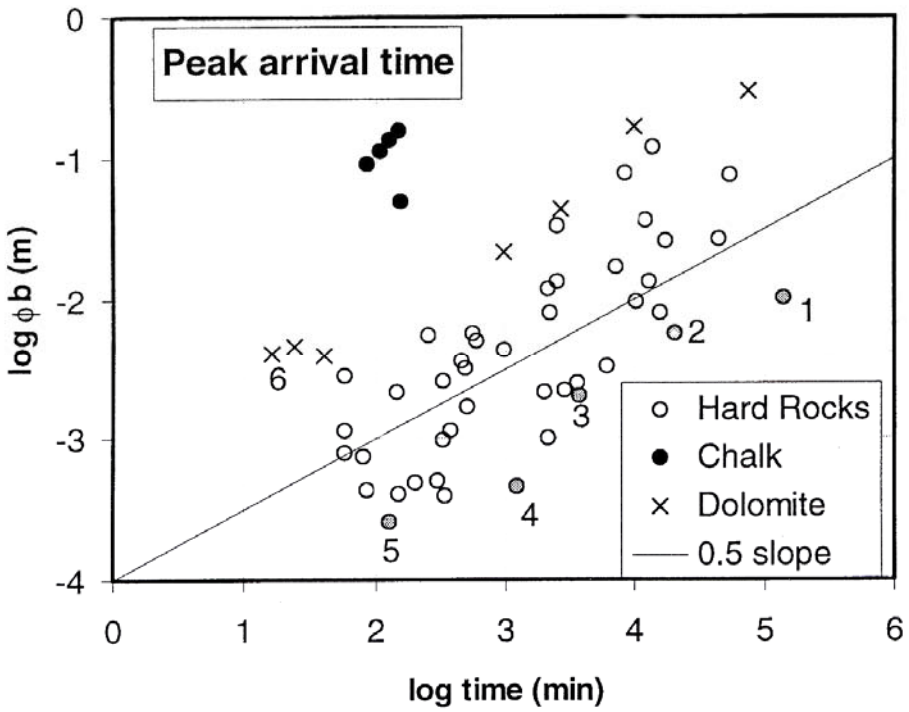

Figure 2.3. Travel time and apparent thickness porosity values for peak concentration arrival times (from Guimerà and Carrera 2000)

2.2.2 Hydrodynamic dispersion

Hydrodynamic dispersion results from the spreading of solutes around the mean advective position, caused by a combination of two processes (Figure 2.4):

- mechanical dispersion due to the distribution of the velocity around the mean value defined on the REV, fluctuations in space of the streamlines around the mean direction of flow and mainly heterogeneity not taken into account in the REV;
- diffusion contaminant from zones of high concentrations to zones of lower concentrations.

The hydrodispersive flux can be expressed, with a Fickian law by:

$$\underline{f_D} = \underline{\underline{D_h}}\,\underline{\nabla C} \tag{2.2}$$

where $\underline{f_D}$ is the hydrodispersive flux [$ML^{-2}T^{-1}$]; C is the volumic concentration of contaminant [ML^{-3}]; $\underline{\underline{D_h}}$ is the tensor of hydrodynamic dispersion [L^2T^{-1}] that is equal to:

$$\underline{\underline{D_h}} = D_m \underline{\underline{I}} + \underline{\underline{D}} \tag{2.3}$$

where D_m is the diffusion coefficient in the porous media [L^2T^{-1}]; $\underline{\underline{I}}$ is the unity tensor; $\underline{\underline{D}}$ is the tensor of mechanical dispersion [L^2T^{-1}].

If the axes are chosen in such a way that the x axis coincides with the direction of the average velocity (Frenet referential), the tensor $\underline{\underline{D}}$ can be expressed by:

$$\underline{\underline{D}} = \begin{bmatrix} \alpha_L |v| & 0 & 0 \\ 0 & \alpha_T |v| & 0 \\ 0 & 0 & \alpha_T |v| \end{bmatrix} \tag{2.4}$$

where α_L and α_T are respectively the longitudinal and lateral dispersivity coefficients [L], $|v|$ is the magnitude of the velocity vector [LT^{-1}].

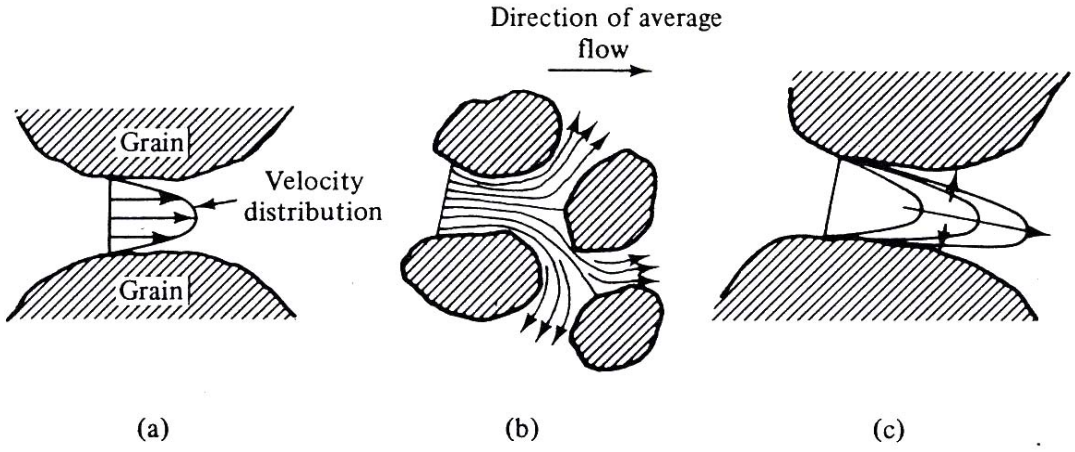

Figure 2.4. Spreading due to mechanical dispersion (a, b) and molecular diffusion (c) (Bear and Verruijt 1987).

It is also well known that dispersivity coefficients are scale dependant. For example, Gelhar *et al* (1992) synthesised dispersivity values obtained at different test sites. Data indicate a systematic increase of the longitudinal dispersivity with observation scale (Figure 2.5).

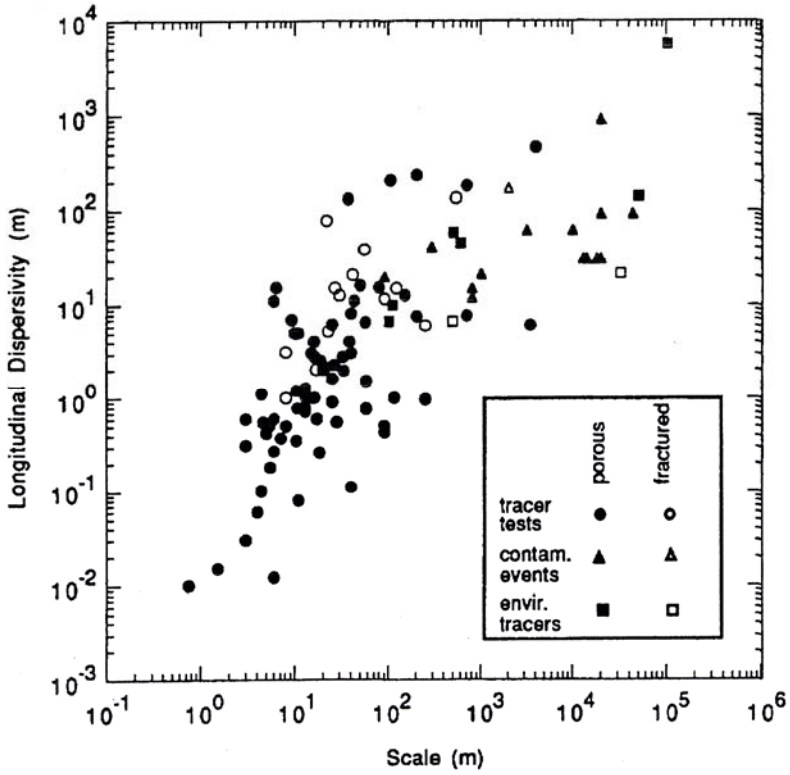

Figure 2.5. Longitudinal dispersivity versus scale of observation identified by type of observation and type of aquifer. The data are from 59 field sites characterized by widely differing geologic materials (Gelhar *et al.* 1992).

2.2.3 Degradation

Chemical, biochemical or physical processes that produce the disappearance of the solute (and eventually producing other derived solute compounds) are grouped together under the notion of degradation. The simplest way to consider degradation is to take it into account through an equation of radioactive decay:

$$\frac{\partial C}{\partial t} = -\lambda\, C \qquad \textbf{(2.5)}$$

where λ is the first-order linear degradation coefficient [T^{-1}].

2.2.4 Retardation and trapping

Retardation effects can be divided into two major categories (Brouyère 2001):

- chemical retardation, including all physico-chemical reactions between the solute and the porous medium;
- physical retardation or dual-porosity effects.

Sorption group together different processes such as adsorption-desorption, absorption and cation exchange, that are dependant of the physico-chemical nature of the solute. It refers to mass transfer processes between the contaminants dissolved in groundwater and the contaminant sorbed on the porous media. It is often assumed that equilibrium conditions exist between the aqueous phase and the solid phase concentrations and that the sorption reaction is fast enough in comparison to the velocity of groundwater to be treated numerically as instantaneous. Different types of equilibrium controlled sorption isotherms are proposed in the literature (linear, Freundlich and Langmuir isotherms). The simplest relation expresses a linear sorption isotherm, which considers that the sorbed concentration C_{sorb} is directly proportional to the solute concentration:

$$C_{sorb} = K_d\, C \qquad \textbf{(2.6)}$$

where K_d is the distribution coefficient [L^3M^{-1}].

Physical retardation processes affect all the solutes transported in the porous medium. Physical retardation mainly depends on the heterogeneity of the aquifer, solutes being trapped in less permeable parts of the aquifer (micropores, silty and clayey lenses, dead-end pores…).

The dual-porosity concept, introduced by Coats and Smith (1964) following the failure of the advection-dispersion model to represent solute transport in heterogeneous media, considers two domains of porosity respectively mobile and immobile (or much less mobile). In chalk aquifers, immobile water is assumed to represent groundwater in the matrix, while the mobile water is associated to groundwater present in the fissures (Biver 1993; Hallet 1998; Brouyère 2006). Advection and dispersion take place only in the mobile zone, while chemical retardation can occur in both zones, although not necessary at the same rate. Diffusion is generally considered as the main process controlling the transfer of solutes from one zone to the other one.

Mass conservation equation applied to the immobile domains can be expressed using a first order coefficient by:

$$\theta_{im} \frac{\partial C_{im}}{\partial t} = \alpha (C_m - C_{im}) - \lambda \theta_{im} C_{im} \qquad \textbf{(2.7)}$$

where α is the first-order transfer coefficient between mobile and immobile water [T^{-1}]; θ_{im} is the immobile porosity [-]; θ_m is the effective mobile porosity [-]; C_m and C_{im} are respectively the solute concentration in the mobile and immobile water [ML^{-3}]; λ is the first-order linear degradation coefficient [T^{-1}].

Brouyère (2001) analysed the parameters obtained by the interpretation, considering interaction between mobile and immobile water, of different tracer tests performed in the aquifer of the alluvial plain of the Meuse river at Hermalle-sous-Argenteau. He noticed that an increase in the tracing distance, the modal transit time of the tracer and the modal effective porosity do not seem to affect the interpreted values of immobile porosity. On the contrary, he found that the transfer coefficient between the mobile and immobile water is clearly affected by scale and temporal effects. It decreases as a function of the tracing distance and of the transfer modal transit time and increases as a function of the modal effective velocity (Figure 2.6).

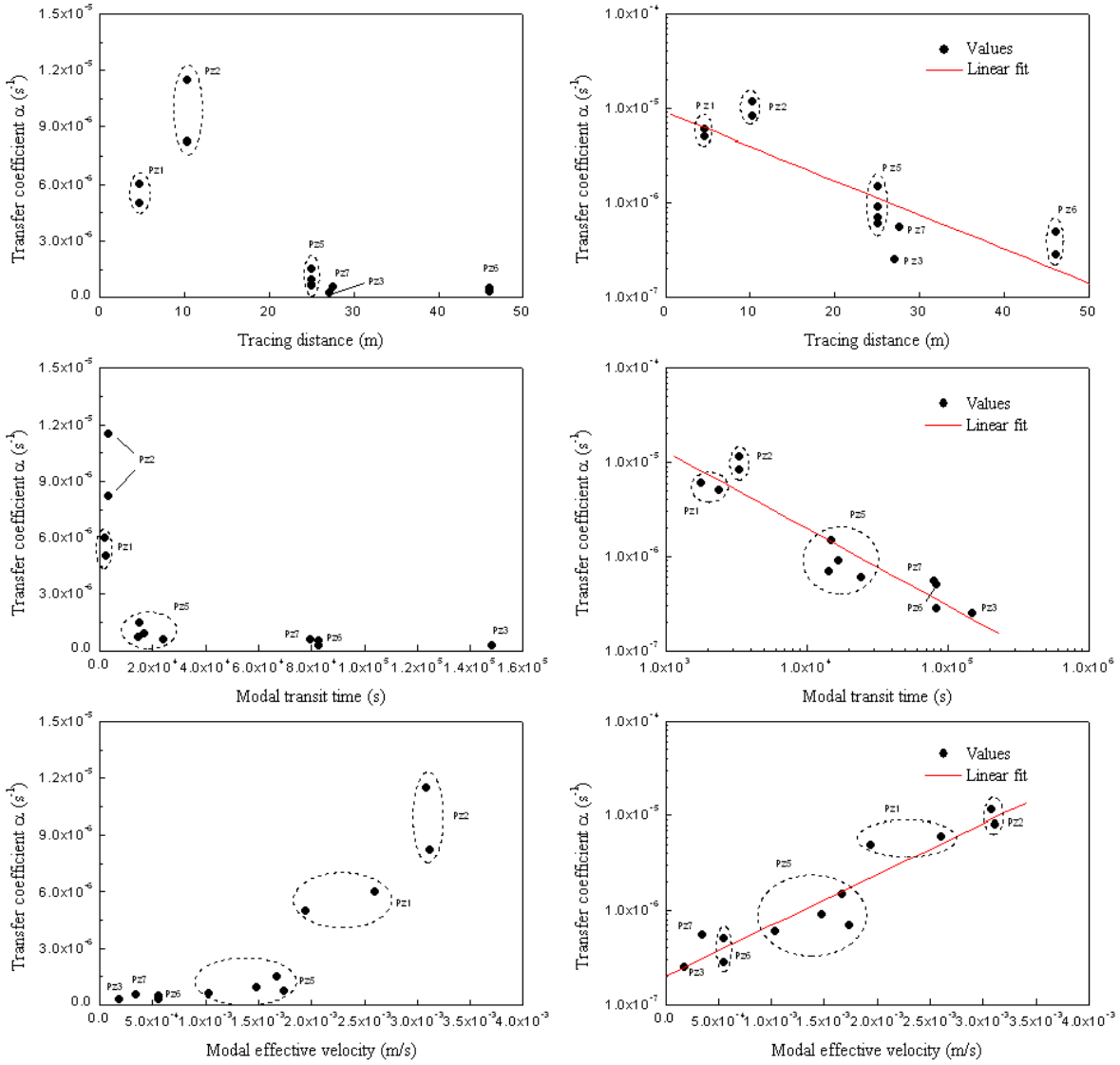

Figure 2.6. Evolution of the transfer coefficient as a function of the tracing distance, the modal transit time and the modal effective velocity (modified from Brouyère 2001).

2.2.5 Solute transport equations

Regrouping the different processes described here above, the solute transport equation can be written:

$$\theta_m \frac{\partial C_m}{\partial t} = -\underline{\nabla}.(\underline{v}_D\, C_m) + \underline{\nabla}.(\theta_m\, \underline{\underline{D}}_h\, \underline{\nabla} C_m) - \lambda\, \theta_m\, C_m - \alpha\, (C_m - C_{im}) + q\,(C' - C_m) \qquad \textbf{(2.8)}$$

where θ_m is the effective mobile porosity [-]; C_m and C_{im} are respectively the solute concentration in the mobile and immobile water [ML^{-3}]; t is the time [T]; v_D is the Darcy's flux [LT^{-1}]; D_h is the hydrodynamic dispersion [L^2T^{-1}]; λ is the linear degradation coefficient [T^{-1}]; q are the volumetric fluxes associated to the source and sink [T^{-1}]; C' is the concentration associated to these sources [ML^{-3}].

2.3 Existing approaches for modelling solute transport in groundwater at the regional scale

Solute transport in groundwater is generally conceptualised using the different processes described in the previous section. At the regional scale, the acquisition of the relevant data and the development of solute transport models in groundwater remains a challenge. Generally speaking, existing conceptual and mathematical approaches used to model contaminant transport at large scale can be grouped into three main categories: transfer function approaches, compartment models and models relying on advanced solution of the advection-dispersion equation, in function of the way the different processes are taken into account or represented.

2.3.1 Transfer function models

Transfer function models, sometimes referred to as "black-box" or "lumped parameters" models, are usually used for the interpretation and correlation of datasets at the entry and outlet of the underground system (e.g. recharge and discharge zones). Transfer functions can be obtained through deconvolution of available time series when the structure and the functioning of the system are unknown. They can also be expressed as more or less elaborated parametric mathematical equations (e.g. Jury *et al.* 1982a; Amin and Campana 1996; Skaggs *et al.* 1998; Stewart and Loague 1999). Such approaches are relatively simple and they require

a limited number of parameters to be assessed. However, they provide a relatively low accuracy and because these models rely on integral mass balance formulations relating mass flux and concentrations at the system entry and output, the detailed spatial distribution and time evolution of concentrations within the underground system remain unknown. Such approaches have been mostly applied to isotopic and environmental tracer data (e.g. Duffy and Gelhar 1986; Ritzi *et al.* 1991; Maloszewski and Zuber 1996).

This type of model can be expressed mathematically by the following convolution product:

$$Y(t) = F(t) * X(t) \quad \textbf{(2.9)}$$

where $X(t)$ is the input function or the solicitation of the system; $Y(t)$ is the output function or the response of the system; $F(t)$ is the transfer function or impulse response.

Transfer function approaches proposed in the literature differ essentially one from another by the way of representing and computing the transfer function $F(t)$. Applied to solute transport through aquifers, Equation (2.9) becomes:

$$C_{out}(t) = \int_0^{\infty} C_{in}(t-\tau) g(\tau) d\tau \quad \textbf{(2.10)}$$

where $C_{out}(t)$ is the temporal evolution of concentration at the outlet of the aquifer system; $C_{in}(t)$ is the temporal evolution at the entry of the aquifer system; τ is the time of entrance of the solute in the system and $t-\tau$ the transit time; $g(\tau)$ is the impulse response of the system whom the mathematical formulation depends on the mathematical model considered to represent the behaviour of solute moving in the system.

If degradation is considered, Equation (2.10) becomes:

$$C_{out}(t) = \int_0^{\infty} C_{in}(t-\tau)\, g(\tau) \exp(-\lambda\tau)\, d\tau \quad \textbf{(2.11)}$$

where λ is the degradation rate of the tracer and $g(\tau)$ is the impulse response of the system.

2.3.1.1 Non-parametric transfer functions

A non-parametric transfer function is not explicitly described by a function or a mathematical model. It is obtained by deconvolution of the system response $Y(t)$ by the solicitation $X(t)$ applied to the system. Long time series of data at the entry and outlet of the system are thus required to establish the transfer function $F(t)$ for that system. This form of the transfer function is static and the system is assumed to be perfectly linear and invariant. Skaggs *et al.* (1998) proposed an algorithm for the deconvolution that allow determining the non-parametric transfer function for 1D solute transfer across soil based on concentrations measured at the entry and outlet of the soil column. They concluded that one of the limits of such formulations is the impossibility to generalise the result to, for example, other soil thicknesses.

2.3.1.2 Transfer functions based on empirical or physical mathematical models

Such transfer functions are based on more or less complex mathematical equations, including a few parameters used to adjust the model from measurements of the stresses and responses of the system. Such transfer functions require time series of data long enough to adjust the parameters. Due to the large set of mathematical functions that are available, it is theoretically possible to consider non-linear or time-variant systems. Jury (1982b) proposed a log-normal function to represent the distribution of transit times (indeed the transfer function) of solutes through soils. The transfer function can also be based on a physical model, for example an analytical solution of the advection-dispersion equation that allows the evaluation of the distribution of transit times in the medium (Jury and Roth 1990; Roth and Jury 1993). Stewart and Loague (1999) proposed a generalization of the works of Jury (1982b) at large scale by introducing the notion of type transfer functions.

The advantages of such approaches are mainly their simplicity and the limited number of required parameters. Their main drawback is the low precision that they provide and, above all, the fact that such models give information on the concentrations and mass fluxes at the outlet of the system but not on the spatial distribution of the concentrations inside the system. For example, the application of a transfer function aiming to represent the transit of a contaminant from agriculture to the river network, through the underground, allows estimating the mass flux associated to groundwater discharge but does not give information on the spatial distribution of the contaminant inside the aquifer.

In most cases, the transfer functions are characterised by one or two unknown parameters determined solving the inverse problem. Different codes have been developed to solve such inverse problems selecting different kinds of transfer functions, e.g. FLOWPC (Maloszewski and Zuber 1996), TRACER (Bayari 2002), LUMPED (Ozyurt and Bayari 2003).

Different authors have proposed syntheses of the main existing models and applications generally based on the use of these models for the interpretation of isotopic or environmental tracer data (Maloszewski and Zuber 1982; Duffy and Gelhar 1985; Duffy and Gelhar 1986; Ritzi *et al.* 1991; Maloszewski and Zuber 1996; Maloszewski *et al.* 2004 among others).

A summary of most common mathematical models used in transfer functions is presented hereafter.

2.3.1.2.1 Perfect mixing model

The perfect mixing model relies on the assumption of perfect mixing of solutes within the considered reservoir. This implies that any solute entering the system is instantaneously and completely mixed with the entire volume of groundwater and solute already present in the aquifer reservoir. The concentration at the outlet of the system is assumed to be equal to the mean concentration within the reservoir. Knowing the concentration at the outlet of the system, it is theoretically possible to know the mean concentration within the aquifer. The transfer function representing perfect mixing can be mathematically expressed by:

$$g(\tau) = \frac{1}{T}\exp\left(-\frac{\tau}{T}\right) \qquad \textbf{(2.12)}$$

where $g(\tau)$ is a function of the distribution of the transit time in the aquifer; T is the mean transit time of water in the underground.

In regards to the mathematical formulation of the function representing the model, it is often also called exponential model.

This model is, for example, applicable when the groundwater sampling induces a mixing of groundwater with different travel times (Figure 2.7).

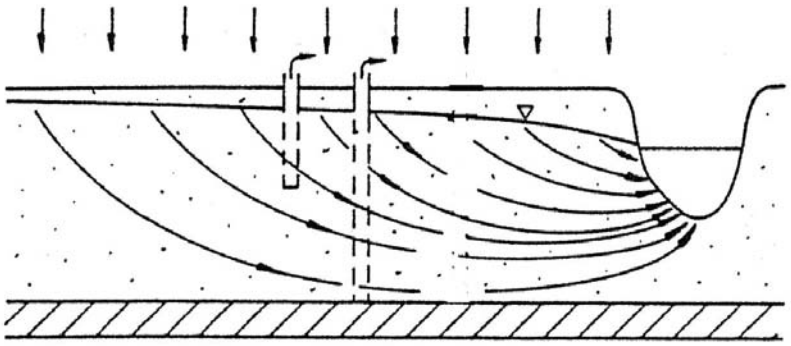

Figure 2.7. Situation for which the mixing model is applicable (modified from Maloszewski and Zuber 1982)

2.3.1.2.2 Piston-flow model

The piston-flow model assumes that solutes move from the entry to the outlet of the system by a purely advective process, introducing simply a delay corresponding to the travel time within the aquifer. This model assumes thus that the solute travel time between the entry and the outlet of the system is equal for all the stream lines and that mechanisms of dispersion and molecular diffusion are negligible. Mathematically, the transfer function representing piston-flow can be expressed by:

$$g(\tau) = \delta(\tau - T) \qquad \textbf{(2.13)}$$

where $g(\tau)$ is a function of the distribution of the travel times in the aquifer; T is the mean transit time of water in the underground.

The piston-flow model is, for example applicable, neglecting the dispersion in the case of a confined aquifer with a recharge zone limited in space and located far away from the pumping wells (Figure 2.8).

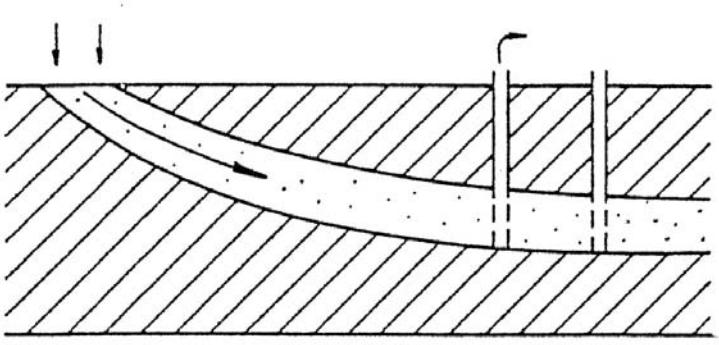

Figure 2.8. Situation for which the piston-flow model is applicable (modified from Maloszewski and Zuber 1982)

2.3.1.2.3 Dispersion model

The dispersion model links concentrations at the entry and the outlet of the system by a transfer function based on a simplified analytical one-dimensional solution of the advection-dispersion equation. Mathematically, the transfer function representing the dispersion model can be expressed by:

$$g(\tau) = \frac{1}{\sqrt{4\pi P_D \tau / T}} \frac{1}{\tau} \exp\left(- \frac{(1-\tau/T)^2}{4P_D \tau/T} \right) \quad \textbf{(2.14)}$$

where P_D is the dispersion parameter reflecting the relative importance of the dispersion processes to the advection processes. This parameter is the inverse of the Peclet number which is the ratio between advection and dispersion and which is defined for a flow parallel to the direction x by:

$$P_e = \frac{v_x \Delta x}{D_x} = \frac{\Delta x}{\alpha_L} \quad \textbf{(2.15)}$$

Where P_e is the Peclet number [-]; v_x is the advective velocity in the x direction [LT^{-1}]; Δx is the cell dimension in the x direction [L]; D_x is the xx component of the dispersion tensor [L^2T^{-1}]; α_L is the longitudinal dispersivity [L].

This model is applicable when dispersion process can not be neglected. Maloszewski (1994) showed that, for dual-porosity media, the dispersion model is usable when the travel time T is larger than 2-3 years. However, the application of the dispersion model to dual-porosity media yields to determine an apparent mean travel time T^* instead of the real travel time of groundwater T. This apparent mean travel time T^* can be expressed by:

$$T^* = \left(\frac{\theta_m + \theta_{im}}{\theta_m} \right) T = RT \quad \textbf{(2.16)}$$

where T* is the apparent mean travel time of groundwater [T]; θ_m is the effective mobile porosity [-]; θ_{im} is the immobile water porosity [-] ; T is the real mean travel time [T] and R is the retardation factor resulting from the diffusion of tracer into stagnant water [-].

2.3.1.2.4 Combined models

In the models mentioned here above, only one fitting parameter is generally considered. To model real cases, it is often necessary to have a greater flexibility for the calibration of the transfer functions with observed time series of concentrations. Several authors have thus proposed more elaborated models based on the combination of simple models. Amin and Campana (1996) proposed a general model from which, by fixing in a appropriate way the parameters, it is possible to infer most of the models cited here above, as well as several combinations of these models.

One generalisation of the approaches presented here above is the example of the combined exponential – piston-flow model. This model includes a parameter called mixing efficiency that allows for the continuity from the piston-flow model (corresponding to a mixing efficiency equal to zero) to the exponential model (corresponding to perfect mixing with a mixing efficiency of 1).

Mathematically, the transfer function representing the combined exponential – piston-flow model can be expressed by:

$$g(\tau) = \frac{\eta}{T}\exp\left(-\frac{\eta\tau}{T} + \eta - 1\right) \qquad \text{for } \tau > (\eta - 1)T/\eta \qquad \textbf{(2.17)}$$

$$g(\tau) = 0 \qquad \text{for } \tau \leq (\eta - 1)T/\eta \qquad \textbf{(2.18)}$$

where η is the mixing efficiency.

This model is, conceptually, applicable to unconfined aquifers with a thick unsaturated zone (Figure 2.9). The piston flow component of the combined model allows representing solute transport in the unsaturated zone and the exponential component transport in the saturated one.

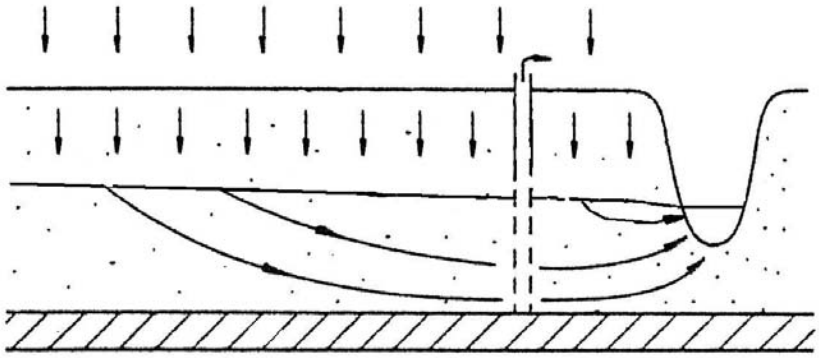

Figure 2.9. Situation for which the combined exponential - piston-flow model is applicable (modified from Maloszewski and Zuber 1982)

2.3.2 Compartment models

Simple transfer function models consider and represent the underground as a whole by a "black box", without considering the heterogeneity and the spatial distribution of physical properties of the underground medium. Among these approaches, combined models differentiate a series of fluxes or processes, however, from a spatial point of view, they remain non-spatially-distributed. These black-box models work more or less when the number of observed data and available measurements are limited or when the actual groundwater flow and transport conditions are not too far from the ideal situation described by the model. Unfortunately, groundwater flow and transport conditions met in reality are often strongly different from idealized situations described by transfer functions and it becomes necessary to develop spatially-distributed groundwater models that take into account the spatial heterogeneity of the media and of its physical properties.

Compartment models constitute a first category of approaches taking into account the heterogeneity of the media. Even if they are still based on simplified mathematical concepts, such as simple mathematical formulations, compartment modelling approaches have the advantage of being spatially-distributed. They are usually made of "black-box" models connected in series or spatially-distributed (e.g. Campana and Simpson 1984; Adar 1996; Campana *et al.* 1997; Van Herpe *et al.* 1998; Harrington *et al.* 1999). Existing approaches essentially differ one from another in the way of evaluating the exchanged fluxes between the different compartments of the model.

One of the most used compartment models is the spatially-distributed mixing cell model. In this model, the aquifer is divided into cells within which transported solutes are assumed to

undergo complete mixing. Different ways of evaluating the flux between the cells have been proposed in literature (Bajracharya and Barry 1992; Bajracharya and Barry 1994). In some approaches, the cell contents is displaced downward by one cell at the beginning of each time step (Appelo and Willemsen 1987). In other approaches, the advective term of the solute transport equation is solved using more traditional tools such as for example an implicit backward finite-difference scheme (Dudley *et al.* 1991). Recently, Carroll *et al.* (2008) used fluxes computed with the code MODFLOW (solving the groundwater flow equation) as boundary conditions of a mixing model.

In a general way, the equation of mass conservation of solute in steady state condition can be written for a constituent k, in cell n:

$$C'_{nk}\ Q_n - \overline{C}_{nk}\left[W_n + \sum_{j=1}^{J_n} q_{nj}\right] + \sum_{i=1}^{I_n} q_{in}\ \overline{C}_{ink} = 0 \qquad \textbf{(2.19)}$$

where C'_{nk} is the average concentration [ML^{-3}] of constituent k associated with source Q_n [L^3T^{-1}]; $\overline{C}_{nk}$ is the average concentration [ML^{-3}] of solute k within cell n; W_n are the sink terms [L^3T^{-1}]; q_{nj} is the flux from cell n to cell j [L^3T^{-1}]; $\overline{C}_{ink}$ is the average concentration of solute k entering cell n together with the flux q_{in} coming from cell I.

Mixing cell models have been used for a wide variety of applications at different scales, ranging from 1D columns (Bajracharya and Barry 1994) to regional scale (Harrington *et al.* 1999; Carroll *et al.* 2007; Carroll *et al.* 2008). Such models have also been predominantly applied to studying isotopic and environmental tracer distributions in groundwater systems (Adar 1996; Campana *et al.* 1997; Dahan *et al.* 2004) but also to study salt water intrusion (Appelo and Willemsen 1987) or temporal and spatial distribution of pesticides in a soil profile (Basagaoglu *et al.* 2002). Chemical reactions, adsorption and degradation have also been introduced in these models (Van Ommen 1985; Bajracharya and Barry 1992)

2.3.3 Advection-dispersion models applied at the regional scale

The most advanced existing solution consists in modelling solute transport in groundwater using spatially-distributed solutions of the advection-dispersion equation. Such approaches are based on the resolution of the physical equation describing the transport processes, most

often with the help of numerical methods (finite differences, finite elements, finite volume…). These approaches generally offer a higher flexibility in terms of the choices of the considered processes, of boundary conditions and of stresses. Distributed physically-based models developed at the regional scale have to face different problems (Barthel *et al.* 2008), (1) the growing in degree of complexity of groundwater systems if more than one aquifer have to be considered or if the geology is diversified, (2) the frequent scarcity of data and their inadequacy with the modelling scale, (3) the time and spatial discretisation not only related to the physical phenomena but also with numerical issues such as model stability, numerical dispersion and oscillations.

2.3.3.1 Parametrisation

The development of advection–dispersion models at the regional scale requires a lot of parameters quantifying the different processes described in the equation. The first problem thus concerns the availability of such data. Data should theoretically cover the whole modelled domain, which is generally not the case, since values of the parameters are generally measured in particular points within the aquifer. The second problem relates to representativeness of existing data at the considered modelling scale. In particular, as discussed in the first section of this chapter (e.g. Figure 2.5), parameters used in the advection-dispersion equations are scale-dependant. At the regional scale, it becomes difficult to evaluate precisely the hydrodispersive parameters introduced in the models (effective porosity and the terms of the dispersivity tensor). Classical techniques used to quantify transport processes in the field, such as tracer experiments (Käss 1998; Brouyère 2005) apply only at local to medium scales (from a few meters to a few hundred meters). Because of these limitations, important research efforts have been devoted to upscaling techniques from local to large scale. For hydraulic conductivities, a large number of research have been lead to make the link between values measured locally and more global equivalent values (King 1989; Durlofsky 1991; Desbarats 1992a; Desbarats 1992b; Durlofsky 1992; Desbarats 1994; Neuman 1994; Sánchez-Vila *et al.* 1995; Sánchez-Vila *et al.* 1996; Renard and de Marsily 1997; Renard *et al.* 2000; Hristopulos 2003; Nastev *et al.* 2004; Efendiev *et al.* 2005; Eaton 2006). For solute transport, works mainly related to the dispersion mechanisms at large scale have also been done. These researches are however essentially confined to the theoretical domain (Gelhar and Axness 1983; Desbarats 1990; Dagan 1994; Fernandez-Garcia *et al.* 2005), probably because of a lack of enough experimental data that allow proposing really effective upscaling tools. Different authors (Scheibe and Yabusaki 1998; Kasteel *et al.* 2000;

Cassiraga *et al.* 2005) have investigated and tested upscaling methods and their influence on transport modelling. In most of these approaches, advective processes only are taken into account and upscaling of hydraulic conductivities is performed.

2.3.3.2 Numerical solution to the advection-dispersion equation

Even if hydrodispersive data are available at the required work scale, numerical difficulties would occur when solving the advection-dispersion equations. Transport equations are indeed generally difficult to solve due to the conditionality of the stability of the numerical scheme linked to the spatial and temporal discretisations of the system. Classical numerical techniques require long computation times and large computer memory because refined meshes are required in order to avoid problems such as numerical dispersion or instabilities. Modelling large scale transport models based on the advection-dispersion equation need that a compromise is found between the degree of spatial refinement and computational costs (memory and time). Most numerical methods for solving the advection-dispersion equation can be classified as Eulerian, Lagrangian and mixed Eulerian-Lagrangian (Neuman 1984).

Eulerian approaches solve the transport equations using a fixed grid method such as the standard finite difference or finite element methods. This approach is mass conservative but for advection-dominated problems (which are the problems the most common in hydrogeology), Eulerian method are susceptible to excessive numerical dispersion or artificial oscillations. To avoid these problems, small grid spacing and time steps are required which can be translated mathematically by the fact that, the Peclet (Equation(2.15) and Courant number should be lower than 1.

The Courant number [-] is the ratio between the advective travel during one time step Δt over the cell dimension Δx :

$$C_r = \frac{v_x \, \Delta t}{\Delta x} \qquad \textbf{(2.20)}$$

Lagrangian approaches solve the transport equations in either a deforming grid or deforming coordinate in a fixed grid through particle tracking. Lagrangian approaches provide highly efficient solution to advection-dominated problems, virtually free of numerical dispersion (Zheng and Wang 1999). However, Lagrangian methods can lead to numerical instability and

computational difficulties in non-uniform media with multiple sink/sources terms and complex boundary conditions (Yeh 1990).

Mixed Eulerian–Lagrangian methods try to combine the advantages of both the Eulerian and Lagrangian approaches by solving the advection and dispersion terms of the transport equation respectively with a Lagrangian (the method of characteristics, the modified method of characteristics and the hybrid method of characteristics) and an Eulerian method. However these mixed approaches do not guarantee mass conservation (Zheng 1990).

Promising TVD (Total Variation Diminishing) numerical schemes have been proposed that are able to control numerical dispersion inherent to using less refined meshes (Harten 1983).

Several examples of groundwater flow and solute transport model at the regional scale using less refined meshes are available (Loague *et al.* 1998; Loague and Abrams 1999; Refsgaard *et al.* 1999; Christiansen *et al.* 2004; Almasri and Kaluarachchi 2007; Ledoux *et al.* 2007).

Refsgaard *et al.* (1999) developed a coupled soil-groundwater spatially-distributed model using the Daisy-MikeShe model to simulate groundwater contamination from nitrate leaching in two Danish catchments of about 500 km². The underground is conceptualised using two layers with uniform values of hydraulic conductivities, porosity and storage coefficients. No information is provided concerning the transport processes taken into account or their parameterisation. The models were not calibrated but were validated using the statistical distribution of nitrate concentrations in groundwater. Different sizes of the grid were tested.

Almasri and Kaluarachchi (2007) coupled a soil model with the code MODFLOW and MT3D to model the nitrate contamination in an agricultural watershed of 388 km². No information is provided concerning the parameters introduced in the model and the discretisation and numerical scheme used to solve the transport equation. Nitrate concentrations have been assumed to be quasi-steady state and a trial-and-error calibration was performed by comparing observed and computed nitrate concentration in groundwater.

Ledoux *et al* (2007) developed a software package combining the different existing codes MODCOU, NEWSAM and STICS to model nitrate contamination in groundwater in the Seine basin (95560 km²). Advection is the only transport process taken into account in groundwater. The groundwater solute transport model was calibrated using a probability distribution of measured nitrate concentrations.

2.3.4 Comparisons between the approaches of the transfer function type and the spatially-distributed models

As described previously, simple transfer functions and spatially-distributed physical models have relatively contrasted possibilities and are generally used to reach different objectives. The first kind of approaches are tools that allow a rough and global analysis of the functioning of the underground system in terms of transit time of groundwater and solute. These approaches have the advantage to require a limited number of parameters. The second kind of approaches are more performing tools, usable when spatially-distributed information are required for management and predictive tasks. However, they are more difficult to implement and require a more important number of data to furnish reliable and accurate results.

A comparison between the different approaches is interesting for several reasons. First of all, it allows better understanding their respective advantages and drawbacks, and on the other hand identifying their similarities and differences that characterise them. It is, among others, interesting to determine in which conditions an approach of the transfer functions can be used to replace physical spatially-distributed models when data of good quality or in a sufficient number are not available and also to determine the kind of errors or approximations introduced by the use of these simplified approaches. Several authors have already performed some interesting comparisons. The main results of these comparisons are described here after.

Maloszewski and Seiler (1999) compared a simplified 2-dimensional horizontally stratified aquifer different transfer function approaches (exponential model, piston-flow model, dispersion model and combined exponential piston flow model) and the results of a numerical, spatially-distributed groundwater flow and solute transport model. They were generally able to fit the evolution of concentration generated with the numerical model with the help of transfer functions but frequently, they had to assume that a part of the groundwater contained in the aquifer was stagnant and isolated from the solute travel area. This is particularly true when using the exponential model that reproduced with difficulty the effect of stratification of hydraulic conductivities on groundwater flow and the confinement of the solute in the upper part of the aquifer (the most permeable part of the aquifer).

Baracharya and Barry (1994) compared solutions obtained with a mixing cell approach and a finite difference scheme used to reproduce transport of adsorbing solutes in a column. It was found that the results obtained using the mixing cell approach coupled with a non-linear isotherm were very accurate when compared with results obtained with the finite difference

scheme. They also observed that the accuracy of the results was dependant on the spatial discretisation used to describe the column. Best results were obtained for a size of the mixing cells close to twice the dispersivity value.

Duffy and Lee (1992) evaluated the concentration in the base flow resulting from a diffuse pollution for a vertical 2-dimensional steady state flow. Using a non-dimensional formulation of the problem, they performed a sensitivity analysis on transport parameters (dispersion and adsorption), on the relative extension and intensity of the diffuse pollution area in surface and on the variability of initial conditions in the aquifer and of the heterogeneity of the media. These tests showed that the concentration in the base flow was not very sensitive to variations of the hydrodynamic dispersion in the underground medium. This hydrodynamic dispersion becomes indeed rapidly negligible as compared to the dispersion implicitly introduced by the spatial distribution of the contamination. Variability of the hydraulic conductivities, of the concentrations of the source of contamination and of the initial concentrations seemed to have a secondary role. On the contrary, the mean concentration of the source of contaminant, the initial concentrations in the aquifer and the mean residence time in the aquifer had a key role. The same authors compared the concentrations in the base flow obtained with the numerical model with those obtained applying an exponential transfer function model, showing that this transfer function model is a relatively good representation of the phenomena regarding diffuse pollution. These observations seem to be strongly linked to the fact that the source of contamination is spatially-distributed (diffuse pollution) while the outlet of the system is relatively spatially concentrated, producing a mixing of the different stream lines at the outlet of the system and thus a mixing of solutes coming with different concentrations from different zones of the aquifer. In the end, they proposed and applied another transfer function model (the Weibull residence time distribution) that provided results in better agreement with the numerical model than those provide by the exponential model.

Eldor et Dagan (1972) determined analytical solution for the hydrodynamic dispersion in porous media for a vertical two-dimensional flow towards ditches from uniform and steady recharge. The authors computed the concentrations in the aquifer and the motion of the contamination front when adding tracer to the recharge. The authors showed that the amount of tracer crossing a vertical section of the aquifer is practically uninfluenced by the hydrodynamic dispersion.

2.4 Nitrates in groundwater

Nitrate is a component of the nitrogen cycle (Figure 2.10) and its conversion from nitrogen is part of the functioning of any ecosystem. Nitrate is a stable nitrogen species in certain natural conditions and it forms compounds that are highly soluble. These characteristics allow nitrate to be transported in groundwater (Korom 1992). Anthropogenic activities of modern society, such as organic waste disposal and the use of fertilizers for agriculture are the primary contributors to the contamination of groundwater by nitrate (Hallberg and Keeney 1993; Hudak 2000; Harter *et al.* 2002; Johnsson *et al.* 2002; Collins and McGonigle 2008). Nitrate is identified as one of the most problematic and widespread contaminant of groundwater which has been widely documented throughout the world (e.g. Mitchell *et al.* 2003; Mohamed *et al.* 2003; Thorburn *et al.* 2003; Oren *et al.* 2004; Jackson *et al.* 2008). Links between nitrate ingestion and diseases are supposed (Canter 1997; Sandor *et al.* 2001) and recommendations have been emitted in Europe (1998/83/EC) and by the World Health Organisation (WHO 2004) to restrict the concentration of nitrate in drinking water to 50 mg/l.

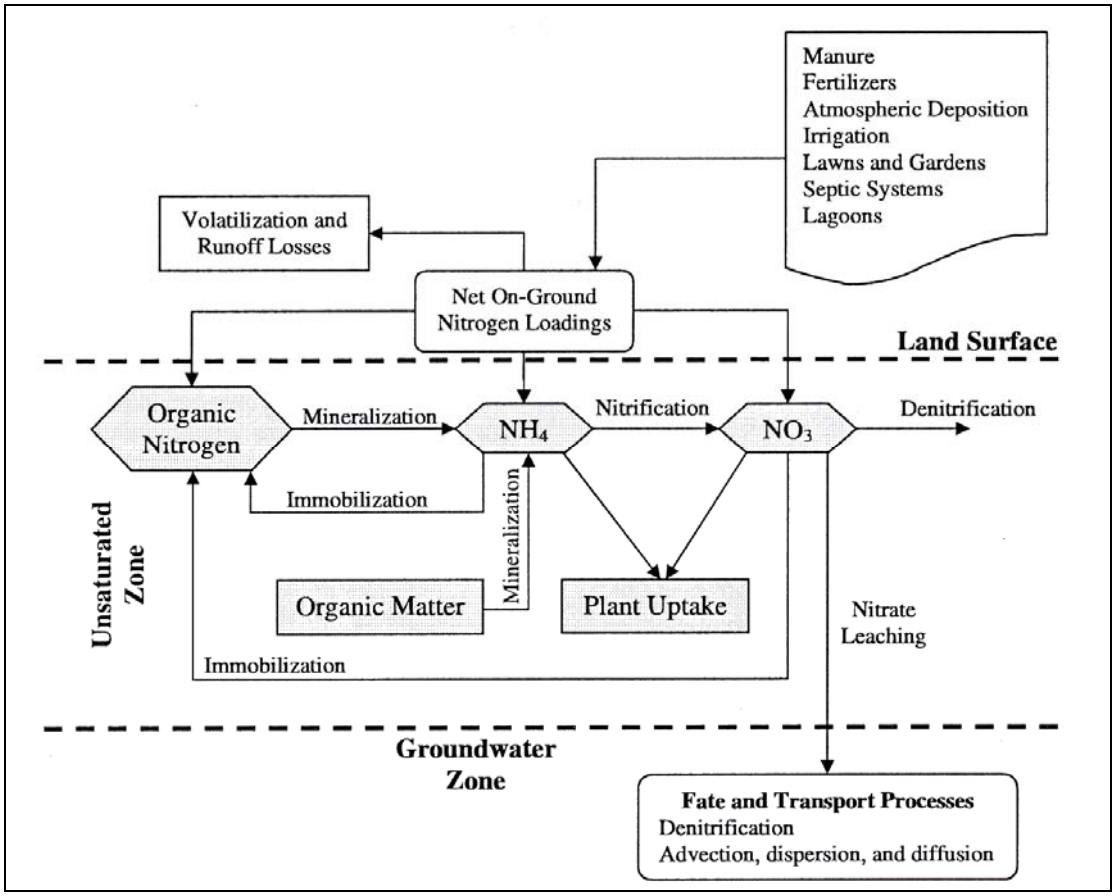

Figure 2.10. Nitrogen cycle (Almasri and Kaluarachchi 2007)

It is generally assumed that, in the deep unsaturated zone and unconfined groundwater, nitrate is effectively conservative (Price *et al.* 1993; Brouyère *et al.* 2004). In practice, the only effective way for nitrate to be removed from groundwater is by chemical reduction, a process often called denitrification (Postma *et al.* 1991). This reduction is a multi-step reducing reaction:

$$NO_3^- \rightarrow NO_2^- \rightarrow NO^- \rightarrow N_2O \rightarrow N_2 \quad \textbf{(2.21)}$$

Four prerequisites for denitrification are the concomitant presence of (1) N oxides (NO_3^-, NO_2^-, NO, and N_2O) as terminal electron acceptors (2) bacteria possessing the metabolic capacities of denitrification (3) suitable electron donors (4) anaerobic conditions or restricted O_2 availability (Firestone 1982).

Bacteria in aquifers obtain energy from the oxidation of organic or inorganic compounds. Electron donors can be in the form of dissolved organic carbon (DOC) (Mengis *et al.* 1999 among others) or inorganic (reduced manganese Mn_2^+, ferrous iron Fe_2^+, sulfides) (Schwientek *et al.* 2008 among others). The electron donors are oxidised by electron acceptors that yield the most energy to the bacteria (Korom 1992). In the presence of dissolved oxygen, bacteria use preferentially oxygen to oxidise the electron donors. When O_2 levels decrease, denitrification becomes competitive and NO_3^- becomes the electron acceptor (Korom 1992). As a consequence, denitrification processes are most often relatively limited in unconfined aquifers, denitrification being only significant when confined conditions are met (Rivett *et al.* 2007).

Different methods are proposed in the literature to highlight denitrification processes in groundwater (Mariotti 1994). A first approach consists in detecting a gradient of redox potentials in the aquifer, allowing denitrification and decrease in relevant geochemical parameters such NO_3^-, DOC, Fe^{2+} as well as increase in HCO_3^-, Fe^{3+}, Mn^{4+}, SO_4^{2-} (Appelo and Postma 2005). A second approach consists in detecting the increase of N_2 gas concentrations that is the final product of the denitrification chain (Vogel *et al.* 1981). Another approach consists in relating the presence or absence of nitrate in groundwater with the age of this water (see next section for more details) (Schwientek *et al.* 2008). As denitrification processes generate isotopic fractionation, the monitoring of nitrogen isotopes could also be used as denitrifying bacteria preferentially metabolise the light isotopes (Aravena and Robertson 1998; McMahon *et al.* 1999; Lehmann *et al.* 2003)

2.5 Environmental tracers

Significant global changes in the shallow groundwater chemistry due to human activities have occurred during the last 50 years. as a result of increasing concentrations of anthropogenic tracers in the atmosphere, e.g. 3H, 36Cl, 85Kr, chlorofluorocarbons (CFC) and Sulfur hexaFluoride (SF_6) (Figure 2.11) (Loosli *et al.* 1991; Cook and Solomon 1997; Busenberg and Plummer 2000; Loosli *et al.* 2000; Hinsby *et al.* 2001) and infiltration of a large range of contaminants from agricultural and industrial activities e.g. pesticides nitrate, sulphate (Robertson *et al.* 1989; Postma *et al.* 1991; Rao and Alley 1993; Edmunds 1996). These anthropogenic pollutants can be considered as tracers and can be used for age dating of young shallow groundwater.

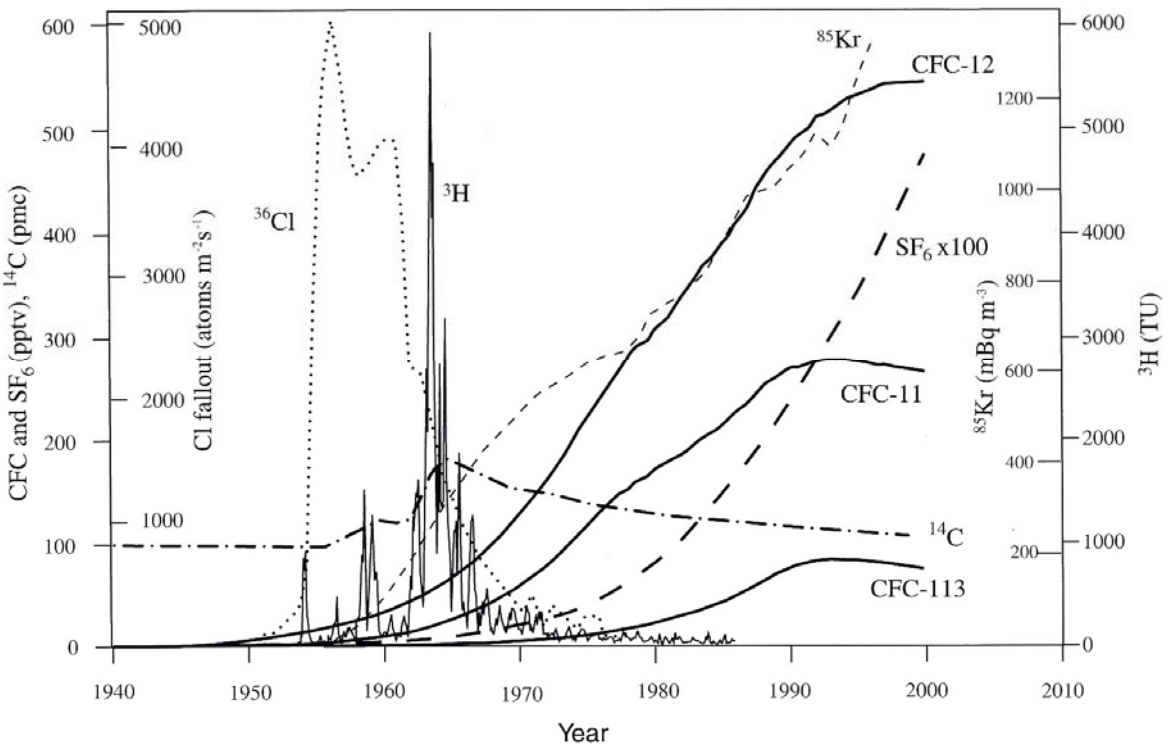

Figure 2.11. Atmospheric Northern hemisphere concentrations of CFC, SF_6, ^{85}Kr, ^{14}C and precipitation concentration of ^{3}H (from Hinsby *et al.* 2001).

For the last fifty years, concerns for these environmental tracers in hydrogeology have been demonstrated through numerous studies related to the characterisation, the use, the management and the protection of groundwater resources (Schlosser *et al.* 1988; Olive *et al.* 1996; Szabo *et al.* 1996; Katz *et al.* 2004; Cook *et al.* 2005). Groundwater dating using environmental tracers allows estimating mean residence times in the aquifers and the mean

ages of groundwater. Different authors (Broers 2004; Koh *et al.* 2006 among others) have highlighted the importance of groundwater age for the understanding of diffuse pollution and as a key factor determining the distribution of solute in groundwater.

Tritium, CFC's and SF_6 are the most commonly used environmental tracers, providing information on groundwater residence times and mixing processes for waters up to 50 years old (Figure 2.12). They can be rapidly determined and sampling require no sophisticated equipments (Gooddy *et al.* 2006). Groundwater dating with tritium, CFC's and SF_6 is possible because (1) the atmospheric mixing ratios of these compounds are known or have been reconstructed for the last sixty years and is essentially a function of the latitude, (2) detection levels are low enough to allow detection, (3) the solubility in water (Henry's law) of CFC's and SF6 that are gazes is known (Plummer and Busenberg 2000).

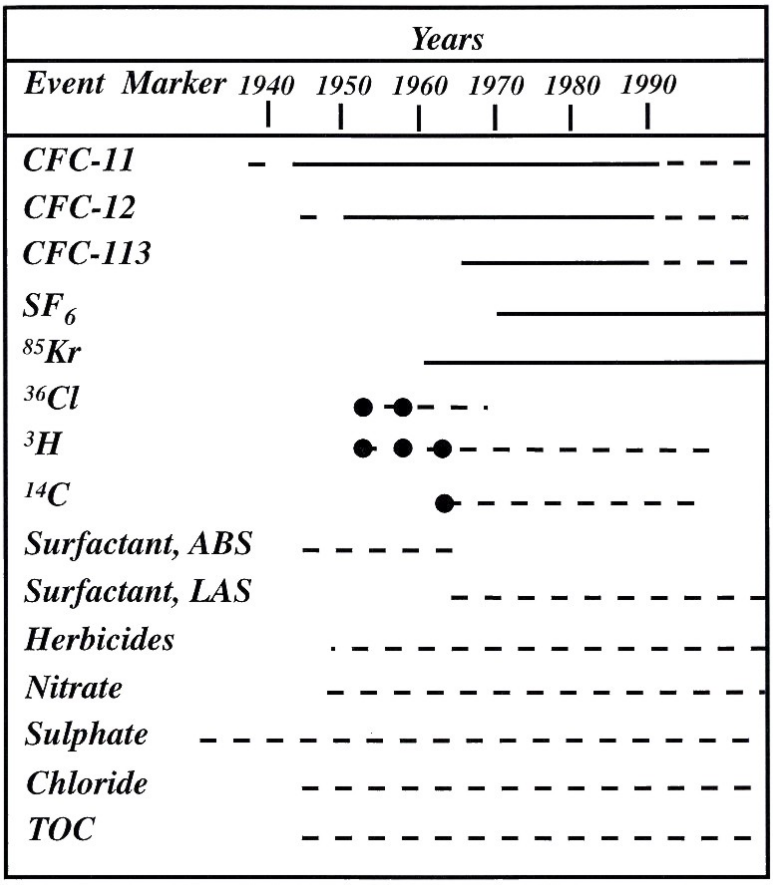

Figure 2.12. Approximate range of absolute dating applications of selected environmental tracers and event markers (black dots) (Modified after Plummer *et al.* 1993)

Tritium ^{3}H, the radioactive isotope of hydrogen has a period or a half-life of 12,43 ± 0,05 year (Unterweger *et al.* 1980), its concentration is generally expressed in tritium unit (TU) corresponding to one atom of ^{3}H for 10^{18} atoms of hydrogen that is 0,118 Bq/l. Naturally produced by reactions of protons and neutrons with nitrogen and oxygen in the upper atmosphere, tritium concentrations in atmospheric waters (and thus in precipitations) were constant and low (about 5-10 TU) before the thermonuclear aerial tests. Following these tests, tritium contents in atmospheric waters increased to reach a peak of about 6000 TU in the Northern hemisphere during the summer months in 1962 and 1963. Since the end of aerial tests, atmospheric tritium concentrations have exponentially decreased, reaching 10-20 TU in the late 90-ties. The high concentrations in tritium of the 60-ties still allow dating young groundwaters, which means of an age lower than 50 years.

Chorofluorocarbons (CFC's) gazes are stable, synthetic, halogenated alkanes developed in the early 30-ties for industrial and refrigerant applications. Release of CFC's to the atmosphere and subsequent incorporation into the earth's hydrologic cycle has closely followed their industrial production (Plummer and Busenberg 2000). CFC-11 ($CFCl_3$), CFC-12 (CF_2Cl_2) and CFC-113 ($C_2F_3Cl_3$) concentrations in the atmosphere steadily increased in the atmosphere between 1945 and 1990. After 1990, this fast increase changed abruptly, as a consequence of regulations limiting the use of CFC's in the industry, resulting in nearly constant atmospheric concentrations. CFC's are used as tracers of post-1950 water and dating tools of pre-1990's water. An important drawback is that all CFC's can be degraded under anaerobic conditions. Consequently, the use of such tracers for absolute dating is limited in aquifers where such conditions occur. However, occurring degradation can be identified thanks to the fact that CFC's degrade at different rates (Oster *et al.* 1996; Plummer and Busenberg 2000). Another drawback is the possibility of local contamination resulting from anthropogenic point sources such as discharges from septic tanks, leachage from sewage treatment plants (Plummer and Busenberg 2000). These local contaminations can mask the contamination from atmospheric CFC's and lead to the impossibility to interpret CFC's data because the input function is not anymore known.

Sulfur hexaFluoride (SF_6) is a stable gas of primarily anthropogenic origin produced since 1953 for its excellent electrical insulating and arc-quenching properties. SF_6 has been predominantly released in the mid latitude of the Northern hemisphere and subsequently incorporated in the hydrosphere (Busenberg and Plummer 2000). SF_6 concentrations in the

atmosphere have increased rapidly over the last 30 years. This tracer is thus very useful to date very young groundwater (Hinsby *et al.* 2001). SF_6 has the highest greenhouse warming potential, and consequently production and release controls are expected in a near future. However due to its very long lifetime (800-3200 years), SF_6 could be therefore used as groundwater tracer in the 21st century (Busenberg and Plummer 2000). An advantage of SF_6 over CFC's is that SF_6 apparently does not degrade in aquifers even in anaerobic conditions. On the contrary, a drawback is that natural (mainly volcanic) sources of SF_6 exist (Harnisch and Eisenhauer 1998).

These three environmental tracers do not behave in the same way in regards to water. Tritium is part of the water molecule that makes it a nearly-perfect tracer. CFC's and SF_6 are gazes partly dissolved in water. Behaviour of these tracers in the unsaturated zone is also different. As tritium is part of water, it follows strictly the water molecules in the unsaturated zone and passes the unsaturated zone advectively with the seepage water. As CFC's and SF_6 are gazes, they move mainly by diffusion in the gas phase of the unsaturated zone before they enter groundwater in which they dissolved according to Henry's law (Cook and Solomon 1995). This transport mechanism is much faster then the advective transport with the seeping water. When the unsaturated zone is relatively thin, the unsaturated zone air composition is similar to the air composition of the troposphere (Oster *et al.* 1996). It is reasonable to assume that SF_6 and CFC's concentrations in the unsaturated zone are similar to tropospheric concentrations to unsaturated zone depths of less than 10 meters (Busenberg and Plummer 2000). In deeper unsaturated zones, there is a lag time for diffusive transport of CFC's and SF_6.

2.6 Quality trend assessment in groundwater

The increasing concern for groundwater quality over the last few decades has led to the acquisition of long-term water quality data records (Hirsch *et al.* 1991). The long-term changes in these records, also called temporal trends have been defined more accurately by Loftis *et al.* (1991) as "*a change in groundwater quality over a specific period in time, over a given region, which is related to land use or water quality management"*. Trend assessment consists in determining whether the measured values of water quality increase or decrease during a time period and to describe the rate or amount of such changes (Antonopoulos *et al.* 2001).

The notion of trend has also been introduced in the Water Framework Directive (WFD) (2000/60/EC). The directive requires, among others, Member States to take measures to identify and reverse significant upward trends in pollutant concentrations. For EU Member States, a series of recommendations were made for trend assessment for different type of time series (for example seasonally varying or not water quality time series), proposing parametric and non-parametric methods owing to their capability to detect different types of patterns of change and their robustness (Grath *et al.* 2001). Following these guidelines, Batlle-Aguilar *et al.* (2007) have proposed a methodology for trend assessment based on a three steps procedure (Broers *et al.* 2005) (Figure 2.13).

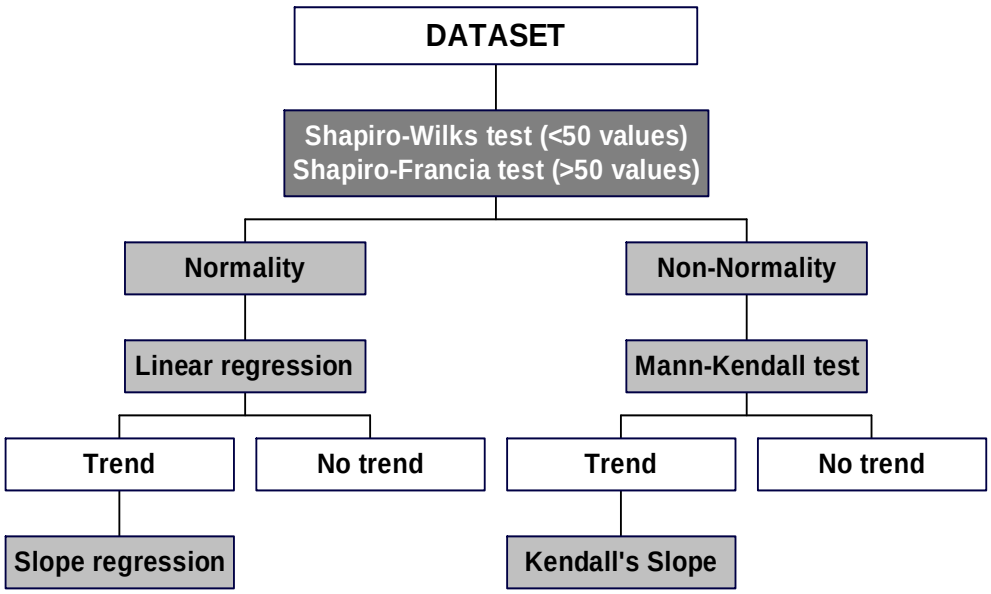

Figure 2.13. Three step procedure adopted for trend analysis: 1) normal/non-normal distribution data; 2) trend detection; 3) trend estimation (from Batlle-Aguilar *et al.* 2007).

The first step of the procedure consists in testing the normality of the dataset to select the techniques to be applied in the second and third steps.

For normally distributed dataset, trend detection is performed the correlation coefficient r:

$$r = \frac{\sum_{i=1}^{n}\left(t_i - \bar{t}\right)\left(C_i - \overline{C}\right)}{\sqrt{\sum_{i=1}^{n}\left(t_i - \bar{t}\right)^2 \sum_{i=1}^{n}\left(C_i - \overline{C}\right)^2}} \qquad \textbf{(2.22)}$$

where C_i are concentration data at time i.

The value of the indicator r is then compared to threshold values to determine if a trend exist (Carr 1995). If a trend exists, its magnitude is estimated using the slope of the linear regression.

For non-normally distributed dataset, trend detection is performed using the Mann-Kendall test (Mann 1945; Kendall 1975). The Mann-Kendall test determines whether a trend is present or not with an indicator T based on the calculation of differences between pairs of successive data:

$$T = \sum_{i=1}^{n-1} \sum_{j=i+1}^{n} \mathrm{sgn}\left(C_j - C_i\right) \quad \textbf{(2.23)}$$

where:

$$\mathrm{sgn}\left(C_j - C_i\right) = \begin{Bmatrix} 1 \;\; if \;\; C_j - C_i > 0 \\ 0 \;\; if \;\; C_j - C_i = 0 \\ -1 \;\; if \;\; C_j - C_i < 0 \end{Bmatrix} \quad \textbf{(2.24)}$$

where C_j and C_i are concentration data at different time i and j, with $j > i$ and n is the size of dataset.

The value of the indicator T is then compared to threshold values defined in function of the significance level required to determine if a trend exist or not. If a trend is detected, its magnitude is estimated using the Sen's slope estimator (Hirsch *et al.* 1991; EPA 2000):

$$b = median\left(\frac{C_j - C_i}{t_j - t_i}\right) \text{ for all i, j} \quad \textbf{(2.25)}$$

where C_i *and* C_j are nitrate concentrations at time t_i and t_j, respectively.

If these statistical tools allow detecting and quantifying trends, they do not allow, by themselves, predicting their future evolution or identifying trend reversal (Grath *et al.* 2001) because they do not consider changes in land-use which are the main drivers of the contamination evolution (Gardner and Vogel 2005; Ritter *et al.* 2007).

2.7 References to chapter 2

Adar, E. M. (1996). Quantitative evaluation of flow systems, groundwater recharge and transmissivities using environmental tracers. Vienna, Austria, IAEA**:** 113-154.

Almasri, M. N. and J. J. Kaluarachchi (2007). "Modeling nitrate contamination of groundwater in agricultural watersheds." Journal of Hydrology **343**: 211-229.

Amin, I. E. and M. E. Campana (1996). "A general lumped parameter model for the interpretation of tracer data and transit time calculation in hydrologic systems." Journal of Hydrology **179**: 1-21.

Antonopoulos, V. Z., D. M. Papamichail and K. A. Mitsiou (2001). "Statistical and trend analysis of water quality and quantity data for the Strymon River in Greece." Hydrology and Earth System Sciences **5**(4): 679-691.

Appelo, C. A. J. and D. Postma (2005). Geochemistry, Groundwater and Pollution. Rotterdam, A.A. Balkema.

Appelo, C. A. J. and A. Willemsen (1987). "Geochemical calculations and observations on salt water intrusions, I. A combined geochemical/mixing model." Journal of Hydrology **94**: 313-330.

Aravena, R. and W. D. Robertson (1998). "Use of multiple isotope tracers to evaluate denitrification in ground water: study of nitrate from a large-flux septic system plume." Ground Water **36**(6): 975-982.

Bajracharya, K. and A. Barry (1994). "Note on common mixing cell models." Journal of Hydrology **153**: 189-214.

Bajracharya, K. and D. A. Barry (1992). "Mixing cell models for nonlinear nonequilibrium single species adsorption and transport." Water Resources Research **29**(5): 1405-1413.

Barthel, R., J. Jagelke, J. Götzinger, T. Gaiser and A. Printz (2008). "Aspects of choosing appropriate concepts for modelling groundwater resources in regional integrated water resources management - Examples from the Neckar (Germany) and Ouémé catchment (Benin)." Physics and Chemistry of the Earth **33**(1-2): 92-114.

Basagaoglu, H., T. R. Ginn and B. J. Mc Coy (2002). "Formulation of a soil-pesticide transport model based on a compartmental approach." Journal of Contaminant Hydrology **56**: 1-24.

Batlle-Aguilar, J., P. Orban, A. Dassargues and S. Brouyère (2007). "Identification of groundwater quality trends in a chalk aquifer threatened by intensive agriculture in Belgium." Hydrogeology Journal **15**: 1615-1627.

Bayari, S. (2002). "TRACER : an EXCEL workbook to calculate mean residence time in groundwater by use of tracers CFC-11, CFC-12 and tritium." Computers & Geosciences **28**: 621-630.

Bear, J. (1972). Dynamics of fluid in porous media. New-York, American Elsevier Publishing Co.

Bear, J. and A. Verruijt (1987). Modeling groundwater flow and pollution. Dordercht (NL), Kluwer Academic.

Biver, P. (1993). Etude phénoménologique et numérique de la propagation des polluants miscibles dans un milieu à porosité multiple (Phenomenological and numerical study of miscible contaminant propagation in a multi-porosity medium). PhD thesis. Faculty of Applied Sciences. Liège (Belgium), University of Liège**:** 389.

Broers, H. P. (2004). "The spatial distribution of groundwater age for different geohydrological situations in the Netherlands: implications for groundwater quality monitoring at the regional scale." Journal of Hydrology **299**: 84-106.

Broers, H. P., A. Visser, J.-L. Pinault, D. Guyonnet, I. G. Dubus, N. Baran, A. Gutierrez, C. Mouvet, J. Batlle-Aguilar, P. Orban and S. Brouyère (2005). Report on extrapolated time trends at test sites, Deliverable T2.4, AquaTerra (Integrated Project FP6 no. 505428)**:** 81.

Brouyère, S. (2001). Etude et modélisation du transport et du piégeage des solutés en milieu souterrain variablement saturé (Study and modelling of transport and retardation of solutes in variably saturated media). Faculty of Applied Sciences. Liège (Belgium), University of Liège**:** 640.

Brouyère, S. (2005). "Solute contaminant transport in variably saturated dual-porosity/dual-permeability chalk: field tracer experiments and modelling." Reactive transport in soil and groundwater processes and models: doi 10.1007/b138022.

Brouyère, S. (2006). "Modelling the migration of contaminants through variably saturated dual-porosity, dual-permeability chalk." Journal of Contaminant Hydrology **82**: 195-219.

Brouyère, S., A. Dassargues and V. Hallet (2004). "Migration of contaminants through the unsaturated zone overlying the Hesbaye chalky aquifer in Belgium: a field investigation." Journal of Contaminant Hydrology **72**: 135-164.

Busenberg, E. and L. N. Plummer (2000). "Dating young groundwater with sulfur hexafluoride: Natural and anthropogenic sources of sulfur hexafluoride." Water Resources Research **36**(10): 3011-3030.

Campana, M. E., N. Sadler, N. L. Ingraham and R. L. Jacobson (1997). "A deuterium-calibrated compartmental model of transient flow in a regional aquifer system." Tracer Hydrology: 389-396.

Campana, M. E. and E. S. Simpson (1984). "Groundwater residence times and discharge rates using discrete-state compartmental model and ^{14}C data." Journal of Hydrology **72**: 171-185.

Canter, L. W. (1997). Nitrates in groundwater. USA, CRC Press.

Carr, J. R. (1995). Numerical analysis for the geological sciences. Englewood Cliffs, New Jersey, EUA, Penitence-Hall, Inc.

Carroll, R. W. H., G. M. Pohll, S. Earman and R. L. Hershey (2007). "Global optimization of a deuterium calibrated, discrete-state compartment model (DSCM): Application to the eastern Nevada Test Site." Journal of Hydrology **345**(3-4): 237-253.

Carroll, R. W. H., G. M. Pohll, S. Earman and R. L. Hershey (2008). "A comparison of groundwater fluxes computed with MODFLOW and a mixing model using deuterium: Application to the eastern Nevada test site and vicinity " Journal of Hydrology **361**(3-4): 371-385.

Cassiraga, E. F., D. Fernandez-Garcia and J. J. Gomez-Hernandez (2005). "Performance assessment of solute transport upscaling methods in the context of nuclear waste disposal." International Journal of Rock Mechanics and Mining Sciences **42**: 756-764.

Christiansen, J. S., M. Thorsen, T. Clausen, S. Hansen and J. C. Refsgaard (2004). "Modelling of macropore flow and transport processes at catchment scale." Journal of Hydrology **299**: 136-158.

Clauser, C. (1992). "Permeability of Crystalline Rocks." EOS Transaction American Geophysical Union **73**(21): 233-237.

Coats, K. H. and B. D. Smith (1964). "Dead-end pore volume and dispersion in porous media." Society Petroleum Engineers Journal **4**: 73-84.

Collins, A. L. and D. F. McGonigle (2008). "Monitoring and modelling diffuse pollution from agriculture for policy support: UK and European experience." Environmental Science & Policy **11**(2): 97-101.

Cook, P. G., A. J. Love, N. I. Robinson and C. T. Simmons (2005). "Groundwater ages in fractured rock aquifers." Journal of Hydrology **308**: 284-301.

Cook, P. G. and D. K. Solomon (1995). "Transport of atmospheric trace gases to the water table: Implications for groundwater dating with chlorofluorocarbons and krypton 85." Water Resources Research **31**(2): 263-270.

Cook, P. G. and D. K. Solomon (1997). "Recent advances in dating young groundwater : Chlorofluorocarbons, $^{3}H/^{3}He$ and ^{85}Kr." Journal of Hydrology **191**: 245-265.

Dagan, G. (1994). "Upscaling of dispersion coefficients in transport through heterogeneous formations." Computational Methods in Water Resources **12**: 431-439.

Dahan, O., D. McGraw, E. Adar, G. Pohll, B. Bohm and J. Thomas (2004). "Multi-variable mixing cell model as a calibration and validation tool for hydrogeologic groundwater modeling." Journal of Hydrology **293**: 115-136.

de Marsily, G. (1986). Quantitative hydrogeology. San Diego, California, Academic.

de Marsily, G., F. Delay, J. Gonçalvès, P. Renard, V. Teles and S. Violette (2005). "Dealing with spatial heterogeneity." Hydrogeology Journal **13**(1): 161-183.

Desbarats, A. J. (1990). "Macrodispersion in sand-shale sequences." Water Resources Research **26**(1): 153-163.

Desbarats, A. J. (1992a). "Spatial averaging of hydraulic conductivity in three-dimensional heterogeneous porous media." Mathematical Geology **24**(3): 249-267.

Desbarats, A. J. (1992b). "Spatial averaging of transmissivity in heterogeneous fields with flow toward a well." Water Resources Research **28**(3): 757-767.

Desbarats, A. J. (1994). "Spatial averaging of hydraulic conductivity under radial flow conditions." Mathematical Geology **26**(1): 1-21.

Dudley, L. M., J. E. McLean, T. H. Furst and J. J. Jurinak (1991). "Sorption of cadmium and copper from an acid waste extract by two calcareous soils: column studies." Soil Sciences **151**: 121-135.

Duffy, C. J. and L. W. Gelhar (1985). "A frequency domain approach to water quality modelling in groundwater: Theory." Water Resources Research **21**(8): 1175-1184.

Duffy, C. J. and L. W. Gelhar (1986). "A frequency domain analysis of groundwater quality fluctuations: Interpretation of field data." Water Resources Research **22**(7): 1115-1128.

Duffy, C. J. and D.-H. Lee (1992). "Base flow response from non-point source contamination: spatial variability in source, structure, and initial condition." Water Resources Research **28**(3): 905-914.

Durlofsky, L. J. (1991). "Numerical calculation of equivalent grid block permeability tensors for heterogeneous porous media." Water Resources Research **27**(5): 699-708.

Durlofsky, L. J. (1992). "Representation of grid block permeability in coarse scale models of randomly heterogeneous porous media." Water Resources Research **28**(7): 1791-1800.

Eaton, T. T. (2006). "On the importance of geological heterogeneity for flow simulation." Sedimentary Geology **184**: 187-201.

Edmunds, W. M. (1996). Indicators in the groundwater environment of rapid environmental change. Geoindicators - Assessing Rapid Environmental Changes in Earth Systems. A. R. Berger and W. J. Iams. Rotterdam, Balkema**:** 135-150.

Efendiev, Y., A. Datta-Gupta, I. Osako and B. Mallick (2005). "Multiscale data integration using coarse-scale models." Advances in Water Resources **28**: 303-314.

Eldor, M. and G. Dagan (1972). "Solutions of hydrodynamic dispersion in porous media." Water Resources Research **8**(5): 1316-1331.

EPA (2000). Practical Methods for Data Analysis. Washington, DC 20460, US Environmental Protection Agency (USEPA)**:** 219.

Fernandez-Garcia, D., T. H. Illangasekare and H. Rajaram (2005). "Differences in the scale-dependence of dispersivity estimated from temporal and spatial moments in chemically and physically heterogeneous porous media." Advances in Water Resources **28**(7): 745-759.

Firestone, M. K. (1982). Biological denitrification. Nitrogen in Agriculture Soils. F. J. Stevenson. Madison, Wis., American Society of Agronomy**:** 289-326.

Gardner, K. K. and R. M. Vogel (2005). "Predicting ground water nitrate concentration from land use." Ground Water **43**(3): 343-352.

Gelhar, L. W. and C. L. Axness (1983). "Three-dimensional stochastic analysis of macrodispersion in aquifers." Water Resources Research **19**(1): 161-180.

Gelhar, L. W., C. Welty and K. R. Rehfeldt (1992). "A critical review of data on field-scale dispersion in aquifers." Water Resources Research **28**(7): 1955-1974.

Gooddy, D. C., W. G. Darling, C. Abesser and D. J. Lapworth (2006). "Using chlorofluorocarbons (CFCs) and sulphur hexafluoride (SF_6) to characterise groundwater movement and residence time in a lowland Chalk catchment." Journal of Hydrology **330**(1-2): 44-52.

Grath, J., A. Scheidleder, S. Uhlig, K. Weber, M. Kralik, T. Keimel and D. Gruber (2001). The EU Water Framework Directive: Statistical aspects of the identification of ground water pollution trends, and aggregation of monitoring results. Final report. Vienna, Austrian Federal Ministry of Agriculture and Forestry, Environment and Water Management (Ref.: 41.046/01-IV1/00 and GZ 16 2500/2-I/6/00), European Comission (Grant Agreement Ref.: Subv 99/130794), in kind contributions by project partners**.:** 63.

Guimerà, J. and J. Carrera (2000). "A comparison of hydraulic and transport parameters measured in low-permeability fractured media." Journal of Contaminant Hydrology **41**: 261-281.

Hallberg, K. B. and D. R. Keeney (1993). Nitrate. Regional Ground-Water quality. W. M. Alley. New York, Van Nostrand Reinhold**:** 297-322.

Hallet, V. (1998). Étude de la contamination de la nappe aquifère de Hesbaye par les nitrates: hydrogéologie, hydrochimie et modélisation mathématique des écoulements et du transport en milieu saturé (Contamination of the Hesbaye aquifer by nitrates: hydrogeology, hydrochemistry and mathematical modeling). Faculty of Sciences. Liège (Belgium), University of Liège**:** 361.

Harnisch, J. and A. Eisenhauer (1998). "Natural CF_4 and SF_6 on Earth." Geophysical Research Letters **25**: 2401-2404.

Harrington, G. A., G. R. Walker, A. J. Love and N. K. A. (1999). "A compartmental mixing-cell approach for the quantitative assessment of groundwater dynamics in the Otway Basin, South Australia." Journal of Hydrology **214**: 49-63.

Harten, A. (1983). "High resolution schemes for hyperbolic conservation laws." Journal of Computational Physics **49**: 357-393.

Harter, T., H. Davis, M. C. Mathews and R. D. Meyer (2002). "Shallow ground water quality on dairy farms with irrigated forage crops." Journal of Contaminant Hydrology **55**: 287-315.

Hinsby, K., W. M. Edmunds, H. H. Loosli, M. Manzano, M. Melo and F. Barbecot (2001). The modern water interface : recognition, protection and development-advance of modern waters in European aquifer systems. Palaeowaters in coastal Europe : evolution of groundwater since the Late Pleistocene. W. M. Edmunds and C. J. Milne. London, The Geological Society. **189:** 271-288.

Hirsch, R. M., R. B. Alexander and R. A. Smith (1991). "Selection of methods for the detection and estimation of trends in water quality." Water Resources Research **27**(5): 803-813.

Hristopulos, D. T. (2003). "Renormalization group methods in subsurface hydrology: overview and applications in hydraulic conductivity upscaling." Advances in Water Resources **26**: 1279-1308.

Hudak, P. F. (2000). "Regional trends in nitrate content of Texas groundwater." Journal of Hydrology **228**: 37-47.

Jackson, B. M., C. A. Browne, A. P. Butler, D. Peach, A. J. Wade and H. S. Wheater (2008). "Nitrate transport in Chalk catchments: monitoring, modelling and policy implications." Environmental Science & Policy **11**(2): 125-135.

Johnsson, H., M. Larsson, K. Martensson and M. Hoffmann (2002). "SOILNDB: a decision support tool for assessing nitrogen leaching losses from arable land." Environmental Modelling & Software **17**(6): 505-517.

Jury, W. A. (1982b). "Simulation of solute transport using a transfer function model." Water Resources Research **18**(2): 363-368.

Jury, W. A. and K. Roth (1990). Transfer functions and solute movement through soils: Theory and applications. Basel, Birkhaûser Verlag.

Jury, W. A., L. H. Stolzy and P. Shouse (1982a). "A field test of the transfer function model for predicting solute transport." Water Resources Research **18**(2): 369-375.

Käss, W. (1998). Tracing technique in geohydrology, A.A.Balkema P.O.Box 1675, 3000 BR Rotterdam, Netherlands.

Kasteel, R., H.-J. Vogel and K. Roth (2000). "From local hydraulic properties to effective transport in soil." European Journal of Science Science **51**: 81-91.

Katz, B. G., A. R. Chelette and T. R. Pratt (2004). "Use of chemical and isotopic tracers to assess nitrate contamination and groundwater age, Woodville Karst Plain, USA." Journal of Hydrology **289**: 36-61.

Kendall, M. G. (1975). Rank correlation methods. London.

King, P. R. (1989). "The use of renormalisation for calculating effective permeability." Transport in porous media **4**: 37-58.

Koh, D.-C., L. N. Plummer, D. K. Solomon, E. Busenberg, Y.-J. Kim and H.-W. Chang (2006). "Application of environmental tracers to mixing, evolution, and nitrate contamination of ground water in Jeju Island, Korea." Journal of Hydrology **327**: 258-275.

Korom, S. F. (1992). "Natural denitrification in the saturated zone: a review." Water Resources Research **28**(6): 1657-1668.

Ledoux, E., E. Gomez, J.-M. Monget, C. Viavattene, P. Viennot, A. Ducharne, M. Benoit, C. Mignolet, C. Schott and B. Mary (2007). "Agriculture and groundwater nitrate contamination in the Seine basin. The STICS-MODCOU modelling chain." Science of the Total Environment **375**: 33-47.

Lehmann, M. F., P. Reichert, S. M. Bernasconi, A. Barbieri and J. A. McKenziz (2003). "Modelling nitrogen and oxygen isotope fractionation during denitrification in a lacustrine redox-transition zone. ." Geochimica et Cosmochimica Acta **67**(14): 2529-2542.

Loague, K. and R. H. Abrams (1999). "DBCP contaminated groundwater : hot spots and nonpoint sources." Journal of Environmental Quality **28**(2): 429-446.

Loague, K., R. H. Abrams, S. N. Davis, A. Nguyen and I. T. Stewart (1998). "A case study simulation of DBCP groundwater contamination in Fresno County, California 2.Transport in the saturated subsurface." Journal of Hydrology **29**: 137-163.

Loftis, J. C., C. H. Taylor and P. L. Chapman (1991). "Multivariate tests for trend in water quality." Water Resources Research **27**(7): 1419-1429.

Loosli, H. H., B. E. Lehmann and G. Däppen (1991). Dating by radionuclides. Applied isotope hydrology. A case study in Northern Switzerland. F. J. Pearson Jr. Amsterdam, Elsevier. **43**.

Loosli, H. H., B. E. Lehmann and W. M. Smethie (2000). Noble gas radiosotopes (^{37}Ar, ^{85} Kr, ^{39}Ar, ^{81}Kr). Environmental tracers in subsurface hydrology. P. G. Cook and A. Herczeg. Dordrecht, Kluwer**:** 379-396.

Maloszewski, P. (1994). "Mathematical modelling of tracer experiments in fissured aquifers." Freiburger Schriften zur Hydrologie **2**: 1-107.

Maloszewski, P. and K.-P. Seiler (1999). Modeling of flow dynamics in layered groundwater system - Comparative evaluation of black box and numerical approaches. IAEA.

Maloszewski, P., W. Stichler and A. Zuber (2004). "Interpretation of environmental tracers in groundwater systems with stagnant water zones." Isotopes in Environmental and Health Studies **4**(1): 21-33.

Maloszewski, P. and A. Zuber (1982). "Determining the turnover time of groundwater systems with the aid of environmental tracers. 1. Models and their applicability." Journal of Hydrology **57**: 207-231.

Maloszewski, P. and A. Zuber (1996). Lumped parameter models for the interpretation of environmental tracer data. in : Manual on mathematical models in isotope hydrology. Vienna, IAEA**:** 9-58.

Mann, H. B. (1945). "Nonparametric tests against trend." Econometrica **13**: 245-259.

Mariotti, A. (1994). "Dénitrification in situ dans les eaux souterraines, processus naturels ou provoqués : une revue." Hydrogéologie **3**: 43-68.

McMahon, P. B., J. K. Böhlke and B. W. Bruce (1999). "Denitirification in marine shales in northeastern Colorado." Water Resources Research **35**: 1629-1642.

Mengis, M., S. L. Schiff, M. Harris, M. C. English, R. Aravena, R. J. Elgood and A. MacLean (1999). "Multiple geochemical and isotopic approaches for assessing ground water NO_3^- elimination in a riparian zone." Ground Water **37**(3): 448-457.

Mitchell, R. J., R. Scott Babcock, S. Gelinas, L. Nanus and D. E. Stasney (2003). "Nitrate distributions and source identification in the Abbotsford-Sumas aquifer, Northwester Washington state." Journal of Environmental Quality **32**: 789-800.

Mohamed, M. A. A., H. Terao, R. Suzuki, I. S. Babiker, K. Ohta, K. Kaori and K. Kato (2003). "Natural denitrification in the Kakamigahara ground water basin, Gifu prefecture, central Japan." The Science of the Total Environment **307**: 191-201.

Nastev, M., M. M. Savard, P. Lapcevic, R. Lefebvre and R. Martel (2004). "Hydraulic properties and scale effects investigation in regional rock aquifers, south-western Quebec, Canada." Hydrogeology Journal **12**(3): 257-269.

Neuman, S. P. (1984). "Adaptative Eulerian-Lagrangian finite element method for advection-dispersion." International Journal of Numerical Methods in Engineering **20**: 321-337.

Neuman, S. P. (1994). "Generalized scaling of permeabilities: validation and effect of support scale." Geophysical Research Letters **21**: 349-352.

Olive, P., P. Hubert and S. Ravailleau (1996). "Estimation pratique de "l'âge" des eaux souterraines en Europe par le tritium." Revue des sciences de l'eau **4**: 523-533.

Oren, O., Y. Yechieli, J. K. Böhlke and A. Dody (2004). "Contamination of groundwater under cultivated fields in a arid environment, central Arava Valley, Israel." Journal of Hydrology **290**: 312-328.

Oster, H., C. Sonntag and K. O. Münnich (1996). "Groundwater age dating with chlorofluorocarbons." Water Resources Research **32**(10): 2989-3001.

Ozyurt, N. N. and C. S. Bayari (2003). "LUMPED: a Visual Basic code of lumped-parameter models for mean residence time analyses of groundwater systems." Computers & Geosciences **29**: 79-90.

Plummer, L. N. and E. Busenberg (2000). Chlorofluorocarbons. Environmental tracers in subsurface hydrogeology. P. G. Cook and A. Herczeg. Dordrecht, Kluwer**:** 441-478.

Plummer, L. N., R. L. Michel, E. M. Thurman and P. D. Glynn (1993). Environmental tracers for age dating young ground water. Regional Ground-Water Quality. W. M. Alley. New York, Van Nostrand Reinhold**:** 255-296.

Postma, D., C. Boesen, H. Kristiansen and F. Larsen (1991). "Nitrate reduction in an unconfined sandy aquifer: water chemistry, reduction processes and geochemical modeling." Water Resources Research **27**(8): 2027-2045.

Price, M., R. A. Downing and W. M. Edmunds (1993). The chalk as an aquifer. The Hydrogeology of the Chalk of the North-West Europe. R. A. Downing, M. Price and G. P. Jones. Oxford, U.K., Oxford University Press**:** 35-58.

Rao, P. S. C. and W. M. Alley (1993). Pesticides. Regional Ground-Water Quality. W. M. Alley. New-York, Van Nostrand Reinhold**:** 345-382.

Refsgaard, J. C., M. Thorsen, J. B. Jensen, S. Kleeschulte and S. Hansen (1999). "Large scale modelling of groundwater contamination from nitrate leaching." Journal of Hydrology **221**: 117 - 140.

Renard, P. (1996). Modélisation des écoulements en milieux poreux hétérogènes. Calcul des perméabilités équivalentes. Paris, Ecole des Mines de Paris**:** 246.

Renard, P. and G. de Marsily (1997). "Calculating equivalent permeability : a review." Advances in Water Resources **20**(5-6): 253-278.

Renard, P., G. Le Loc'h, E. Ledoux, G. de Marsily and R. Mackay (2000). "A fast algorithm for the estimation of the equivalent hydraulic conductivity of heterogeneous media." Water Resources Research **36**(12): 3567-3580.

Ritter, A., R. Munoz-Carpena, D. D. Bosch, B. Schaffer and T. L. Potter (2007). "Agricultural land use and hydrology affect variability of shallow groundwater nitrate concentration in South Florida." Hydrological Processes **21**(18): 2464-2473.

Ritzi, R. W., S. Sorooshian and V. K. Gupta (1991). "On the estimation of parameters for frequency domain models." Water Resources Research **27**(5): 873-882.

Rivett, M. O., J. W. N. Smith, S. R. Buss and P. Morgan (2007). "Nitrate occurence and attenuation in the major aquifers of England and Wales." Quarterly Journal of Engineering Geology and Hydrogeology **40**(4): 335-352.

Robertson, W. D., J. A. Cherry and S. L. Schiff (1989). "Atmospheric sulfur deposition 1950-1985 inferred from sulfate in groundwater." Water Resources Research **25**: 1111-1123.

Roth, K. and W. A. Jury (1993). "Linear transport models for adsorbing solutes." Water Resources Research **29**(4): 1195-1203.

Sánchez-Vila, X., J. Carrera and J. P. Girardi (1996). "Scale effects in transmissivity." Journal of Hydrology **183**: 1-22.

Sánchez-Vila, X., J. P. Girardi and J. Carrera (1995). "A synthesis of approaches to upscaling of hydraulic conductivities." Water Resources Research **31**(4): 867-882.

Sandor, J., I. Kiss, O. Farkas and I. Ember (2001). "Association between gastric cancer mortality and nitrate content of drinking water: ecological study on small area inequalities." European Journal of Epidemiology **17**(5): 443-447.

Scheibe, T. and S. Yabusaki (1998). "Scaling of flow and transport behavior in heterogeneous groundwater systems." Advances in Water Resources **22**(3): 223-238.

Schlosser, P., M. Stute, H. Dörr, C. Sonntag and K. O. Münnich (1988). "Tritium/^{3}He dating of shallow groundwater." Earth and Planetary Science Letters **89**: 353-362.

Schwientek, M., F. Einsiedl, W. Stichler, A. Stögbauer, H. Strauss and P. Maloszewski (2008). "Evidence for denitrification regulated by pyrite oxidation in a heterogeneous porous groundwater system." Chemical Geology **255**(1-2): 60-67.

Skaggs, T. H., Z. J. Kabala and W. A. Jury (1998). "Deconvolution of a nonparametric transfer function for solute transport in soils." Journal of Hydrology **207**: 170-178.

Stewart, I. T. and K. Loague (1999). "A type transfer function approach for regional-scale pesticide leaching assessments." Journal of Environmental Quality **28**(2): 378-387.

Szabo, Z., D. E. Rice, L. N. Plummer, E. Busenberg, S. Drenkard and P. Schlosser (1996). "Age dating of shallow groundwater with chlorofluorocarbons, tritium/helium 3, and flow path analysis, southern New Jersey coastal plain." Water Resources Research **32**(4): 1023-1038.

Thorburn, P. J., J. S. Biggs, K. L. Weier and B. A. Keating (2003). "Nitrate in ground waters of intensive agricultural areas in coastal Northeastern Australia." Agriculture, Ecosystems and Environment **94**: 49-58.

Unterweger, M. P., B. M. Courset, F. J. Schima and W. B. Mann (1980). "Preparation and calibration of the 1978 National Bureau of Standarts tritiated water standarts." Journal of Applied Radiation and Isotopes **31**: 611-614.

Van Herpe, Y., P. A. Troch, L. Callewier and P. F. Quinn (1998). "Application of a conceptual model catchment scale nitrate transport model on two rural rivers catchments." Environmental Pollution **102**(S1): 569-577.

Van Ommen, H. C. (1985). "The "Mixing-cell" concept applied to transport of non-reactive and reactive components in soils and groundwater." Journal of Hydrology **78**: 201-213.

Vogel, J. C., A. S. Talma and T. H. E. Heaton (1981). "Gaseous nitrogen as evidence for denitrification in groundwater " Journal of Hydrology **50**: 191-200.

WHO (2004). Guidelines for drinking water quality 3rd. Geneva, World Health Organization.

Yeh, G. T. (1990). "A Lagrangian-Eulerian method with zoomable hidden fine-mesh approach to solve advection-dispersion equations." Water Resources Research **26**(6): 1133-1144.

Zheng, C. (1990). MT3D: A Modular, Three-Dimensional Transport Model for Simulation of Advection, Dispersion and Chemical Reactions of Contaminants in Groundwater Systems. Ada, Oklahoma (USA), U.S. Environmental Protection Agency**:** 169.

Zheng, C. and P. P. Wang (1999). MT3DMS: a modular three-dimensional multispecies transport model for simulation of advection, dispersion, and chemical reactions of contaminants in groundwater systems; documentation and user's guide. Tuscaloosa, USA, University of Alabama**:** 169.

3 THE HYBRID FINITE ELEMENT MIXING CELL APPROACH

3.1 The need for regional scale groundwater model

Today, sustainable management of water resources is widely understood as an integrative, cross border task, in particular in Global Change research (Barthel *et al.* 2008). Groundwater is an important link of the water cycle and evaluating and predicting the availability of groundwater quantity and quality under changing scenarios is a central task in integrated water resources management (Sophocleous 2002; Quinn 2004). Models are essential tools in the comprehension and the representation of the state of groundwater.

Regional scale groundwater models can be developed for examples:

- to assess and predict the impact of climate change or increasing exploitation on groundwater and the evolution of groundwater fluxes feeding the surface river network;
- to estimate the long term evolution of groundwater quality for different scenarios of land-use and agricultural practices.

3.2 Specificities of regional scale groundwater modelling

When modelling at the regional scale (at the groundwater body scale or at the scale of hydrological or hydrogeological basin), the zone to be modelled is often characterised by a wide variety of geological and hydrogeological contexts. It is, for example, the case in the Walloon region in which granular aquifers (Bruxellian sands, alluvial deposits) coexist with karstified basins (Devonian limestone) or fractured and fissured aquifers (limestones, sandstones…) (Figure 3.1). The level of knowledge on the hydrogeology (often called hydrogeological characterisation) can differ widely from one part to another in the modelled zone. For example, in the Walloon region, chalk deposits and their hydrogeologic characteristics have been well studied and described (Dassargues and Monjoie 1993; Hallet 1998; Brouyère 2001). On the contrary, the shally-sandstones have not been or at least less studied as they have less hydrogeological potential (Figure 3.2). Moreover, even in high density data regions, these data can not be in adequacy to the scale of work (see Chapter 2, data scale dependence).

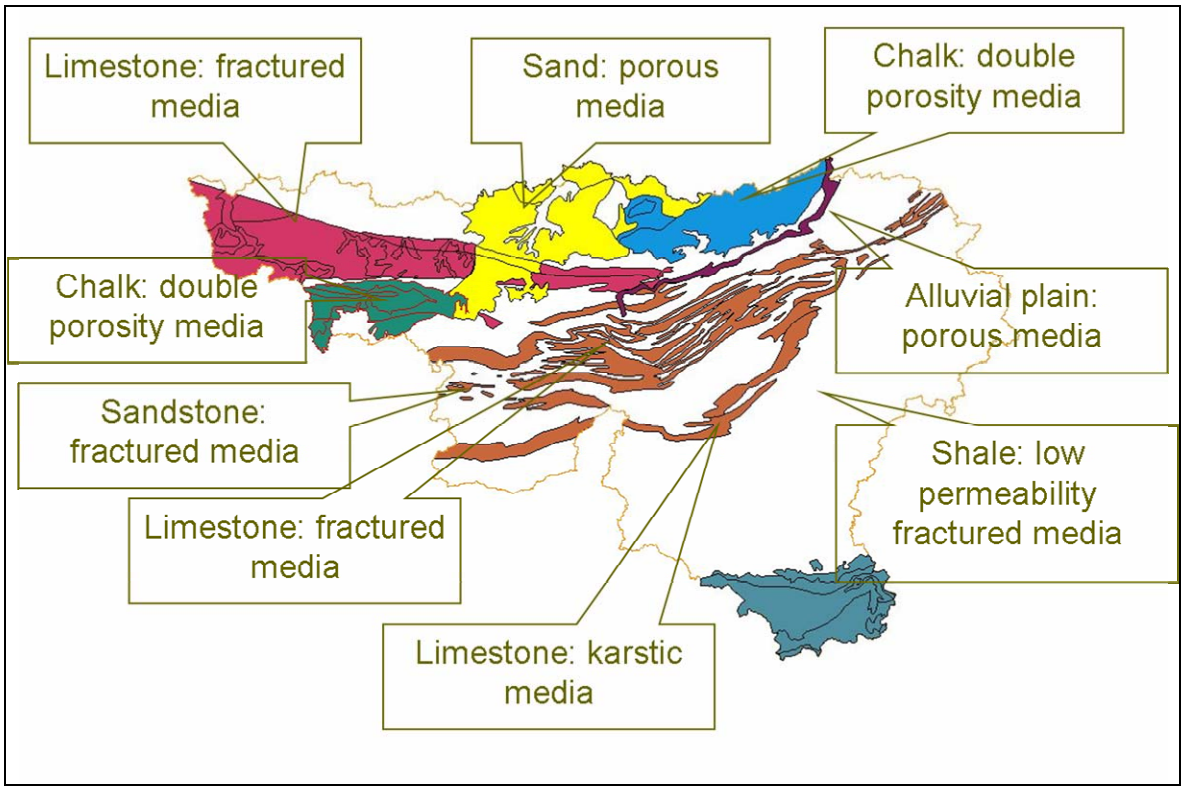

Figure 3.1. Diversity in geological and hydrogeological contexts in the Walloon region.

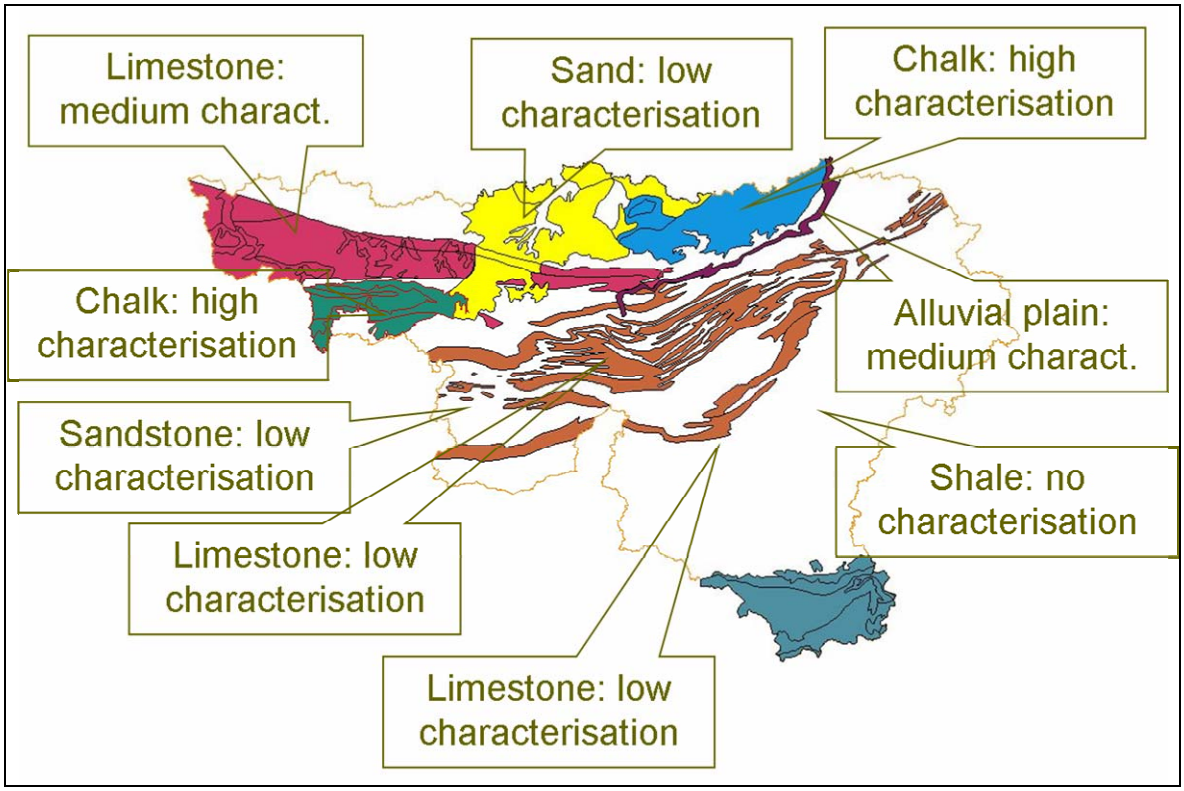

Figure 3.2. Diversity in the degree of hydrogeological characterisation in the Walloon region (situation in 2001).

It is thus difficult to define and use a unique conceptual, mathematical and numerical approach for all these different contexts.

3.3 General methodology

A general methodology has been developed for regional scale groundwater modelling application by the Hydrogeology Group of the University of Liège. This methodology includes: (1) data management and processing using databases and Geographic Information Systems (GIS); (2) original development, the Hybrid Finite Element Mixing Cell approach (HFEMC) implemented within the code SUFT3D; (3) the development and use of specific interfaces.

The originality of this methodology consists in the HFEMC approach that allows adaptating to the variability of available data and to the hydrogeological conditions using different mathematical approaches within one model. Mathematical formalisms of variable complexity have been selected and implemented in the SUFT3D code to model groundwater flow and solute transport. Additionally, the approach allows moving from a simplified approach to a more complex one when new information is collected.

3.3.1 Data management and processing

Large amount of data are required for large-scale groundwater flow and transport modelling when adopting a spatially-distributed and physically-consistent approach. Geological data such as maps, borehole data and logs, data from geophysical survey have to be used in an optimal way to create the spatial discretization. Parameters such as values of hydraulic conductivity, specific yield and porosity of the different distinguished hydrogeological units are needed to constrain the calibration of the model. Historical values of piezometric levels and concentrations are needed for calibration and validation procedures. These data have been collected and introduced in a hydrogeological data base (HYGES) coupled with a GIS system (ArcGIS®) (Gogu *et al.* 2001; Wojda *et al.* 2005). Based on queries and GIS pre-processing, data are transferred into the pre- and post-processor package Groundwater Modelling System (GMS®) (Figure 3.3). A conceptual model is developed that consists in different layers of information built independently of any numerical and discretization choices. This information is transferred in a further step to the mesh used for the computation. This procedure allows new data being easily introduced and processed. After computation, visualization of results

can be performed using GMS, ArcGIS, or any other visualization tools for calibration and output production.

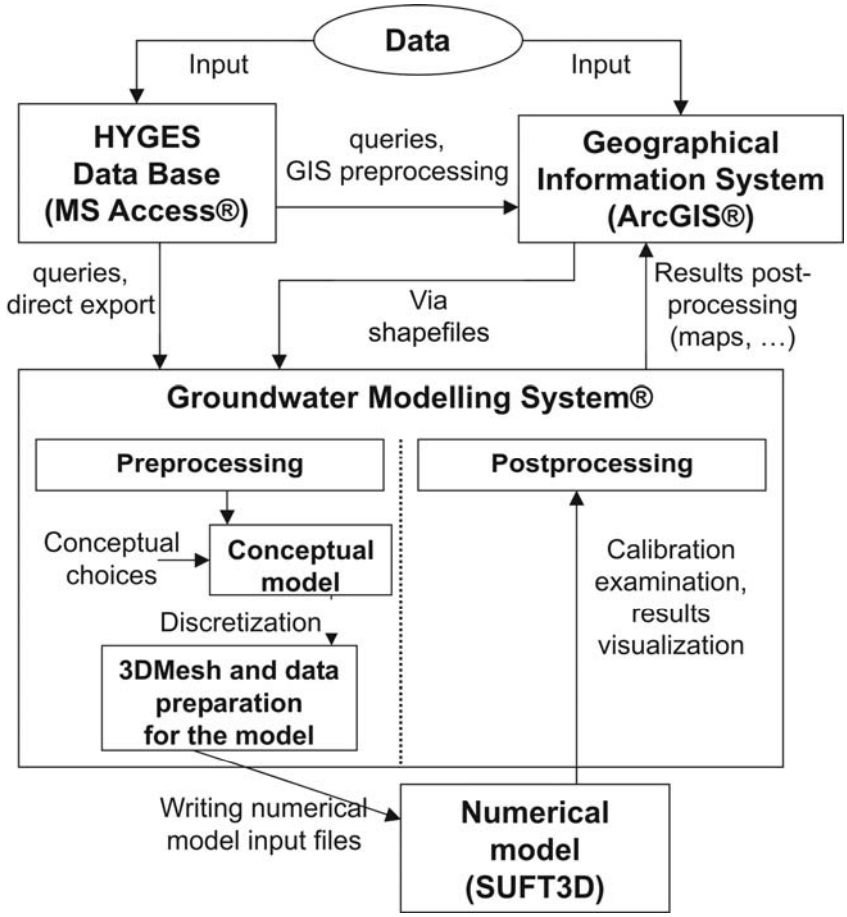

Figure 3.3. Scheme of the data management procedure developed for regional scale groundwater modelling (Orban *et al.* 2005).

3.3.2 The Hybrid Finite Element Mixing Cell approach

3.3.2.1 Concepts

The originality of the Hybrid Finite Element Mixing Cell (HFEMC) approach consists in combining, in a single, fully integrated simulator, different mathematical approaches of different complexity to model groundwater flow and solute transport. These mathematical approaches can be used either simultaneously in different portions of the modelled area (called subdomains) or for different successive simulations keeping the same spatial representation of the geometry of the studied area.

The approach is based on the finite element formalism: the modelled area is discretized with a finite element mesh. This mesh can then be subdivided in different subdomains representing different hydrogeologically separate areas, either because they cover different hydrogeological basins, either by their aquifer characteristics (karstic media, porous media …) or even by their current degree of hydrogeological characterisation. In each subdomain, the mathematical approach used to describe the groundwater flow and solute transport phenomena will be chosen according to the hydrodynamic characteristics of the media, the present investigation degree and the data availability.

At the interfaces between subdomains, internal boundary conditions are defined to allow considering and modelling the exchanged water fluxes. Three types of internal boundary conditions can be used:

- Dirichlet or 1st type dynamic boundary condition where the coupling between subdomains implies the equality of the piezometric heads along the internal boundary but these values can vary in time and remains an unknown of the problem.

$$h_{SD,i}(x,y,z,t) = h_{SD,j}(x,y,z,t) \quad \textbf{(3.1)}$$

  where $h_{SD,i}$ is the hydraulic head in subdomain *i* [L], $h_{SD,j}$ is the hydraulic head in subdomain *j* [L]

  This kind of internal boundary conditions keeps the continuity in the calculated piezometry but it allows calculating water budget across the corresponding limit (exchanged flux between the two connected subdomains).

- Neumann or 2nd type boundary condition where the first derivative of the piezometric head is set to 0 on a portion of the internal boundary if there is no exchange of water between the subdomains.

$$\frac{\partial h(x,y,z,t)}{\partial n} = 0 \quad \textbf{(3.2)}$$

- Fourier or 3rd type dynamic boundary condition where the piezometric level can not be considered as continuous. The exchanged flux along such an internal boundary depends on (1) the difference of piezometric heads on each side of the boundary (once

more, these values can vary and remains unknowns of the problem) and (2) a conductance coefficient between the two subdomains.

$$Q_{SD,i-SD,j} = \alpha_{SD,i-SD,j} \; A \left[h_{SD,j}(x,y,z,t) - h_{SD,i}(x,y,z,t) \right] \quad \textbf{(3.3)}$$

where $Q_{SD,i-SD,j}$ is the exchanged flow between subdomains *i* and *j* through the third type *internal* boundary condition [L^3T^{-1}], $\alpha_{SD,i-SD,j}$ is a first order exchange coefficient [T^{-1}], A is the exchange area [L^2].

Trough the use of low values of $\alpha_{SD,i-SD,j}$, this kind of internal boundary conditions can also be used to model implicitly thin low permeable layers avoiding introducing very thin element in the 3D mesh.

Two examples of subdivision into subdomains are proposed to illustrate the concept of subdomains and internal boundary conditions. In the first one, a subdivision of the groundwater body RWM021 (limestones and sandstones of the Condroz), modelled in the framework of the Synclin'Eau project (DGRNE-SPGE - Aquapôle), into subdomains is proposed (Figure 3.4). The division into subdomains is based on:

- the different hydrogeological units. For example, Carboniferous limestones were distinguished from Famennian sandstones. Between these formations, thin shale layers induce a jump in the piezometry. The use of internal Fourier boundary conditions allows representing this discontinuity.
- the aquifer characteristics. The Givetian limestones that are karstified are distinguished using separate subdomains.
- the limits of the hydrological basins. The Carboniferous limestones are divided into subdomains on the basis of these hydrological limits. Internal Dirichlet boundary conditions are defined between these subdomains to keep the continuity in the calculated piezometry. This choice allows computing the exchange of groundwaters between the hydrological basins.

In the second example, a subdivision of the aquifer of the Geer basin is proposed. The aquifer consists mainly in chalk that is divided in two formations separated by a thin layer of low permeability hardened-chalk. Such a system can be modelled by two subdomains interacting trough an internal Fourier boundary condition.

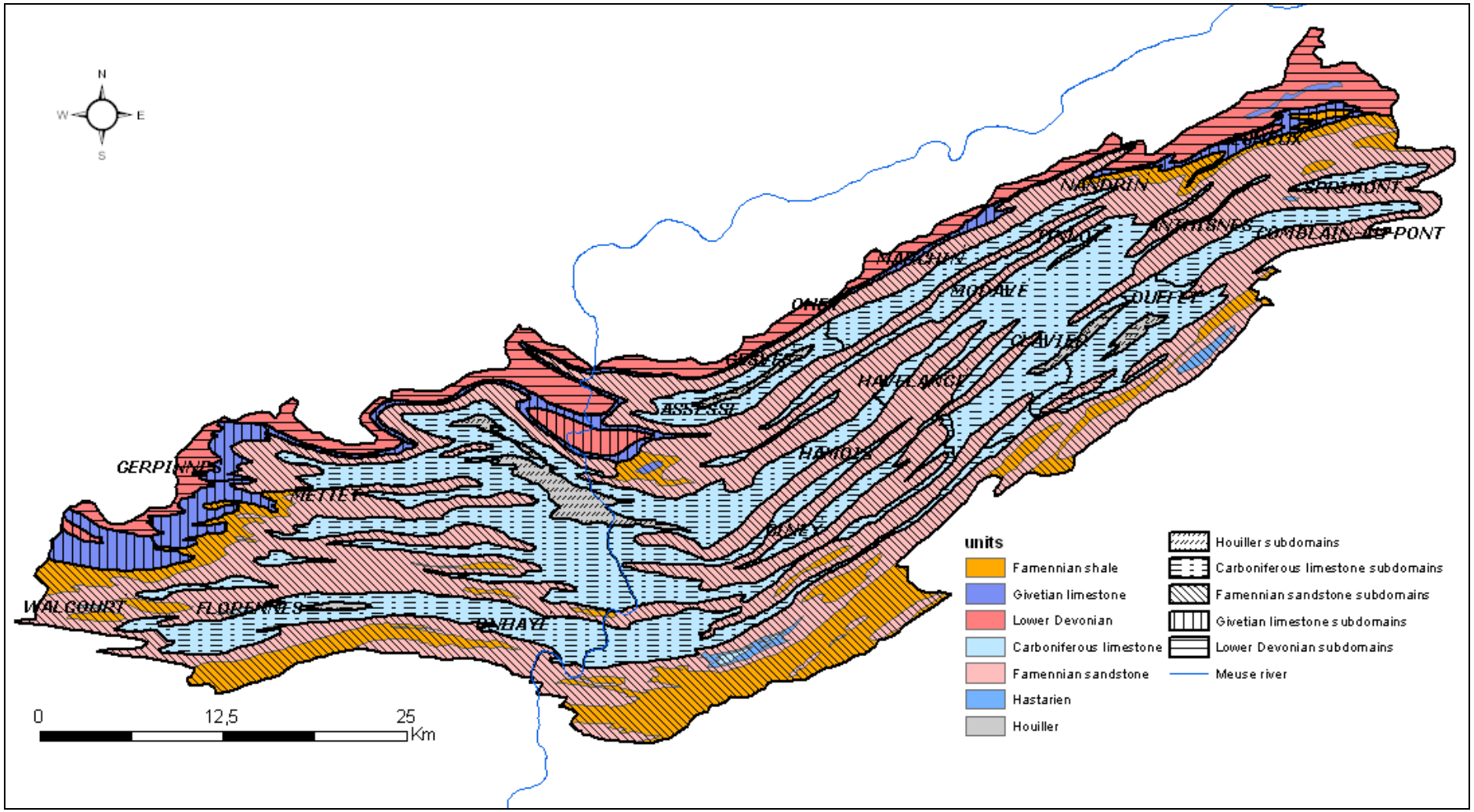

Figure 3.4. Division of the groundwater body RWM021 into subdomains (Synclin'Eau project).

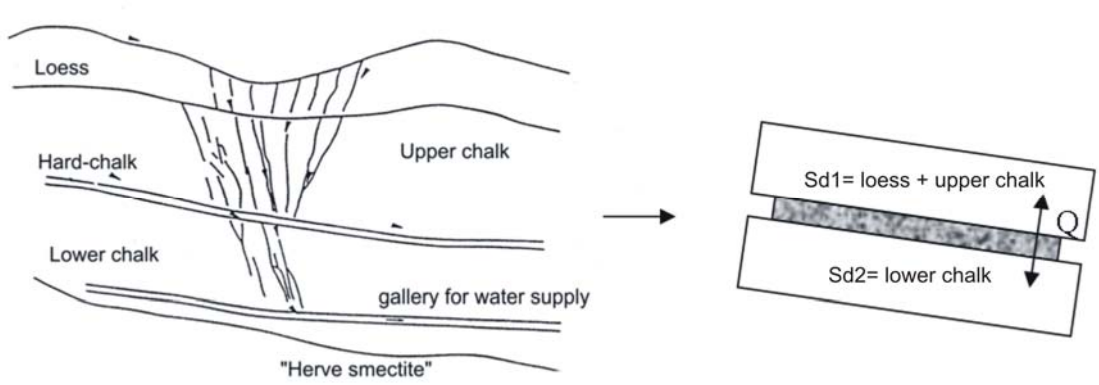

Figure 3.5. Schematic cross-section in the Geer basin and division in subdomains (modified from Orban *et al.* 2005).

3.3.2.2 Adapted version of the SUFT3D code: Hybrid Finite Element Mixing Cell (HFEMC) method

The SUFT3D (Saturated Unsaturated Flow Transport 3D) is a control volume finite element (CVFE) code developed by the Hydrogeology Group at the University of Liège (Carabin and Dassargues 1999; Brouyère 2001; Brouyère *et al.* 2004). It can treat full 3D cases under steady state or transient conditions. In its original version, the code solves the classical flow (based on the Richard's law and a mass budget) and advection-dispersion equations using a classical finite element method or a control volume finite element method. Besides advection and dispersion, the transport processes that can be simulated are linear degradation, adsorption/desorption and dual-porosity concepts.

For the HFEMC method, other physically-based mathematical approaches have been selected among the solutions presented in Chapter 2 and implemented in the SUFT3D simulator to compute groundwater flow and solute transport processes. Three mathematical and numerical formulations can be considered for solving the groundwater flow problem and three formulations for the solute transport problem in each subdomains (Table 3.1).

As mentioned in Chapter 2, linear reservoir models imply that the characteristics at the outlet of the aquifer are linearly linked to the mean behaviour of the reservoir which is made of a single entity. In continuity between the linear reservoir model and the classical flow model, distributed linear reservoir models have also been implemented in the SUFT3D. This continuity allows, if further data are acquired, to move from a simplified approach to a more complex one.

		TRANSPORT		
		Simple Linear Reservoir	***Distributed Mixing Model***	***Advection-dispersion***
FLOW	***Simple Linear Reservoir***	OK	impossible	impossible
	Distributed Linear Reservoirs	OK	OK	impossible
	Flow in porous media	OK	OK	OK

Table 3.1. Solutions implemented in the SUFT3D code and restrictions of use.

The choice of a simplified solution for simulating groundwater flow conditions implies to choose also a simplified method for solving the transport problem (Table 3.1). As an example, if a linear reservoir is used to model groundwater flow in a karstic medium, it is not possible to compute the solute transport in this medium using a spatially-distributed model such as the advection-dispersion equation as the spatial distribution of the groundwater fluxes in the system remain unknown. On the other hand, if available data allow a spatially-distributed computation for groundwater flows but not for solute transport, it is possible to use "the flow in porous media" equation to solve the groundwater flow problem coupled with a simple mixing reservoir to model the transport problem.

3.3.2.2.1 Implementation of the simple linear reservoir model in the SUFT3D

The equation of a simple linear reservoir implemented in the SUFT3D is:

$$Q_{LR} = S_{LR}\ A_{LR}\ \frac{\partial \overline{H}_{LR}}{\partial t} = -\alpha_{LR}\ (\overline{H}_{LR} - H_{ref}) + Q \qquad \textbf{(3.4)}$$

where S_{LR} is the storage of the linear reservoir [-], A_{LR} is the surface area of the linear reservoir [L^2], $\overline{H}_{LR}$ is the mean water level in the linear reservoir [L], α_{LR} is the exchange coefficient of the linear reservoir [L^2T^{-1}], H_{ref} is the drainage level of the linear reservoir [L], Q is source/sink term [L^3T^{-1}].

In order to apply the simple linear reservoir in a given subdomain, all the elements of the subdomain are grouped together, a single unknown (i.e. mean groundwater level) being considered for the whole subdomain. The finite element discretisation is then only used to define the external boundary of the subdomain and its interactions with the other subdomains or with the other compartments of the water cycle (such as infiltration or exchange with surface water bodies). The global volume of the reservoir is computed as the sum of the effective volumes associated to each element. Subsequently, the discretisation within the subdomains could be used to apply a more detailed mathematical approach, when new data would allow a spatially-distributed description of the groundwater flow.

3.3.2.2.2 Implementation of the distributed linear reservoirs model in the SUFT3D

The equation corresponding to the distributed linear reservoir implemented in the SUFT3D is:

$$Q_{LR,i} = S_{LR,i}\ A_{LR,i}\ \frac{\partial H_i}{\partial t} = \sum_{j=1}^{n} \alpha_{ij}\ (H_j - H_i) + Q_i \qquad \textbf{(3.5)}$$

where $S_{LR,i}$ is the storage of the linear reservoir i [-], $A_{LR,i}$ is the surface area of the linear reservoir i [L^2], H_i is the water level in the linear reservoir i [L], H_j is the water level in the linear reservoirs j hydraulically connected with cell j [L], α_{ij} is the exchange coefficient between the linear reservoirs i and j [L^2T^{-1}], Q_i is source/sink term in the linear reservoir i [L^3T^{-1}].

Classical spatial discretisations used in distributed linear reservoir models are based on simple geometric forms like parallelepiped elements. Such kinds of mesh simplify the discretisation work and the computation of the fluxes exchanged between cells; however it is not possible to represent complex geometries such as met in hydrogeology. The HFEMC method is adapted to complex spatial discretisation (non structured finite element mesh), using the finite element formulation with control volume. In addition to the flexibility of the mesh, this method allows defining very simply the reservoirs associated to each point of computation and the fluxes exchanged between these reservoirs.

3.3.2.2.3 Flow in porous media equation implemented in the SUFT3D

In a porous medium, the classical groundwater flow equation can be written:

$$F\frac{\partial h}{\partial t} = \underline{\nabla}.(\underline{\underline{K}}\,\underline{\nabla}(h+z)) + q \qquad \textbf{(3.6)}$$

where F is the generalised specific storage coefficient [L^{-1}], $\underline{\underline{K}}$ is the hydraulic conductivity tensor [LT^{-1}], h is the pressure potential [L], z is the gravity potential [L] , q is the source/sink term by unit volume [T^{-1}].

In the SUFT3D code, this equation is solved by the control volume finite element (CVFE) method (Brouyère 2001). With this formulation, the discretised form of Equation (3.6) can be written:

$$V_I\frac{\partial \theta_I}{\partial t} - \sum_{J\in\eta_I}(H_J - H_I)\int_V \underline{\nabla}N_I.\underline{\underline{K}}.\underline{\nabla}N_J\,dV - Q_I = 0 \qquad \textbf{(3.7)}$$

where V_I is called the control volume associated to node I; θ_I is the porosity associated to V_I; η_I is the set of nodes J connected to node I ($J \neq I$); H_J and H_I are the total head computed at the nodes J and I respectively; N_I and N_J are the spatial interpolation functions of the nodes I and J respectively; Q_I is source/sink term.

Different laws linking the water content, the pressure and the relative hydraulic conductivity are implemented in the SUFT3D code to model the flow in the unsaturated zones. More details can be found in Brouyère (2001).

3.3.2.2.4 Implementation of the simple mixing reservoir model in the SUFT3D

Solutes migrating in the subsoil are subject to hydrodynamical dispersion and diffusion leading to a progressive mixing with groundwater. The physical parameters quantifying these processes are difficult to obtain at the regional scale and a simplified description of the phenomena is required. The assumption of perfect mixing consists in assuming that water entering is instantly and perfectly mixed with the water in a cell. The solute concentration within this volume is thus assumed uniform. The assumption of linearity is reflected

mathematically by the fact that the concentration in the flow rate coming out of the reservoir is set equal to the mean concentration in the reservoir.

The equation of simple mixing reservoir implemented in the SUFT3D is:

$$\frac{\partial(V_{eff,res}\ \overline{C})}{\partial t} = Q_{in}\ C' - Q_{out}\ \overline{C} \qquad \textbf{(3.8)}$$

where $V_{eff,res}$ is the effective mixing volume of the reservoir [L^3]; $\overline{C}$ is the mean concentration in the reservoir [ML^{-3}]; Q_{in} and Q_{out} [L^3T^{-1}] are flow rates coming in and out the reservoir at concentrations C' and $\overline{C}$ [ML^{-3}] respectively.

As in the case of the linear reservoir model for flow, all the elements of the subdomain are grouped together, a single unknown (i.e.: mean concentration) being applied for the whole subdomain.

3.3.2.2.5 Implementation of the distributed mixing reservoirs model in the SUFT3D

To apply the simple mixing model, the volume of the mixing cell and the fluxes exchanged with its neighbourhood has to be defined. If the mixing cell exchanges with other mixing cells, we have a compartment mixing cell or a distributed mixing model.

In a general way, the distributed mixing cell model can be written:

$$\frac{\partial(V_{eff,i}\ C_i)}{\partial t} = \sum_{j=1}^{n} Q_{ij}\ C_{ij} + Q_i\ C' \qquad \textbf{(3.9)}$$

where $V_{eff,i}$ is the effective mixing volume of the reservoir i [L^3]; C_i is the concentration in the reservoir i [ML^{-3}]; Q_{ij} [L^3T^{-1}] are flow rates exchange between the cell i and the cell j hydraulically connected to i; C_{ij} [ML^{-3}] are the concentrations associated to the exchanged flow rate Q_{ij}.

The original aspect of the approach relies on the way to evaluate the different terms of Equation (3.9). The evaluation of these terms is function of the formulation used to solve the groundwater flow problem.

If the distributed linear reservoirs model is used, the flux Q_{ij} exchanged between the nodes *i* and *j* is computed by:

$$Q_{ij} = -\alpha_{ij} \, (H_j - H_i) \tag{3.10}$$

If the CVFE method is used for the groundwater flow problem, Q_{ij} is expressed by:

$$Q_{ij} = -\left(H_j - H_i\right) \int_V \underline{\nabla} N_i \cdot \underline{\underline{K}} \cdot \underline{\nabla} N_j \, dV \tag{3.11}$$

The term C_{ij} is evaluated as follow. If groundwater flows from node *i* to node *j* ($\left(H_j - H_i\right) < 0$), groundwater leaves the mixing volume centred on the node i with a concentration C_i. If groundwater flows from node *j* to node *i* ($\left(H_j - H_i\right) > 0$), C_{ij} is equal to C_j. The concentration C_{ij} in the exchanged flux is always equal to the concentration in the mixing cell located upstream of each couple *i,j*, i.e. $C_{ij} = C_{upstream}$(i,j).

The discretised form of the mixing cell equation can thus be written:

- If the distributed linear reservoirs model is used for the groundwater flow:

$$V_{res,i} \frac{\partial(\theta_i \, C_i)}{\partial t} - \sum_{j \in \eta_I} \alpha_{ij} \left(H_j - H_i\right) C_{upstream}(i,j) - Q_i \, C' = 0 \tag{3.12}$$

- If the CVFE method is used for the groundwater flow:

$$V_{res,i} \frac{\partial(\theta_i \, C_i)}{\partial t} - \sum_{j \in \eta_I} \left(H_j - H_i\right) C_{upstream}(i,j) \int_{Vi} \underline{\nabla} N_i \cdot \underline{\underline{K}} \cdot \underline{\nabla} N_j \, dV - Q_i \, C' = 0 \tag{3.13}$$

where $V_{res,i}$ is the volume of the reservoir i [L^3]; θ_i is the porosity of the reservoir i [-].

3.3.2.2.6 Advection-dispersion equation implemented in the SUFT3D

The advection-dispersion equation can be written:

$$\frac{\partial(\theta_m \, C)}{\partial t} = -\underline{\nabla}.(\underline{v}_D \, C) + \underline{\nabla}.(\theta_m \, \underline{\underline{D_h}} \, \underline{\nabla} C) + q \, (C' - C) \tag{3.14}$$

where θ_m is the effective porosity [-]; v_D is the Darcy flux [LT^{-1}]; $\underline{\underline{D_h}}$ is the hydrodynamic dispersion [L^2T^{-1}]; C' is the concentration [ML^{-3}] associated to the source/sink term q [T^{-1}].

This equation is solved by the finite element method (Galerkin or SUPG methods) (Brouyère 2001).

Some particular hydrodispersive processes such as immobile water effect, linear degradation or equilibrium sorption laws traditionally used with the advection-dispersion equation remain applicable with the distributed mixing model.

3.3.3 Development of interfaces

In its first versions, the interface with the SUFT3D code was limited to a few operations of pre-processing (mesh development) and post-processing (visualization of the simulation results) with the help of the software "Groundwater Modeling System (GMS)" developed by the Brigham Young University and the Aquaveo Company. To carry out a groundwater flow and solute transport simulation with the SUFT3D, input files had to be written manually using text editors. When modelling at the regional scale, it becomes complicated and time consuming to create these input files manually. Specific tools have thus been designed to automate operations such as the cutting of the mesh into subdomains, the definition of the boundary conditions linked to the interactions between the surface and groundwater or to create the input files. Important efforts during this PhD thesis have been thus devoted to the development and to the tests of three interfaces of the SUFT3D code. The two first tools are related to the cutting of the mesh and the spatial definition of the river boundary conditions. The third interface is a more general tool to prepare the input files for the SUFT3D. All these interfaces were developed using the MatLab software.

3.3.3.1 Cutting the mesh into subdomains

As mentioned previously, the basic principle of the HFEMC method consist in dividing the modeled area in different subdomains (Section 3.3.2.1). In practice, a global finite element mesh covering the whole area to be modeled is created using classical tools such as the GMS® preprocessor. This global mesh had then to be divided into different submeshes representing the different subdomains (Figure 3.6).

To perform this cutting, an interface called MESHDIV was developed. The subdivision of this global mesh can be made in two ways: (1) on the basis of polygons or arcs defining, in a horizontal plane, the limits between the subdomains or (2) by distinguishing the elements defining the subdomains on the basis of the material ID initially attributed to the element

during the building of the mesh with GMS. The first approach allows cutting the mesh following vertical limits between subdomains, the second approach allows an arbitrary cutting on the basis, for example, of geological boundaries.

To perform the cutting, nodes located on the boundaries between subdomains have to be doubled. Once the cutting performed, in each subdomains, nodes and elements are renumbered successively in a continuous way (Figure 3.6).

Internal boundary conditions prescribed between subdomains are defined and parameterized. The mathematical approaches chosen to solve the groundwater flow and solute transport problems are chosen.

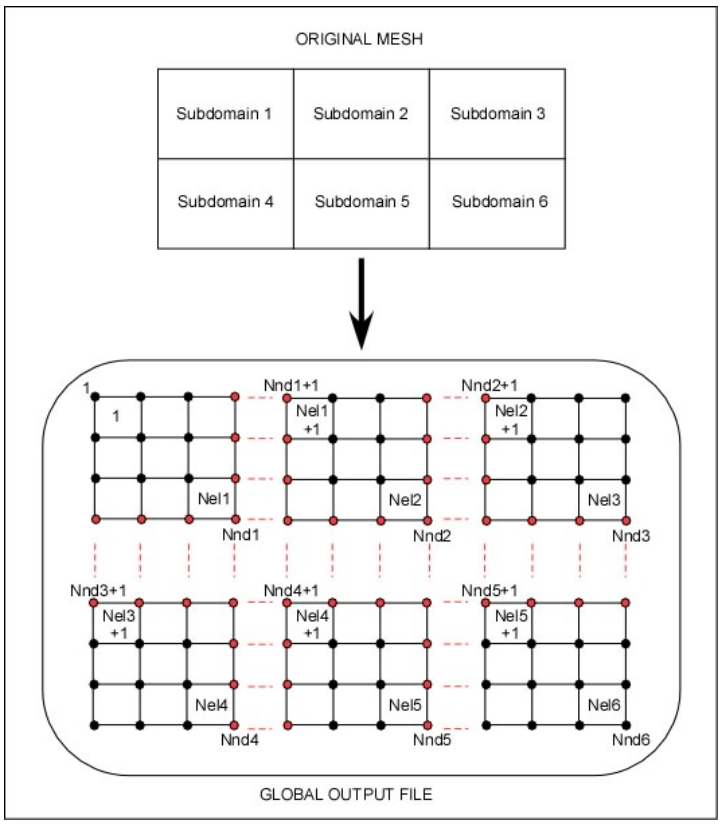

Figure 3.6. Division of the global mesh into submeshes representing the subdomains and renumbering of the mesh within each subdomain (Orban *et al.* 2005)

3.3.3.2 Definition of river boundary conditions

The interactions between groundwater and rivers are defined using third-type boundary conditions (Fourier) considering the characteristics of the river flowing on the upper face of each element of the mesh. When developing groundwater models at the regional scale, it becomes difficult to take explicitly into account the location of the river network in the spatial discretisation, i.e. it is unrealistic to have a node of the mesh corresponding to each node of the river network. A dedicated tool (RIVERMESH) was created to automate the interfacing of the surface-groundwater interactions.

Rivers are assumed to be equivalent to one-dimensional networks of nodes and arcs located on the upper faces of the mesh made of 3D finite elements. Intersections between the river and the limits of the upper face of the finite elements crossed by the river are determined to compute the length (L) of the river segment in the element (Figure 3.7). For each element, the width (w) of the river crossing this element, the thickness (b) and the hydraulic conductivity (K_r) of the river sediments are defined in the interface. Based on this information, a conductance coefficient α_R [L^2T^{-1}] is computed. This coefficient is used to compute, based on the Darcy's Law, the flux Q_{riv}^{GW} (Equation (3.15) exchanged between the river and the groundwater:

$$Q_{riv}^{GW} = \frac{K_r \, L \, w}{b}\left(H_{riv} - H_{GW}\right) = \alpha_R\left(H_{riv} - H_{GW}\right) \quad \textbf{(3.15)}$$

where H_{riv} is the mean water level in the river for the considered segment (interpolated in the middle of the segment on the basis of the water level values at the upstream and downstream nodes), H_{GW} is the groundwater level (unknown of the groundwater flow problem).

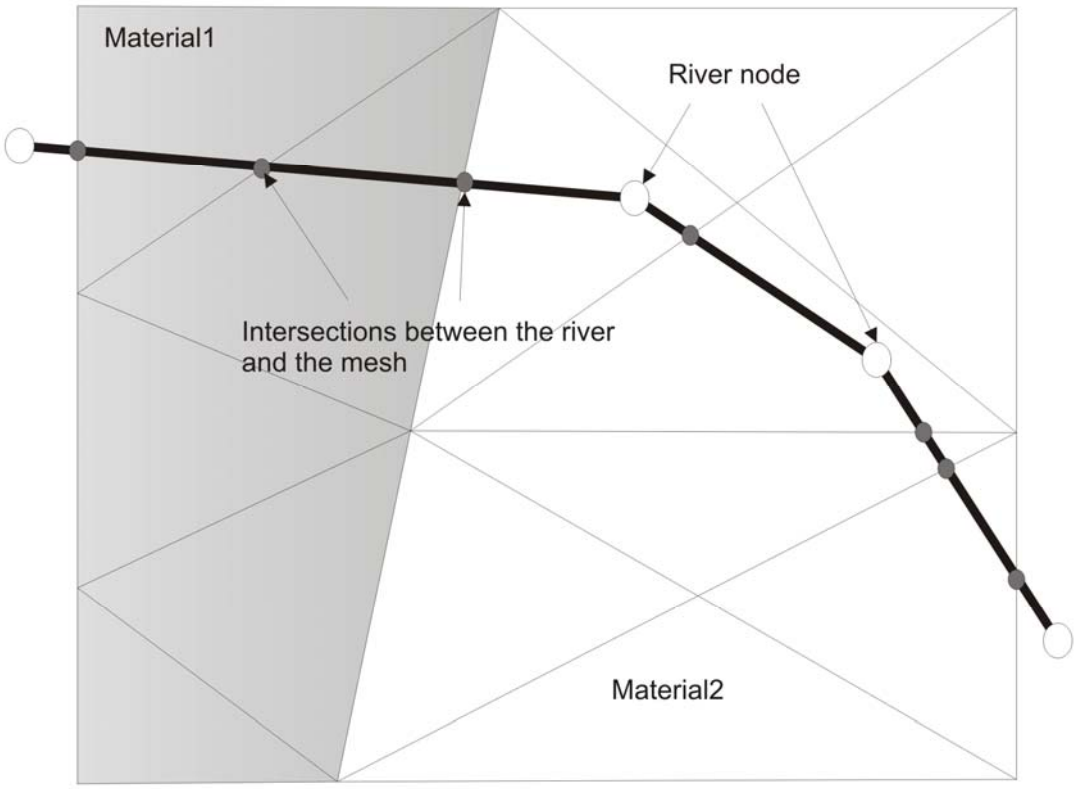

Figure 3.7. Intersection between a 3Dmesh and a river (black line). The grey dots correspond to intersections between the river network and the lateral limits of the elements of the mesh while white dots are the nodes defining the river.

3.3.3.3 Creation of the input files for the SUFT3D

The interface to the code SUFT3D was developed to create the input files needed for the computation. In a first step, the mesh and boundary conditions files, prepared with the help of GMS software, the MESHDIV and RIVERMESH tools, are read by the interfaces and are used to define information required for the simulation files (simulation type, numerical parameters, hydrodynamic and hydrodispersive properties, solicitations…). Information such as hydrodynamic and hydrodispersive parameters can be introduced manually or imported from an external database. The content of each window is dynamically adapted to the choices of the user.

Once the spatial data (location and characteristics of the pumping wells for example) are introduced, this information has to be mapped to the mesh. For example, volumes extracted in a pumping well have to be attributed to a node or a group of nodes in function of the depth of the well, the location of the screen and of the user's choices.

3.4 Test of the HFEMC approach implemented in the SUFT3D code

Different tests were performed to validate the implementation of the HFEMC approach in the SUFT3D. In a first step, the different approaches implemented in the SUFT3D to model the groundwater flow were tested. The linear reservoir approach was not used in the application developed in the framework of this thesis. Nevertheless, the performed tests are presented here to illustrate the method. These tests have been used in the framework of another project devoted to the groundwater flow modelling in mined area (Gardin *et al.* 2005; Brouyère *et al.* in press) in which mined areas are modelled using linear reservoirs coupled with a traditional finite element approach to represent the surrounding bed-rock.

3.4.1 Validation of the flow equations implemented in the SUFT3D

3.4.1.1 Comparison of the linear reservoir solution and an analytical solution

A groundwater flow model made of a single subdomain was simulated using a single linear reservoir. The model consisted in a parallelepiped (150 m long, 100 m width, 100 m high) divided in two layers of 12 prismatic elements. A third type boundary condition (Fourier with H_{ref} = 5 m and α_{LR} = 1×10^{-6} m²/s) was applied on one of the lateral face (Figure 3.8). Two cases were considered: (1) steady state conditions considering a uniform recharge of 1×10^{-5} m/s and, (2) transient condition considering a time variable recharge (Figure 3.9).

For the steady state case, the groundwater level computed with the SUFT3D code was equal to 5.0009 m in the reservoir. This result was similar to the one calculated analytically with Equation (3.4).

For the transient case, the mean groundwater level can also be computed analytically on the basis of Equation (3.4):

$$H_{LR} = \left(H_0 - \frac{\alpha_{LR} H_{ref} + Q}{\alpha_{LR}} \right) e^{-\frac{\alpha_{LR}}{S_{LR} A_{LR}} t} + \frac{\alpha_{LR} H_{ref} + Q}{\alpha_{LR}} \qquad \textbf{(3.16)}$$

The analytical solution (continuous line) and the SUFT3D solution (symbols) were compared (Figure 3.9).

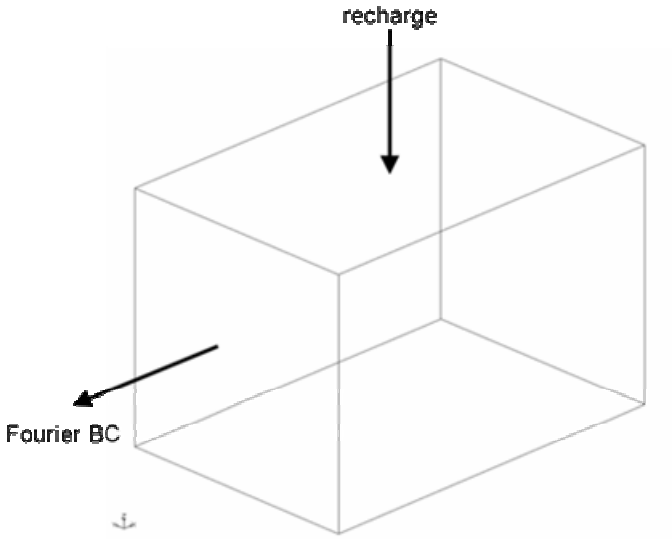

Figure 3.8. Scheme of the geometry, boundary conditions and solicitations applied to the reservoir linear model.

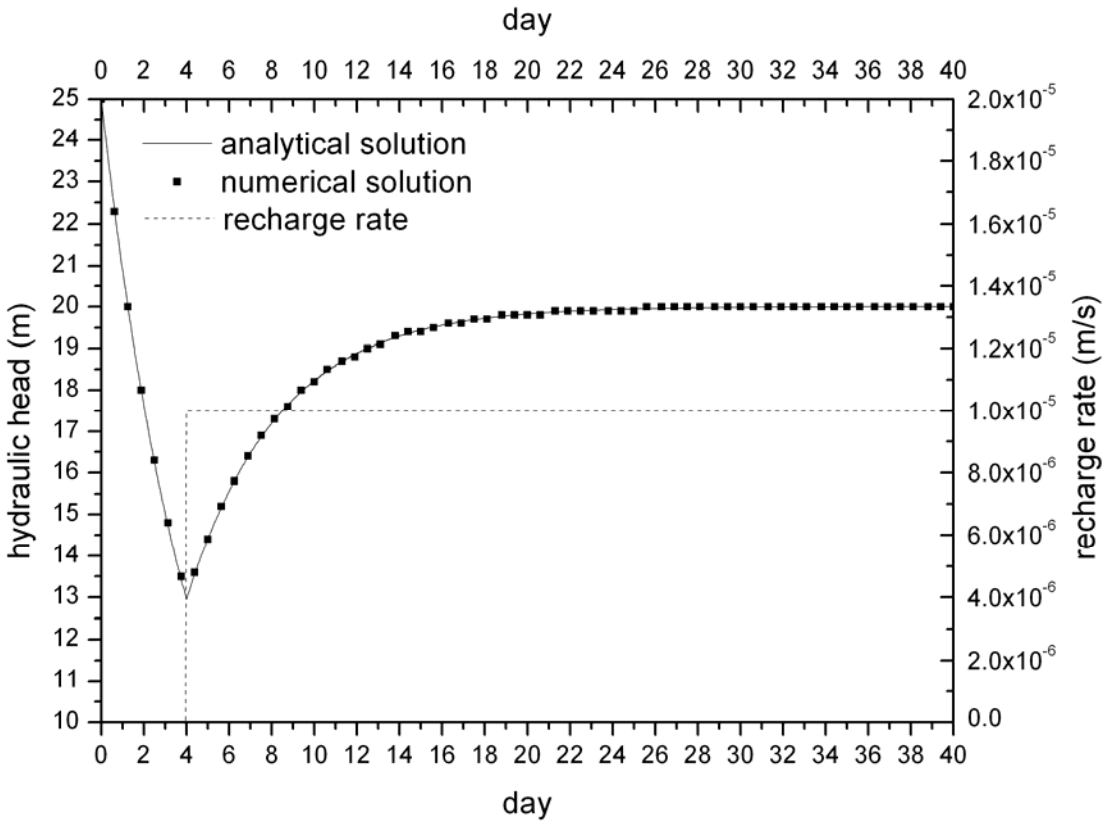

Figure 3.9. Temporal comparison between the analytical solution and the solution computed with the SUFT3D for the reservoir linear model in transient state.

3.4.1.2 Comparison with an analytical solution for combination of a linear reservoir and a traditional approach in a column

A saturated column was built to verify the implementation of the internal Fourier boundary condition and the possibility to use a combination of a linear reservoir and traditional approach to model the groundwater flow. A column of 15 m high was built using 15 cubic elements of 1 m. This column was divided into two subdomains of 10 elements and five elements for the upper and lower subdomains respectively. The flow is simulated using a classical flow equation and a reservoir linear approach in respectively the upper and lower subdomains.

An external Fourier boundary condition is prescribed at the bottom of the column (H_{ref} = 15 m and α_{LR} = 1×10^{-5} m²/s). An infiltration rate of 1×10^{-6} m/s is prescribed at the top of the column. An internal Fourier boundary condition ($\alpha_{interface}$ = 1×10^{-5} m^2/s) is used to model the flux exchanged between the two subdomains. The hydraulic conductivity in the upper suddomain is equal to 1×10^{-3} m/s.

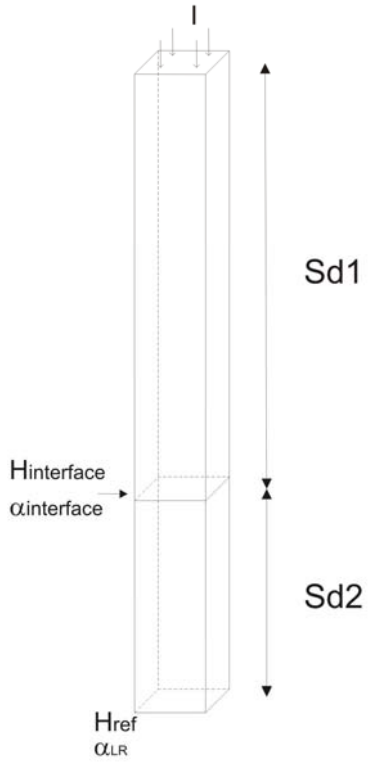

Figure 3.10. Scheme of the geometry, boundary conditions and solicitations applied to the model.

In steady state, the groundwater level can be computed analytically for the whole column using Equation (3.4) for the lower subdomain and the Darcy's law for the upper one. The concordance between the analytical solution (continuous line) and the SUFT3D solution (symbols) is perfect, confirming the precision of the approach implemented in the code (Figure 3.11).

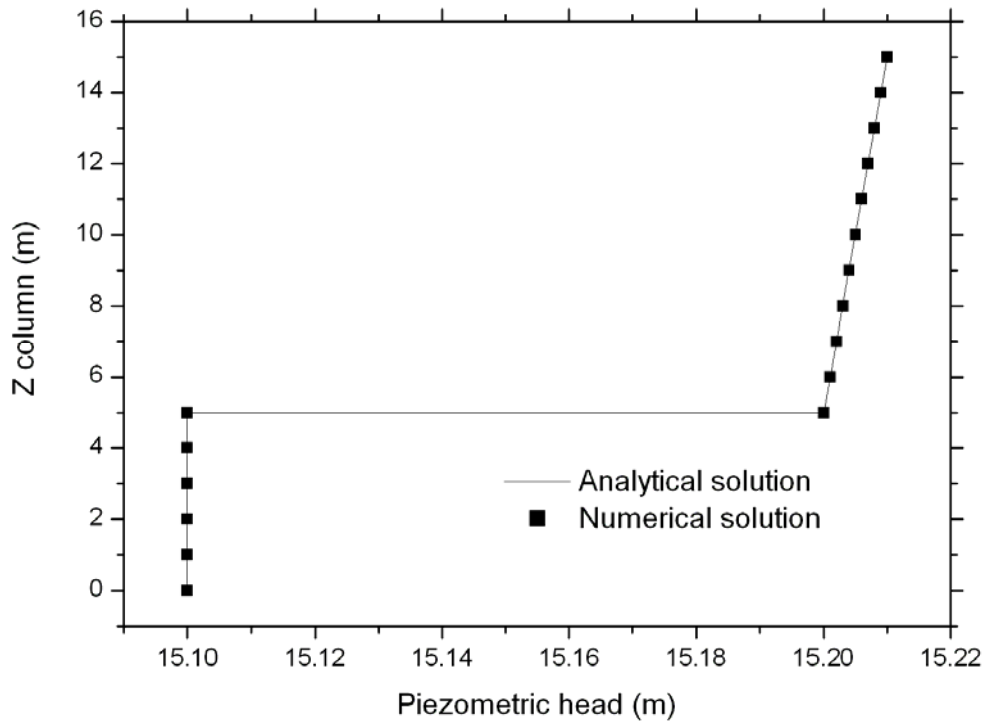

Figure 3.11. Comparison between the analytical solution and the solution computed with the SUFT3D as a function in the depth in the column.

3.4.1.3 Comparison with an analytical solution for combination of a linear reservoir and a traditional approach in a 3D model

A parallelepipedic 3D model was built to verify the implementation of the internal Fourier boundary condition and the possibility to use a combination of a linear reservoir and a traditional approach to model groundwater flow. The model is 300 m long, 250 m width and 300 m high and was discretised in two layers of 60 prismatic elements. The model is divided into two subdomains (Figure 3.12). In the first subdomain (SD1), groundwater flow is modelled using the classical groundwater flow equation; in the second one (SD2), a linear reservoir approach is used.

An external Fourier boundary condition is prescribed on the external faces of SD2 (H_{ref} = 5 m and α_{LR} = 1×10^{-5} m^2/s). An infiltration rate of 6×10^{-9} m/s is prescribed on the upper faces of the two subdomains. An internal Fourier boundary condition ($\alpha_{interface}$ = 1×10^{-1} m^2/s) is used to model the flux exchanged between the two subdomains. The hydraulic conductivity in SD1 is equal to 1×10^{-5} m/s.

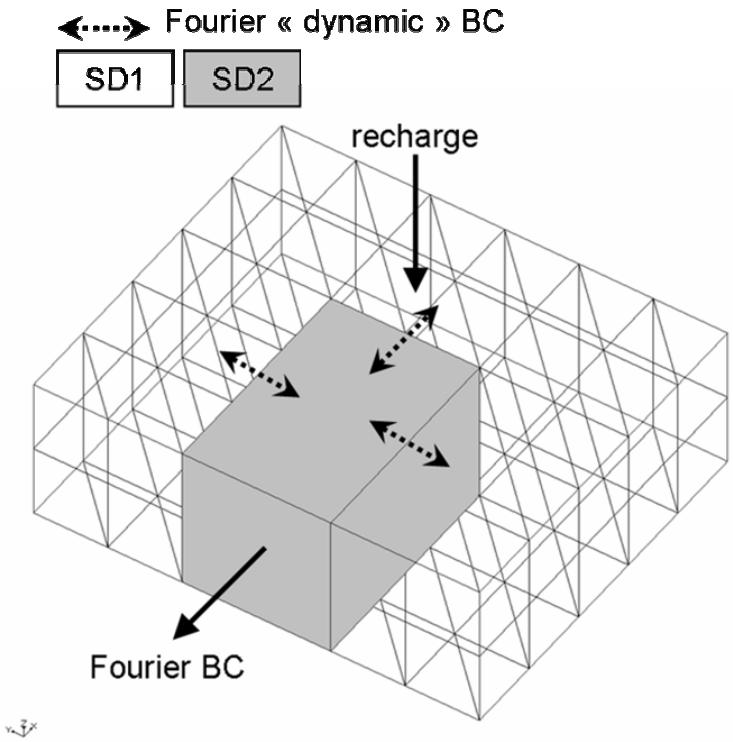

Figure 3.12. Schema of the geometry, boundary conditions and solicitations applied to the model.

In steady state, an analytical solution can be used to calculate a mean groundwater level equal to 5.0045 m in the linear reservoir. This value is equal to that computed with the SUFT3D (Figure 3.13). The subdomain SD1 is drained laterally to the subdomain SD2 modelled by a linear reservoir model.

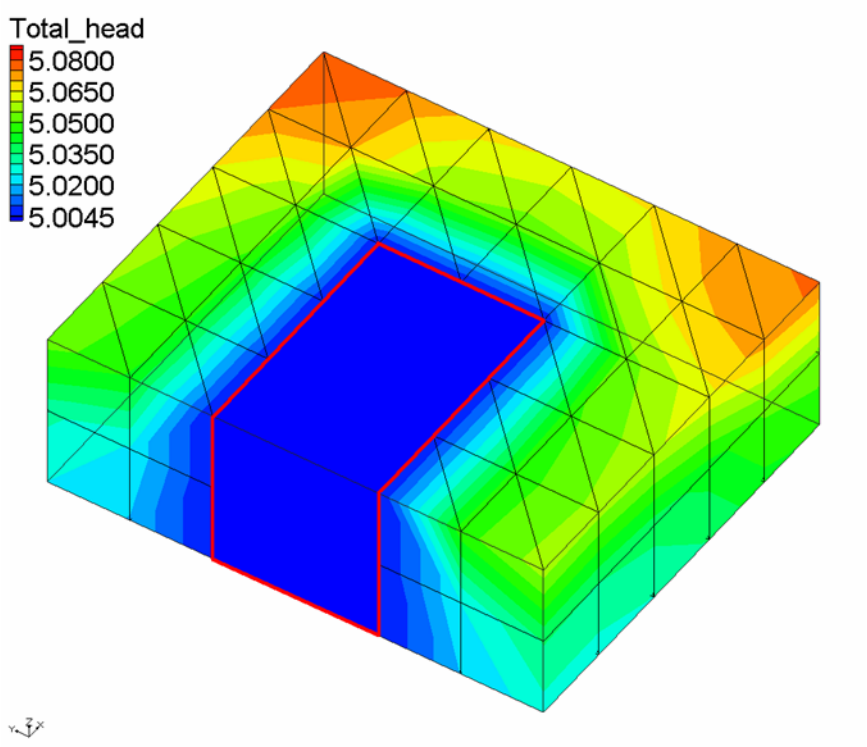

Figure 3.13. Groundwater levels computed with the SUFT3D.

3.4.2 Validation of the implementation of the transport equations in the SUFT3D

3.4.2.1 Comparison of the mixing cell solution of the SUFT3D and a semi-analytical solution

Under few simplifying assumptions, the equation describing the distributed mixing model (Equation (3.8) can be solved semi-analytically and used to validate the implementation of this model in the SUFT3D code. A solute is injected at a unitary concentration in a 1D column divided in mixing cells connected in series. The flow is steady state and a constant recharge of 1×10^{-6} m/s is prescribed at the top of the column; the height of each cell is 0.1 m. The effective porosity in each cell is equal to 10% of the total volume of the cells.

The mass balance equation applied to a mixing cell i (Figure 3.14) can be written:

$$V_i \frac{dC_i}{dt} = Q_{i-1,i}C_{i-1} - Q_{i,i+1}C_i \qquad \textbf{(3.17)}$$

where V_i (L^3) is the mixing volume associated to the mixing cell *i*, the terms $Q_{i-1,i}$ (L^3T^{-1}) is the flow rate between the upstream cell *i-1* and the cell *i*, $Q_{i,i+1}$ (L^3T^{-1}) is the flow rate

between the cell *i* and the downstream cell *i+1*, C_i (ML^{-3}) is the concentration in the mixing cell *i*, C_{i-1} (ML^{-3}) is the concentration in the upstream cell *i-1*.

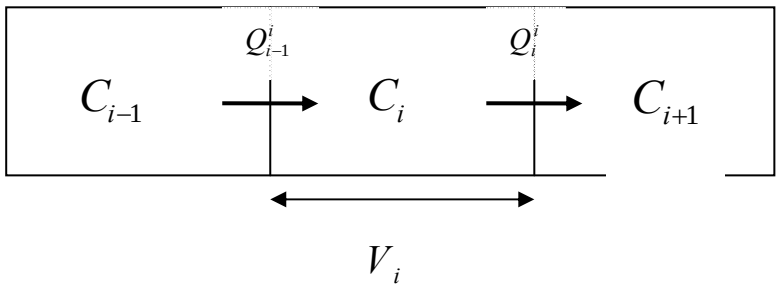

Figure 3.14. Scheme of the mixing cells used for the validation test

As the flow is steady state, $Q_{i-1,i} = Q_{i,i+1} = Q_{in}$ and the mixing equation becomes:

$$V_i \frac{dC_i}{dt} = Q_{in}\left(C_{i-1} - C_i\right) \tag{3.18}$$

An approximate solution can be easily derived, expressing the evolution of the concentration in the mixing cell *i*. The temporal derivative is approximated by a finite difference schema; the other terms of the equation being estimated explicitly.

The discrete form of the equation is written:

$$V_i \frac{C_i(t+\Delta t) - C_i(t)}{\Delta t} = Q_{in}\left(C_{i-1}(t) - C_i(t)\right) \tag{3.19}$$

The evolution of the concentration in the cell *i* can be computed as follow:

$$C_i(t+\Delta t) = \frac{Q_{in}\Delta t}{V_i}\left(C_{i-1}(t) - C_i(t)\right) + C_i(t) \tag{3.20}$$

In Figure 3.15 and Figure 3.16, the concentrations computed with the semi-analytical solution (continuous lines) and the SUFT3D (symbols) are compared.

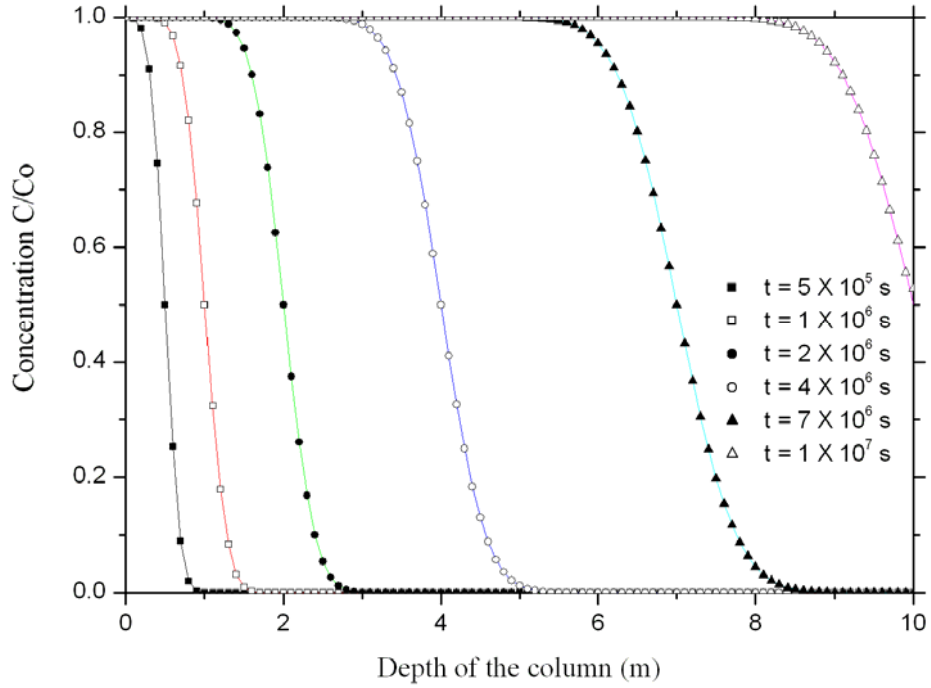

Figure 3.15. Spatial comparison between the results of the mixing cell model implemented in the SUFT3D code (symbols) and the one-dimensional semi-analytical solution (continuous lines).

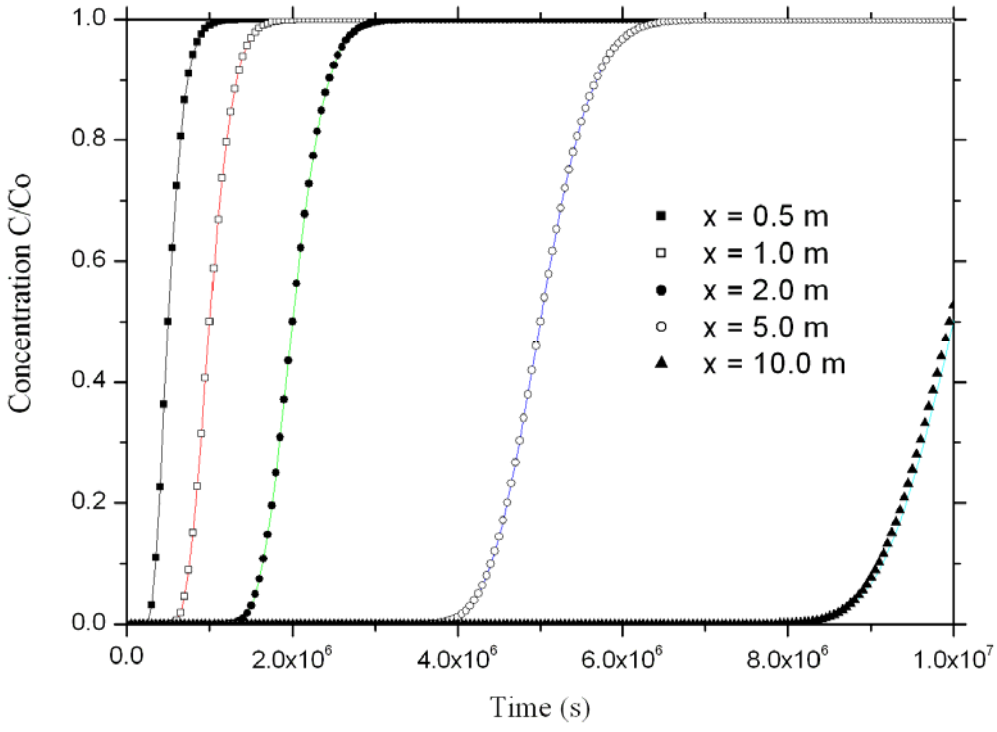

Figure 3.16. Time comparison between the results of the mixing cell model implemented in the SUFT3D code (symbols) and the one-dimensional semi-analytical solution (continuous lines).

3.4.2.2 Transport from a point source in a uniform two-dimensional flow field

An analytical solution for a two-dimensional solute dispersion problem proposed by Wilson and Miller (1978) was used to validate the implementation of the resolution of the advection-dispersion equation within the SUFT3D. The problem concerns two-dimensional dispersion of solute injected from a point source in a steady groundwater flow field (Figure 3.17). The specific objectives of this example is to test the ability of the code to predict two-dimensional concentration distribution taking into account the combined effect of advection and longitudinal and transverse dispersion.

Values of the parameters used in the simulation summarized in Table 3.2 are taken from Huyakorn *et al.* (1984). The selected parameters are based on data from a field study of hexavalent chromium contamination reported by Perlmutter and Lieber (1970). Simulation is performed on a finite element rectangular mesh containing 741 elements of 30 × 30 m and 14 time steps of 100 days each. In Figure 3.18 and Figure 3.19, numerical results from SUFT3D (symbols) are compared with the analytical solution (continuous lines).

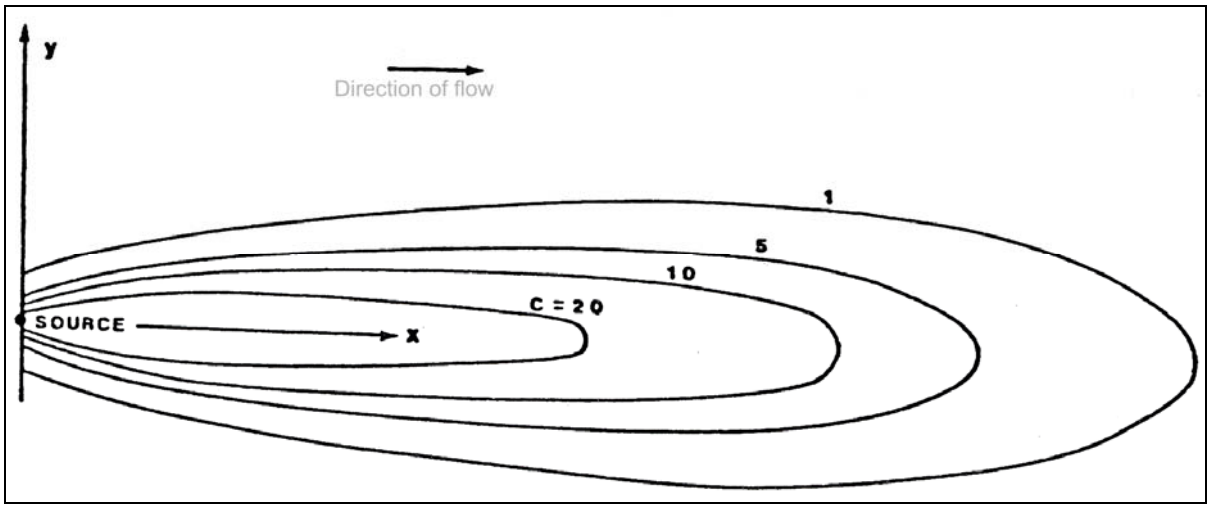

Figure 3.17. Schematic description of the problem (Huyakorn *et al.* 1984)

Parameter	Value
Darcy velocity, v_D	0.161 m/d
Porosity, θ_m	0.35
Longitudinal dispersivity, α_L	21.3 m
Transverse dispersivity, α_T	4.3 m
Aquifer saturated thickness, b	33.5 m
Contaminant mass flux, QC_0	704 g/m.d
Retardation factor, R	1.0
Decay constant, λ	0.0 d^{-1}

Table 3.2 Values of the parameters used in the simulation (Huyakorn *et al.* 1984)

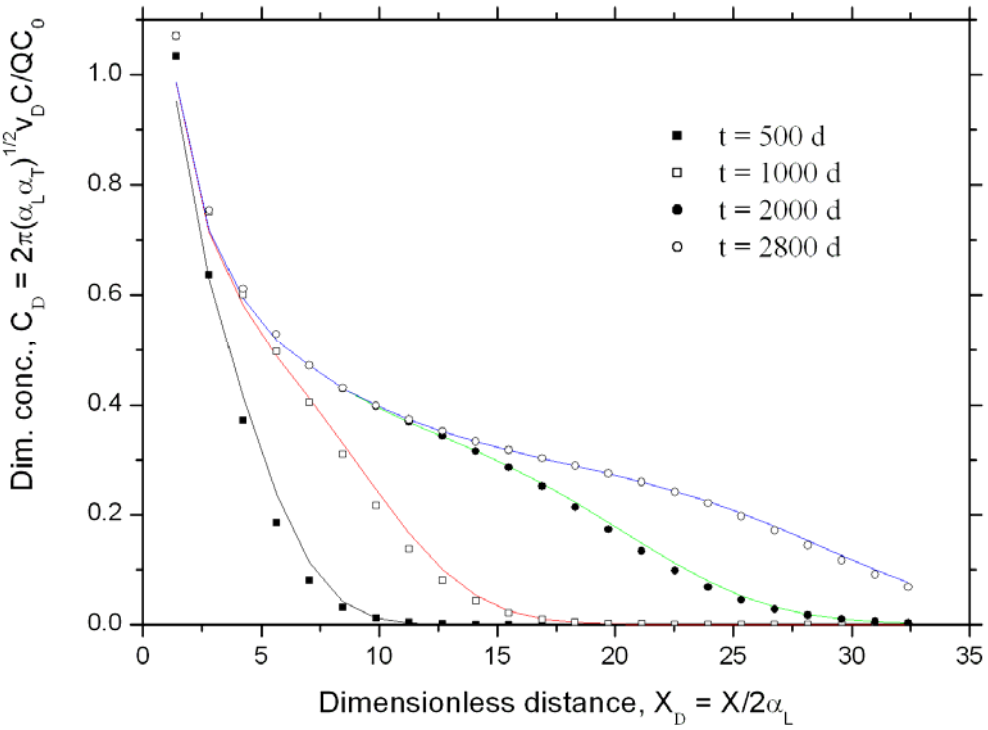

Figure 3.18. Concentration distributions along the x-axis showing analytical (continuous lines) and numerical (symbols) solutions.

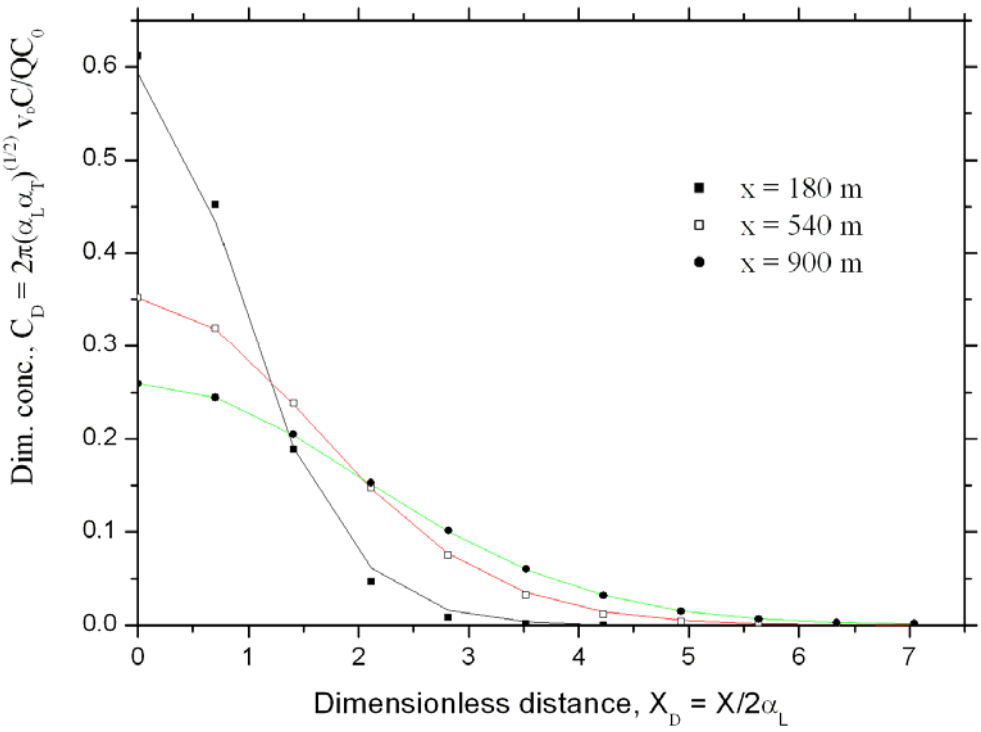

Figure 3.19. Concentration distributions along section perpendicular to the X-axis showing analytical (continuous lines) and numerical (symbols) solutions, t = 2800 days.

3.4.2.3 Comparison of mixing cell and advection dispersion solutions in a saturated column

The mixing cell approach implies that perfect mixing occurs instantly when solutes enter in a cell. Bajracharya and Barry (1994) showed that the concordance between results obtained with a mixing cell approach and with an advection-dispersion approach was dependant on the cell size. Best results were obtained with a cell size close to twice the hydrodynamic dispersivity of the medium (see chapter 2). Different tests have been performed to evaluate the validity of their conclusions for multi-dimensional problems. As a first step, the classical advection-dispersion equation was solved with the SUFT3D code under basic assumptions for 1D flow in a saturated column of 20 m with a slug injection at a concentration of 1 mg/l introduced at the top of the column during the first hour of simulation. To minimize numerical dispersion, the mesh was sized to have a very low numerical Peclet number (the cell dimensions is equal to 5cm). Different solutions were computed for different values of dispersivity.

In a second step, the same problem was solved with the SUFT3D simulator using the mixing cell approach for different discretisation levels. The two results were then compared to quantify the numerical dispersion introduced by the mixing cell approach as a function of the mesh size.

Figure 3.20 presents breakthrough curves computed with the classical advection-dispersion approach (continuous line) for different values of dispersivity and with the mixing cell approach (symbols) for two spatial discretisation of the column (100 elements of 20 cm and 200 elements of 10 cm). This confirms that the mixing cell solution reproduce the solution obtained with the advection-dispersion equation when the size of the mixing cell is twice the dispersivity.

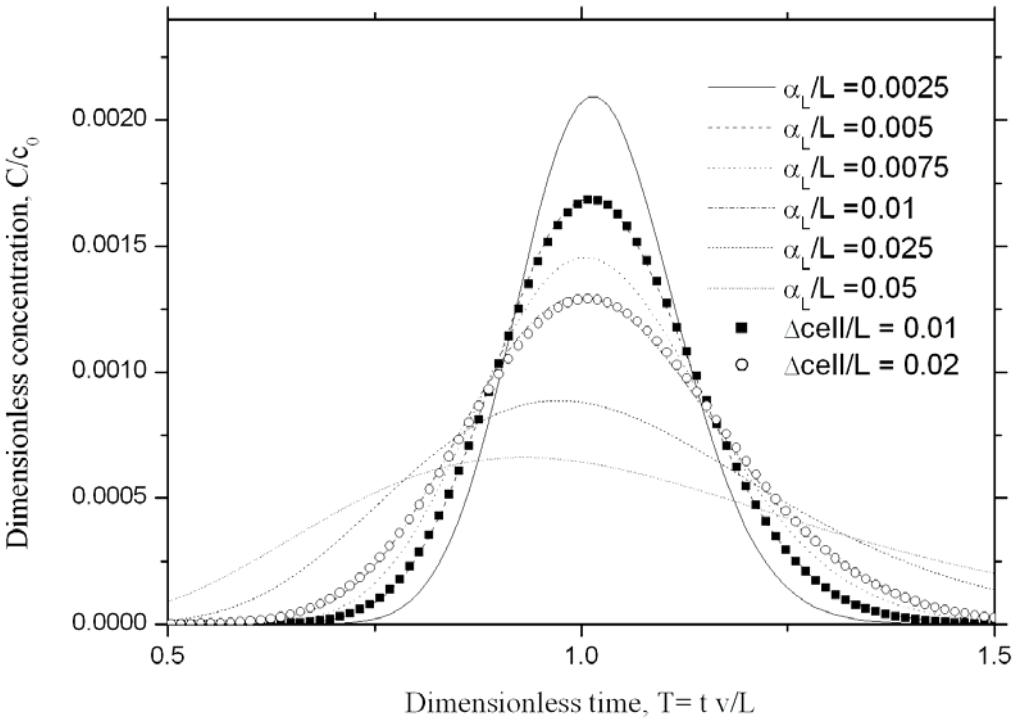

Figure 3.20. Comparison of solutions obtained using the mixing cell approach (symbols) and the advection-dispersion approach (lines). T is the dimensionless time, v the advective velocity, L the depth of observation in the column, c_0 is the injected mass multiplied by the volume of water within the column and Δcell the size of the mixing cell.

3.4.2.4 Comparison of mixing cell and advection dispersion solutions in a 2D problem

In order to compare mixing cell and advection dispersion solutions in a 2D problem, the example proposed by Wilson and Miller (1978) was revisited to quantify the numerical dispersion introduce by the use of the mixing cell in a 2D model. The modelled situation is similar to that described in section 3.4.2.2. The injection of solute is limited to the first time step.

Firstly, the problem was solved using the classical equation of advection dispersion was solved with the SUFT3D on a 2D mesh of cubic elements of 10 meters. To minimize numerical dispersion, dispersivity coefficients were chosen to have low Peclet number. Different solutions were computed for different values of longitudinal and lateral dispersivity.

In a second step, the same problem was solved with the SUFT3D simulator using the mixing cell approach with elements of 30 m. The results of the two approaches were then compared to estimate the numerical dispersion introduced by the mixing cell as a function of the mesh size.

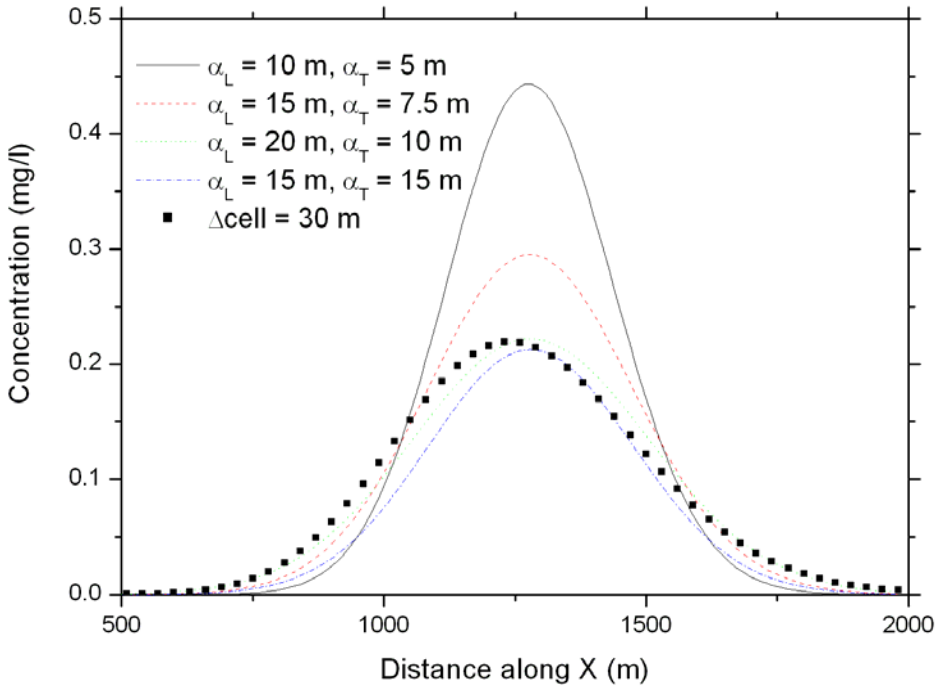

Figure 3.21. Concentration distributions along the x-axis showing advection-dispersion (lines) and mixing cell (symbols) solutions, t = 2800 jours

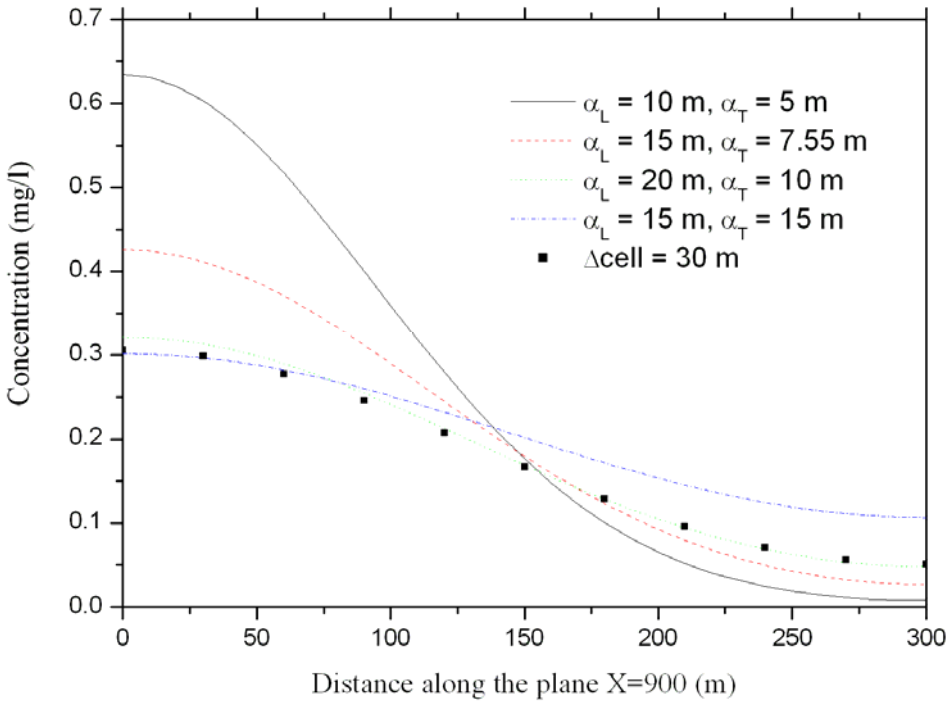

Figure 3.22. Concentration distributions along the plane X = 900m -axis (perpendicular to the groundwater flow) showing comparison of advection-dispersion (lines) and mixing cell (symbols) solutions, t = 1900 days

Figure 3.21 presents the concentrations along the flow direction (X axis) computed with the classical advection-dispersion approach for different values of dispersivity and with the mixing cell approach with cells of 30 m. The breaktrough curve computed with the mixing cell approach is similar to the two curves computed with the advection-dispersion approach for longitudinal and lateral dispersivities of 20 m and 10 m for the first one and 15 m and 15 m for the second one. However, if looking at the computed concentrations on planes perpendicular the direction of the flow (e.g. Figure 3.22), the mixing cell approach reproduced adequately only the advection-dispersion solution for longitudinal and lateral dispersivities of 20 m and 10 m respectively.

3.4.2.5 Example MIM from van Genuchten (1976)

To test and verify the mobile-immobile water effect as implemented in the SUFT3D to represent dual-porosity media, results computed by the code have been compared with an analytical solution of the one-dimensional transport of a solute pulse in sorbent soil with immobile water (van Genuchten and Wierenga 1976).

The column is supposed to be semi-infinite. Practically, its length is sufficient for the solute concentration not to be influenced by the boundary condition at the bottom of the column. A Dirichlet transport boundary condition is prescribed at the bottom of the column. At the entry of the column, the total flux of solute (Cauchy BC) is prescribed.

The same problem is modelled with the SUFT3D on a one meter length column, made of 100 elements of one centimetre high in the direction of the flow. In the perpendicular directions, parameters and stresses are constant to reproduce a one-dimensional problem. Values of the parameters are presented in Table 3.3

Parameter	**Value**
Darcy velocity, v_D	10 cm/d
Total porosity, θ	0.40
Mobile porosity θ_m	0.26
Dispersion, D_h	30 cm²/d
Bulk density ρ_b	1.30 g.cm³
Transfer coefficient between mobile and immobile water, α	0.15 d^{-1}
Partionning coefficient of the adsorbing site, f	0.4
Adsorption constant K_d	0.5 cm³/g
Injction length (dimensionless number) T_1^*	3
Distance at which the concentration is observed, L	30 cm

Table 3.3. Values of the parameters used in the simulation (van Genuchten and Wierenga 1976)

* T is an dimensionless number defined as:

$$T = \frac{v_m t \phi}{L} \tag{3.21}$$

where v_m (LT^{-1}) is the mean porous velocity in mobile water; $\phi = \frac{\theta_m}{\theta} = \frac{\theta_m}{\theta_m + \theta_{im}}$; θ, θ_m, θ_{im} are respectively the total water content, the mobile water content, the immobile water content.

In Figure 3.23, examples of results computed with the SUFT3D (symbols) are compared with those obtained with the CXTFIT code (continuous line) (Toride *et al.* 1995) in which the analytical solutions proposed by van Genuchten & Wierenga (1976) were implemented.

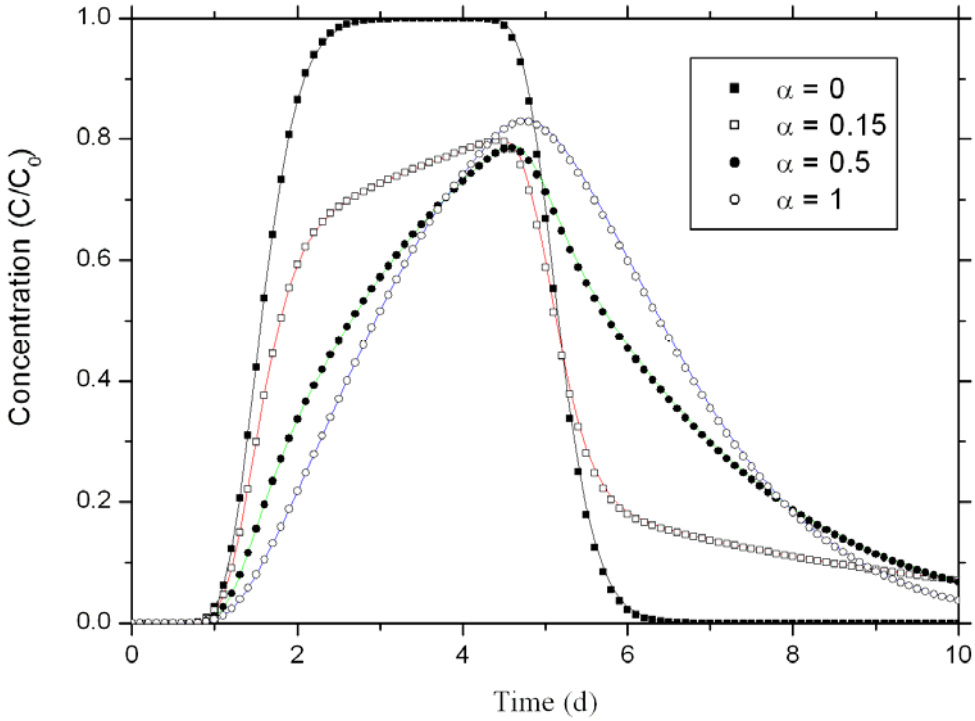

Figure 3.23. Comparison of the concentrations in the mobile water obtained with the SUFT3D (symbols) and CXTFIT (lines) for the example from van Genuchten and Wierenga (1976)

3.4.3 Conclusions of the tests

The different tests performed allow validating the implementation of the different equations (linear reservoir, mixing cell…) in the SUFT3D. The HFEMC approach can thus be used for practical applications.

3.5 References to chapter 3

Bajracharya, K. and A. Barry (1994). "Note on common mixing cell models." Journal of Hydrology **153**: 189-214.

Barthel, R., J. Jagelke, J. Götzinger, T. Gaiser and A. Printz (2008). "Aspects of choosing appropriate concepts for modelling groundwater resources in regional integrated water resources management - Examples from the Neckar (Germany) and Ouémé catchment (Benin)." Physics and Chemistry of the Earth **33**(1-2): 92-114.

Brouyère, S. (2001). Etude et modélisation du transport et du piégeage des solutés en milieu souterrain variablement saturé (Study and modelling of transport and retardation of solutes in variably saturated media). PhD Thesis Faculty of Applied Sciences. Liège (Belgium), University of Liège**:** 640.

Brouyère, S., G. Carabin and A. Dassargues (2004). "Climate change impacts on groundwater resources: modelled deficits in a chalky aquifer, Geer basin, Belgium." Hydrogeology Journal **12**: 123-134.

Brouyère, S., P. Orban, S. Wildemeersch, J. Couturier, N. Gardin and A. Dassargues (in press). "The hybrid finite element mixing cell method: a new flexible method for modelling mine water problems." Mine Water and the Environment.

Carabin, G. and A. Dassargues (1999). "Modeling groundwater with ocean and river interaction." Water Resources Research **35**(8): 2347-2358.

Dassargues, A. and A. Monjoie (1993). The chalk in Belgium. The hydrogeology of the chalk of the North-West Europe. R. A. Downing, M. Price and G. P. Jones. Oxford, UK, Oxford University Press**:** Chapter 8: 153 - 269.

Gardin, N., S. Brouyère and A. Dassargues (2005). Modélisation de la remontée des niveaux piézométriques dans les massifs affectés par des travaux miniers dans l'ancien bassin charbonnier de Liège. Liège, Université de Liège - Département GEOMAC - Secteur Hydrogéologie et Géologie de l'Environnement**:** 99.

Gogu, C. R., G. Carabin, V. Hallet, V. Peters and A. Dassargues (2001). "GIS-based hydrogeological databases and groundwater modelling." Hydrogeology Journal **9**: 555-569.

Hallet, V. (1998). Étude de la contamination de la nappe aquifère de Hesbaye par les nitrates: hydrogéologie, hydrochimie et modélisation mathématique des écoulements et du transport en milieu saturé (Contamination of the Hesbaye aquifer by nitrates: hydrogeology, hydrochemistry and mathematical modeling). PhD Thesis Faculty of Sciences. Liège (Belgium), University of Liège**:** 361.

Huyakorn, P. S., A. G. Kretschek, R. W. Broome, J. W. Mercer and B. H. Lester (1984). Testing and validation of models for simulating solute transport in ground-water: Development, evaluation and comparison of benchmark techniques. Indianapolis, International ground water modeling center**:** 419.

Orban, P., S. Brouyère, H. Corbeanu and A. Dassargues (2005). Large-scale groundwater flow and transport modelling: methodology and application to the Meuse Basin, Belgium. Bringing Groundwater Quality Research to the Watershed Scale, 4th International Groundwater Quality conference, Waterloo, Canada, IAHS.

Perlmutter, N. M. and M. Lieber (1970). "Dispersal of plating wastes and sewage contaminants in groundwater and surface water, South Farmingdale-Massapequa Area, Nassau County, New York." Water Supply Paper **1879-G**.

Quinn, P. (2004). "Scale appropriate modelling : representing cause-and-effect relationships in nitrate pollution at the catchmment scale for the purpose of catchment scale planning." Journal of Hydrology **291**(3-4): 197-217.

Sophocleous, M. (2002). "Interactions between groundwater and surface water: the state of the science." Hydrogeology Journal **10**: 52-67.

Toride, N., F. J. Leij and M. T. van Genuchten (1995). The CXTFIT code for estimating transport parameters from laboratory or field tracer experiments, Version 2.0. Riverside, CA, U.S. Salinity Laboratory, USDA, ARS**:** 121.

van Genuchten, M. T. and P. J. Wierenga (1976). "Mass transfer studies in sorbing porous media: I. Analytical solutions." Soil Sci. Soc. Am. J. **40**: 473-480.

Wilson, J. L. and P. Miller (1978). "Two-dimensional plume in uniform ground-water flow." Journal of the hydraulics division, Proceedings of the american society of civil engineers **104**(HY4): 503-514.

Wojda, P., M. Dachy, I. C. Popescu, I. Ruthy, N. Gardin, A. Dassargues and S. Brouyère (2005). Appui à la conception de la structure, à l'interfaçage et à l'enrichissement de la base de données hydrogéologiques de la Région Wallonne (Support to structuring, interfacing and developing the Walloon Region Hydrogeological Database), University of Liège, GeomaC (Hydrogeology) - Walloon Region**:** 48.

4 CASE STUDY: THE GEER BASIN

4.1 Introduction

A first application of the large-scale modelling approach has consisted in the development of a groundwater flow and transport model for the Geer sub-catchment (tributary of the Meuse) (Figure 4.1) to study and predict the mid-term temporal evolution of nitrate concentration in the chalk aquifer of the Geer basin.

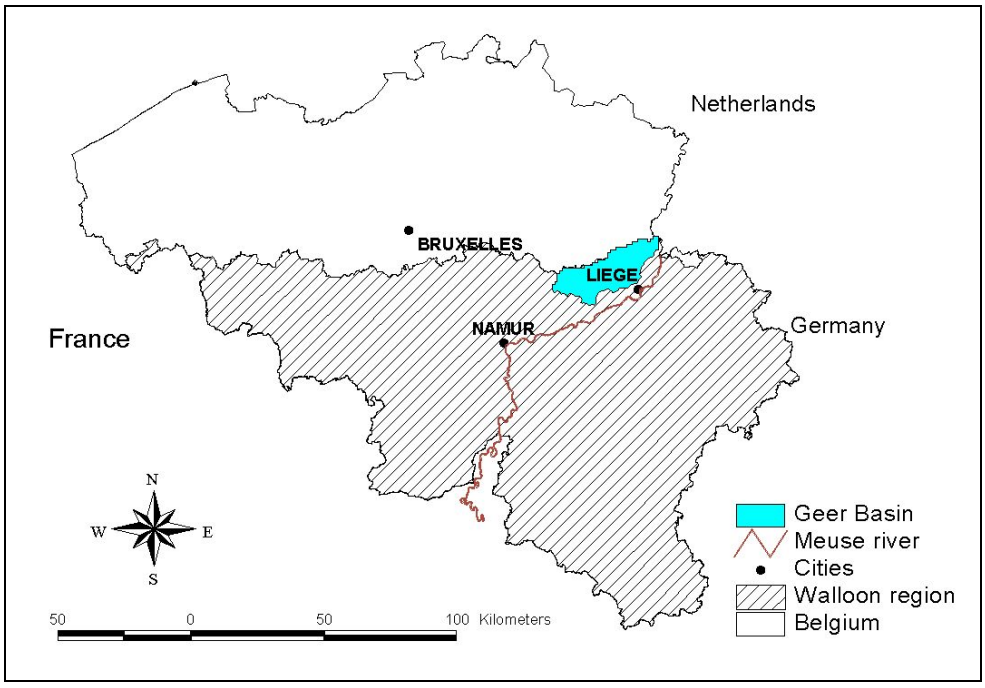

Figure 4.1. Location of the Geer basin

The Geer basin has been selected because of several interesting characteristics.

1. This basin has been the topic of several research projects and investigations, including modelling. An important dataset is available, including time series of nitrate concentration and environmental tracer data.

2. From a quantitative point of view, this groundwater resource is of major importance for the Walloon region. Groundwater provides drinking water to the city of Liège and to an important part of its suburbs.

3. Because of the existence of a thick layer of loess, the region is intensively cultivated. From 1960, nitrate concentrations have risen. Presently, nitrate concentrations are close to the drinking water limit (50 mg/l). These last years, pesticides (mainly atrazine) have also been detected in some observations and pumping wells. Estimation of present and future groundwater quality trends in the basin is of primary importance

for supporting any decisions in terms of land use and for supporting the administration in the implementation of the Water Framework Directive.

The objective of the two first sections of this chapter is to describe the hydrogeological characteristics of this case study and to present an overview of the available dataset. In this chapter, main features relevant for the development of the model are highlighted. More information can be found in previous studies as the "Programme Action Hesbaye" (Dautrebande *et al.* 1996), multi-tracer experiments carried out in the basin (Biver 1993; Hallet 1998; Brouyère *et al.* 2004a), the study of the impact of climate change on groundwater resources (Brouyère *et al.* 2004b) and the PIRENE project (Brouyère *et al.* 2004c; Orban *et al.* 2005). In the third section, new information related to environmental tracers and the age of groundwater are presented. The last section is devoted to the development of the groundwater model.

4.2 Description of the Geer basin

4.2.1 Geographical and geomorphologic context

The Geer sub-catchment (480 km^2) is located in Eastern Belgium. The Southern part of the basin is part of the geomorphologic region called the Hesbaye Plateau. Altitudes range from 206 m in the South-West to 80 m in the North-East.

Except for the Geer, which is the main drainage axis flowing from South-West to North-East, the density of the hydrographic network is very small (Figure 4.2).

- The Yerne River, flowing from SSW-NNE, drains the aquifer in its upstream and downstream part; it is perched above the aquifer in the middle part. Except the Geer River, the Yerne is the only permanent natural river.
- The Roua River, flowing to the North towards the Geer, is perched in its upstream part and it drains the aquifer in the downstream part.

The low density of the network is in direct relation with the underground hydraulic conductivity (loess formations of hydraulic conductivity of the order of 10^{-7} m/s) and the depth of the groundwater table.

Dry valleys with main directions S-N, SW-NE, SE-NW, define a fossil hydrographic network. These dry valleys deepen to the North. Most of them have a periglacial origin. These valleys

are associated with zones of higher hydraulic conductivity in the fissured chalk, producing drawdowns of groundwater levels and lower hydraulic gradient.

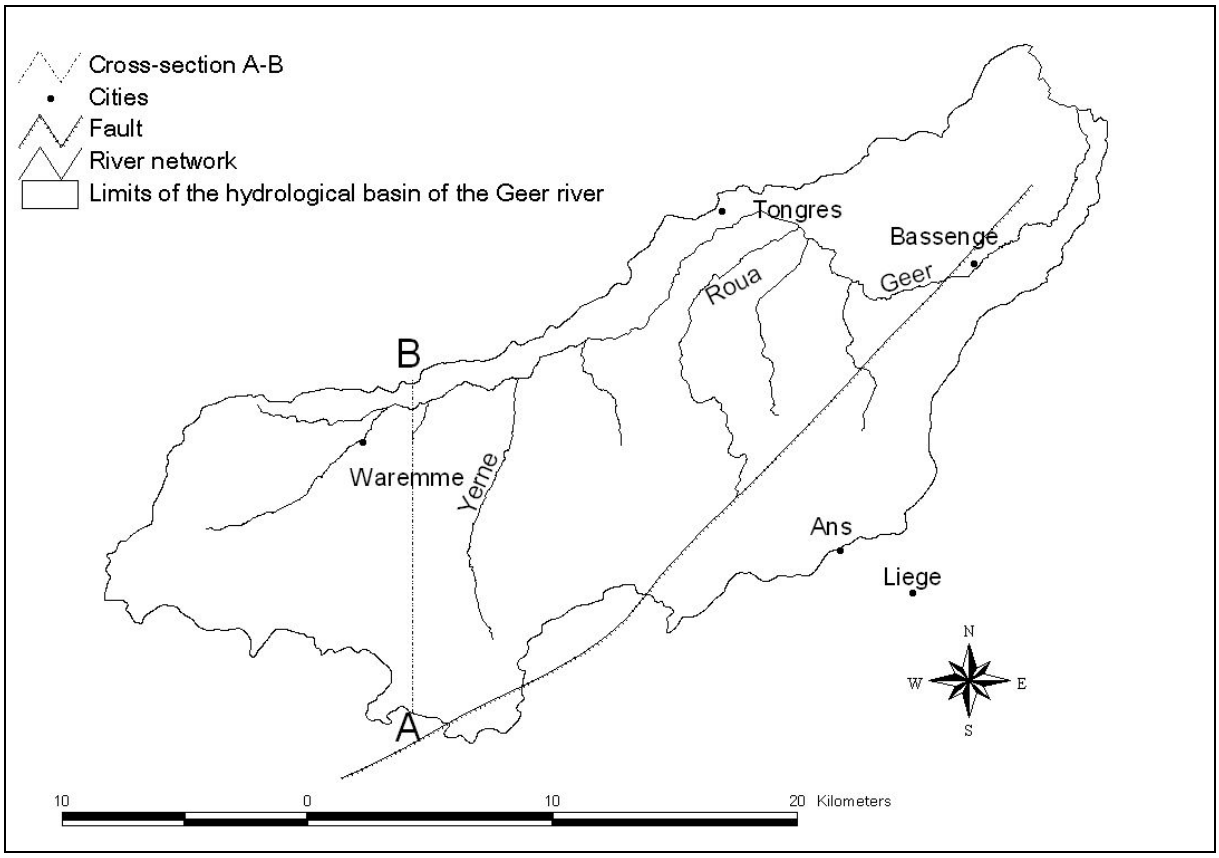

Figure 4.2. Location of the river network in the Geer basin, the Horion-Hozémont fault and the AB cross-section

4.2.2 Geological context

The deep substratum in the Geer basin is made up of a Primary peneplaned platform. This peneplain is covered by Cretaceous marine formations (orientation West-East with a slight slope to the North).

In the Southern part of the basin, the substratum is made of, from top to bottom, (Figure 4.3):

- Quaternary loess of variable thickness, from 2 m up to 20 m;
- locally, several meters of Tertiary sand deposits;
- a maximum of 10 m of flint conglomerate, which is a heterogeneous material made of dissolved chalk residues (flints, sand, clay and locally phosphate residuals);

- Senonian chalks showing depth ranging from a few meters up to 70 m, in which the aquifer is located;
- several meters of smectite clay of low hydraulic conductivity, considered as the aquifer basis.

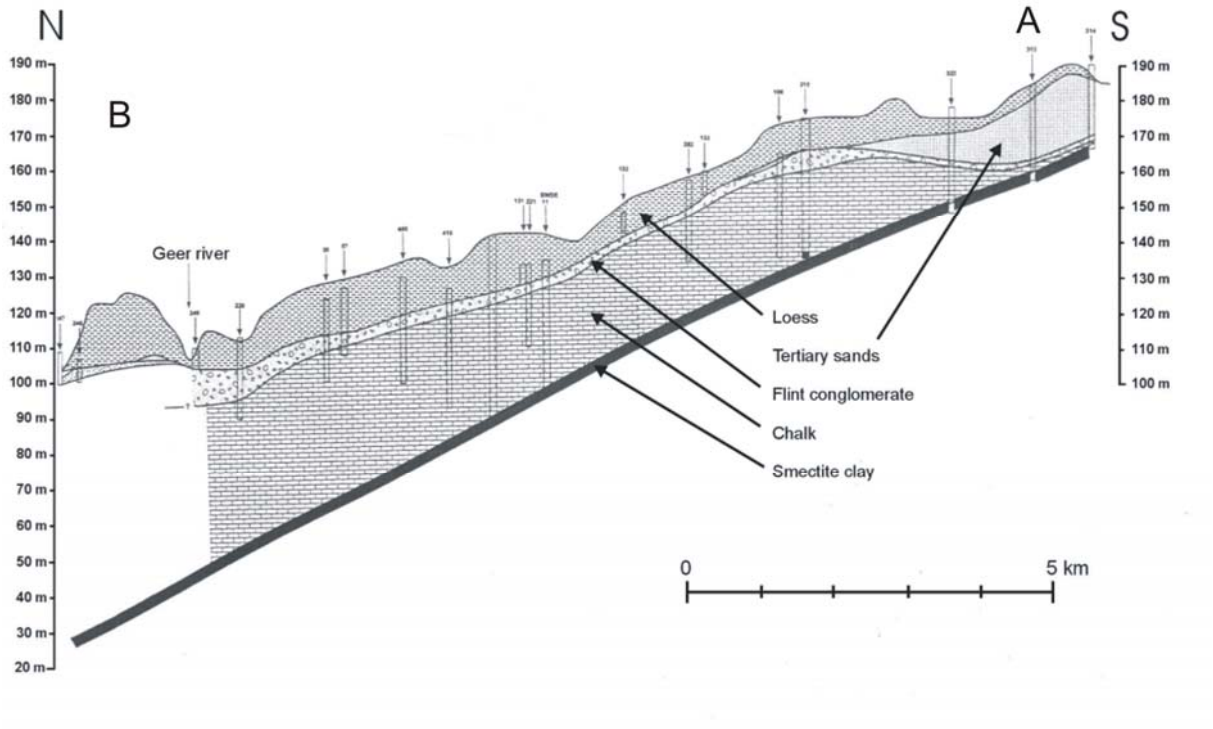

Figure 4.3. North-South simplified geological AB cross-section in the Hesbaye aquifer (Brouyère *et al.* 2004b).

The Senonian chalk can be divided into two groups, the Campanian and the Maastrichtian chalks, separated by a level of indurate chalk of less than one meter, called “The Hardground” or “Horizon de Froidmont” (Hallet 1998). In the Northern part of the basin, the chalk is covered by Tertiary sands and by clays of Heersian and Landenian ages.

Geological logs, available for one hundred points in the basin, are used to define the vertical extension of the different layers. As the direction and slope of the layer are known, interpolation can be easily performed to assess the interface between these layers.

Primary formations were faulted during the Hercynian orogeny. Some of the faults (and in particular the major one, the “Horion-Hozémont” fault, Figure 4.2) moved again after the

Secondary deposits leading to the fracturation of the chalk and an increase of its hydraulic conductivity.

4.2.3 Hydrogeological context

The aquifer is mainly located in the chalk formations. In the Southern part of the basin, in an area also called “the Hesbaye aquifer”, unconfined conditions prevail in an area of about 350 km². Near the Geer River the aquifer becomes semi-confined under the loess deposits. In the Northern part and to the North of the basin, the aquifer is confined under the Tertiary deposits.

4.2.3.1 Data on groundwater abstraction

Data on groundwater abstraction is collected by the administration of the Walloon region and stored in a database. For year 2003, about 24 millions m^3 of groundwater were abstracted in the Geer basin. This groundwater is mainly used for drinking water supply (86%), for the industrial sector (13%), agriculture and services (1%) (Orban *et al.* 2006).

Three companies pump groundwater in the chalky aquifer of the Geer basin for drinking water production, the Companie Intercommunale Liégoise des Eaux (CILE), the Sociéte Wallonne des Eaux (SWDE) and the Vlaamse Maatschappij voor Watervoorziening (VMW).

The CILE uses a network of 45 km of draining galleries dug in the chalk, allowing for the production between 15 millions and 20 millions m^3 of groundwater. These galleries are oriented following the East/West direction. The galleries can be subdivided in two networks (Hodiaumont *et al.* 1999):

- the Southern galleries dug at a depth of approximately 30 metres which drain groundwater in the shallowest part of the aquifer;
- the Northern galleries dug at a depth of approximately 60 metres which drain groundwater in the deeper aquifer.

The Southern galleries feed by gravity two reservoirs located in Hollogne and Ans through a system of aqueducs to supply water to the city of Liège and its suburbs. Groundwater in the Northern galleries has to be lifted up into aqueducs to flow to the Southern galleries. Groundwater is mainly abstracted in the Northern galleries when the production of the Southern galleries are not sufficient or when the nitrate content in the Southern galleries are

too high (Hodiaumont *et al.* 1999). A small amount of groundwater is also pumped directly in the Northern and Southern galleries to provide drinking water to villages located in the Geer basin.

The SWDE and VMW pump groundwater using different wells drilled in the chalk. In 2003, they produced respectively about 2.5 and 0.5 millions m^3 of groundwater.

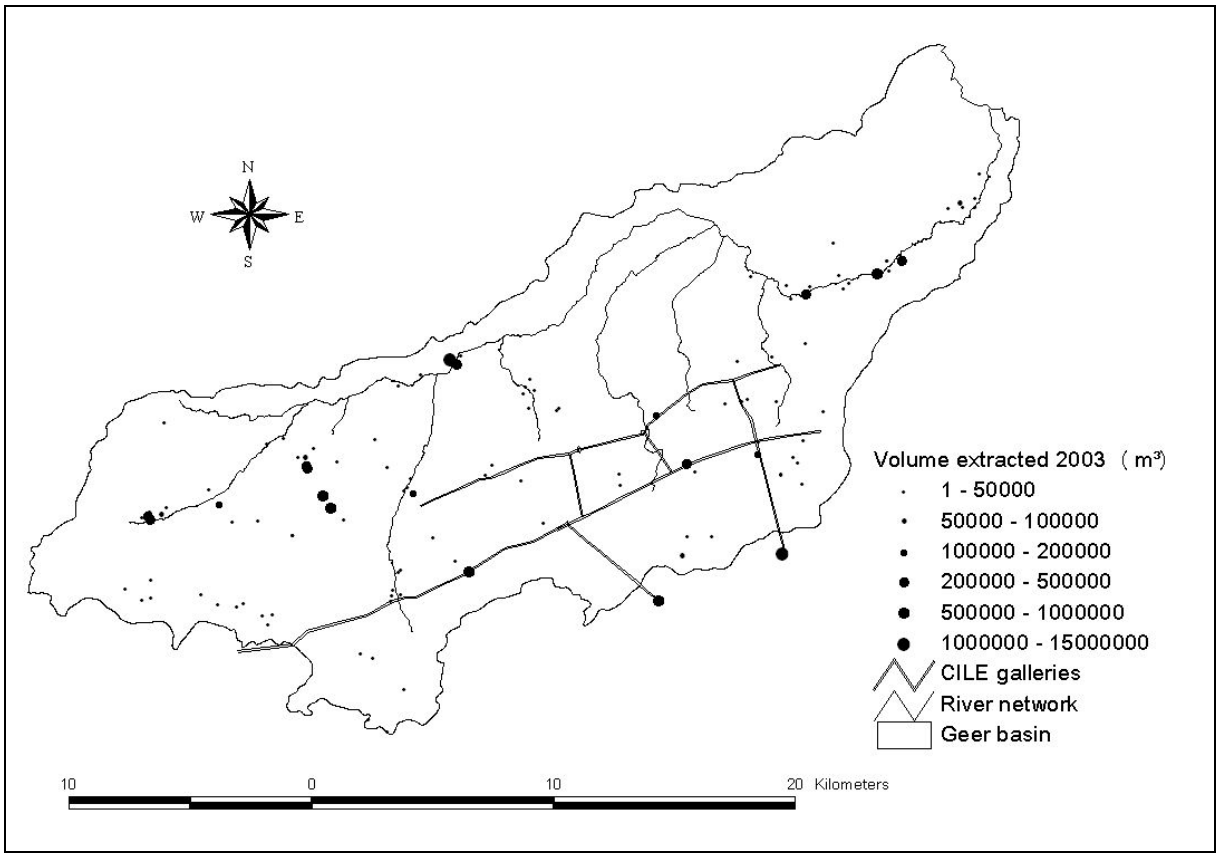

Figure 4.4. Groundwater abstraction volumes for 2003 (m^3)(data extracted from the database of the administration of the Walloon region. The two points outside the basin corresponds to the reservoir of Hollogne and Ans which collect the groundwater drained in the galleries

4.2.3.2 Piezometry

Recently, for the purpose of the hydrogeological maps of the Walloon region, a new piezometric map of the chalky aquifer of the Geer basin for the period January-April 2008 has been drawn on the basis of updated data.

The interpretation of this new piezometic map allows confirming the information already obtained from the previous piezometric maps for the years 1951, 1966, and 1984:

- groundwater flows mainly from South to North;

- the groundwater table has a high piezometric gradient, around 1 % in the vicinity of the galleries; downstream the gradient is lower, around 0.5 %;
- the groundwater table is poorly influenced by the course of the Geer and the Yerne except downstream for the Geer and upstream for the Yerne.

The main contribution of this survey is to allow a better understanding of the piezometry in the North-Eastern part of the Geer basin. Actually, groundwater level measurements have been performed in this area or extracted from the database of the Flemish region and included in a piezometric map of the whole Geer basin for the first time. The piezometric map highlights the presence of a piezometric dome to the East of the city of Tongres. Locally, groundwater flows from North to South to feed the Geer river. The importance of the aquifer drainage by the Geer in this area is also highlighted. Isolines of piezometry lines 65 and 70 metres, sketched at the proximity of the outlet of the basin seem to indicate that the Geer is not draining in this downstream zone.

4.2.3.3 Time evolution of the piezometry

Groundwater levels have been measured at least once in more than 258 piezometers, for some of them since 1951. At some locations, groundwater level fluctuations with time can reach more than 15 metres (Figure 4.6). However, Hallet (1998) showed that the shape of the groundwater table remains relatively constant in time and the amplitude of the fluctuations are smaller in the North of the basin, where the Geer river tends to regulate groundwater levels in the aquifer. Futhermore, a delay ranging from a few weeks to one year and a half is observed between precipitations and variations in groundwater levels. Fluctuations of groundwater levels allow distinguishing contrasted periods of high and low groundwater levels such as those existing respectively in 1983-1984 and 1991-1992. Even if fluctuations are important no evidence of global upward or downward trends in piezometry has been demonstrated.

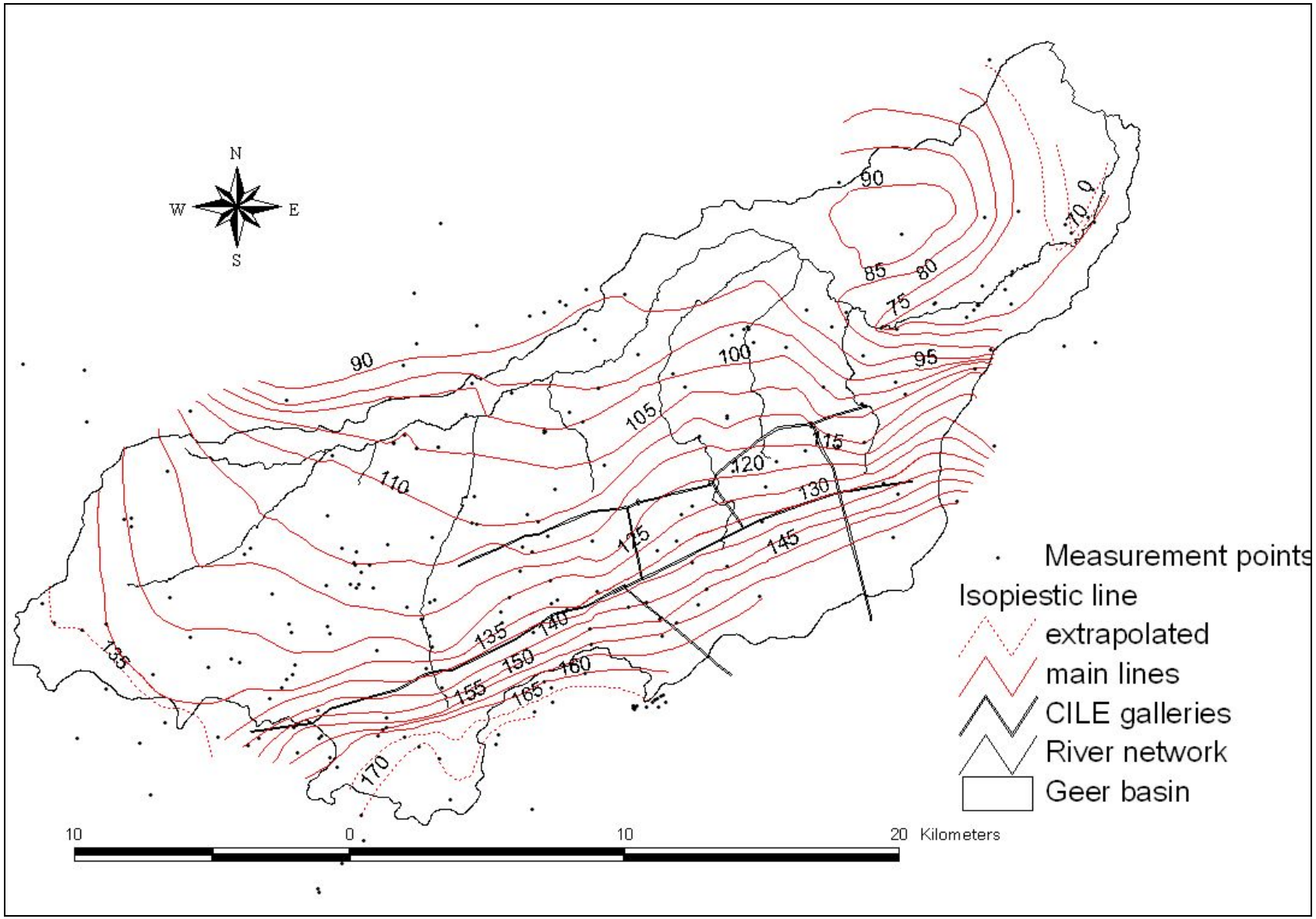

Figure 4.5. Piezometric map of the chalk aquifer based on 2008 data (in metre a.s.l.)

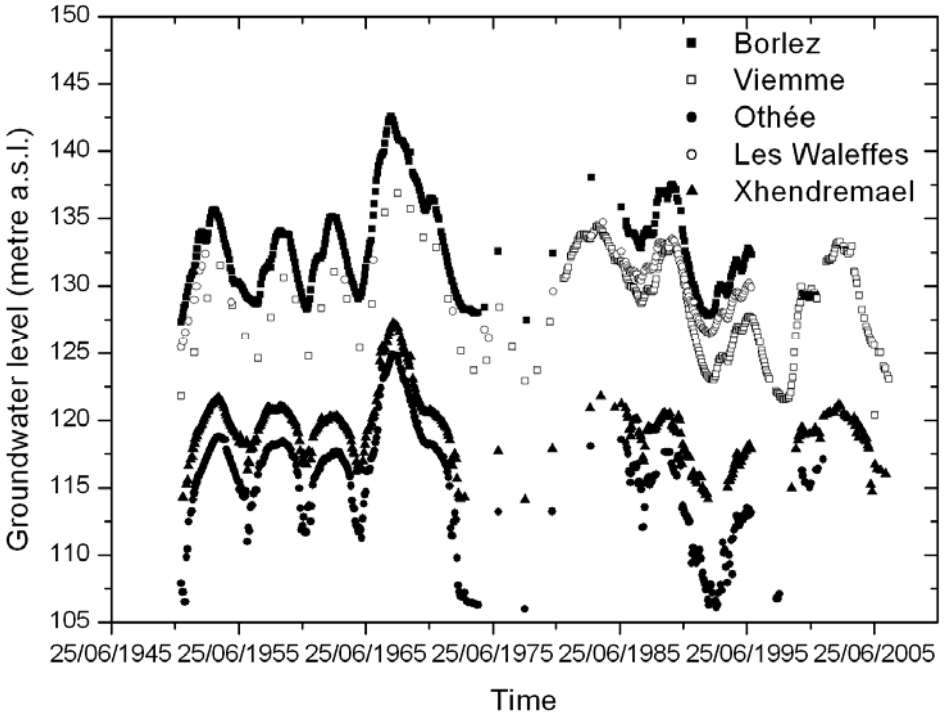

Figure 4.6. Examples of groundwater level variations from 1951 to 2005 (source: DGRNE database)

4.2.3.4 Limit of the hydrogeological basin

Examination of the piezometric maps allows locating the limits of the hydrogeological basin (Hallet 1998) which are corresponding to those of the hydrological basin:

- in the South-Western part of the basin, the hydrogeological limit is located between a few hundreds metres and more then two kilometres to the South of the hydrologic limit;
- in the South-Eastern part of the basin, in the vicinity of the city of Grace-Hollogne, the hydrogeological limit is more uncertain but seems to be located slightly to the North of the limit of the hydrological basin;
- to the West, in the vicinity of the city of Oupeye, the limit of the hydrogeological basin is located 100 or 200 metres to the East of the limit of the hydrological basin;
- to the North of the Geer River, the aquifer is confined under the Tertiary deposits. In this area, groundwater flows through the limit of the hydrological basin and leaves the Geer basin, as highlighted by the hydrogeological water budget and the piezometry.

4.2.3.5 Hydrogeological water budget

Two hydrogeological water budgets were calculated for the Geer basin, respectively for the period 1951-1967 (Monjoie 1967) and 1975-1995 (Hallet 1998). The hydrogeological balance can be expressed using the following formula:

$$P = E + D + Q + \Delta S + L \quad \textbf{(4.1)}$$

where P is the mean annual precipitation [L]; E is the mean annual true evapotranspiration [L]; D is the mean annual discharge of the Geer river at the outlet of the basin [L]; Q is the mean annual volume of groundwater abstracted in the Geer basin [L]; ΔS is the variation in groundwater storage over the period over which the budget is calculated [L]; L represent the losses [L] including the sum of errors in the estimation of the different terms of the budget and groundwater leaving the hydrological basin through its Northern boundary.

Applying Equation (4.1) to the observed data of period 1951-1964 gives a balance of:

$$\begin{aligned} &740 \text{ mm} = 525 \text{ mm} + 120 \text{ mm} + 65 \text{ mm} + 15 \text{ mm} + 15 \text{ mm} \\ &100 \text{ \%} = 71 \text{ \% mm} + 16 \text{ \%} + 9 \text{ \%} + 2 \text{ \%} + 2 \text{ \%} \end{aligned} \quad \textbf{(4.2)}$$

Applying Equation (4.1) to the observed data of period 1975-1994 gives a balance of:

$$\begin{aligned} &810 \text{ mm} = 508 \text{ mm} + 145 \text{ mm} + 88 \text{ mm} + 7.5 \text{ mm} + 61.5 \text{ mm} \quad \text{or} \\ &100 \text{ \%} = 63 \text{ \% mm} + 18 \text{ \%} + 11 \text{ \%} + 1 \text{ \%} + 7 \text{ \%} \end{aligned} \quad \textbf{(4.3)}$$

A comparison between these two water budgets shows:

- the period 1975-1994 was more rainy than the period 1951-1964 resulting in a higher discharge at the outlet of the basin;
- the extracted volume of groundwater has increased by more than 35% between the two considered periods;
- the losses have also increased between these two periods.

This increase in the losses could be explained, at least partly, by the development of the pumping activities in the confined part of the chalk aquifer, in the adjacent basin located to

the North of the Geer basin, resulting in increased groundwater transfer through the Northern boundary of the basin.

Based on statistical analysis of mean annual climatic data and hydrographs at the outlet of the basin, Hallet (1998) proposed an empirical formula to estimate the mean annual infiltration I [L] in the Geer basin.

$$I = 0.845\,P - 422 \quad \textbf{(4.4)}$$

where I is the mean annual direct infiltration [L]; P is the mean annual precipitation [L]

4.2.3.6 Hydrodynamics of the chalk aquifer

The hydraulic conductivity and the porosity of the chalk vary strongly in function of the scale of observation (Dassargues and Monjoie 1993):

- at the microscopic scale (a few centimetres), the chalk is a porous compact material (porosity of 40 %) in which groundwater can only flows very slowly (hydraulic conductivity around 1 x 10^{-9} m/s);
- at the macroscopic scale (a few tens of metres), fissures networks are observed. They increase notably the hydraulic conductivity of the chalk (hydraulic conductivity around 1 x 10^{-4} m/s). The effective porosity associated to these fissures is around 5 % of mobile water;
- at the scale of the aquifer, rocks are fractured by tectonic accidents. Up to these faults, often located below dry valleys, the hydraulic conductivity of the chalk could be high (around 1 x 10^{-3} m/s) and the effective porosity could be around 10 to 15 %.

Values of hydraulic conductivity can be found in different studies (Dassargues and Monjoie 1993; Dautrebande *et al.* 1996; Hallet 1998; Brouyère 2001). These values range from 1×10^{-9} to 1×10^{-7} m/s, from 1×10^{-4} to 5×10^{-3} m/s and from 1×10^{-5} to 5×10^{-4} m/s for the loess, the Maastrichtian upper chalk and the Campanian lower chalk respectively. Hydraulic conductivity values for the chalk being essentially obtained by performing pumping tests, these values are representative of large volume of aquifer. The spatial distribution of the pumping tests performed in the chalk (Figure 4.7) allows having a good representativity of the whole aquifer.

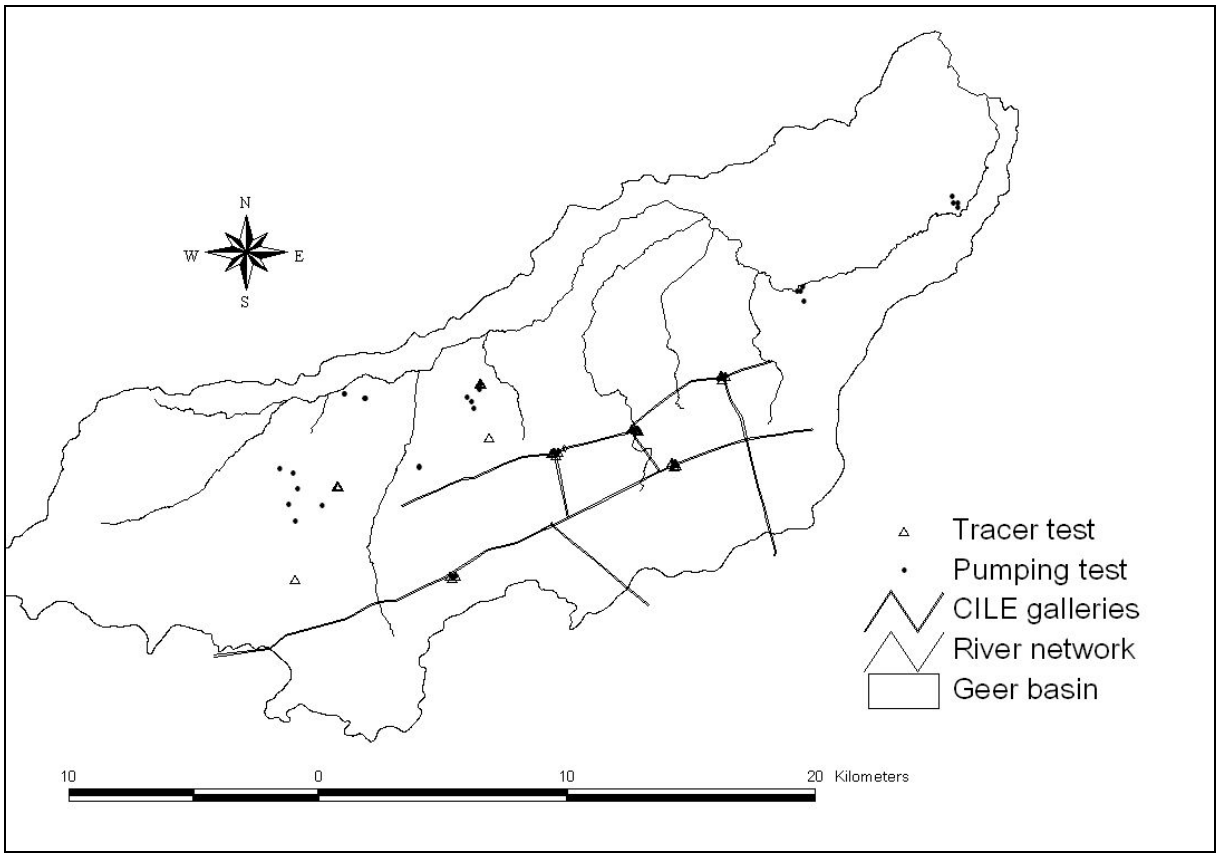

Figure 4.7. Location of the pumping tests and tracer tests performed in the Geer basin (information extracted from the hydrogeological database of the Administration of the Walloon region, 2006)

4.2.3.7 Hydrodispersive properties

Hallet (1998) compiled results of different tracer tests performed in the saturated chalk in the framework of the determination of protection zones around the different pumping wells and galleries (Table 4.1). Numerical modelling of these tracer tests allowed determining hydrodispersive parameters for the chalk.

Location	Chalk type	Porosity of mobile water $\theta_{m,evr}$ (%)	Longitudinal dispersivity α_L (m)	Porosity of immobile water θ_{im} (%)	Transfer coefficient between mobile and immobile water α (1×10^{-7} s^{-1})
Bertrée	Slightly fractured	1.0	0.15	15	1.5
	Fractured	2.5	2.0	20	3.0
	Very fracture	7.5	4.0	30	10.0
Crisnée	Slightly fractured	0.5 to 1.5	2.5 to 3.2	10 to 19	1.2 to 3.7
	Fractured	1.0 to 2.7	3.2 to 5.0	13 to 24	2.5 to 6.7
	Very fractured	1.5 to 5.3	5.0 to 7.0	18 to 31	5.0 to 7.9
Orp Jauche	Fractured	2.9	50	nd	nd
Fize	Heterogeneous	1.0 to 4.0	35	25	0.98
Bovenistier	Karstified	1.0 to 2.0	15	10	0.1
	Wheathered	0.6 to 1.0	10 to 15	10	2.0
Viemme	Wheathered	0.06	20	10	0.1
Jeneffe	Matrix	0.3 to 0.6	8 to 60	nd	nd
	Fractured	2.4	7	nd	nd
Waroux	Matrix	3.2	50	nd	nd
	Fractured	0.2 to 0.58	5 to 7	nd	nd
Kemexhe	Fractured	0.005 to 0.1	2.6 to 4.5	nd	nd
Xhendremael	Fractured	0.15 to 3.0	1.0 to 6.5	nd	nd
Juprelle	Fractured	0.02 to 0.6	1 to 10	nd	nd
Wonck - Roclenge	Fractured	0.3 to 1	3 to 10	nd	nd

Table 4.1. Estimated values of hydrodispersive properties (modified from Hallet 1998), nd corresponds to parameters not taken into account in the code used for the interpretation.

The scale dependence of the dispersivity coefficient is well described in literature (see Chapter 2). Hallet (1998) showed that the values of longitudinal dispersivity obtained by the interpretation of tracer tests performed in the chalk of the Geer basin confirm the scale dependence of the dispersivity coefficient (Figure 4.8).

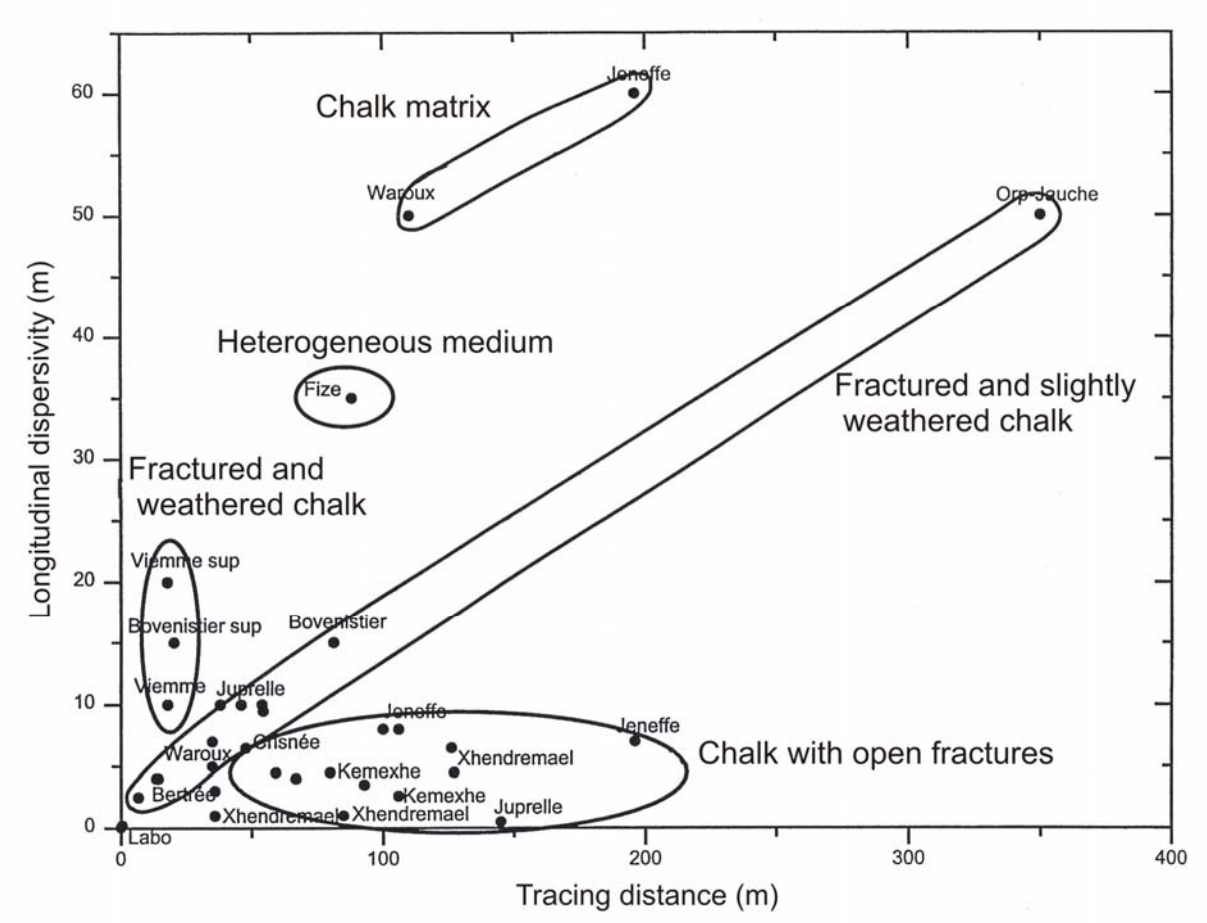

Figure 4.8. Variations of the dispersivity values in function of the distance between the injection well and the pumping well (from Hallet 1998)

4.2.3.8 Data on the unsaturated zone

Between 1998 and 2001, a pilot-site investigation, financed by the Walloon region, was performed at Bovenistier, for studying groundwater and nitrate recharge processes across the thick unsaturated zone overlying the Hesbaye chalk aquifer. Various laboratory measurements were performed on core samples collected during the drilling of borehole in the experimental site. In the field, experiments consisted in well logging, infiltration tests in the unsaturated zone, pumping tests in the saturated zone and tracer tests in both the saturated and unsaturated zones (Brouyère 2001; Brouyère *et al.* 2004a).

In the loess, water recharge mechanisms are dominated by gravitational flow, without evidence of preferential flows. The average velocity of solute downward migration is very low, estimated to 1 m/year (Dautrebande *et al.* 1999). Because of the presence of the loess layer, the water infiltration rate at the top of the unsaturated chalk is attenuated and not sufficient to keep the fractures fully saturated. Water infiltrates slowly downwards across the matrix and solutes migrate at a velocity of the order of 1 m/year, this solute transport being strongly influenced by the low hydraulic conductivity and the large porosity of the matrix (Brouyère *et al.* 2004a).

4.2.3.9 Hydrogeochemistry

The hydrogeochemical facies of groundwater in the Hesbaye aquifer is bicarbonate calcite with a hardness ranging from 35 to 45 °F. For years now, the water companies exploiting the aquifer have observed an increasing influence of man activities and more particularly a slow but constant increase in nitrate content and apparition of pesticides in groundwater of the Hesbaye aquifer. More information on the nitrate contamination will be provided in section 4.3.

4.3 Nitrates in the Geer basin

The Hesbaye aquifer has been identified as the most affected groundwater body by agricultural pressure in the Walloon Region (DGRNE 2005). The Hesbaye aquifer has also been designated as vulnerable to nitrates in the sense of the European Nitrate Directive (91/676/CEE). As a consequence, several studies have been performed to understand the origin of the nitrate contamination in the chalk aquifer of the Geer basin, its spatial distribution, its temporal evolution and the mechanisms of nitrate propagation in the chalk (Biver 1993; Dautrebande *et al.* 1996; Hallet 1998; Brouyère 2001; Batlle Aguilar *et al.* 2007 among others). This chapter presents a synthesis of the main results of these previous studies.

4.3.1 Characterisation of nitrate pressure on groundwater

Agriculture is the dominant activity in the Geer basin (DGRNE 2005). Crops and pastures cover 83 % of the surface of the Geer basin (Figure 4.9). According to Dautrebande and Sohier (2004), agriculture represents the main source of nitrate loads, followed by domestic sources (contributions of respectively 88% and 12%).

Farms located in the Geer basin have mainly specialised in field crops and cattle (dayring and fattening). In 2005, cereals and industrial crops (sugar beets, flax and chicory) represented the main part of the agricultural land use (41% and 29% respectively). Pastures use about 14% of agricultural land. Figure 4.10 shows the evolution of agricultural land use from 1997 to 2005, with a decrease in pasture area (-11%), cereals (-91%) and sugar beet (-16%), while other industrial and horticultural crops area increased (flax: +48%, chicory: +105%, horticulture: +96%) during the same period.

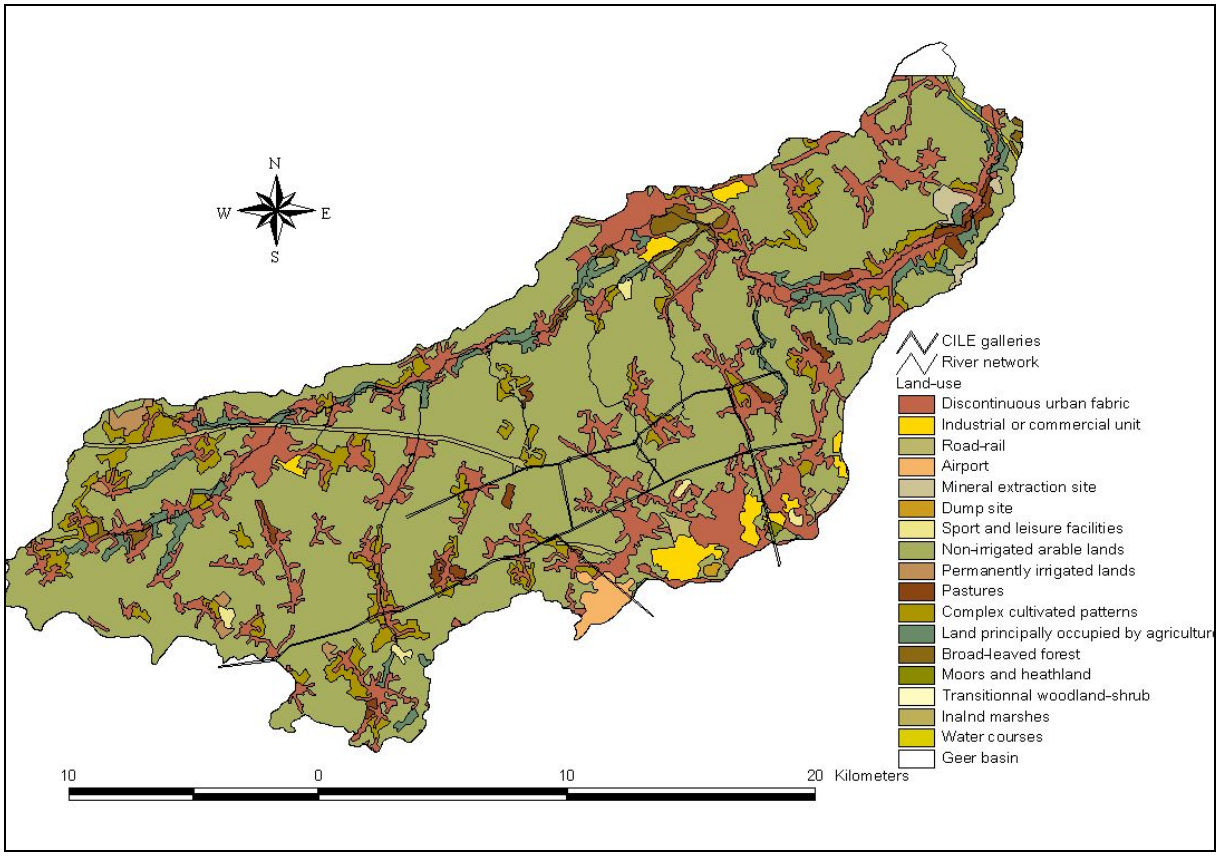

Figure 4.9. Land-use in the Geer basin (based on CORINE database, data provided by DGRNE)

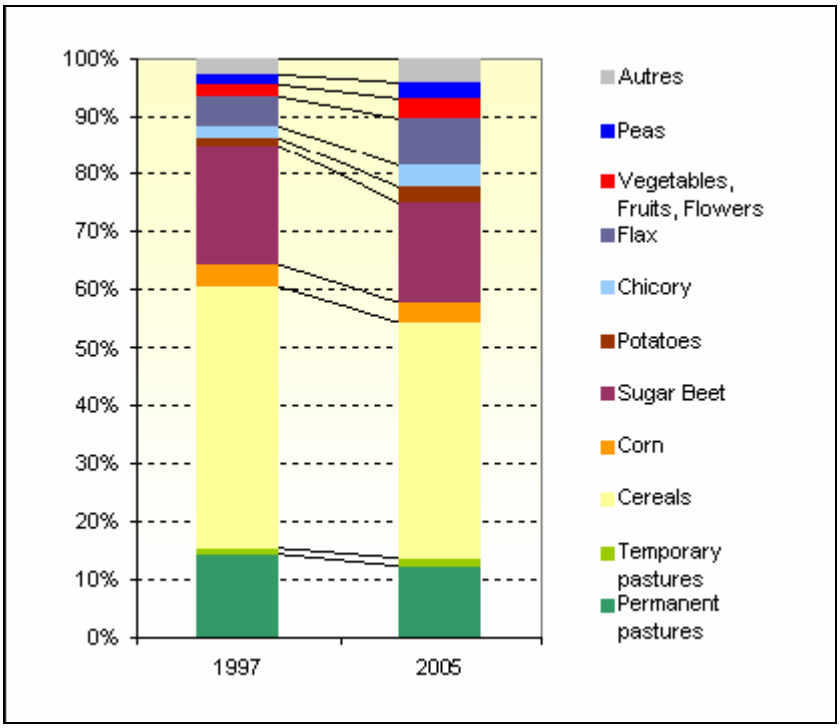

Figure 4.10. Crops and pastures evolution from 1997 to 2005 on the Geer basin (Source: Department of Environmental Sciences in Arlon, University of Liege)

As in other European countries, the use of fertilizers in agriculture started to increase in Belgium at the beginning of the fifties to reach a peak in the eighties (Figure 4.11). More details about the evolution of nitrogen load in Belgium and in the Geer basin can be found in Broers *et al.* (2005a). There is no direct relationship between nitrogen load on crops and nitrate concentration leaching to groundwater. Different factors can affect the fate of nitrogen spread on the land such as the meteorological conditions, the kind of crop and the crop rotation. Different kinds of approaches can be used to estimate the nitrate fluxes to groundwater, among them: (1) a soil model approach or (2) an empirical approach based on statistics. These nitrate fluxes will be used as an input for the groundwater model.

Nitrate fluxes to groundwater resulting from environmental pressures on soil were evaluated for most watersheds in the Walloon region using the semi-distributed model EPICgrid (Dautrebande and Sohier 2004) as part of the PIRENE project. Using a resolution of 1 km^2, the model simulates crop growth and agricultural practices (Dautrebande and Sohier 2001; Broers *et al.* 2005a). The simulated fluxes include direct runoff, groundwater recharge, subsurface lateral flows, real evapotranspiration, nitrate fluxes. The model is considered, by its authors, as physically-based, but without calibration. The model also simulates the transfer of water and nitrate through the unsaturated zone. In the framework of the PIRENE project,

water and nitrate fluxes to groundwater were computed at a "mean" groundwater depth. Based on historical meteorological data and agricultural statistics, simulations were performed for the period 1970-2000. These modelling results predict that, at the end of the nineties, more than 73% of the Hesbaye aquifer surface is affected by NO_3 concentration exceeding 50 mg/l in leaching waters.

On the basis of land use maps (for example, the CORINE project, Copyright EEA, Copenhagen, 2007) and on agricultural statistics (published by the Agricultural Centre of Economics or the National Institute of Statistics), it has been possible to estimate the temporal evolution of the nitrogen loads to crops (Figure 4.11). Based on simplifying assumptions, it is possible to estimate the temporal evolution of the mean nitrate concentrations in water fluxes seeping beneath the crops. In the framework of the European FP6 AquaTerra project, Herivaux (2008) has estimated the mean nitrate concentration in leaching water to 67 mg/l under agricultural land in 2005 in the Geer basin, on the basis of agricultural statistics and standard nitrate emission rate per type of crop (AERM 2005).

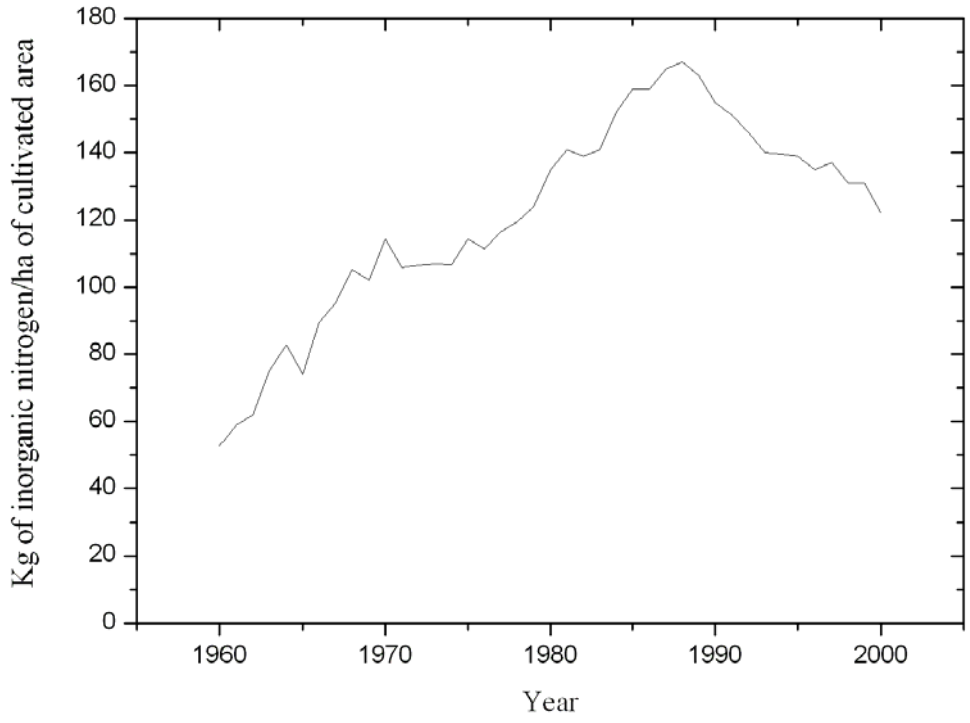

Figure 4.11. Evolution of the consumption of inorganic nitrogen in Belgium (data from "Centre Economie Agricole")

4.3.2 Spatial variations in nitrate concentrations in the Geer basin

Hydrogeological conditions prevailing in the chalk aquifer change from unconfined in the Southern part of the basin to confined conditions in the Northern part. Nitrate concentrations observed in the chalk aquifer of the Geer basin (Figure 4.12) seem closely related to these hydrogeolocical conditions. Hallet (1998) distinguished three zones in the spatial distribution of nitrate concentrations related to these hydrogeological conditions :

- the South of the basin, corresponding to the unconfined part of the aquifer in agricultural zone where high nitrate concentrations are observed (close or even over the drinking limit of 50 mg/l);
- the semi-confined part of the aquifer located along the Geer river and in the East of the basin, where lower nitrate concentrations are observed (around 25 mg/l);
- the North-West of the basin, where the aquifer is confined under Tertiary sediments, where nitrate concentrations are very low or even not detected.

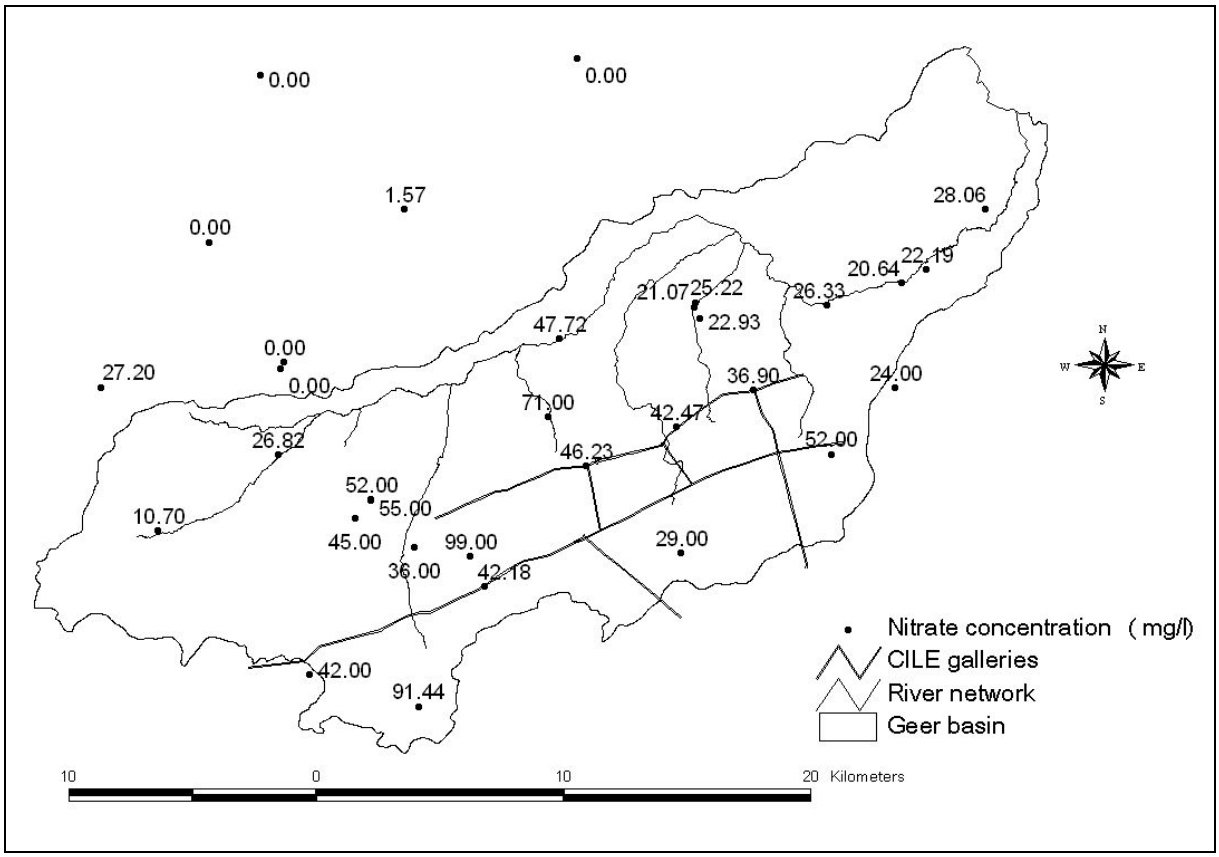

Figure 4.12. Nitrate concentrations observed in 2005 in the Hesbaye aquifer (survey performed between January and April)

Besides this classification in three zones, wells with high nitrate concentration up to 99 mg/l can be found in the unconfined part of the aquifer in the survey performed in 2005. Hallet (1998) showed that these high concentrations are generally associated with shallow wells and with local point-source contaminations.

In the aquifer, samples taken at different depths at the Bovenistier test sites of the Belgian Geological Survey (SGB) allowed also detecting a decrease in nitrate concentrations with depth (Hallet 1998). Unfortunately, for a large number of wells or piezometers located in the Geer basin, the depth of the wells and/or the exact location of the screens remain unknown. Deducing a relation between nitrate concentrations and depths of sampling is thus difficult and most of the samples represent depth averaged concentrations.

4.3.3 Time evolution of the nitrate contamination

4.3.3.1 Periodic variations in nitrate concentrations

Datasets from the aquifer of the Geer basin exhibit clear periodic variations in nitrate concentrations (Figure 4.13). As discussed by Brouyère *et al* (2004a) and Fretwell *et al.* (2005) among others, such periodic variations are explained by groundwater table fluctuations in the variably saturated dual-porosity chalk. In principle, nitrates spread over the land surface by the use of N-rich fertilizers progressively infiltrate in the unsaturated zone and migrate slowly, downwards through the partially saturated chalk matrix. Under low groundwater level conditions, the nitrate contamination front can be considered as disconnected from the saturated zone of the aquifer and nitrate concentrations in the saturated zone tend to decrease because of dispersion and mixing processes in groundwater. When groundwater levels rise, the contamination front is quickly reached and washed: the contamination source is re-activated and nitrate concentrations are likely to increase rapidly in the saturated zone.

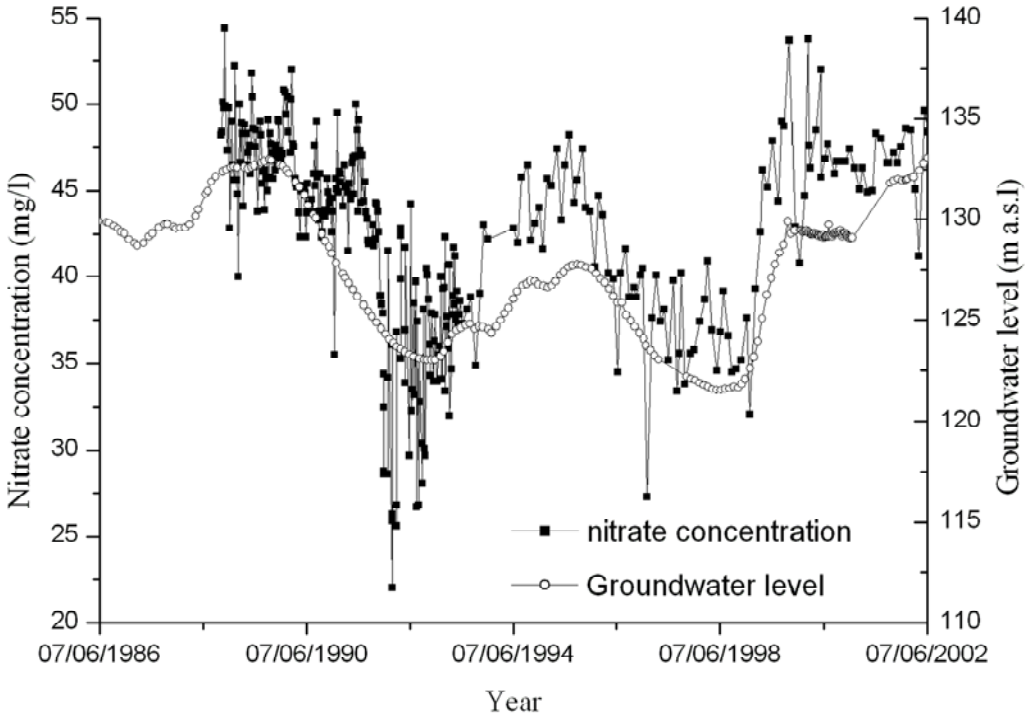

Figure 4.13. Comparison between nitrate concentrations observed in the well of Lantin and groundwater level measured in the piezometer of Viemme (source: DGRNE database).

4.3.3.2 Long-term time evolution of the nitrate contamination

For years now, drinking water supply companies have observed a general global increase in nitrate concentration in the Geer basin. In particular, Hallet (1998) showed that :

- nitrate concentration in the fifties were around 15 mg/l in the Hesbaye aquifer;
- between 1976 and 1998, nitrate content increases by 0.3 mg/l and by 0.7 mg/l respectively in the semi-confined and unconfined part of the aquifer.

In 2007, a statistical approach was applied for trend detection and quantification in groundwater quality (nitrate) datasets in the Geer basin, based on a three-step statistical analysis methodology (see Chapter 2) consisting in (1) analysing the normality of the dataset, (2) detecting the presence of an upward or downward trend or not, (3) quantifying the detected trend (Broers *et al.* 2005b; Batlle Aguilar *et al.* 2007). For this study, 24 groundwater sampling points (Figure 4.14) were selected among the 54 sampling points listed in the groundwater database of the Walloon region and of the VMW for points to the North of the basin (Flemish region). These points were selected because they have been considered as

containing suitable records for statistical trend analysis (i.e. a minimum of 10 nitrate records over time, period of measurement covering more than one periodic variation in nitrate concentration (see Section 4.3.3.1). Nitrate datasets coming from groundwater sampling points located to the North of the basin were not considered as nitrate were not detected there yet (or at very low concentrations only). Samples points H-19 and H-20 correspond to water reservoir tanks storing groundwater drained by the galleries. Even if these reservoirs are not water works located in the aquifer, the nitrate concentrations measured in these two points were analysed because they constitute interesting aggregation points, representative of most of the groundwater in the Hesbaye aquifer, at least of a large portion of the aquifer drained by the subsurface galleries.

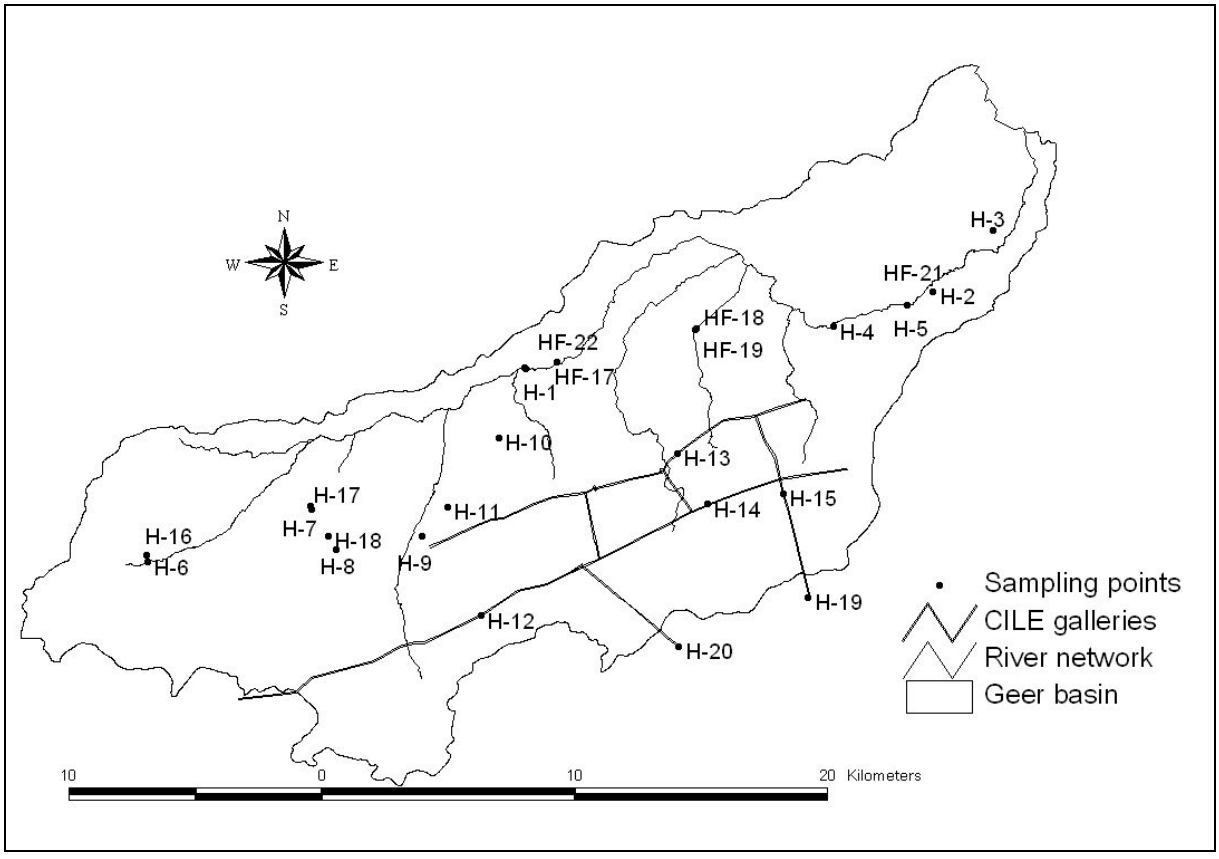

Figure 4.14. Location of sampling points used in the nitrate trend analysis performed by Batlle-Aguilar *et al.* (2007).

The statistical analysis provided point-by-point estimates of nitrate trends, in the form of slopes expressed by an increase or a decrease in nitrate concentration per year. This analysis confirmed, from a statistical point of view, that a general upward trend is observed in the entire Geer basin (Figure 4.15). The spatial distribution of the statistically computed trends can be pointed out. Low values of the trend slopes (around 0.25 - 0.30 mg/l.y) are found for

sampling points located in the Eastern part of the basin. Higher values (between 0.4 and 0.8 mg/l.y) are found for sampling points located in the Southern part of the Hesbaye aquifer. This spatial distribution is in good agreement with observations made by Hallet (1998) even if the slopes computed here are generally lower than the values proposed by Hallet.

Several monitoring points do not show any evidence of upward or downward nitrate trend. They generally correspond to sampling points with limited nitrate records, irregularly distributed in time. In addition, nitrate trend estimates at points H19 and H20 have to be considered with caution and are difficult to interpret because these two points are not abstraction points but correspond to water reservoirs fed by groundwater abstracted in the galleries. The company exploiting the galleries does not take all the groundwater drained by the galleries. Due to the different location and depth of these two galleries, nitrate concentrations are lower in the Northern gallery than in the Southern one. The water company is mixing thus groundwater from both galleries to feed the reservoirs with the three following objectives: (1) to meet the demand of drinking water; (2) to maintain nitrate concentration in the reservoirs below the drinking limit; and (3) to minimize operating costs, the running costs associated to the groundwater extracted in the Northern gallery being higher. In the future, the proportion of groundwater coming from the less contaminated Northern gallery could be increased.

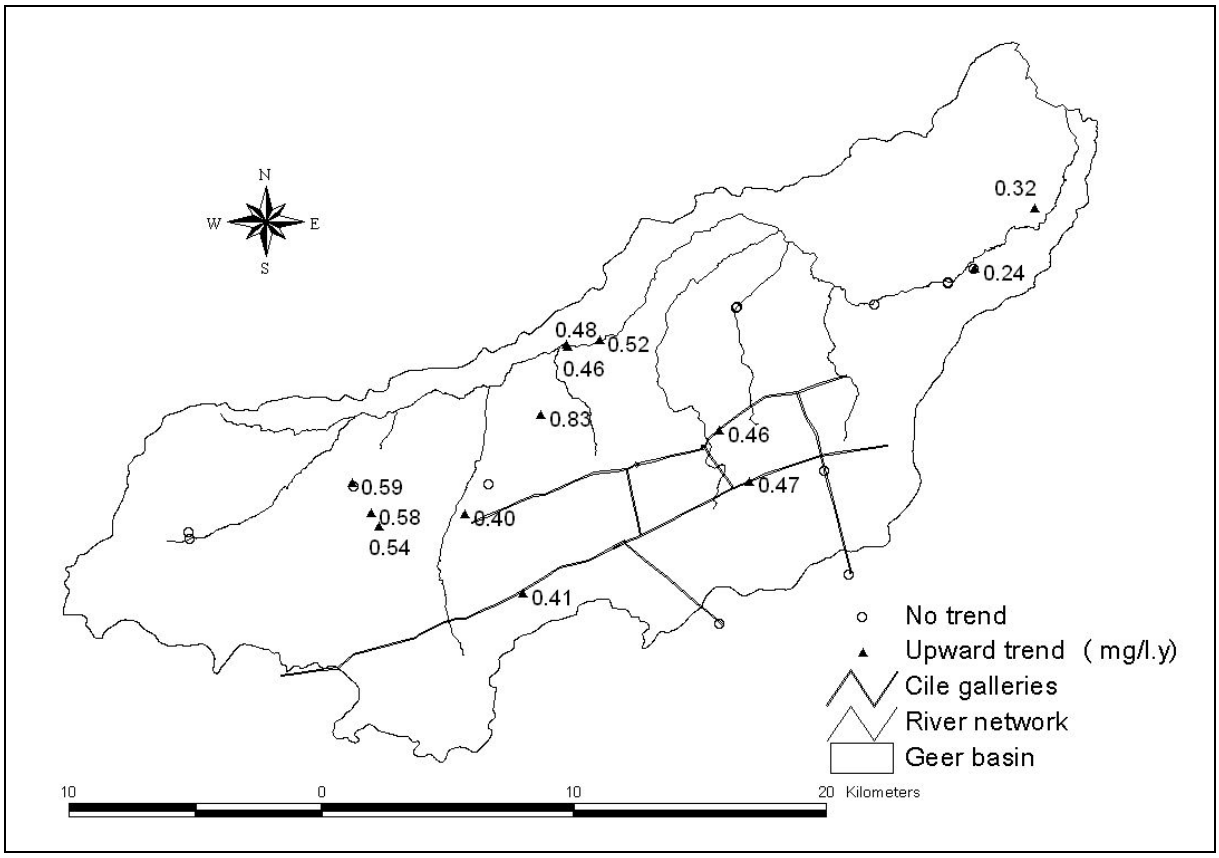

Figure 4.15. Values of the slope of the nitrate trend calculated by Batlle-Aguilar *et al.* (2007).

4.3.4 Discussion on nitrate contamination

Large spatial and vertical variations in nitrate concentration have been highlighted in the previous sections. These spatial gradients of nitrate concentrations can be the result of three phenomena (Landreau *et al.* 1988; Hallberg and Keeney 1993): (1) mixing with less polluted water, (2) differences in the age of groundwater, (3) denitrification processes. Concerning the vertical gradient of nitrate concentrations observed at the SGB Bovenister site in the unconfined part of the aquifer, Hallet (1998) proposed an explanation based on hydrodynamics. Denitrification can not indeed occurs as the concentration in dissolved oxygen are too high (around 4 mg/l) and electron donors such as organic matter and pyrite are mostly absent (Hallet 1998). The vertical gradient of nitrate concentrations could rather be related to subhorizontal fluxes, generated by the decreasing permeability with depth, confining the pollution in the upper part of the aquifer.

The absence (or presence at very low concentration) of nitrate in the confined part of the aquifer (to the North of the Geer basin) is not yet clearly explain. The natural background of nitrate in groundwater in the absence of denitrification is around 5 mg/l of nitrate.

Denitrification should thus occur in the confined part of the aquifer. Nowadays, no evidence of denitrification has been observed. Recently, the VMW exploiting wells located in this part of the aquifer has observed nitrate concentration slightly above the detection limit. This could be due to the arrival of nitrate contaminated groundwater. Actually, the increasing pumping rate to the North of the Geer basin in the confined part of the aquifer seems to increase the transfer of groundwater across the Northern boundary of the Geer hydrological basin as highlighted by the comparison between the two water budgets performed for the period 1951-1964 and 1975-1994.

To go further in the understanding of the spatial distribution of the nitrate contamination in the Geer basin, a tritium survey was performed in 2005, followed in 2007 by a CFC's and SF_6 survey to study and evaluate the age of groundwater in the Geer basin. A description and results of these surveys are presented in the next section.

The trend analysis performed using statistical tools confirms the trend in nitrate concentrations in the Geer basin. The main questions are related to the time remaining before reaching the drinking water limit, or when the trend could be reversed as a result of a stabilisation or decrease in fertiliser load used in agriculture. Statistical techniques do no allow identification of trend reversal (see Chapter 2). They are usually not used as prediction tools because they can not consider possible changes in the inputs. Because of that they can not be used to compare the effects of changes in agricultural practices. Modelling tools are much more appropriate to answer these questions. The groundwater flow and solute transport model developed in the framework of this work has allowed giving first answers to these fundamental questions in terms of management of the groundwater resource (see Section 4.5).

4.4 Survey on environmental tracers

The previous section has led to the conclusion that questions remain about the spatial distribution of the nitrate contamination. Regarding the problematic of diffuse pollution, different authors (Broers 2004; Koh *et al.* 2006 among others) highlighted the importance of the age of water as a key factor explaining the solute distribution in groundwater. On the one hand, it is futile to compare pollutants concentrations in time scale that could be very different, on the other hand, it is interesting to correlate the absence of contaminant with the age of water in some zones of the aquifer, in particular to determine if the absence of nitrate is

due to the fact that the groundwater was infiltrated before 1960, period prior the increase of nitrogen load in agriculture or if it is due to other phenomena such as denitrification.

Thanks to a co-funding of the Administration of the Walloon region ("Direction des Eaux Souterraines, Direction Générale des Ressources Naturelles et de l'Environnement (DGRNE)"), tritium, CFC's and SF_6 surveys were performed in the chalk aquifer of the Geer basin, in the scope of this research.

4.4.1 Materials and methods

4.4.1.1 Sampling network

Samples were taken in the unconfined and the confined part of the aquifer. 34 sampling points, located in the Walloon region, were chosen among the set of points identified in the database of the DGRNE on the basis of the following criteria:

- spatial distribution of the sampling points;
- depth of sampling (depth of the well, location of the screens);
- existence of nitrate data;
- accessibility and possibility of sampling;
- wishes expressed by the DGRNE.

This network has been extended to the North of the Geer basin in the confined part of the aquifer that extends in the Flemisch region of Belgium, under the Tertiary sandy-clayey formations. Sampling points in this part of the aquifer are wells or piezometers belonging to VMW.

Table 4.2 presents the main characteristics (geology, well depths, screens locations …) of each of the 34 groundwater sampling points. The depth of the wells and the location of the screens are known only for some sampling points while this information is often of primary importance during the preparation of the sampling survey or the interpretation of the results. If the depth and the location of screens remain unknown, it is impossible to know from which depth the sampled groundwater is pumped. Actually, many studies have proven that, in chalk aquifers important vertical variations in groundwater chemistry can exist (Barrez 2006 among others). The samples are assumed to be representative of "depth averaged condition", groundwater being pumped from the entire screened zone.

A surface water network made of 10 sampling points located in the Geer river or in springs directly in the vicinity of the river has been defined. The sampling points have been chosen in function of the accessibility of the sampling sites and with the objective to sample along the whole river.

Three field surveys of water sampling for analysis of environmental tracers were organised. During the first one, performed between February and May 2005, 34 samples (referred to as samples 1 to 34 hereafter) were taken in the Hesbaye aquifer by the Hydrogeology Group of ULg and by the "Institut Scientifique de Service Public" (ISSeP) for tritium analysis. During the second sampling survey in November 2005, ten samples (referred to as samples 35 to 44 hereafter) were collected in the surface water for tritium analysis from the Geer basin assuming that a recession period was prevailing, so that the majority of surface waters come from the underground medium. During the third survey in April 2007, six samples (referred to as samples 45 to 50 hereafter) were taken in the Hesbaye aquifer for tritium, CFC's and SF_6 analysis in different wells already sampled during the first tritium survey. The pump installed in one of the selected point (Bovelingen 1) was out of work. The sample (number 46) has been taken in the nearest well (Bovelingen 7) showing the same characteristics of depth and screen location.

Figure 4.16 shows the location of all the sampling points in the Geer basin.

4.4.1.2 Sampling procedures

For groundwater sampling, permanently installed pumps or pumps placed for the sampling were used. Groundwater samples were collected at the pumping taps after stabilisation of physico-chemical parameters (electrical conductivity, pH, temperature). Samples for tritium analysis were stored in 100 ml-HD double capped polyethylene flasks. Samples for major ions analysis were stored in 180 ml-polystyrene flasks. Samples for CFC's and SF_6 analysis were collected without atmospheric contact in 1 litre-glass bottles contained within metal cans by the "displacement method". This method insures that the sample is protected from possible atmospheric contamination by a jacket of the same water (Gooddy *et al.* 2006).

Samples taken in the surface water network were taken manually and stored in the same kind of flasks than the groundwater samples.

Sample number	Name	Type	Depth (m)	Top of the screens (m)	Bottom of the screens (m)	Aquifer
1	Zepperen 2	Pumping well	117.1	--	--	Confined
2 – 45	Vliermaal 1	Pumping well	96.00	44.55	94.05	Confined
3	Alst-bij-Simt-Truiden	Pumping well	102.4	--	--	Confined
4	Voort 3	Piezometer	54.5	16.6	53.6	Confined
5	Montenaken Klein Vorsen 2	Pumping well	77.9	43.5	77.0	Confined
6	Bovelingen 1	Pumping well	92.5	18.6	52.0	Confined
7	Bovelingen 3	Piezometer	95.0	14.0	18.0	Confined
8	Lauw	Pumping well	33.5	13.0	31.5	Unconfined
9	Diets Heur 2	Pumping well	66.5	32.5	68.5	Unconfined
10	Diets Heur 6	Piezometer	15.3	10.3	15.3	Unconfined
11	Diets Heur 7	Piezometer	46.1	41.1	46.1	Unconfined
12	Bassenge	Pumping well	8.45	--	--	Unconfined
13	Roclenge	Pumping well	30.0	15.0	29.0	Unconfined
14	SGB-1	Piezometer	44.4	30.0	40.0	Unconfined
15	SGB-2	Piezometer	16.0	9.0	16.0	Unconfined
16	SGB-3	Piezometer	26.0	16.0	26.0	Unconfined
17 – 47	JEN083	Private well	28.2	--	--	Unconfined
18 – 48	PC-Bovenistier	Piezometer	49.0	--	--	Unconfined
19	PzCS-Bovenistier	Piezometer	34.2	--	--	Unconfined
20	Zone Fret 1	Piezometer	48.0	--		Unconfined
21	Tous Saint	Private well	40.0	--	--	Unconfined
22	P4 + P5	Private well	--	--	--	Unconfined
23	Rondoval	Private well	--	--	--	Unconfined
24	CHS 077	Private well	24.6	--	--	Unconfined
25	LIM 001	Private well	28.3	--	--	Unconfined
26	Abbaye LIE-17	Private well	36.0	--	--	Unconfined
27 – 49	P1-Eben.Mael	Pumping well	--	--	--	Unconfined
28	Pz1-Bas-Slins	Piezometer	44.5	20.5	43.3	Unconfined
29	Rue de la Station 39	Private well	10.0	--	--	Unconfined
30 – 50	Pêcherie Waremme	Private well	25.0	--	--	Semi-confined-
31	Galerie Xendremal	Gallery	--	--	--	Unconfined
32	Galerie Juprelle	Gallery	--	--	--	Unconfined
33	Galerie Kemexhe	Gallery	--	--	--	Unconfined
34	Galerie Jeneffe	Gallery	--	--	--	Unconfined
46	Bovelingen 7	Pumping Well				Confined

Table 4.2. Characteristics of the groundwater sampling points (pumping wells belongs to water supply companies and large volume of groundwater are abstracted, private wells refer to wells, often of large diameter belonging to inhabitants or private companies and the volume of abstracted groundwater is small).

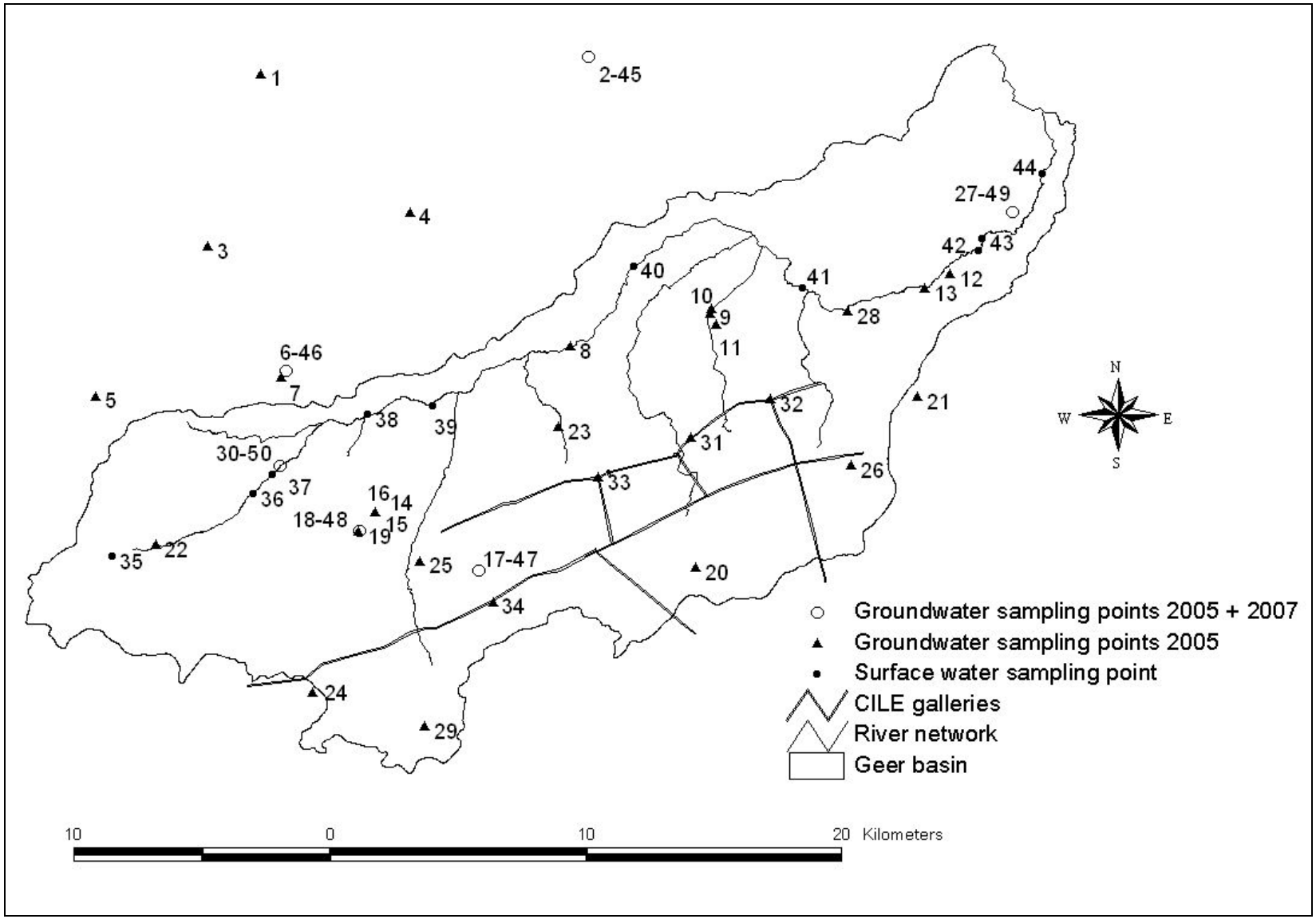

Figure 4.16 Location of the sampling points of the tritium, CFC's and SF_6 surveys (labels correspond to the sample numbers)

4.4.1.3 Analysis procedure

Samples taken for tritium analysis were sent to the Laboratory of Environmental Isotopy (Prof P. Maloszewski, Dr W. Stichler) of GSF-Institute of Groundwater Ecology in Munich (Germany). Tritium concentrations were determined by measuring Beta radiation emitted during the degradation of tritium into helium. As it is difficult to determine absolute specific activity, measures are compared to those done in the same conditions for a reference sample. As the water tritium content is relatively low, the measurement has to be performed for some months.

Samples taken for CFC's and SF_6 analysis were sent to the Trace-Gas-Laboratory (Dr. H. Oster, Wachenheim, Germany). CFC's and SF_6 measurements followed the methods described by Oster *et al.* (1996). After degassing of the samples and preconcentration of the gases, concentrations were measured by isothermal chromatography. The detection limit are close to 1×10^{-4} pmol and 1×10^{-3} fmol[1] for respectively CFC's and SF_6 allowing the measurements of CFC's concentrations down to 0.01 pmol and 0.1 fmol for respectively CFC's and SF_6.

Major elements were analysed either by the Chemistry laboratory of ISSeP either in the Laboratory of Water Analysis of HGULg for samples taken by ISSeP and HGULg respectively.

Results of the analyses are presented in Table 4.3, Table 4.4 and Table 4.5 for the 2005 sampling survey in groundwater, the 2005 survey in surface water and the 2007 survey in groundwater respectively.

[1] pmol and fmol are equal to 1×10^{-12} and 1×10^{-15} moles respectively

4.4.2 Results and interpretation

4.4.2.1 Tritium in groundwater

Tritium concentrations measured in samples taken in the Hesbaye chalky aquifer during the 2005 and 2007 surveys range from the detection limit to 14.7 TU (Table 4.3 and Table 4.5). Waters of different ages coexist thus inside this aquifer. Roughly, three zones can be distinguished from the tritium concentrations (Figure 4.17)

- A zone in the North of the basin (confined part of the Hesbaye aquifer) where tritium concentrations are very low, close to 1 TU. Such concentrations are characteristic of water infiltrated before 1960.
- A zone in the South-West of the basin where tritium concentrations are higher, ranging from 5 to 14 TU. Such concentrations are usually characteristic of water infiltrated after 1960.
- A zone located in the East and North-East of the basin where tritium concentrations range from 2 to 6 TU. These concentrations are probably characteristic of mixing between water infiltrated before and after the sixties.

These three zones can also be distinguished in the spatial distribution of nitrate concentrations (Figure 4.18):

- In the North of the basin, nitrate concentrations are equal to zero or very low.
- In South-Western part of the aquifer, nitrate concentrations range from 30 to 90 mg/l. These high values are indicators of a recent contamination by agriculture.
- In the Eastern part of the Geer basin, nitrate concentrations are close to 25mg/l.

Samples 6 and 7 taken in the confined part of the aquifer show the particularity to have tritium content (respectively 7.9 and 10.1 TU) characteristic of young water but nitrate concentrations equal to zero.

The relatively good correspondence between the spatial distributions of tritium and nitrate in the basin allows one to propose the following interpretation:

- In the confined part of the aquifer (North of the Geer basin), groundwater is still uncontaminated because it has not been reached yet by the nitrate contamination front.

- The South-West of the Geer basin mostly corresponds to the recharge zone of the aquifer, with younger, more contaminated groundwater.
- The North-Eastern and Eastern part of the Geer basin corresponds to the discharge zone of the aquifer (in particular in the Geer River), with a mixture of old groundwater that have flowed all across the aquifer and recent groundwater "directly" recharged in the area.

A comparison between tritium concentrations measured in samples taken in the Hesbaye chalky aquifer during the 2005 and 2007 surveys shows that these concentrations are more or less similar (Figure 4.19). In Figure 4.19, tritium concentrations above 5 TU seem to decrease over time while low tritium concentrations (under 5 TU) seem to increase. As a first assumption, it can be admitted, that at locations where high tritium concentrations are observed, the maximum concentrations have already been reached and tritium concentrations are now decreasing. At locations where low concentrations are observed, low concentrations have still to be reached. More sampling points and the repetition of sampling over time would allow confirming this assumption.

Sample number	^{3}H (TU)	Sp.Elec. Cond. ($\mu S \cdot cm^{-1}$) (laboratory)	pH	Total hardness (°f)	Ca^{2+} (ppm)	Mg^{2+} (ppm)	Na^{+} (ppm)	K^{+} (ppm)	Cl^{-} (ppm)	SO_4^{2+} (ppm)	NO_3^{-} (ppm)	F^{-} (ppm)	$H_2PO_4^{-}$ (ppm)	HCO_3^{-} (ppm)
1	<1.1	708.0	7.40	36.7	115.0	19.3	15.9	5.3	10.8	43.5	0.0	0.2	0.0	420.7
2	<0.8	643.0	7.41	33.7	106.7	17.2	12.2	4.9	10.3	20.1	0.0	0.2	0.0	397.6
3	1.0	717.0	7.40	38.6	123.7	18.7	8.9	4.4	16.8	21.6	0.0	0.0	0.0	437.7
4	1.4	712.0	7.53	37.3	120.8	17.3	11.4	1.5	28.4	54.3	1.6	0.0	0.0	358.3
5	7.3	829.0	7.45	42.4	138.0	19.4	13.9	1.8	39.3	62.4	27.2	0.0	0.0	391.3
6	7.9	843.0	7.48	45.0	149.2	19.0	10.9	1.9	30.6	115.1	0.0	0.0	0.0	386.4
7	10.1	874.0	7.37	46.4	165.4	12.5	11.0	5.6	44.4	112.7	0.0	0.0	0.0	374.6
8	8.1	868.0	7.73	44.2	143.4	20.6	20.0	7.0	54.9	52.9	47.7	0.0	0.0	364.8
9	3.3	706.0	7.41	37.0	120.6	16.8	10.4	1.1	36.4	36.2	21.1	0.0	0.0	338.0
10	9.8	766.0	7.44	40.3	131.2	18.4	8.4	1.3	40.1	57.0	25.2	0.0	0.0	346.4
11	0.8	656.0	7.23	33.8	110.4	15.0	9.7	1.4	29.2	23.1	22.9	0.0	0.0	331.0
12	4.4	621.0	7.34	30.9	104.7	11.7	12.4	2.3	26.7	29.6	22.2	0.0	0.0	296.8
13	2.5	683.0	7.48	34.9	118.0	13.1	11.6	2.2	25.7	26.1	20.6	0.0	0.0	357.3
14	10.0	--	--	--	--	--	--	--	--	--	52.0	--	--	--
15	9.3	--	6.98	--	--	--	--	--	--	--	55.0	--	--	--
16	7.5	--	7.12	--	--	--	--	--	--	--	34.0	--	--	--
17	13.1	--	6.90	--	--	--	--	--	--	--	99.0	--	--	--
18	8.8	--	7.10	--	--	--	--	--	--	--	39.0	--	--	--
19	11.1	--	7.07	--	--	--	--	--	--	--	45.0	--	--	--
20	7.8	--	7.01	44.0	155.0	12.6	10.9	1.7	41.0	69.0	29.0	0.1	0.2	--
21	2.9	--	7.01	46.4	154.0	11.6	10.0	0.9	48.0	38.0	24.0	0.1	0.2	--
22	5.9	--	7.10	44.7	143.0	18.0	14.7	3.1	45.0	74.0	10.7	0.2	0.1	--
23	9.7	--	--	--	--	--	--	--	--	--	71.0	--	--	--
24	14.9	--	7.07	44.2	166.0	13.4	20.0	0.8	42.0	77.0	42.0	0.1	0.2	--
25	10.2	--	6.99	41.4	140.0	13.0	12.3	0.8	42.0	41.0	36.0	0.2	0.2	--
26	10.8	--	--	--	--	--	--	--	--	--	52.0	--	--	--
27	6.0	753.0	7.72	38.1	125.0	16.7	14.9	1.7	39.2	45.7	28.1	0.3	0.0	341.8
28	1.7	731.0	7.59	36.9	127.2	12.5	16.0	1.59	33.6	24.9	26.3	0.0	0.0	367.8
29	9.4	1075.0	7.79	46.6	167.9	11.5	41.8	14.7	53.6	110.4	91.4	0.0	0.0	375.4
30	3.5	730.0	7.66	36.7	121.6	15.4	11.8	3.1	36.3	26.9	26.8	0.0	0.0	360.2
31	7.1	822.0	7.51	40.6	137.9	15.2	11.6	2.0	51.1	52.4	42.5	0.0	0.0	335.3
32	5.8	805.0	7.62	39.9	132.1	16.9	14.1	2.3	50.5	48.2	36.9	0.0	0.0	339.8
33	10.2	891.0	7.40	43.9	145.1	18.7	22.4	2.2	63.7	62.1	46.2	0.0	0.0	356.2
34	14.7	866.0	7.94	0.9	3.6	<=0.01	206.8	0.3	51.7	67.0	42.2	0.0	0.0	328.4

Table 4.3. Tritium and major ions in samples taken in the aquifer of the Geer basin during the 2005 survey

Sample number.	^{3}H (TU)	Sp.Elec. Cond. ($\mu S \cdot cm^{-1}$) (laboratory)	pH	Total hardness (°f)	Ca^{2+} (ppm)	Mg^{2+} (ppm)	Na^{+} (ppm)	K^{+} (ppm)	Cl^{-} (ppm)	SO_4^{2+} (ppm)	NO_3^{-} (ppm)	F^{-} (ppm)	$H_2PO_4^{-}$ (ppm)	HCO_3^{-} (ppm)
35	8.7	696.5	7.63	31.9	97.6	18.2	19.3	3.9	50.8	66.1	33.7	0.55	<=0.2	236.6
36	8.8	1376.0	7.90	46.5	156.3	18.3	99.7	32.2	197.9	51.0	26.7	<=0.2	2.30	438.6
37	9.8	800.0	7.70	39.1	129.1	16.6	16.5	3.9	48.3	47.4	46.6	<=0.2	<=0.2	333.4
38	6.0	684.0	7.71	29.2	92.6	14.8	24.3	4.2	58.4	71.9	47.6	<=0.2	<=0.2	188.0
39	7.6	944.0	8.27	40.2	133.1	16.9	39.9	15.0	89.8	50.5	38.4	<=0.2	0.51	348.7
40	7.6	983.0	7.97	41.8	140.6	16.4	42.6	14.5	88.3	51.9	34.4	<=0.2	1.50	380.1
41	7.2	913.0	7.85	36.3	120.8	14.9	47.7	13.7	89.0	45.7	41.6	0.16	2.50	326.6
42	6.8	934.5	8.00	41.1	138.3	15.9	36.4	11.9	76.8	48.0	34.4	<=0.2	0.87	374.9
43	6.8	943.5	8.04	41.5	139.6	16.0	37.1	12.7	79.8	49.4	36.0	<=0.2	0.79	374.5
44	7.1	943.5	8.12	41.0	138.1	15.8	39.7	12.9	82.4	50.1	29.4	<=0.2	0.80	379.6

Table 4.4. Tritium and major ions in samples taken in the Geer river in November 2005

Sample number.	CFC-11 (pmol//l)	CFC-12 (pmol/l)	CFC-113 (pmol/l)	SF_6 (fmol/l)	^3H (TU)	Sp.Elec. Cond. ($\mu S \cdot cm^{-1}$) (lab.)	pH	Total hardness (°f))	Ca^{2+} (ppm)	Mg^{2+} (ppm)	Na^{+} (ppm)	K^{+} (ppm)	Cl^{-} (ppm)	SO_4^{2+} (ppm)	NO_3^{-} (ppm)	F^{-} (ppm)	$H_2PO_4^{-}$ (ppm)	HCO_3^{-} (ppm)
45	0.22	0.11	0.02	0.1/0.7*	<1.2	645.0	7.03	33.4	106.9	16.4	12.0	4.3	10.1	17.5	0.8	<=0.2	<=0.2	391.3
46	0.31	7.10	0.02	0.5	5.2	827.0	6.92	44.1	145.8	18.7	12.3	4.0	33.0	96.4	0.9	0.20	<=0.2	384.3
47	12.00	8.40	0.33	1.40	12.2	1094.0	6.85	49.8	170.4	17.6	29.6	19.0	69.5	75.3	93.9	<=0.2	<=0.2	387.3
48	40.00	33.00	0.27	1.20	8.6	807.8	6.99	39.9	137.0	13.8	13.4	6.3	47.1	38.1	43.0	<=0.2	<=0.2	340.8
49	10.00	18.00	0.34	1.80	5.5	762	6.98	38.8	131.7	14.4	14.6	1.4	35.9	43.2	26.7	<=0.2	<=0.2	364.0
50	3.60	3.90	0.05	0.30	3.6	734.8	7.00	37.7	126.5	15.0	10.5	2.4	33.7	29.8	21.6	<=0.2	1.50	358.8

Table 4.5. CFC's, SF_6, tritium and major ions in samples taken in the aquifer of the Geer basin during the 2007 survey

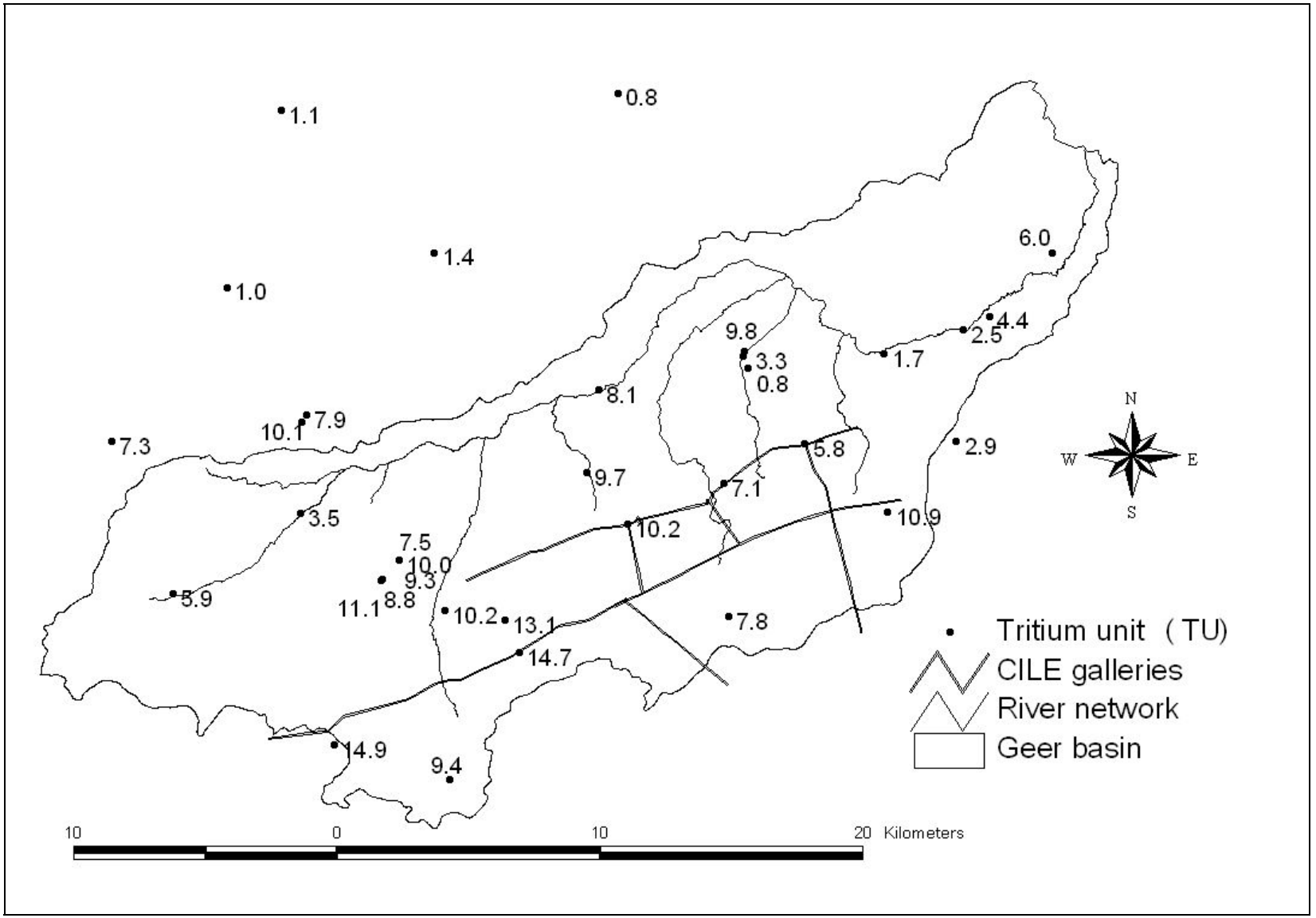

Figure 4.17 Tritium units measured in the groundwater samples taken in the chalk aquifer of the Geer basin in 2005

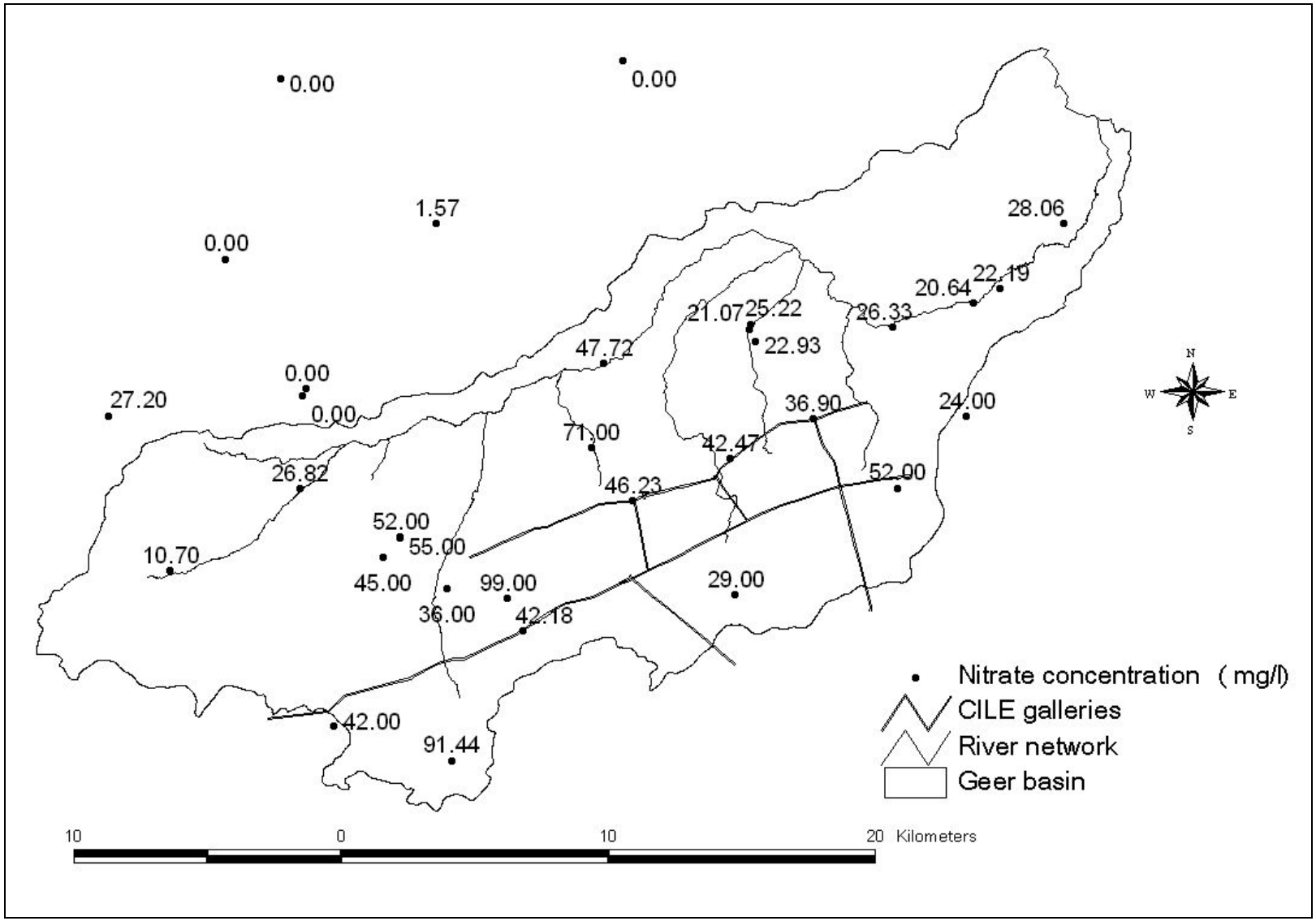

Figure 4.18 Nitrate concentrations measured in the groundwater samples taken in the chalk aquifer of the Geer basin in 2005.

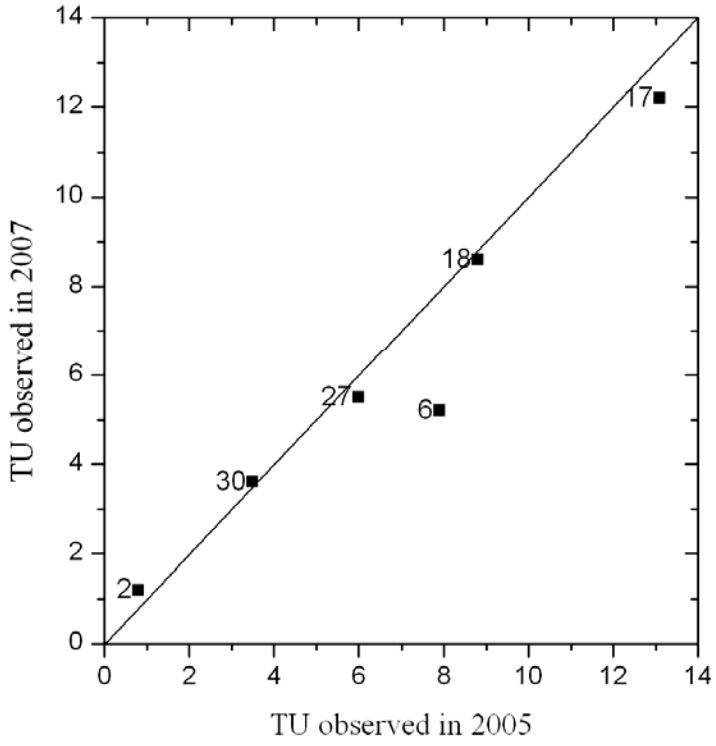

Figure 4.19. Comparison between the tritium concentrations observed in 2005 and 2007 (labels are the sample number of the 2005 survey).

4.4.2.2 Tritium in surface water

Tritium concentrations in the samples, taken in the surface waters of the Geer basin, range from 6.0 to 9.8 TU (Table 4.4). These concentrations are characteristic of young water. The river probably drains the more superficial and thus younger groundwater. The distribution of tritium units observed along the Geer river (Figure 4.20) shows that the tritium concentrations seem to decrease when going downstream (Figure 4.21), reflecting the fact that the proportion of old water in the Geer increases from upstream to downstream. A jump exists in the data around 20 Km from the source of the Geer river, that could be explained by the arrival of young water coming from the Yerne river. More sampling points would, however again be required to confirm these assumptions.

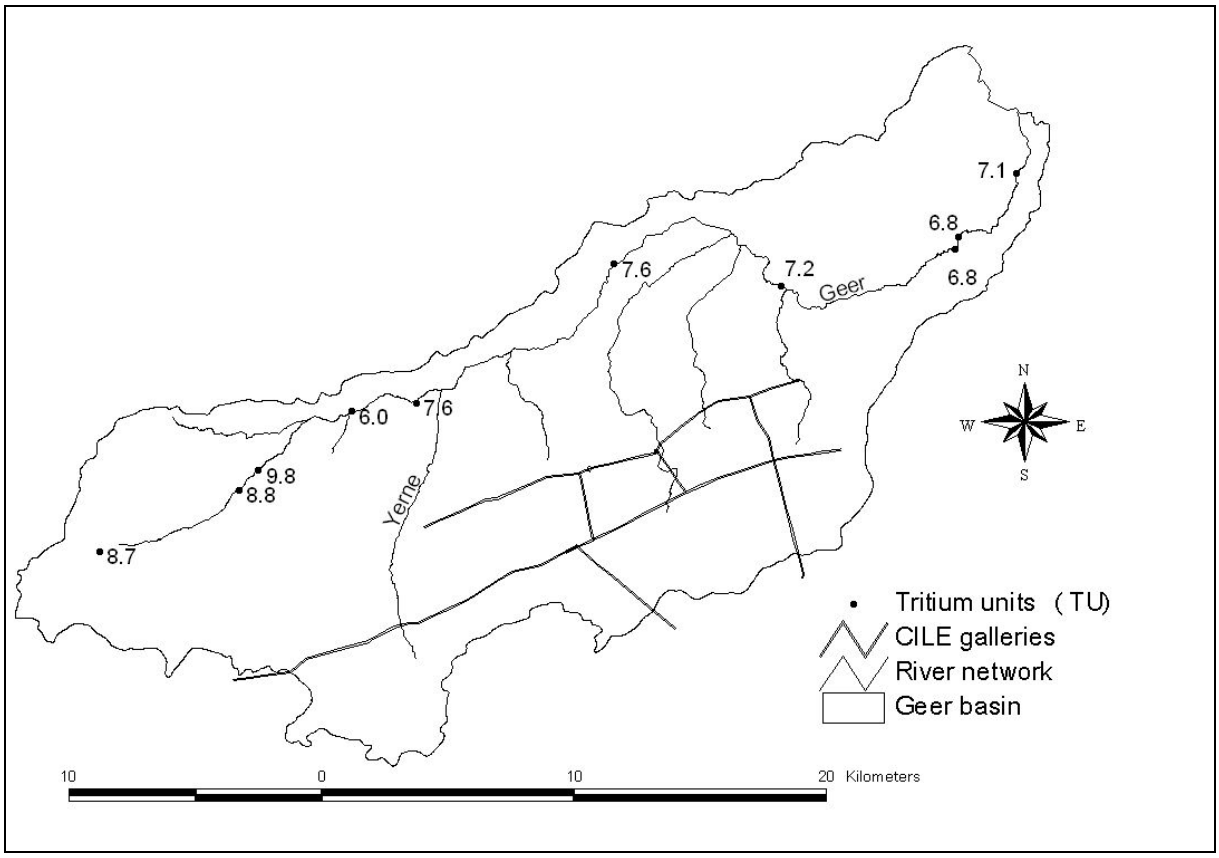

Figure 4.20. Spatial distribution of tritium units in the Geer river (November 2005).

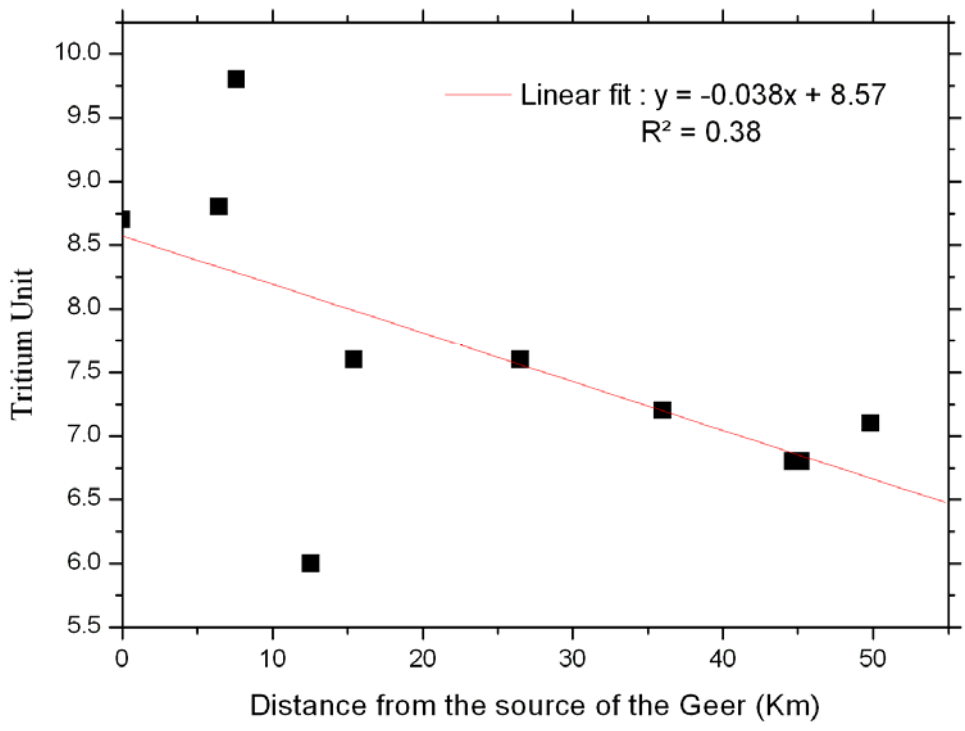

Figure 4.21. Tritium unit in function of the distance from the source of the Geer river.

4.4.2.3 CFC's and SF_6 in groundwater

In all samples, significant amounts of CFC's (ranging from 0.22 to 40 pmol/l for CFC-11, from 0.11 to 33 pmol/l for CFC-12 and from 0.03 to 0.34 pmol/l for CFC-113) and SF_6 (ranging from 0.5 to 1.8 fmol/l) were found (Table 4.5). This indicates that all the samples contain water infiltrated after the 1970-ties (beginning of the production of the SF_6, see Chapter 2). A priori, this result seems in contradiction with tritium results indicating that groundwater found to the North of the Geer basin is old water infiltrated before the tritium peak of the fifties. As it has been explained in Chapter 2, tritium and CFC's-SF_6 do not show the same behaviour in the unsaturated zone. CFC's and SF_6 are gases which travel across the unsaturated zone quickly by diffusion and can reach the saturated zone quicker than tritium.

The results clearly show that several samples are contaminated by local pollution. CFC's are in excess in these samples regarding to the CFC equilibrium concentration (values too high regarding the concentration in the atmosphere and the possible solubility of gas in water). CFC-11 are in excess in samples from P1 Eben, JEN083, PCBov; CFC-12 in samples from Bovenlingen, Pech War, P1 Eben, JEN083, PCBov. No excess values are found for CFC-113 or SF_6. As explained in Chapter 2, these excess values, common in densely populated regions or in industrial/urban sites, are mainly the result of the seepage of contaminated water.

The spatial distribution of the different CFC's (Figure 4.22, Figure 4.23, Figure 4.24) and of SF_6 (Figure 4.25) allows defining two zones corresponding to the confined and unconfined part of the aquifer. The existence of a discharge zone located in North-East of the Geer basin cannot be confirmed by the CFC's and SF_6 concentrations observed in the North-East of the Geer basin. The observed CFC's and SF_6 concentrations observed in this part of the basin are similar to those observed in the unconfined part of the basin.

As mentioned in Chapter 2, CFC's can be used to assess denitrification processes. CFC's, as nitrates, are degraded in anoxic conditions (Oster *et al.* 1996) producing a shift of the CFC-11/CFC-12 ratio. Due to the local contamination of the groundwater, the only sample useful for this comparison comes from Vliermaal (number 45). The concentrations ratio between CFC-11 and -12 is normal. No proof of denitrification can thus be highlighted using this CFC's survey

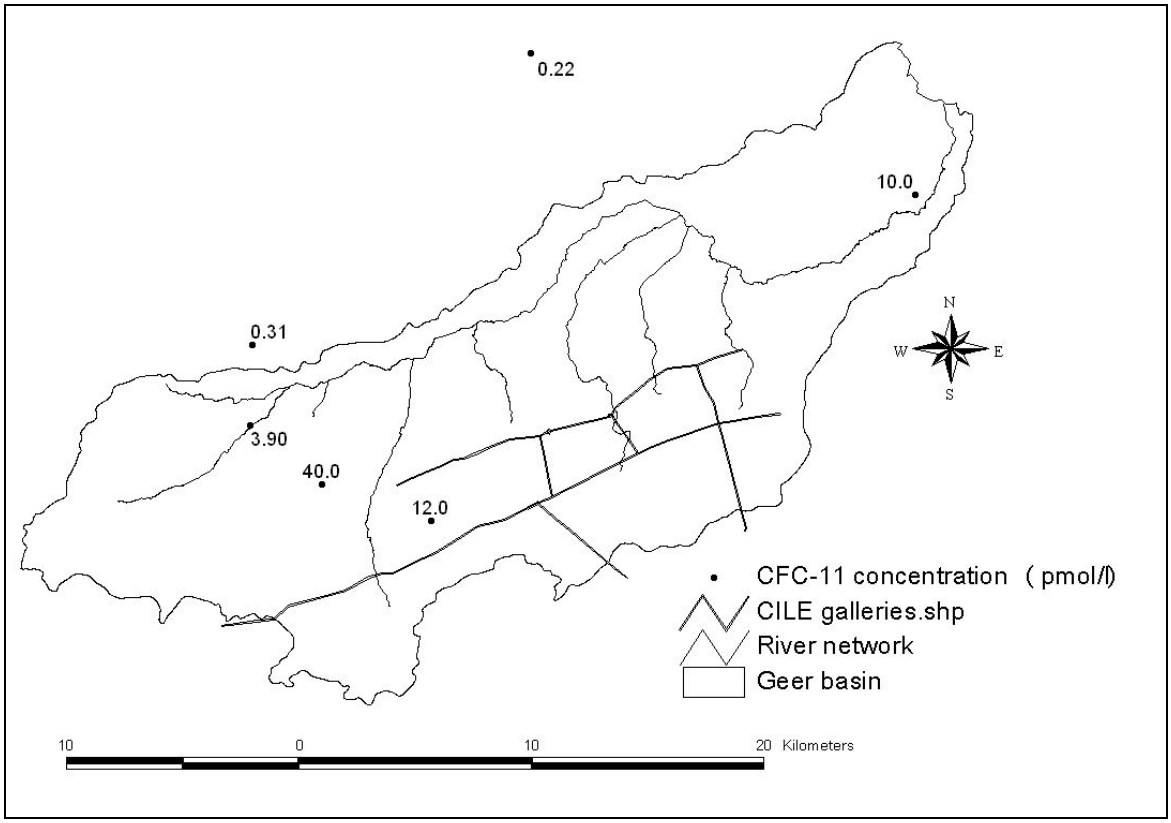

Figure 4.22. CFC-11 concentrations observed in groundwater in 2007.

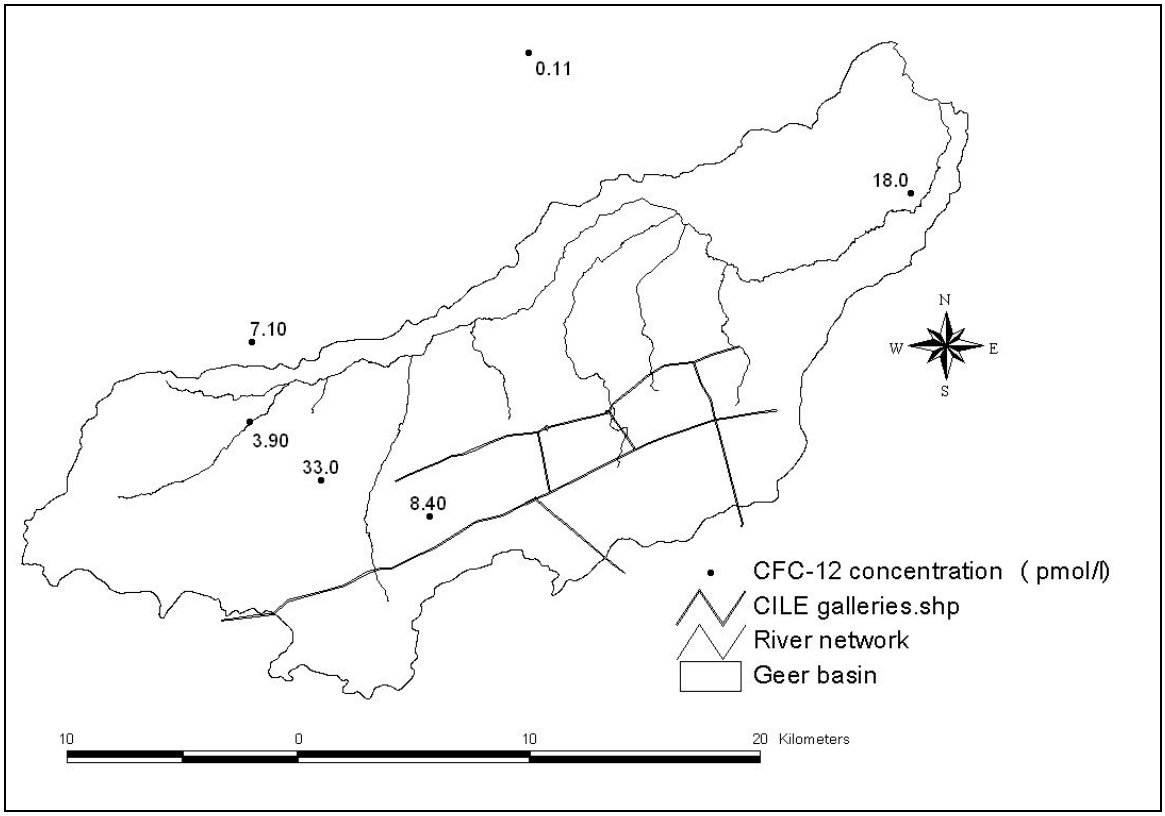

Figure 4.23. CFC-12 concentrations observed in groundwater in 2007.

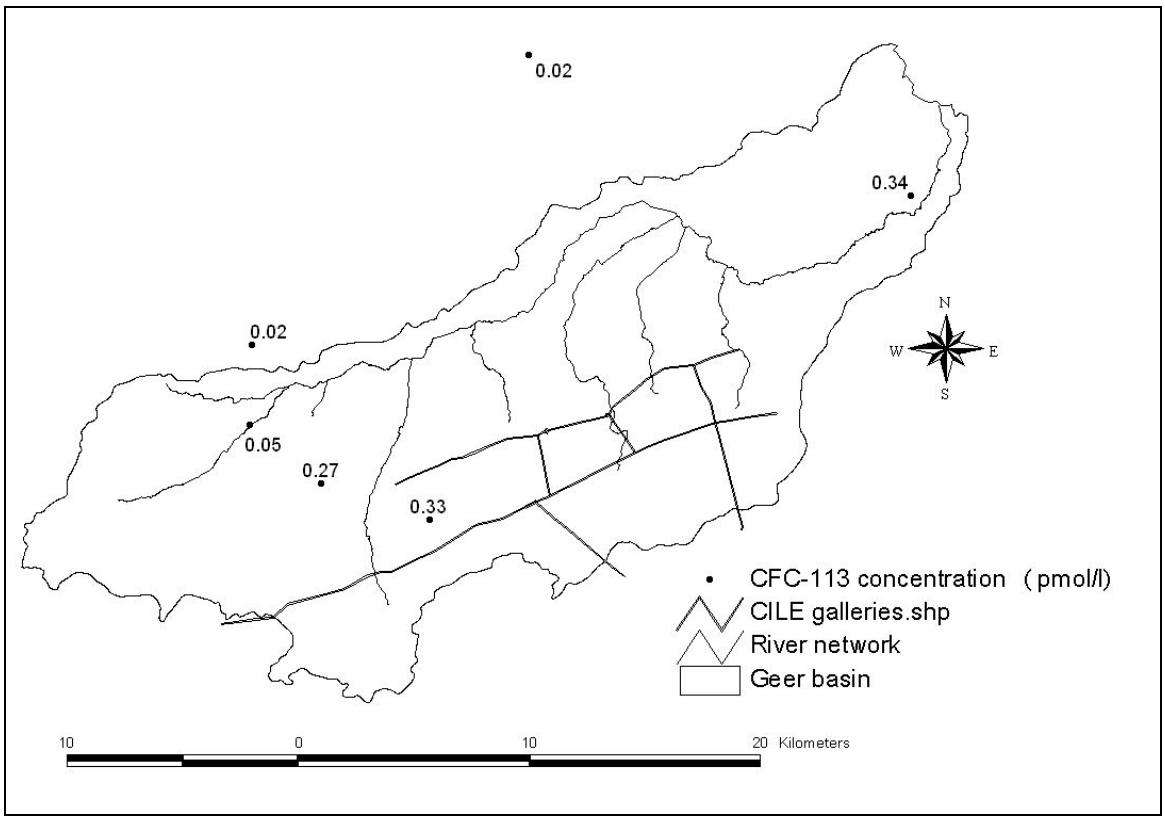

Figure 4.24. CFC-113 concentrations observed in groundwater in 2007.

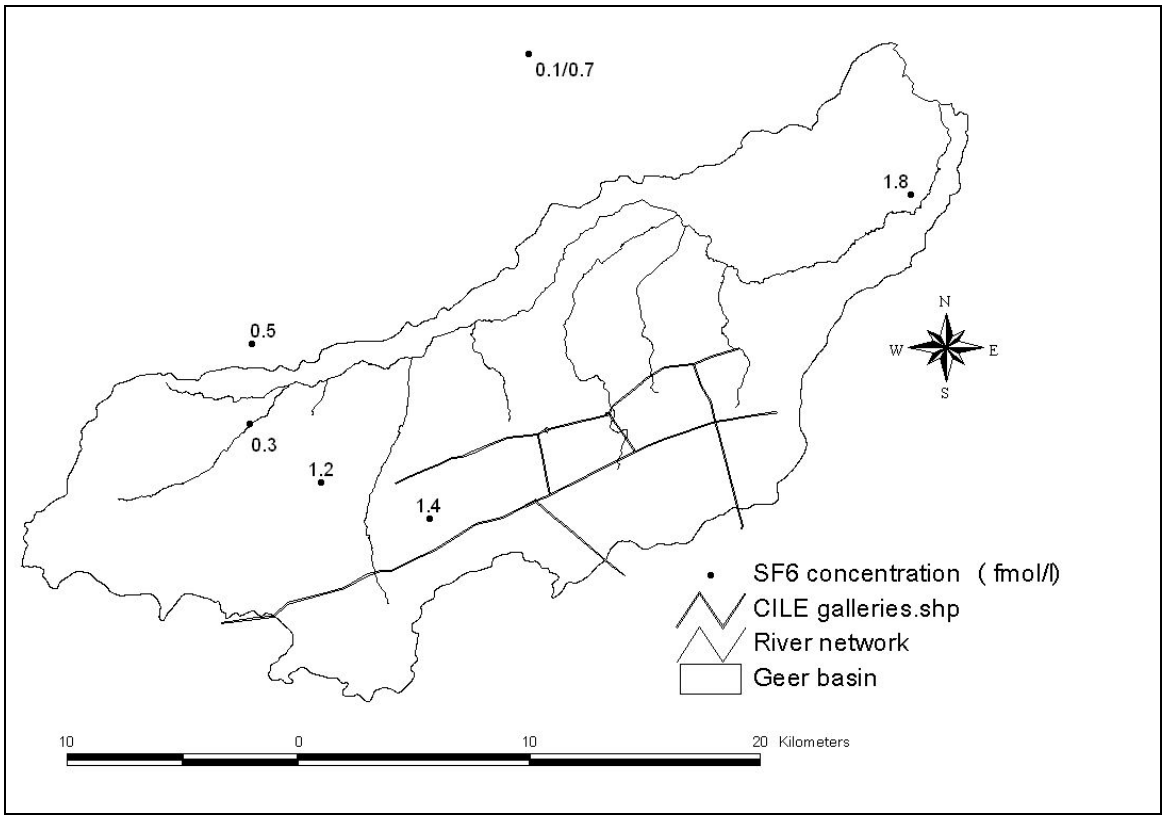

Figure 4.25. SF_6 concentrations observed in groundwater in 2007.

4.4.3 Interpretation of the tritium data

Collected tritium data of the 2005 survey were modelled using the FLOWPC code developed by Maloszewski and published by the IAEA (2002). In this code, different transfer functions are implemented, such as piston-flow, exponential, combined exponential – piston flow and dispersion models. Knowing the tritium concentrations in the leaching water and the concentrations observed at different sampling points and for a specific model chosen by the user, it is possible to compute, by an inverse procedure, the parameters defining the model.

As the chalk is a dual-porosity medium, tritium data were first interpreted using the dispersion model, as proposed by Maloszewski (1994) (see Equation in Chapter 2). For dual-porosity media, the mean transit times computed with the dispersion model are apparent ones and overestimate the real mean transit times of groundwater and a retardation factor has to be applied.

The value of the parameter P_D used in the dispersion model was set to 0.1, considering that advection is the predominant transport process. Considering a porosity of fissure around 1 % and a porosity of the matrix around 40 % (Brouyère *et al.* 2004a), a retardation factor of 40 can be applied to correct the apparent mean transit times, which reflects that the real transit times of the groundwater are then 40 times lower than the apparent transit times. The mean transit times computed with the FLOWPC code range from 71 to more than 200 years (Table 4.6). The real transit times for the mobile water would then range from 2 to 5 years. Such short transit times are unrealistic as the migration velocity in the unsaturated zone alone is estimated to 1 m/y. As the thickness of the unsaturated zone can reach several tens of metres, the transit time in this zone only is larger than the transit time of groundwater estimated with the dispersion model.

The combined exponential - piston flow model is probably more representative of the hydrogeological conditions prevailing in the Geer basin. The piston flow model can be used to represent the unsaturated zone while the exponential model is used for the saturated zone. It was thus applied to the collected data in the unconfined zone in the spring 2005. The mean transit times computed with this combined model are also synthesised in Table 4.6. The mean transit times computed with the piston-flow model (T_{PF}) are on the order of tens years, which correspond to the transfer in the unsaturated zone. As the thickness of the unsaturated zone varies in space, it is difficult to estimate if these transit times are realistic.

Sample number	Name	Aquifer	Dispersion Model	Combined exponential – piston flow model			
			T (years)*	*T (year)*	*η*	T_{PF} *(year)*	T_{EM} *(year)*
1	Zepperen 2	Confined	>200	--	--	--	--
2	Vliermaal 1	Confined	>200	--	--	--	--
3	Alst-bij-Simt-Truiden	Confined	200	--	--	--	--
4	Voort 3	Confined	180	--	--	--	--
5	Montenaken Klein Vorsen 2	Confined	108	--	--	--	--
6	Bovelingen 1	Confined	104	--	--	--	--
7	Bovelingen 3	Confined	90	--	--	--	--
8	Lauw	Unconfined	102	121	1.09	10	111
9	Diets Heur 2	Unconfined	141	--	--	--	--
10	Diets Heur 6	Unconfined	94	96	1.12	10	86
11	Diets Heur 7	Unconfined	200	--	--	--	--
12	Bassenge	Unconfined	130	240	1.02	4.5	235
13	Roclenge	Unconfined	154	--	--	--	--
14	SGB-1	Unconfined	92	--	--	--	--
15	SGB-2	Unconfined	96	101	1.10	9.2	92
16	SGB-3	Unconfined	106	133	1.08	9.8	123
17	JEN083	Unconfined	78	64	1.20	10.6	53
18	PC-Bovenistier	Unconfined	98	110	1.10	10.0	100
19	PzCS-Bovenistier	Unconfined	87	88	1.10	7.2	81
20	Zone Fret 1	Unconfined	105	128	1.08	10	118
21	Tous Saint	Unconfined	147	370	1.03	10	360
22	P4 + P5	Unconfined	116	175	1.06	10	165
23	Rondoval	Unconfined	95	97	1.12	10	87
24	CHS 077	Unconfined	70	48	1.27	10	38
25	LIM 001	Unconfined	88	90	1.12	10	80
26	Abbaye LIE-17	Unconfined	88	84	1.14	10	74
27	P1-Eben.Mael	Unconfined	126	180	1.12	19	161
28	Pz1-Bas-Slins	Unconfined	170	213	1.10	19	194
29	Rue de la Station 39	Unconfined	95	95	1.05	5	95
30	Pêcherie Waremme	Semi-confined	140	--	--	--	--
31	Galerie Xendremal	Unconfined	110	--	--	--	--
32	Galerie Juprelle	Unconfined	117	--	--	--	--
33	Galerie Kemexhe	Unconfined	88	--	--	--	--
34	Galerie Jeneffe	Unconfined	71	--	--	--	--

Table 4.6. Values of the parameters obtained by application of the dispersion and the combined exponential-piston flow models to the tritium data obtained during the 2005 survey.

4.4.4 Discussion and conclusions on the environmental tracer survey

The tritium surveys confirm the importance of studying the age of groundwater to better understand the spatial distribution of diffuse pollution and the functioning of the chalk aquifer of the Geer basin. The spatial distribution of measured tritium units is in concordance with the spatial distribution of nitrates. This allows proposing a coherent interpretative schema of the groundwater flow and solute transport at the regional scale, with three zones corresponding to contrasted hydrogeological contexts in the aquifer (Figure 4.26).

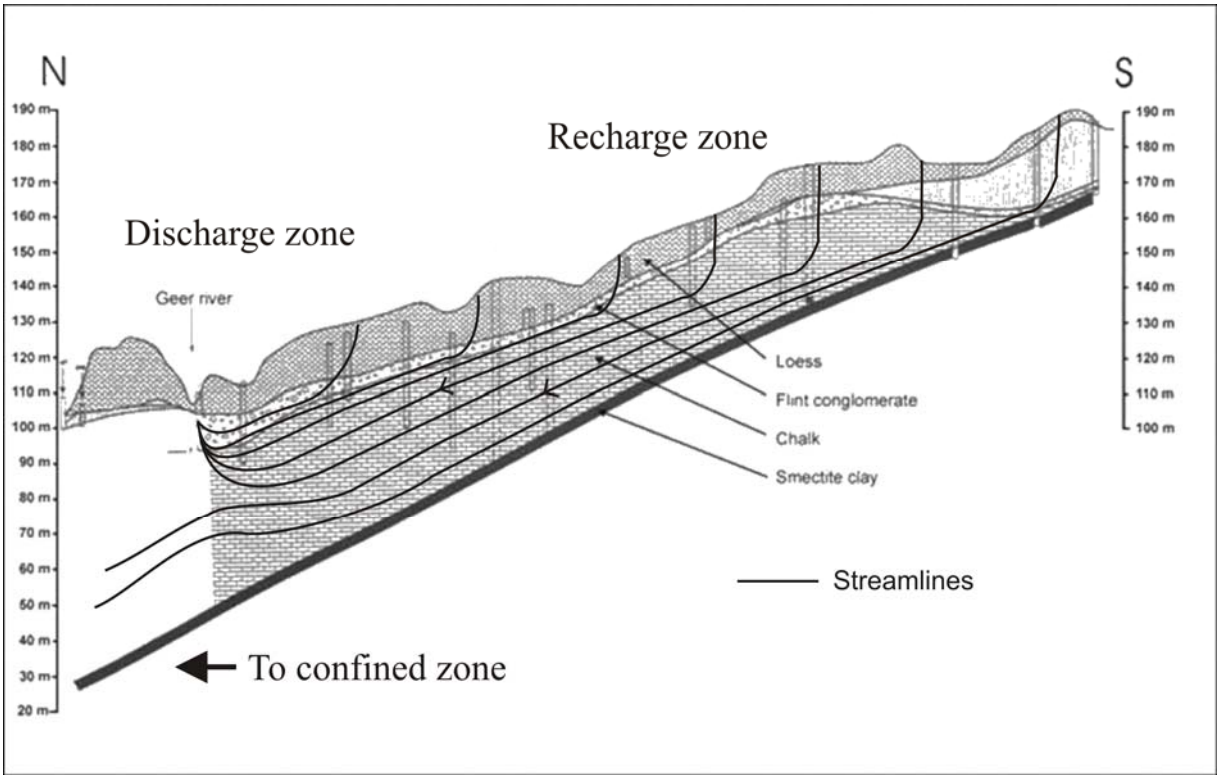

Figure 4.26. North-South cross-section in the Geer basin and schematic representation of groundwater flow at the regional scale.

The results of the CFC's and SF_6 survey are difficult to interpret. Unfortunately, the groundwater is contaminated by local pollution inducing limitations to interpret the data. No conclusion can be drawn concerning denitrification using the CFC's survey.

Various authors (Zoellmann *et al.* 2001; Koh *et al.* 2006 among others) highlighted the difficulty to interpret isotopic data in complex media (unsaturated zone of variable thickness, double porosity media, spatial and vertical heterogeneity…) with the help of simplified analytical models. They propose as an alternative to use spatially-distributed groundwater flow and solute transport model to interpret these data.

4.5 Groundwater model of the Geer basin

Different 3D groundwater models of the Geer basin were already developed at different scales in the framework of different projects. In the MOHISE project, for example, a regional scale spatially-distributed groundwater flow model was developed to study the impact of climate change on groundwater resources (Brouyère *et al.* 2004b). Different groundwater flow and solute transport models were also developed at local scale for the delineation of protection zones around pumping wells and galleries in the basin. The challenge in this work was to develop a spatially-distributed groundwater flow and solute transport model that allows reproducing and predicting the evolution of nitrate concentrations at regional, groundwater body scale using the new Hybrid Finite Element Mixing Cell approach and the available nitrate and environmental tracer datasets for calibration purposes.

In the first part of this chapter, the conceptual choices are described and discussed in terms of geometry, appropriate boundary conditions (recharge, exchanges with rivers, flowing boundaries,…) and stress factors (galleries, pumping wells,…). The different calibration steps of the model are then presented. The developed calibrated model is then used to predict the future evolution of nitrate trends in the Geer basin under a realistic scenario of nitrate concentration evolution in the infiltrating water. The results of the sensitivity analysis to main parameters of the model are then proposed.

4.5.1 Conceptual model for the Geer basin

4.5.1.1 Boundaries of the model

The modelled area has been defined as corresponding to the Geer hydrological basin. More details are provided in Section 4.5.1.4 concerning boundary conditions. In the 3D mesh, the shape of the Northern boundary differs slightly from the actual limit of the hydrological basin because it has been taken similar to the boundary of the soil model EPIC-Grid (developed by the Faculty of Agronomic Sciences of Gembloux) used by the Administration of the Walloon Region over the Geer basin to simulate the fate and behaviour of nitrate used in agriculture (see Section 4.3 devoted to nitrates). This will allow, in a further step, to couple both models.

For defining the bottom and top of the model, different aspects have to be taken into account:

- The main aquifer is located in the chalk

The aquifer is made up of two main layers of chalk separated by a thin layer (approximatively 1 m) of indurated chalk called “Hardground”. This layer has a lower hydraulic conductivity than the surrounding chalk. It does not have any aquifer capacity and it rather acts as a confining unit with an impact on vertical groundwater exchanges between the upper and lower chalk aquifer layers.

- The influence of the unsaturated zone

The unsaturated zone plays a key role in the transfer of contaminant to the aquifer. It is responsible of the delay between application of fertilisers on field and their arrival in the aquifer. It is, therefore, important to represent adequately the unsaturated zone in the model.

4.5.1.2 Discretisation

A two-dimensional finite element mesh was first created considering explicitly the boundaries of the hydrological basin and the location of the pumping galleries. As the developed model is at the regional scale, rivers and pumping wells were not taken explicitly into account in the discretisation process to avoid introducing too much nodes and/or elements with various shapes and sizes. The mesh is based on triangular elements with a mean dimension of 500 m. The resulting 2D mesh is made up of 2115 nodes and 3992 triangular elements.

This two-dimensional mesh was then used to elevate six levels of nodes delimiting five layers of elements: one for the bottom layer of chalk, two for the top layer of chalk and two for the loess layer. The bottom and the top of the different layers were linearly interpolated based on available information from different boreholes drilled in the basin.

As already mentioned, the Hardground being very thin, it is not represented explicitly. In order to take into account its influence on groundwater flows, it is taken advantage of the possibility to define, in the SUFT3D code, the upper and lower chalk aquifer layers as separated subdomains, the Hardground being assimilated to the separating interface, using a leakage coefficient (Figure 4.27) represented by a dynamic third-type boundary conditions between these two subdomains.

The three-dimensional mesh is finally made up of 14805 nodes and 19960 prismatic elements.

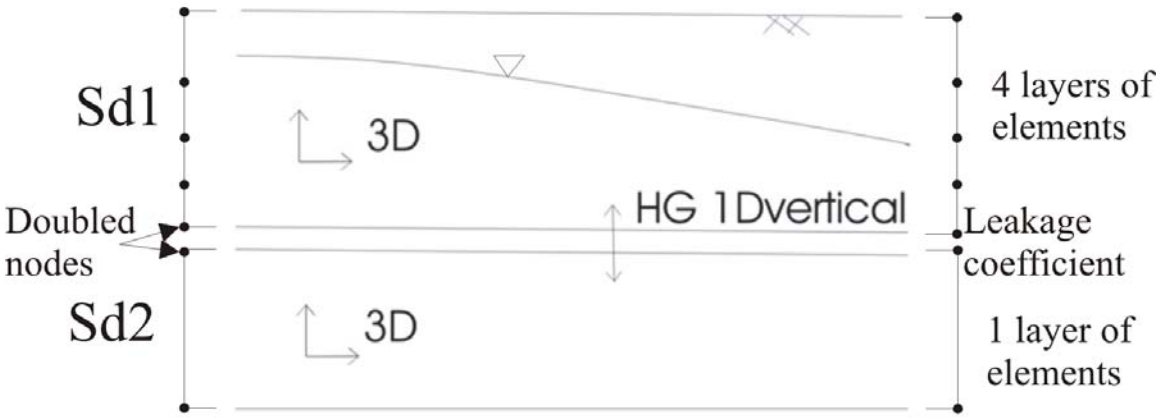

Figure 4.27.Subdomains Sd1 and Sd2 corresponding respectively to the upper and lower chalk

4.5.1.3 Parameterisation of the model

Vertically and laterally, the hydrodynamic properties of the chalk can vary as highlighted by the results of the different surveys and pumping tests performed in the basin. Different zones (symbolised by different colours in Figure 4.28) were distinguished in the chalk layers based on geological information (faulted zone, fractured zone associated to dry valleys…) mainly. As little information is available about the loess hydrodynamic properties, this layer was considered as homogeneous. All materials were assumed to be isotropic. A van Genuchten relationship (van Genuchten 1980) was used to link the water content, the pressure and the relative hydraulic conductivity in the unsaturated zone. Parameters introduced in the van Genuchten model were taken from Brouyère (2001) and Brouyère *et al.* (2004a). The loess layer was considered as a single-porosity medium while the chalk layers are modelled as first-order transfer dual-porosity media using the mobile-immobile model presented Chapter 2.

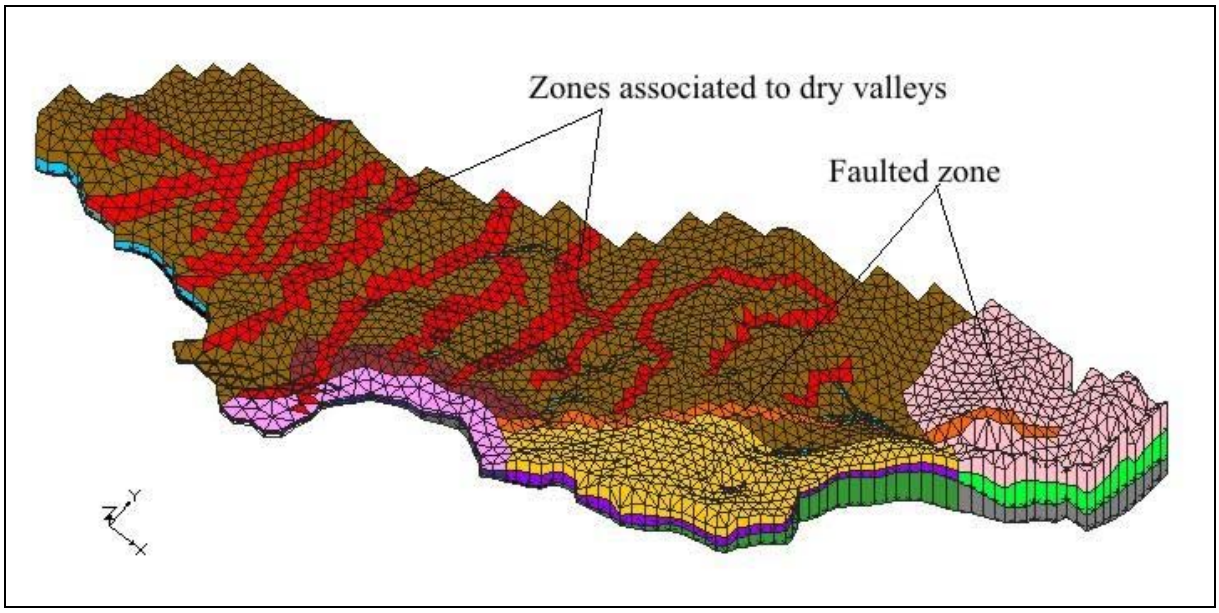

Figure 4.28. 3D mesh (without the layers of elements representing the loess). The different colours symbolised zones in the chalk with different properties. (Vertical scale multiplied by 100)

4.5.1.4 Boundary conditions

On the Eastern, Western and Southern lateral boundaries, no-flow boundary conditions are prescribed. The Southern limit of the hydrogeological basin may vary due to fluctuations of groundwater levels. However, these variations are small and can be neglected; consequently this boundary can be considered as a no-flow boundary (groundwater divide). The Geer river is the main outflow of the chalk aquifer. However, on an annual basis, water balance in the Geer basin shows a groundwater loss estimated to range between 15 mm (Monjoie 1967) and 62 mm (Hallet 1998). As mentioned in section 4.2.3.5 and shown on the piezometric map, the lost groundwater flows under the Geer river to the adjacent basin, due to sloping and deepening of chalk layers towards the North. Such variable losses are function of the piezometry. They were thus considered through the definition of a third-type (Fourier) boundary condition prescribed on the lateral Northern boundary of the chalk (Figure 4.29). The calculated fluxes through this boundary depend on the differences between the prescribed levels outside the model and groundwater levels computed in the aquifer and on a calibrated exchange coefficient. On the lateral Northern boundary of the loess layer, a no-flow boundary has been prescribed. Groundwater flow in the loess layer can be considered as mainly vertical.

At the bottom of the chalk aquifer, the smectite clay is of very low hydraulic conductivity and it corresponds also to a no-flow boundary condition.

Interactions between the rivers and the aquifer are modelled using face-based Fourier boundary conditions, the exchanged fluxes being a function of the difference of groundwater level between the river and the aquifer and of a calibrated exchange coefficient. The Geer, which is the main outlet of the aquifer, and the Yerne and Roua rivers, which drain at least partly the aquifer (Hallet 1998), have been taken into account in the model (Figure 4.29).

4.5.1.5 Stresses

The pumping galleries are represented explicitly in the horizontal discretisation. However, it turned out very difficult to consider exactly and explicitly the complex vertical locations of the galleries. As a first approximation, the Southern and the Northern galleries have been defined at the bottom of the lower chalk aquifer. The galleries act as drains in the chalk layers, however the whole drainage capacity of the galleries is not exploited. The CILE takes only the volume of groundwater needed for distribution. The volume of exploited groundwater is known for each portion of the galleries. In a first step, the galleries are represented by nodal sink terms and the volume abstracted in each portion is linearly distributed on the nodes defining this portion of galleries.

Other groundwater fluxes pumped from wells have been taken into account by sink terms defined in the elements in which the well screens are located. The pumping wells taken into account in the model are presented in Figure 4.29. They have been selected as they are active at least since the seventies and/or important volumes are extracted.

At the top of the aquifer, recharge to the aquifer is prescribed using second type (Neumann) boundary conditions.

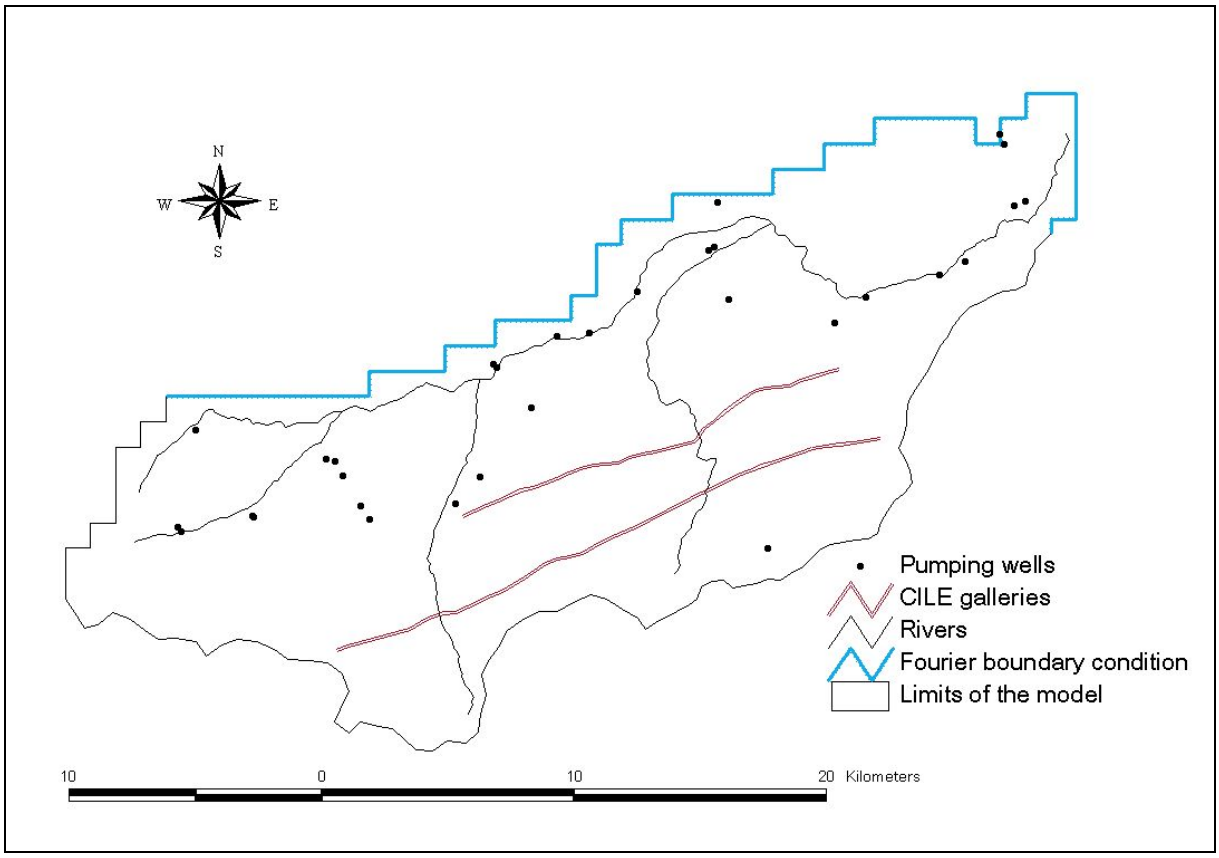

Figure 4.29. Map describing the limit of the model, the location of the Fourier boundary condition on the Northern boundary, the river network, galleries and pumping well taken into account in the model.

4.5.1.6 Mathematical approach to solve the groundwater flow and solute transport problem

As demonstrated in Section 4.3, the observed nitrate trends vary according the location of the observation point in the basin. An explanation to these variations has been proposed and relies on the variations of the depth of the groundwater table, the distinction of a recharge zone and a discharge zone in the aquifer. In regards to management options, it is important to forecast the evolution of nitrate concentrations in specific points corresponding to pumping wells or piezometers belonging to the monitoring network designed to follow the state of the groundwater body. Moreover, the available data set is important and contains spatially-distributed information. There is thus a need but also the possibility to use a spatially-distributed approach to model the groundwater flow and solute transport in the Geer basin.

The hydraulic conductivities of the chalk in the Geer basin were defined mainly using pumping test providing, as explain in Chapter 2, values of the hydraulic conductivities representatives at the scale of few hundreds of meters. These values can thus be used in the

finite elements defining this model. Moreover the chalk of the Hesbaye aquifer can be assimilated to a porous media (Biver 1993; Hallet 1998; Brouyère 2001). The groundwater flow problem was solved using a classical spatially-distributed approach based on the Darcy's Law and assuming a continuous porous medium.

Concerning the solute transport problem, three aspects had to be considered. First, values of available hydrodispersive properties are not very reliable at the scale of the groundwater body. Second, the purpose of the model was mainly to simulate the impact of the nitrate contamination resulting from the agriculture and its future evolution. This pollution is diffuse, widely spread over the whole basin. In this case study, the source of the transported solutes (tritium and nitrate) being fully dispersed at the top of the model, the "true" hydrodynamic dispersion in the model is not an essential process to be modelled since dispersion in groundwater corresponds essentially to the dispersion of the source. Third, the resolution of the advection-dispersion equation at the regional scale remains numerically a challenge. Consequently, the mixing cell approach was chosen to model the transport phenomena. The transport processes considered with the mixing cells were advection, degradation and dual-porosity related to the presence of immobile water.

		TRANSPORT		
		Simple Linear Reservoir	***Distributed Mixing Model***	***Advection-dispersion***
FLOW	***Simple Linear Reservoir***	OK	impossible	impossible
	Distributed Linear Reservoir	OK	OK but data underused	impossible
	Flow in porous media	OK	USED HERE	OK but challenging

Table 4.7. Solutions implemented in the SUFT3D code and restrictions of use.
The combined approach used here corresponds to the simulation of flow in porous medium together with a distributed mixing cell model for solute transport.

4.5.1.7 Steady state vs transient modelling

The solute transport model is developed to study the long-term temporal evolution and to predict the evolution of nitrate concentrations in the Geer basin aquifer at regional scale. Short-term variations in nitrate concentrations associated to groundwater level fluctuations have not to be reproduced. In addition, for the period 1950-2008, no evidence of upward or

downward trends in groundwater levels was observed; the groundwater flow can thus be assumed to be stationary and modelled in steady state using mean stresses for this period. The recharge prescribed to the model was computed using the relation (Equation (4.4) proposed by Hallet (1998):

$$I = 0.845\,P - 422$$
$$262\ mm = 0.845\ 809\ mm - 422\ mm \quad \textbf{(4.5)}$$

Transient conditions were considered for modelling solute transport in order to able to simulate the transient evolution of nitrate trends.

4.5.2 Calibration of the groundwater flow model

The groundwater flow model was calibrated in steady state using two contrasting piezometric situations, each of them being assimilated to a steady state: one corresponding to high groundwater levels (during the period 1983-1984), the second to low groundwater level (during the period 1991-1992). As explain by Brouyère *et al* (2004b), this approach allows assessing the vertical heterogeneity of the chalk. For this calibration step, all stress factors (pumping, recharge…), prescribed to the model, are assumed constant. A recharge of 368 mm/year and 226 mm/year for respectively the period 1983-1984 and 1991-1992 was uniformly spatially-distributed and calculated based on groundwater budgets for the corresponding years. For the period 1983-1984 and 1991-1992, respectively 39 and 50 piezometric measurements relatively well distributed over the whole basin were used (Figure 4.30). The calibration was performed by a trial-and-error procedure, by modifying the spatial distribution of hydraulic conductivity values and the transfer coefficients of the various Fourier boundary conditions defined in the model (interaction between groundwater and surface water, interaction between the two subdomains, external boundary condition used on the Northern boundary). The objective of the calibration process was to minimize the differences between observed and computed groundwater levels. The process was ended when each difference between observed-computed groundwater levels was less than 5 meters. The hydraulic conductivity values obtained at the end of the calibration process are summarized in Table 4.8. These values are of the same order of magnitude than those presented in the section devoted to the description of the Geer basin (10^{-9} to 10^{-7} m/s for the loess and 10^{-5} to 5×10^{-3} m/s for the chalk). Hydraulic conductivity values of the chalk obtained after calibration are lower in the lower chalk than those in the upper chalk, as it has been observed (see Section 4.2.3.6).

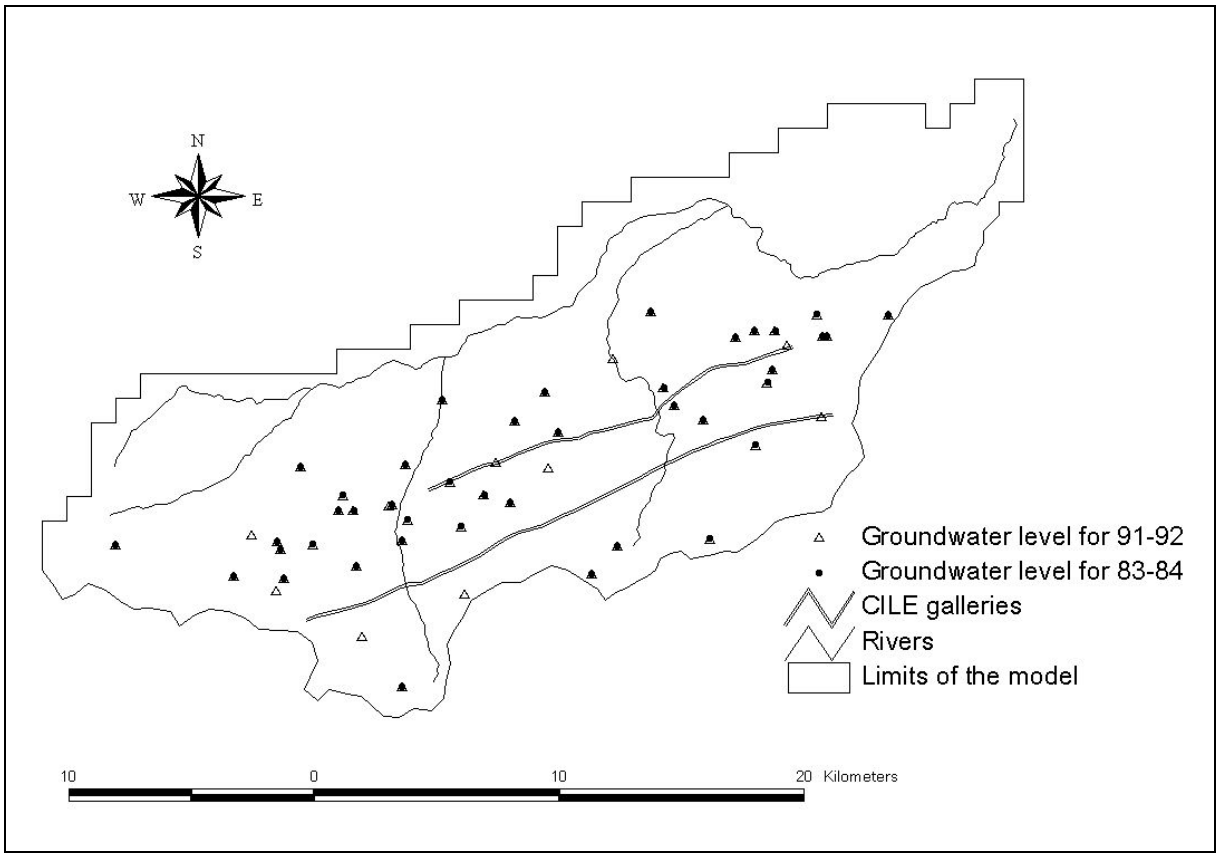

Figure 4.30. Location of the groundwater level measurement points used for the steady state calibration

In Figure 4.31 and Figure 4.32, a general quality of the calibration is presented in the form of scatter plot diagrams of observed versus computed groundwater levels for the periods 1983-1984 and 1991-1992 respectively. The Root Mean Squared Errors (RMSE) obtained after this calibration process is considered as acceptable. Observed values are actually transient values that were here modelled using steady state assumptions and uniform values of recharge. Additionally, the observed values are compared with computed values at the nearest node. As a consequence, two different values of groundwater level observed in two different but very close piezometers or wells can be compared to a unique computed value. A computed piezometric map corresponding to the period 1983-1984 is presented in Figure 4.33. A comparison with the piezometric map presented in Section 4.2.3.2 shows that the model is able to reproduce the following observations:

- groundwater flows mainly from South to North;
- the piezometric gradient is larger in the vicinity of the galleries and lower downstream;

- the groundwater table is not very influenced by the course of the Geer except in its downstream part;
- a piezometric dome is modelled in the North-Eastern part of the basin.

At the end of this groundwater flow steady state calibration process, the exchange coefficient defining the Fourier boundary conditions associated to the Yerne and Roua rivers were very low. The computed exchanged fluxes between the aquifer and these rivers were thus very low. The repartition of the fluxes abstracted in the galleries remains unknown. Only the abstracted total volume per section of gallery can be estimated. During the calibration process, to avoid desaturation in some nodes, the volume of abstracted groundwater in each section was not anymore distributed linearly between the nodes but adapted node by nodes.

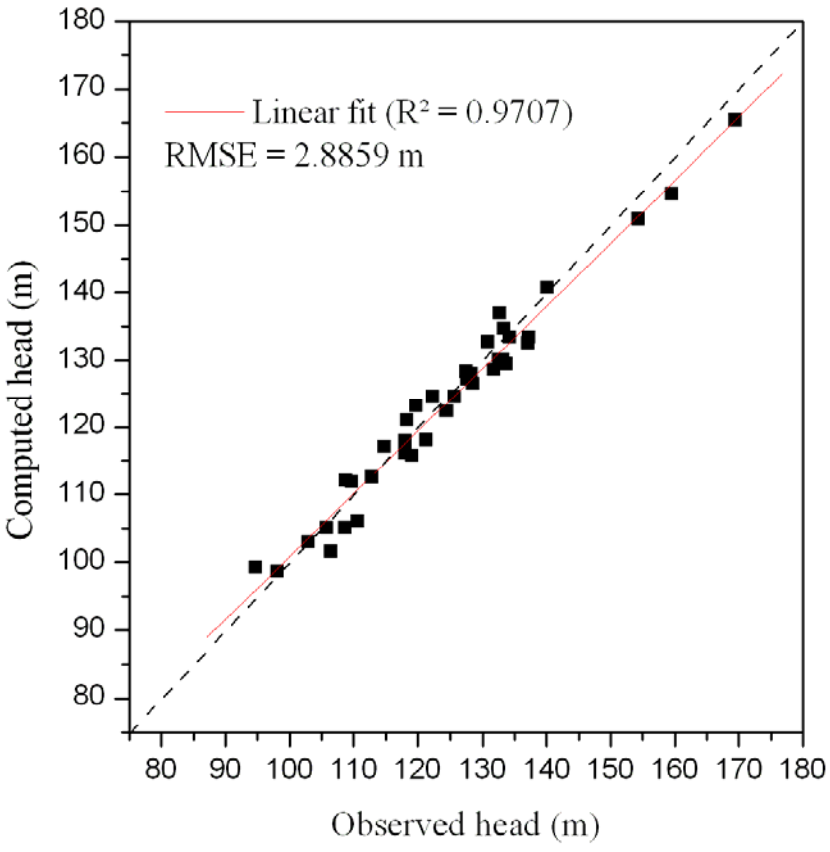

Figure 4.31. Comparison between observed and computed head for the period 1983-1984 assuming steady state conditions.

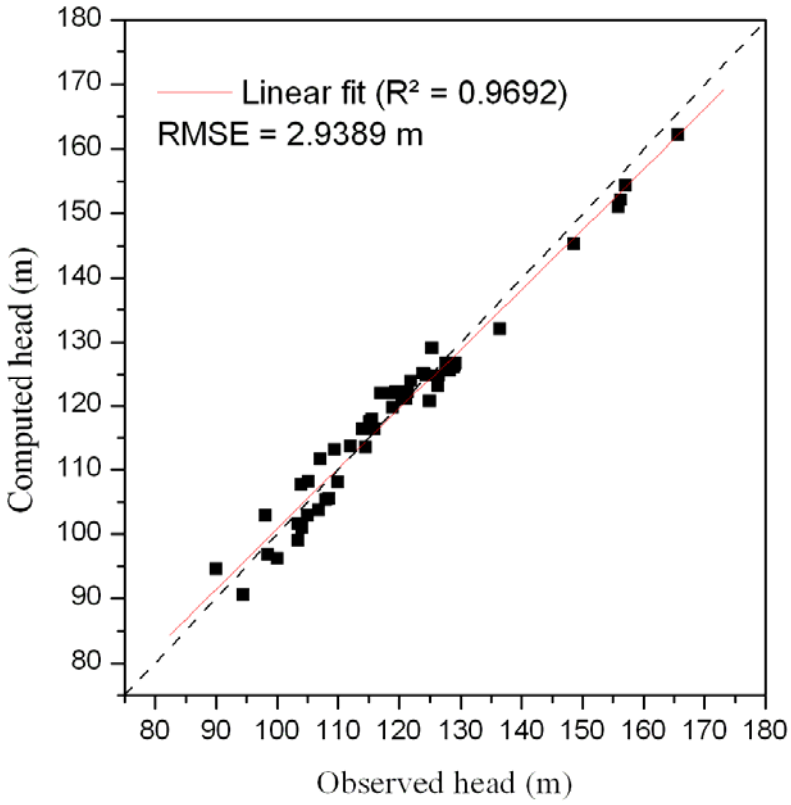

Figure 4.32. Comparison between observed and computed head for the period 1991-1992 assuming steady state conditions.

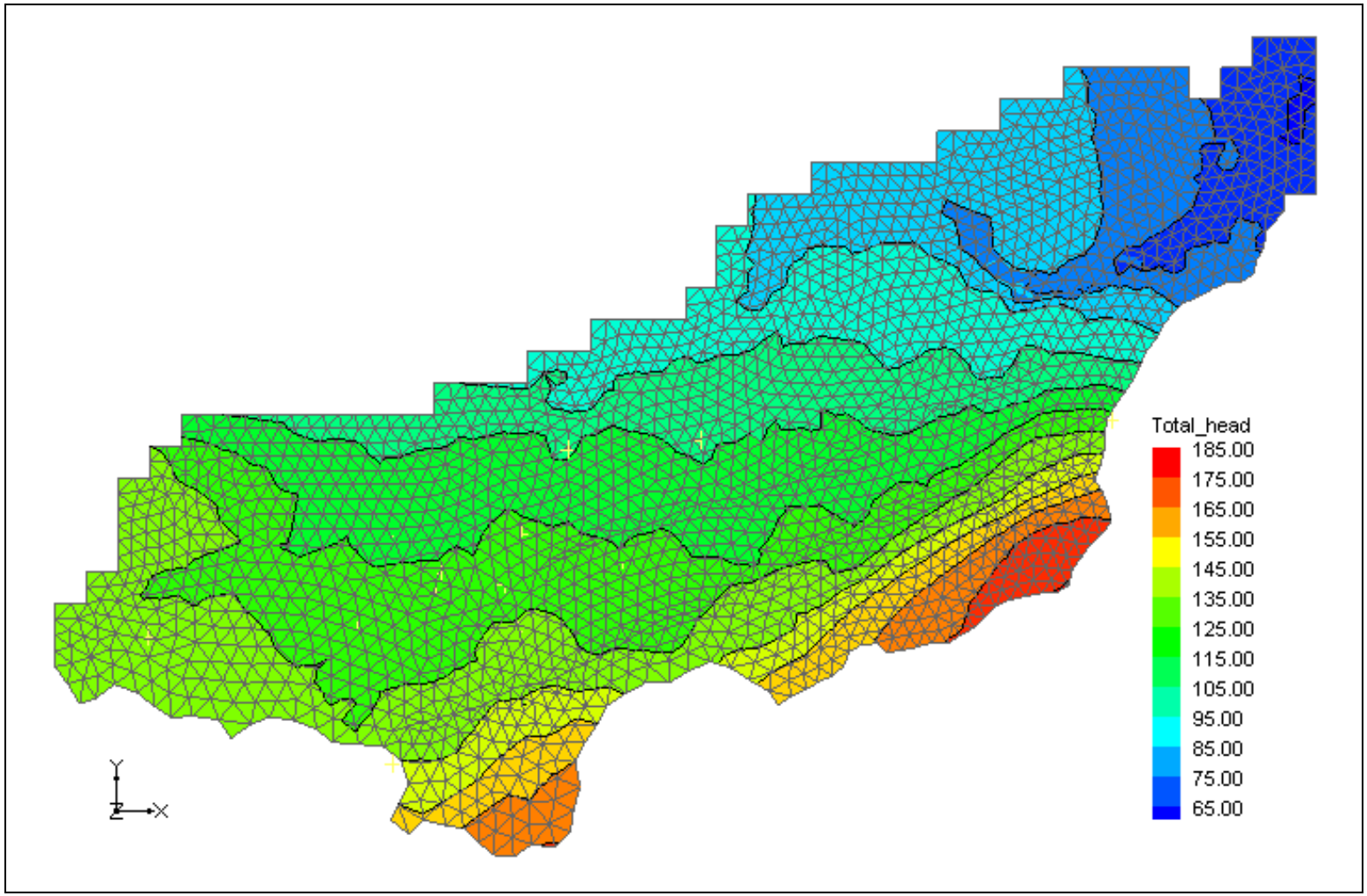

Figure 4.33. Computed piezometric map for the period 1983-1984 assuming steady state conditions.

	Particularity	Saturated hydraulic conductivity (m/s)
Bottom chalk		
Material 1		4.0×10^{-5}
Material 2		2.0×10^{-5}
Material 3		2.0×10^{-5}
Material 4		2.75×10^{-5}
Material 5	Fractured zone	4.0×10^{-4}
Material 6	Fractured zone, Hor.-Hoz. Fault	1.0×10^{-3}
Material 7	Fractured zone, dry valleys	3.0×10^{-3}
Upper chalk (bottom part)		
Material 8		2.0×10^{-4}
Material 9		2.0×10^{-4}
Material 10		7.0×10^{-5}
Material 11		1.5×10^{-4}
Material 12	Fractured zone, Horion-Hozémont Fault	1.0×10^{-3}
Material13	Fractured zone, dry valleys	3.00×10^{-3}
Upper chalk (upper part)		
Material 14		2.0×10^{-4}
Material 15		1.0×10^{-4}
Material 16		1.0×10^{-3}
Material 17		2.0×10^{-4}
Material 18	Fractured zone, Horion-Hozémont Fault	1.0×10^{-3}
Material 19	Fractured zone, dry valleys	2.70×10^{-3}
Material 21		7.0×10^{-5}
Loess		
Material 20		1.0×10^{-7}

Table 4.8. Values of hydraulic conductivity as obtained after calibration of the groundwater flow model assuming steady state conditions.

4.5.3 Calibration of the groundwater solute transport model

Two sets of data were used for calibration of the transport model, one corresponding to tritium data acquired during winter 2004-2005, the second to observed nitrate concentrations and trends (Batlle-Aguilar *et al.* 2007). The advantage of tritium is that the concentration in the infiltrating water can be easily estimated because it is essentially correlated to the latitude (see Chapter 2). Nitrate concentrations in the infiltrating water are more difficult to determine as they are function of land-use and they show temporal as well as seasonal evolutions.

The calibration was performed by trial-and-error changing the values and the spatial distribution of effective porosity, percentage of the immobile water and transfer coefficient between mobile and immobile water.

4.5.3.1 Calibration of the groundwater transport model using the results of the tritium survey

As mentioned in Section4.4, a tritium survey was performed during winter 2004-2005. Samples were taken in the aquifer in the Geer basin and to the North of the basin where the aquifer becomes confined, in continuity with the unconfined part of the aquifer. Concentrations measured during this survey were used to calibrate the model. This calibration step allowed constraining the model in terms of origin of the groundwater and mean transit time.

Tritium concentration in the infiltration was considered as uniformly distributed in the basin, equal to the mean tritium concentration measured in precipitation at the station of Groningen, The Netherlands (Figure 4.34). Tritium concentrations in the recharge were assumed to be constant around 5 Tritium Unit before the thermonuclear tests. Degradation of tritium was considered in the model using a first order degradation constant of 2.55×10^{-9} s^{-1} equal to the inverse of the half-life of tritium.

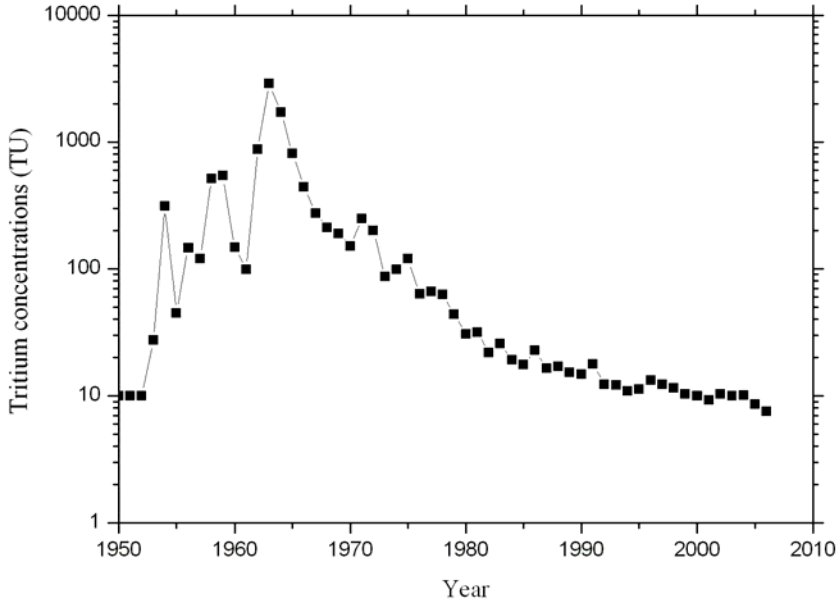

Figure 4.34. Tritium concentrations measured in precipitation at the station of Groningen

The transport model was run in transient state for the period 1950-2004. The modelling period was divided in 2090 time steps of 10 days to respect the criterion of the Courant number (Cr < 1, see Chapter 2). Initial conditions were computed running the model in transient state until stabilisation of computed tritium concentrations at each node. It was assumed that before 1950 the tritium concentrations in groundwater were stabilized. To reach stabilisation of the computed tritium concentrations, the transient solute transport model had to be run for a period of 140 years. This relatively long period is indicative of the long mean residence time of groundwater in the basin and of the global inertia of the system.

The quality of the calibration of the solute transport model was assessed on the basis of three different aspects:

- a qualitative comparison of observed versus computed maps of the spatial distribution of tritium in the aquifer at the end of 2004;
- a scatter plot of observed versus computed tritium concentration for the winter 2004-2005;
- a scatter plot comparing the thickness of the unsaturated zone and the transit time of the tritium peak in this unsaturated zone.

4.5.3.1.1 Computed spatial distribution of the tritium concentrations

A qualitative comparison between the measured concentrations map drawn after the winter 2004-2005 survey (see Section 4.4.2.1) and the computed tritium concentration map at the bottom of the upper chalk of the chalk in 2004 (Figure 4.35) shows that (1) the computed concentrations are on the same magnitude than the observed ones and (2) the computed tritium concentration confirmed the observed zonation based on measured tritium concentrations. As the model is limited to the hydrologic basin of the Geer River, it does not simulate the concentration in the confined part located to the North of the basin. The spatial distribution of the tritium concentration seem to be influenced by the course of the Geer river and the location of the Horion-Hozemont fault which corresponds to an area of higher hydraulic conductivity.

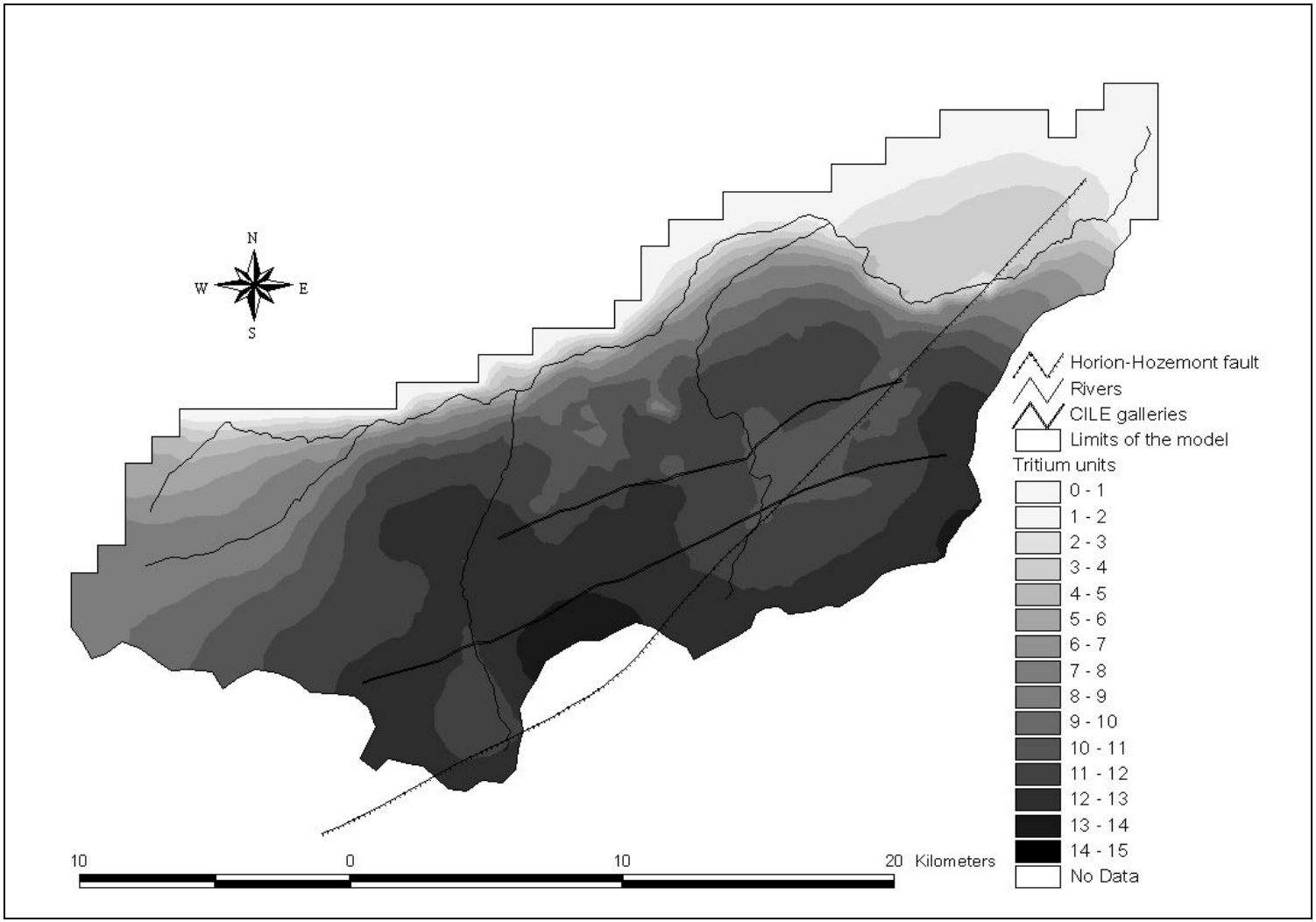

Figure 4.35. Computed tritium concentrations for 2004 at the bottom of the upper chalk layer (Black and white colours correspond to respectively "young" and "old" water)

4.5.3.1.2 Scatter plot of observed versus computed tritium concentrations

25 points where tritium concentrations were measured were used to build a scatter plot of observed versus computed concentrations (Figure 4.36). The computed concentrations used in the comparison are those calculated at the upper nodes in the saturated zone. Unfortunately, most of the piezometers and wells were sampled for tritium analysis assuming depth averaged conditions. However, the depths of the wells and the position of the screens are often unknown. It is therefore difficult to compare depth averaged measured concentrations and concentrations computed at a particular node of the 3D mesh. This can partly explain the dispersion of points around the line Y = X in Figure 4.36

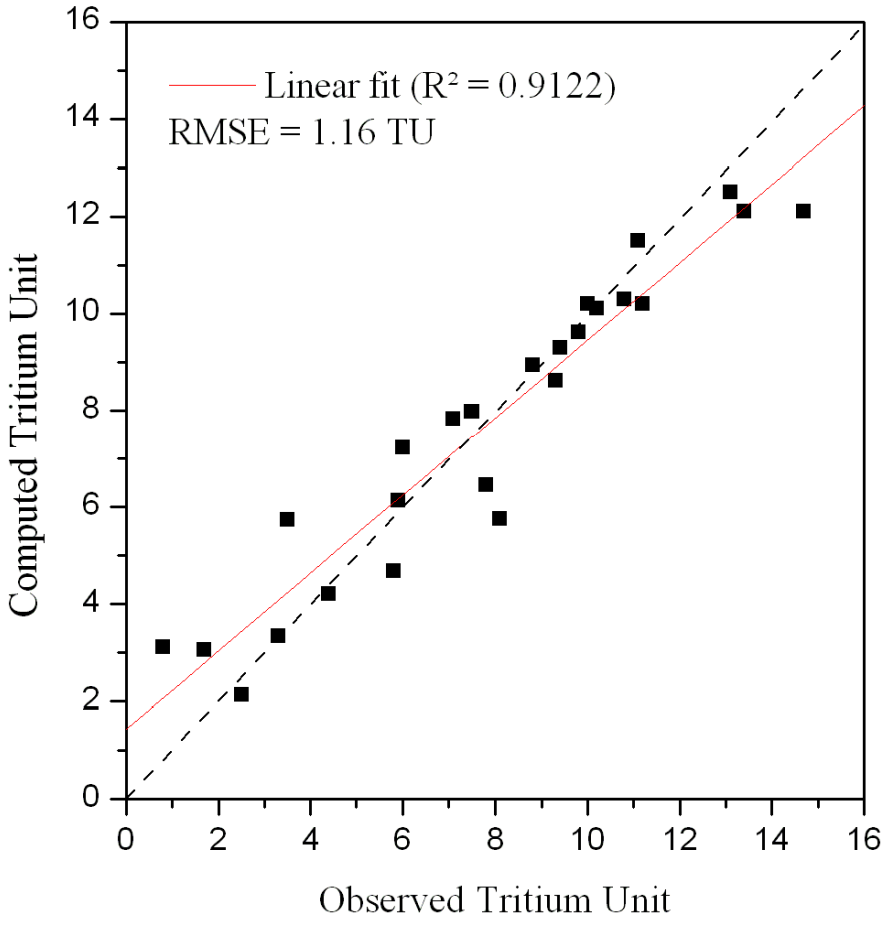

Figure 4.36. Comparison between observed and computed tritium concentrations (winter 2004-2005)

4.5.3.1.3 Vertical variation of computed tritium concentrations

An average velocity of solute in the unsaturated zone (loess and chalk layers) in the Geer basin was estimated at 1m/year (Dautrebande *et al.* 1996; Brouyère *et al.* 2004). The calculated solute velocity in the unsaturated zone at the location of each sampling point of the "tritium 2005" survey confirms the previous estimates of 1m/year (Figure 4.37). It indicates that the tritium transport model is well parameterized in the unsaturated zone. Figure 4.37 shows that the relation 1 m of propagation for 1 m of unsaturated zone is better verified for low thickness of the unsaturated zone. A relatively thin unsaturated zone correspond to a solute transfer essentially in the loess layer, when higher thickness of the unsaturated zone includes as well a part of the solute transfer in the chalk layers. The dispersion observed around the line 1/1 for a large thickness of the unsaturated zone is likely to be due to the high heterogeneity of the unsaturated chalk.

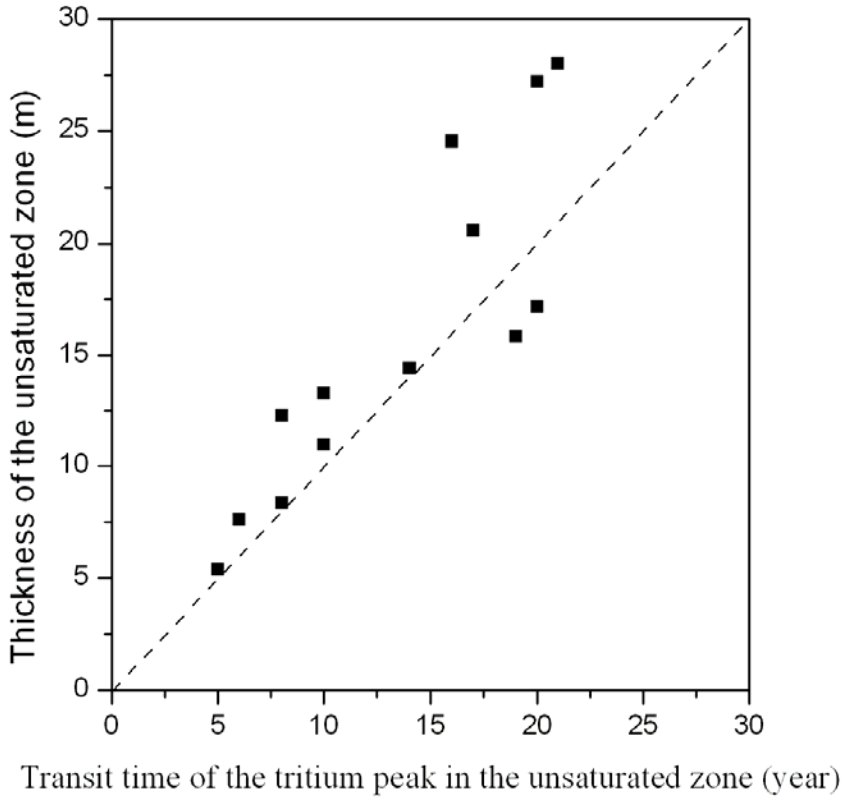

Figure 4.37. Comparison between the thickness of the unsaturated zone and the transit time of the tritium peak in this unsaturated zone

4.5.3.2 Calibration of the groundwater transport model using the time evolution of nitrate concentrations

The capability of the model to reproduce the observed long-term time evolution of nitrate concentrations in groundwater was evaluated comparing observed and computed time series of nitrate concentrations. The model was run in transient state for the period 1950-2008. The modelling period was divided in 2242 time steps of 10 days.

As a first step, a simplified uniform scenario of input (Figure 4.38) was defined on the basis of information from literature (Dautrebande and Sohier 2004; Hérivaux *et al.* 2008). In this scenario, the concentration in the infiltrating water is assumed to be equal to 15 mg/l at the beginning of the fifties. Nitrate concentrations increase between 1950 and the mid of the eighties to reach a plateau with nitrate concentrations of 70 mg/l. This plateau can be related to the stabilization of nitrogen load on the crops observed in Western Europe and in Belgium (see Section 4.3.1and Figure 4.11). In the absence of degradation evidence (see Section 4.3 and 4.4), nitrate is assumed as conservative.

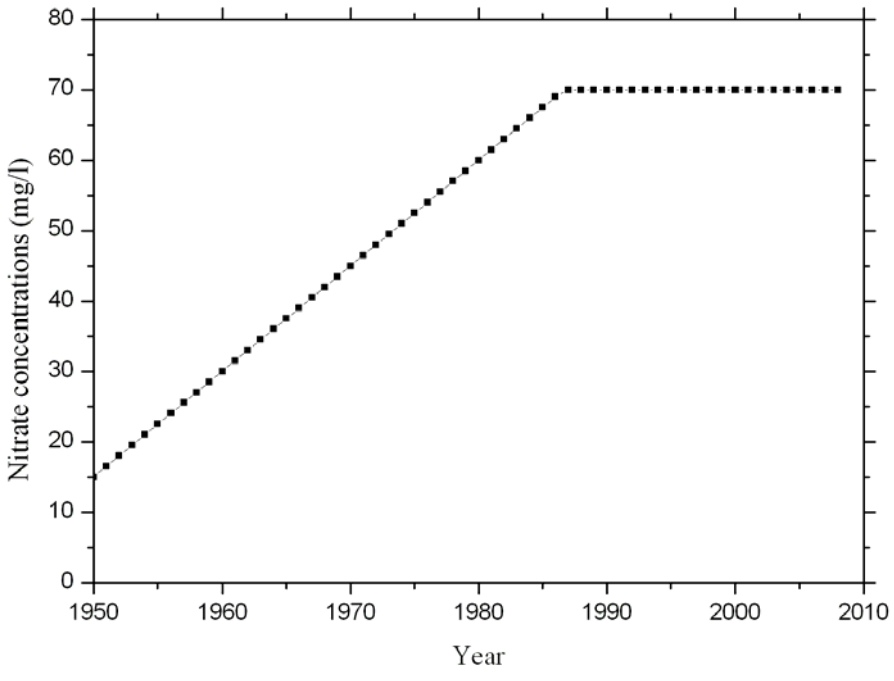

Figure 4.38. Simplified nitrate input used for modelling between 1950 and 2008.

At the beginning of the fifties, nitrate concentrations in groundwater can not be assumed to be in steady state conditions. Nitrate concentration in the Southern part of the basin are around 15 mg/l (Hallet 1998). Nitrate concentrations observed in the Eastern part of the basin are lower, around 10mg/l. Initial conditions for the period 1950-2008 were computed running the model in transient conditions during 70 years considering a concentration in the infiltrating water equal to 15 mg/l. At the end of these 70 years, computed nitrate concentrations in the basin have not stabilised yet but reproduce the observed nitrate concentrations at the beginning of the fifties.

The nitrate dataset used for the statistical trend analysis (Batlle-Aguilar *et al.* 2007) and described in Section 4.3.3 was chosen as reference data for this calibration step. These datasets are representative of the different situations found in the basin and contains sufficient data in each point of observation to be representative of the long-term evolution of nitrate concentrations in the aquifer. The computed concentrations used for the sake of comparison are those computed at the upper node in the saturated zone.

In Figure 4.42, the computed concentrations were compared to the observed one for four locations in the basin, the nitrate concentrations computed in the other observation points can be found in annex. The computed nitrate concentrations are of the same order of magnitude than the observed ones. Long term evolution of nitrate concentrations seems also to be reproduced. In order to assess the quality of the calibration, a “slope” (hereafter named “computed slope”) describing the upward trend of the computed nitrate concentration was calculated and compared with the slope of observed data calculated with statistical tools (hereafter named “observed” slope). This “computed slope” is determined considering the same methodology and tools than for the determination of the “observed slope” (see Chapter 2 and Section4.3.3.2). The values of the “observed” and “computed slopes” are similar (Table 4.9). The “computed slopes” are generally higher than the observed ones but the correspondence is better if the observed time series is long (e.g. points H10 and H18). Low values of “computed slopes” generally correspond to ‘no trend’ determined statistically. The spatial distribution of the different “computed slopes” (Figure 4.39) is similar to the one described by Hallet (1998) on the basis of observed data.

Observation points	Start of the observations	End of the observations	"Observed slope" (mg/year)	"Computed slope" (mg/year)
H1	11/05/1994	30/12/2003	0.48	0.71
HF22	17/06/1981	10/01/2001	0.46	0.71
H2	05/01/1994	30/12/2003	0.25	0.31
HF20	02/02/1990	26/01/2005	NT	0.31
H3	06/01/1958	26/11/2002	0.32	0.52
H4	27/06/1994	11/12/2002	NT	0.37
H5	05/01/1994	30/12/2003	NT	0.29
HF21	29/05/1985	28/01/2005	NT	0.31
H6	11/05/1992	05/08/2003	NT	0.21
H7	16/06/1958	12/12/2002	0.59	0.64
H17	12/11/1987	12/12/2002	NT	0.64
H8	13/08/1976	12/12/2002	0.54	0.69
H9	06/12/1957	24/10/2002	0.40	0.53
H10	06/12/1957	02/02/2000	0.83	0.90
H11	26/11/1998	25/07/2002	NT	0.47
H12	26/11/1990	04/12/2002	0.41	0.67
H13	16/05/1990	04/12/2002	0.46	0.72
H14	16/01/1991	04/12/2002	0.47	0.75
H15	07/10/1988	04/12/2002	NT	0.78
H16	16/04/1996	28/05/2002	NT	0.20
H18	06/07/1976	12/12/2002	0.58	0.64
HF17	01/02/1986	25/01/2001	0.52	0.74
HF18	07/08/1996	08/11/2000	NT	0.37
HF19	15/05/2002	07/12/2004	NT	0.37
H19	31/12/1982	16/12/2002	NT	0.69
H20	15/08/1988	15/12/2002	NT	0.66

Table 4.9. Comparison between the slope of the observed trend and the computed trend

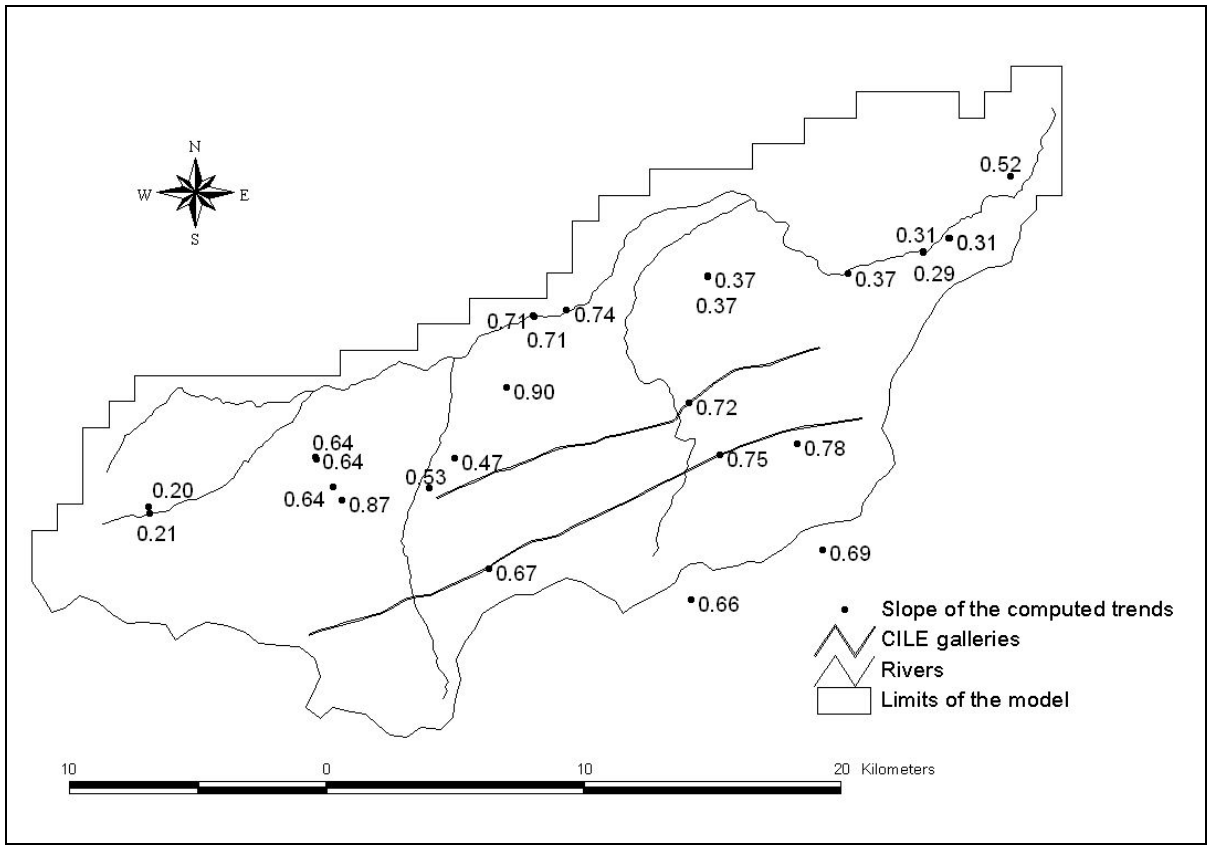

Figure 4.39. Spatial distribution of the slope of the computed trends

Values of parameters obtained at the end of the calibration process are presented in Table 4.10. Calibrated values of effective porosity obtained for the chalk are similar to those presented in Section 4.2.3.7. The value of effective porosity obtained for the loess layer could seem very large. This layer is unsaturated, the flow is mainly governed by gravity and all the porosity participates to the flow. Large value was introduced in the model during the calibration process to simulate the mean observed vertical velocity of 1m/year. The calibrated value corresponds to the total porosity determined at the Bovenistier test site (Brouyère *et al.* 2004a). The calibrated value obtained for the immobile water corresponds at the largest value presented in Section 4.2.3.7. The value of the transfer coefficient between mobile and immobile water is also similar to those presented in Section 4.2.3.7. As little information is available on the spatial distribution of these two last parameters, the same value was prescribed for all the zones defined in the chalk.

	Particularity	Effective porosity (/)	Immobile water porosity (/)	Transfer coefficient (1/s)
Bottom chalk				
Material 1		0.005	0.30	1.0×10^{-7}
Material 2		0.01	0.30	1.0×10^{-7}
Material 3		0.01	0.30	1.0×10^{-7}
Material 4		0.01	0.30	1.0×10^{-7}
Material 5	Fractured zone	0.01	0.30	1.0×10^{-7}
Material 6	Fractured zone, Hor.-Hoz. Fault	0.01	0.30	1.0×10^{-7}
Material 7	Fractured zone, dry valleys	0.02	0.30	1.0×10^{-7}
Upper chalk (bottom part)				
Material 8		0.005	0.30	1.0×10^{-7}
Material 9		0.01	0.30	1.0×10^{-7}
Material 10		0.01	0.30	1.0×10^{-7}
Material 11		0.01	0.30	1.0×10^{-7}
Material 12	Fractured zone, Horion-Hozémont Fault	0.01	0.30	1.0×10^{-7}
Material13	Fractured zone, dry valleys	0.02	0.30	1.0×10^{-7}
Upper chalk (upper part)				
Material 14		0.005	0.30	1.0×10^{-7}
Material 15		0.01	0.30	1.0×10^{-7}
Material 16		0.01	0.30	1.0×10^{-7}
Material 17		0.01	0.30	1.0×10^{-7}
Material 18	Fractured zone, Horion-Hozémont Fault	0.01	0.30	1.0×10^{-7}
Material 19	Fractured zone, dry valleys	0.02	0.30	1.0×10^{-7}
Material 21		0.01	0.30	1.0×10^{-7}
Loess				
Material 20		0.44	/	/

Table 4.10. Effective porosity, immobile water porosity and transfer coefficient between mobile and immobile water as obtained after calibration of the solute transport model.

4.5.4 Nitrate concentration forecasting

To study the evolution of nitrate concentrations in groundwater, a scenario for the evolution of nitrate concentrations in the infiltrating water must be defined. In term of management of the groundwater resource, the main objective is to reverse upward trends and to stabilise nitrate concentrations below the drinking water limit. Two scenarios (Figure 4.40) of nitrate concentrations in the infiltrating water were investigated. The first one is an unrealistic, extreme scenario of nitrate concentration equal to 0 mg/l. In the second one, an optimistic (but still critical) scenario is to a concentration of 50 mg/l.

The future nitrate concentrations in groundwater were computed for the next 50 years (2009-2058) considering the two previously described scenarios. The evolution of nitrate concentrations in groundwater is followed as an example in the different wells used for the trend analysis.

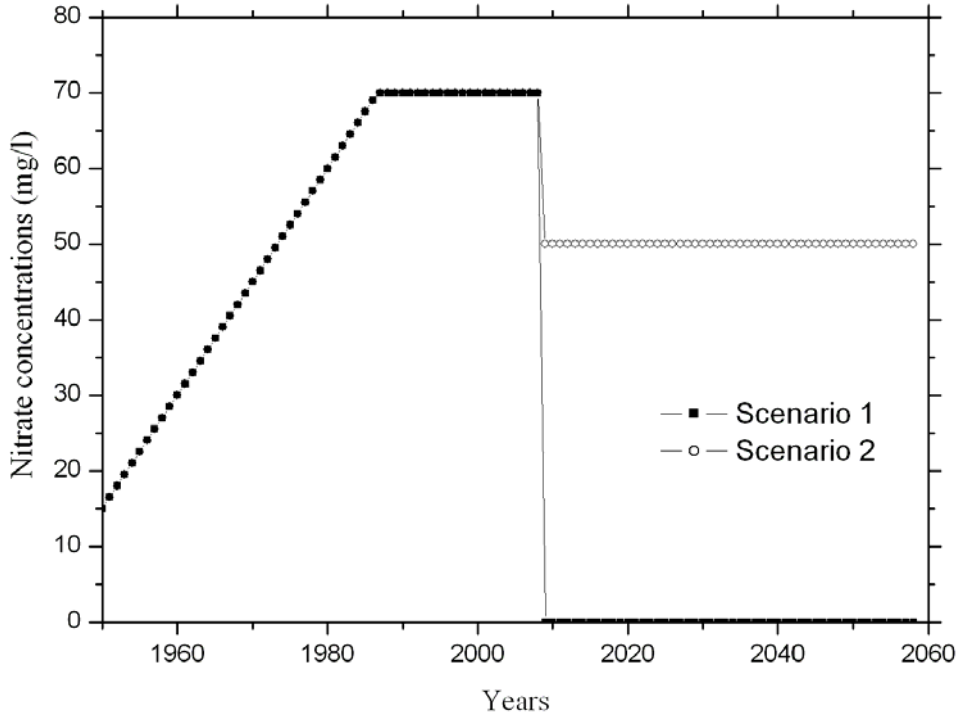

Figure 4.40. Nitrate inputs considered in the modelling for nitrate concentrations forecasting in groundwater

According to the modelling results obtained with the first scenario (nitrate concentration in leaching water of 0 mg/l after 2008), trend reversal is expected to occur between 5 and more

than 30 years after the abrupt change in the input (see examples in Figure 4.41). Even with an unrealistic, extreme scenario, nitrate upward trends observed in the aquifer of the Geer basin are not expected to reverse before 2015 as required by the WFD.

The calculated evolution of nitrate concentrations in groundwater considering the second more realistic scenario is presented for four wells in Figure 4.42. The computed nitrate concentrations for the other observation points are shown in Annex 1. The evolution of the nitrate concentrations is dependent on the location of the wells in the basin. According to the modelling results, in the Southern part of the basin, nitrate trend reversal is expected during the period 2009-2058 (for example, 2025 for H12 and 2016 for H15). The exact period when the inversion is observed is essentially a function of the thickness of the unsaturated zone. Where the thickness of the unsaturated zone is higher, the time needed for a trend reversal is longer. In the Northern and Eastern parts of the basin, the trend reversal will not occur in the simulated period 2009-2058 and the nitrate concentrations will still increase and even reach and exceed the drinking water limit of 50 mg/l.

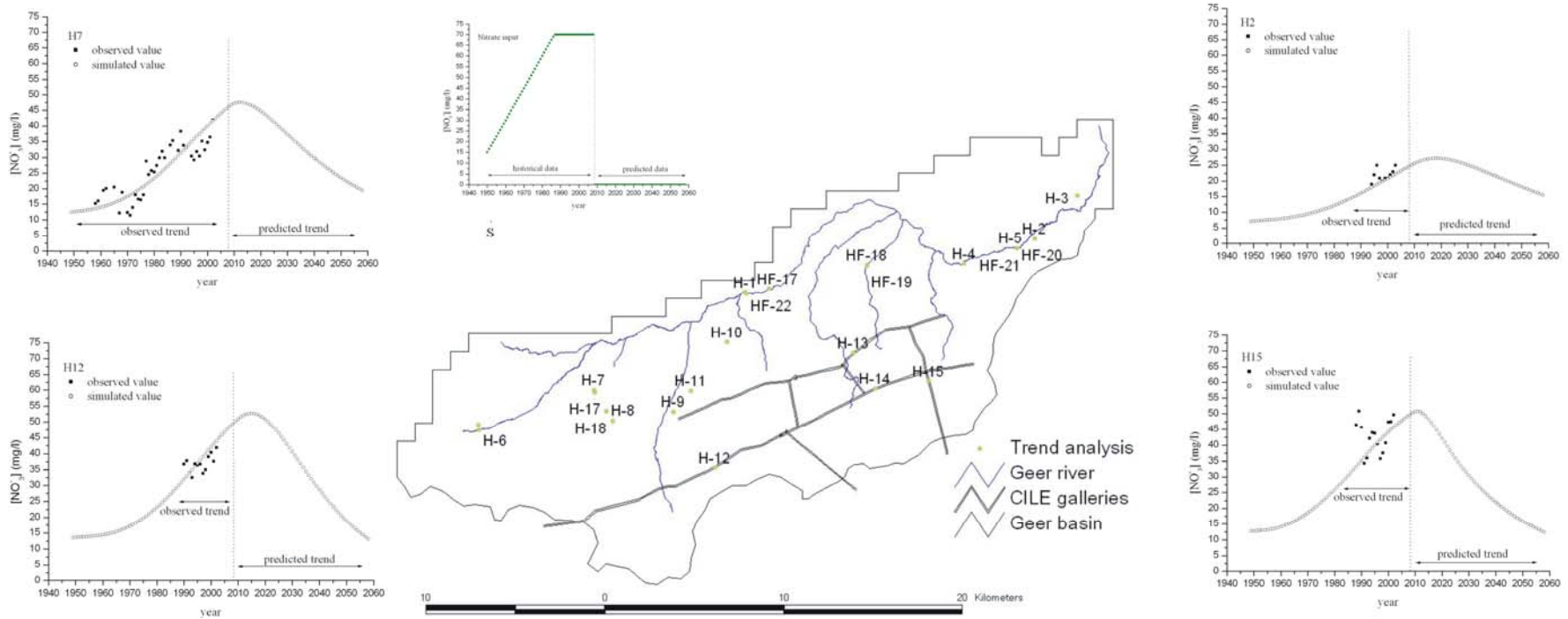

Figure 4.41. Example of computed values of nitrate concentration for the period 1950-2058 considering scenario 1 for the nitrate concentrations in leaching water.

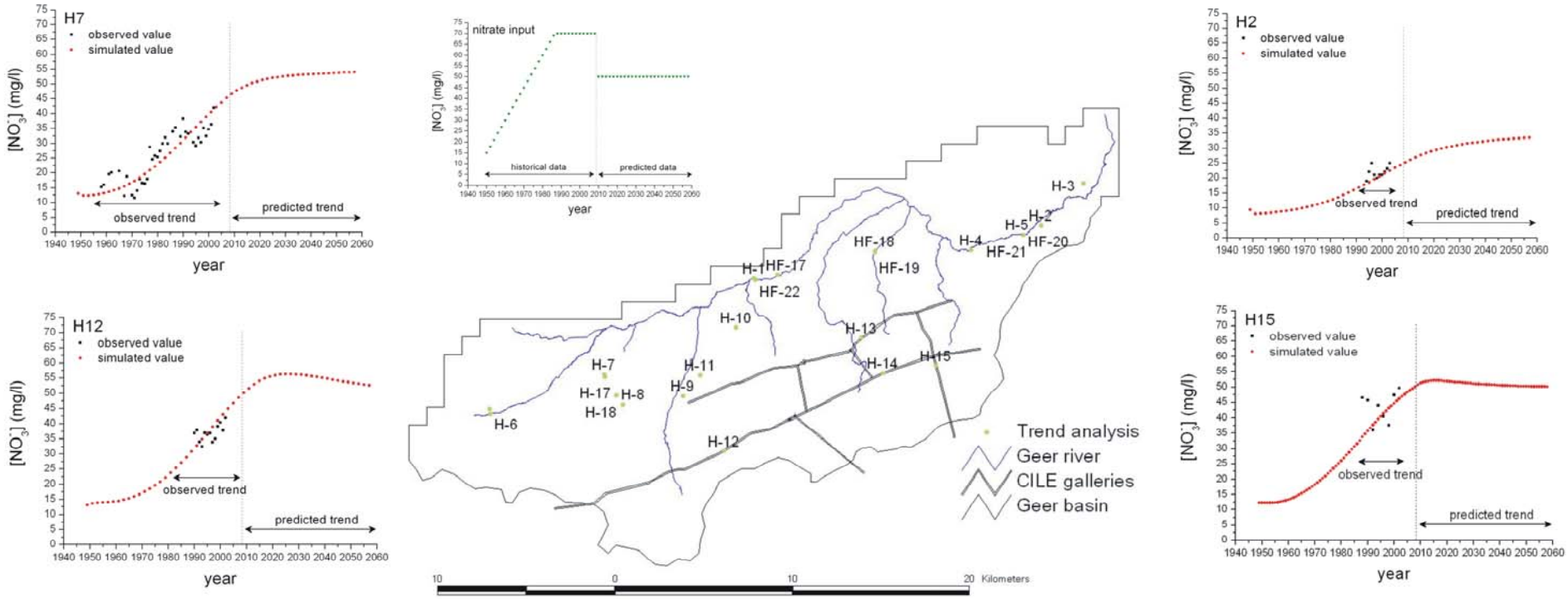

Figure 4.42. Example of computed values of nitrate concentration for the period 1950-2058 considering scenario 2 for the nitrate concentrations in leaching water.

4.5.5 Sensitivity analysis

The purpose of a sensitivity analysis is to quantify the uncertainty in the calibrated model caused by uncertainty in the estimates of the aquifer parameters (Anderson and Woessner 1992). The sensitivity of the model to variations of the considered parameters θ_{ml} (porosity of mobile water in the loess layer), θ_{mc} (porosity of mobile water in the chalk layers),α (transfer coefficient of the solute between mobile and immobile water) θ_{im} (porosity of immobile water), α_{HG} (transfer coefficient between the two subdomains) were tested. The sensitivity of the model to the distribution of the nitrate input was also evaluated. As an example, the sensitivity was evaluated by comparing the computed nitrate concentrations at the points H2, H7, H12, and H15 in the basin, representing different zones of the aquifer.

4.5.5.1 Sensitivity to the variations of effective porosity

4.5.5.1.1 Sensitivity to the variations of the effective porosity in the loess layer θ_{ml}

Three contrasted values (θ_{ml} = 39%, 44%, 49%) of the effective porosity in the loess layer have been used in the sensitivity analysis (Figure 4.43). If θ_{ml} increases, contaminants move more slowly in the loess layer and arrive later in the chalk. If θ_{ml} increases, the slope of the trend decreases. Trend reversal occurs later but the maximum concentration is lower as more mixing occurs.

4.5.5.1.2 Sensitivity to the variations of the porosity of mobile water in the chalk layer θ_{mc}

Values of the porosity of mobile water of the chalk obtained after calibration of the model have been divided and multiplied by two for the sensitivity analysis (Figure 4.44). Surprisingly, the impact of the changes in the values of the effective porosity is very low. One can see that, as expected, the lower is the effective porosity the higher is the concentration in the mobile water is as the contaminant arrives more quickly.

4.5.5.2 Sensitivity to the variations of the transfer coefficient between mobile and immobile water α

Three contrasted values ($\alpha = 1\times10^{-6}$, 1×10^{-7}, 1×10^{-8} s^{-1}) of the transfer coefficient between the mobile and immobile water were used. As an example, the nitrate concentrations computed with these three values are presented for four wells in Figure 4.45. The lower is α, the higher is the concentration in the mobile water as less contaminant is transferred to the immobile water. The slope of the trend is also larger if α decreases. For the wells H12 and H15 where a trend reversal is observed in the reference case, trend reversal occurs earlier if α is lower and the maximum concentration reached is higher. The slope of the downward trend is also larger.

4.5.5.3 Sensitivity to the variations of the porosity of immobile water θ_{im}

Three contrasted values (θ_{im} = 20%, 30%, 40%) of the porosity of immobile water were tested. The resulting computed are presented in Figure 4.46. The lower is θ_{im}, the higher is the computed concentration in the mobile water as the available volume of immobile water to mix the contaminant is lower. The slope of the trend is also larger if θ_{im} decreases. For the wells H12 and H15, the observed trend reversal occurs earlier if θ_{im} is smaller and the maximum concentration is higher. The slope of the downward trend is also larger.

Variations of the two parameters α and θ_{im} plays in the same way and act both on the amount of contaminant diffusing into the immobile water. The more these parameters are large, the more contaminants can diffuse into immobile water. More dilution occurs but the inertia of the system becomes also higher.

4.5.5.4 Sensitivity to the variations of the coefficient α_{HG}

As explained in Section 4.5.1.2, the modelled area was divided in two subdomains in order to take into account the influence of the hardground on the groundwater flow. An internal third type was prescribed at the interface between the two subdomains. Three contrasted values ($\alpha_{HG} = 1\times10^{-4}$, 1×10^{-5}, 1×10^{-6} m^2/s) of the transfer coefficient between the two subdomains. The nitrate concentrations computed with these three values are shown for four wells in Figure 4.47. As explained previously, the computed nitrate concentrations are observed at the upper nodes in the saturated zone. For the wells H2 and H7, the observation node is located in the upper subdomains above the interface but in the lower subdomain under the interface for the wells H12 and H15. Variations in the value of α_{HG} induce an opposite result on the

computed concentrations in the wells H2, H7 and H12, H15. If α_{HG} increases, computed nitrate concentrations decrease in the wells H2 and H7 but increase in the wells H12 and H15. This difference is explained by the position of the nodes at which the computed concentrations are considered. When α_{HG} increases, more pollutant can move from the upper to the lower subdomain and concentrations decrease in the upper subdomain and thus in the wells H2 and H7 and increases in the lower subdomain and thus in the wells H12 and H15. If α_{HG} is low, the trend reversal occurs earlier in H7.

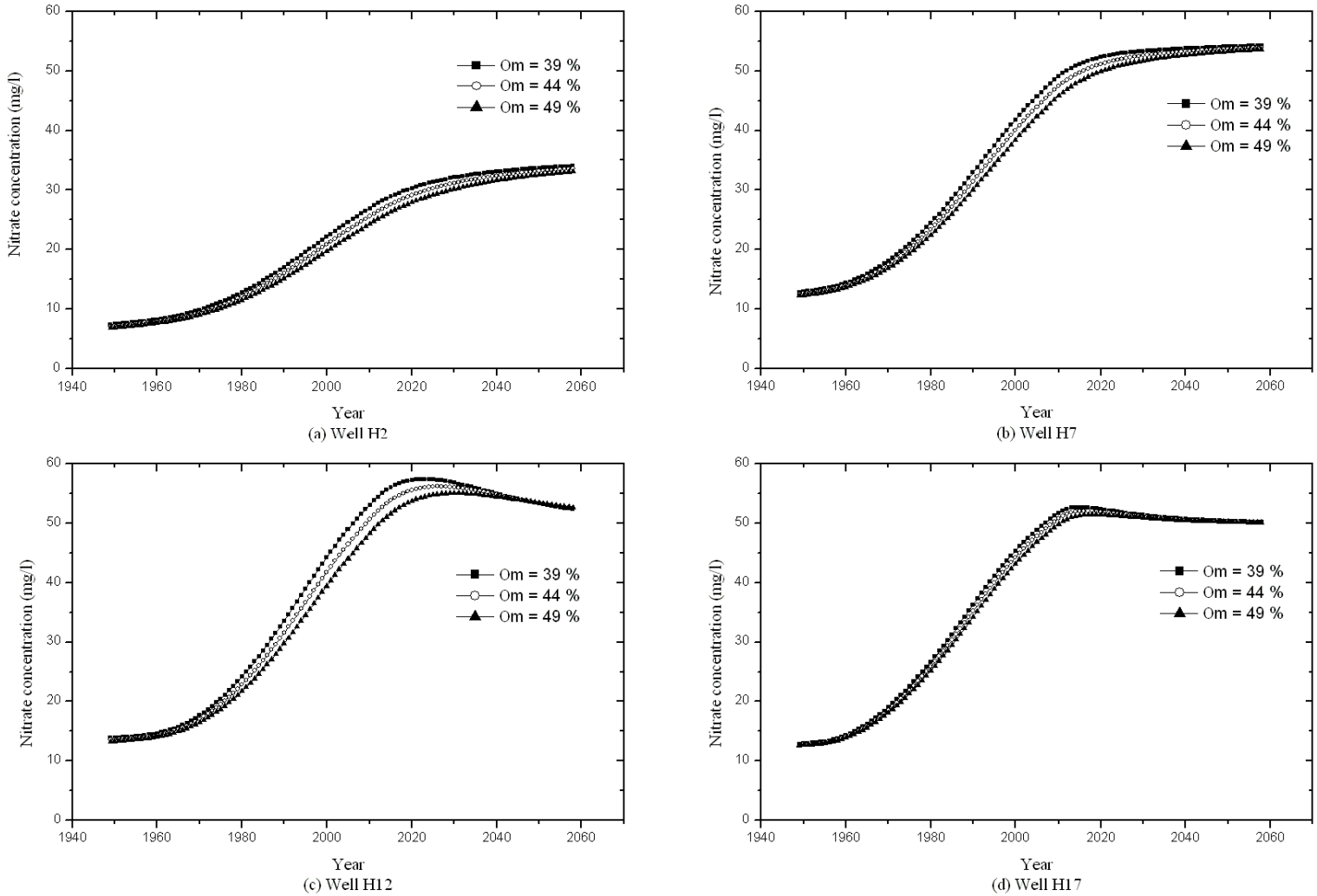

Figure 4.43. Nitrate concentrations computed in wells H2, H7, H12, H15 for different values of the effective porosity in the loess layer.

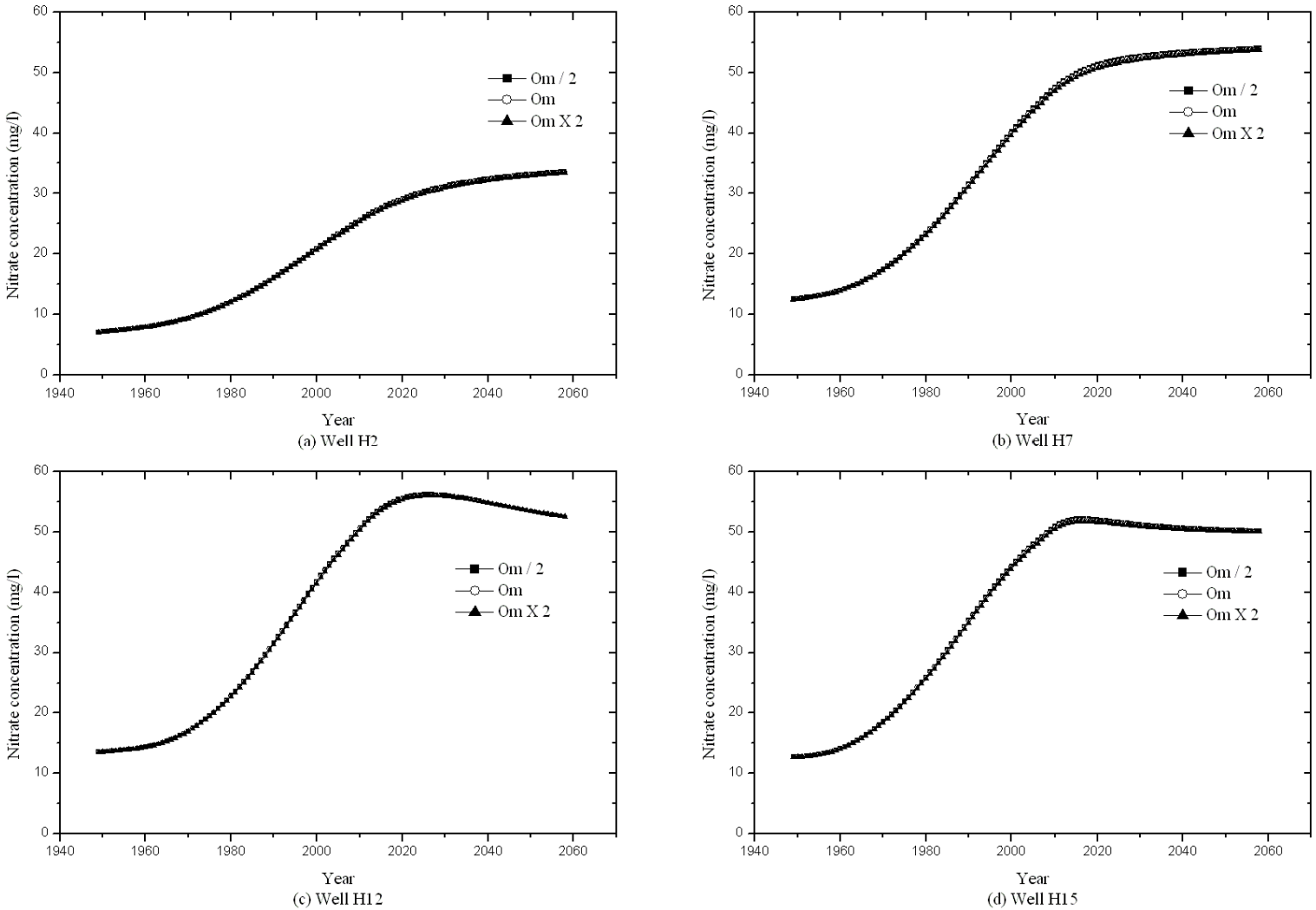

Figure 4.44. Nitrate concentrations computed in wells H2, H7, H12, H15 for different values of the proportion of mobile water in the chalk layers.

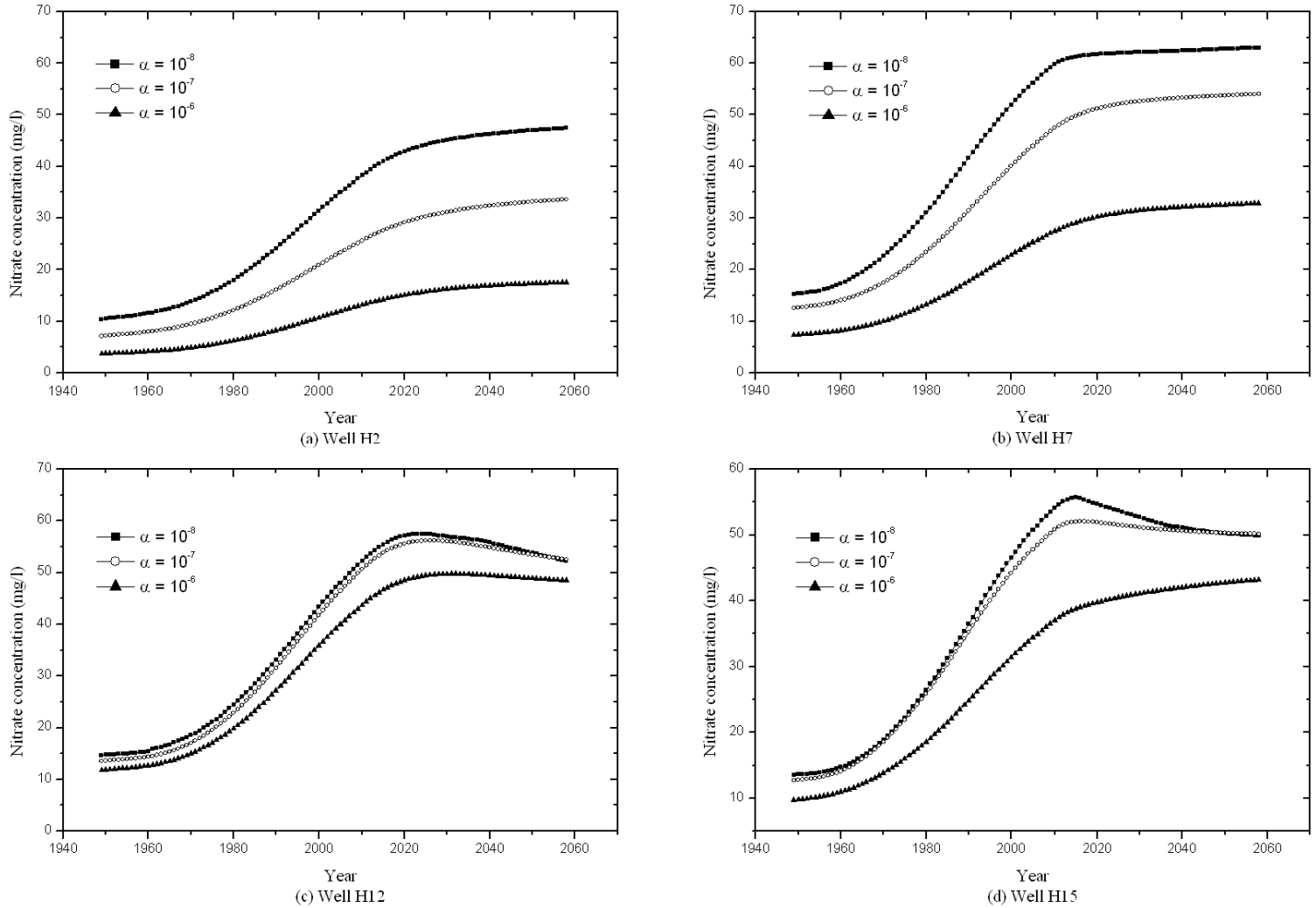

Figure 4.45. Nitrate concentrations computed in wells H2, H7, H12, H15 for different values of the transfer coefficient between the mobile and immobile water.

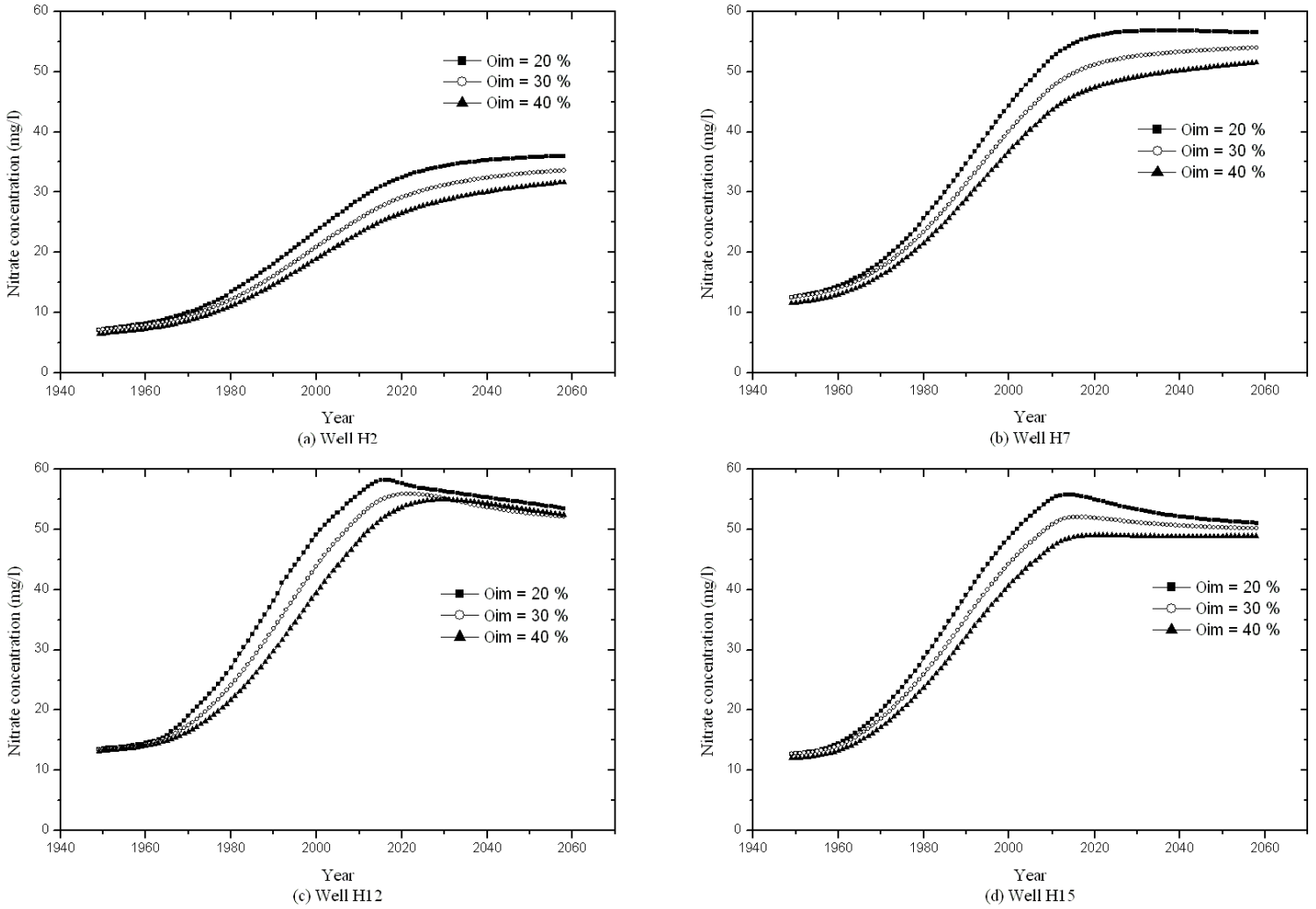

Figure 4.46. Nitrate concentrations computed in wells H2, H7, H12, H15 for different values of the proportion of immobile water in the chalk layers.

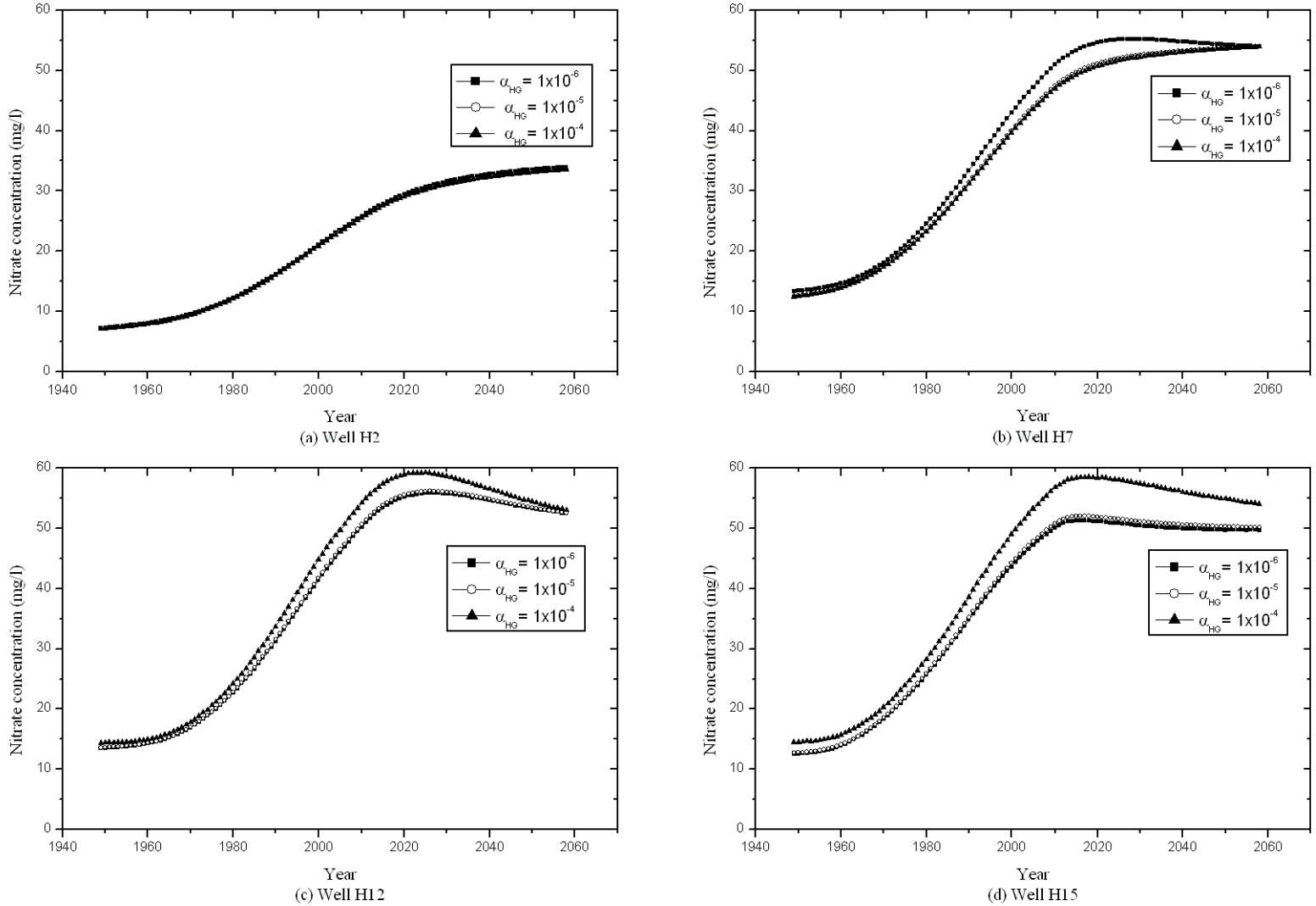

Figure 4.47. Nitrate concentrations computed in wells H2, H7, H12, H15 for different values of the transfer coefficient between the two subdomains.

4.5.5.5 Sensitivity to the distribution of the nitrate input

As explained previously, the nitrate input in the infiltrating water has been assumed to be spatially uniform. However, zones exist in the basin where the nitrate input is suspected to be very different. It is the case of urban zones where the nitrate input is not related to the agricultural practice but to the management of sewage. Point pollutions can also lead to very different nitrate input. However these point pollutions, which are not targeted in this work, are difficult to localise and to quantify.

To test the sensitivity of the model results to the spatial distribution of this nitrate input, three zones (Figure 4.48) were distinguished on the basis of the land-use map and correspond to the "discontinuous urban fabric" zones of this map. In these zones, the nitrate input was considered as equal to 15 mg/l for all the period of simulation (1950-2058). Wells H12 and 15 are located upstream, in the Southern part in the basin. However, their situation is different; H12 is located in an agricultural zone while H15 is located downstream from an urban zone. H2 and H7 are located downstream in the basin, in its Northern part, in or upstream from an urban zone respectively (Figure 4.48). The computed nitrate concentrations for these four wells are presented in Figure 4.49.

Computed concentrations in the well H12 are not affected by this change of input distribution. The well H12 is located upstream in the basin and all the area located upstream of this well receive a nitrate input which is not different from the reference scenario. On the contrary, computed concentrations in H15 are lower due to the lower nitrate input in the zone located upstream (around Bierset). The computed concentration in the wells H2 and H7 are both influenced by the new nitrate input distribution. They are located downstream in the basin and receive the water and contaminant infiltrated upstream.

In conclusion, distribution of the nitrate input should have different effects on the nitrate contamination levels in the Southern and Northern part of the basin. In the upstream part of the basin, the impact of the spatial distribution of the input on the groundwater nitrate concentration should be important. In the downstream part, this impact should be less pronounced as groundwater is a mix of groundwater coming from different parts of the basin.

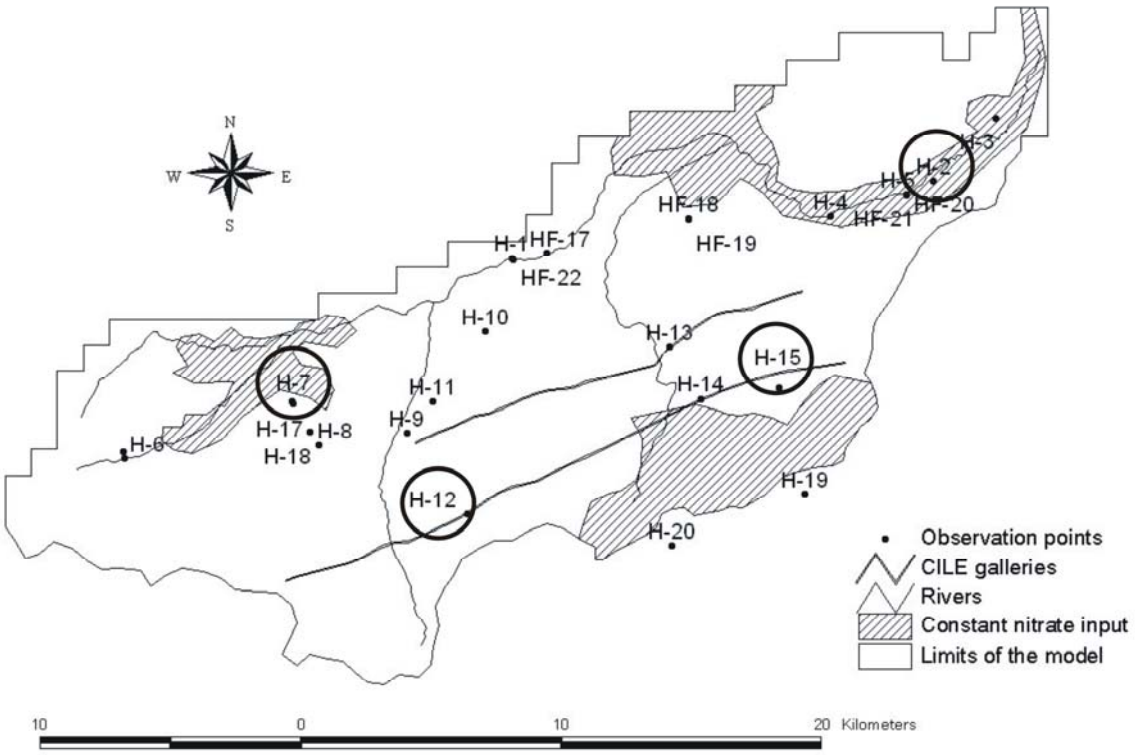

Figure 4.48. Spatial distribution of the nitrate input, hatched areas correspond to discontinuous urban zones where the nitrate input is assumed to be lower.

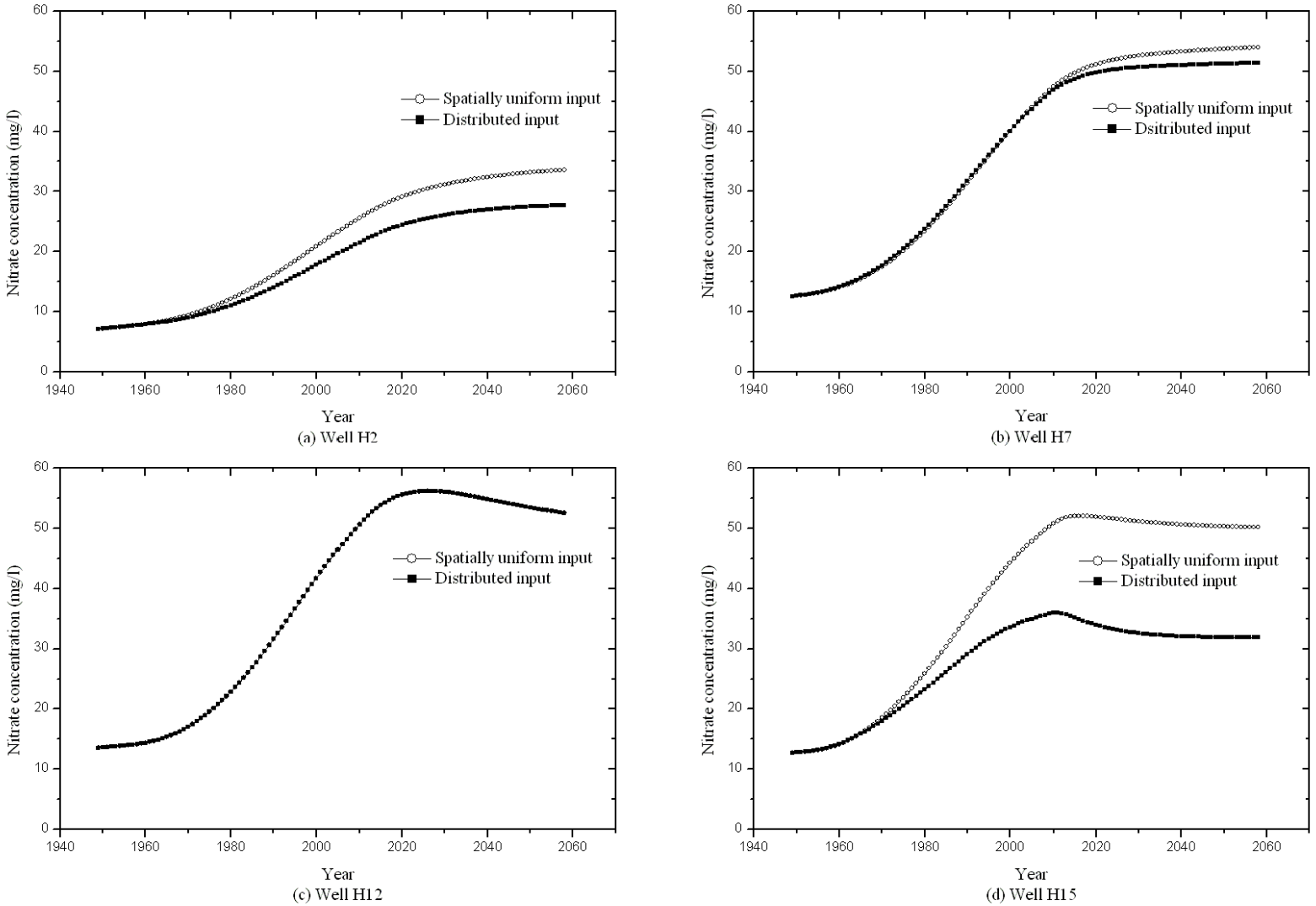

Figure 4.49. Nitrate concentrations computed in the wells H2, H7, H12 and H15 considering or not that the nitrate input is distributed

4.5.6 Discussion of modelling results

A 3D spatially-distributed groundwater flow and solute transport model of the Geer basin has been developed based on: (1) the HFEMC approach and, (2) long time series of nitrate concentration completed by tritium data.

Considering simplified, but realistic and uniformly distributed nitrate input, the model reproduce in a satisfactory way (1) the observed levels and the spatial distribution of nitrate contamination and (2) the time evolution of the nitrate concentration and the spatial repartition of these trends. These results seem to confirm the diffuse character of contamination. More details in the distribution of the nitrate input could potentially explain local variations in the observed groundwater nitrate concentrations but are not necessary to manage the groundwater body globally.

As demonstrated using the results of the environmental tracer survey, the spatial distribution of the contamination in the Geer basin is clearly linked to the hydrodynamic conditions prevailing in the basin. A good understanding and representation of groundwater flows is thus of primary importance to model adequately the nitrate contamination of the groundwater in the Geer basin. The performed sensitivity analysis proves that the model is robust. All the tested variations in values attributed to the parameters have clear effects on the model that can be explained by physical laws. The spatial distribution of the computed nitrate trends seems not to be very affected by the tested variations of the parameters. The parameters that seem to have the most important impacts on the results are the porosity of immobile water and the transfer coefficient between the mobile and immobile water. Further investigations could be done to better quantify these parameters and evaluate their spatial distributions.

The long period of simulation required to stabilise computed concentrations used as initial conditions confirms the high inertia of the chalk aquifer system of the Geer basin. Using the model to predict the future evolution of nitrate trends in the basin, it appears clearly that the objective prescribed by the Water Framework Directive could not be achieved by 2015 even considering an extreme scenario with no nitrate input since 2008. The time needed before trend reversal in the Southern part of the basin is mainly a function of the thickness of the unsaturated zone, which range from a few meters to many tens of meters. The velocity of contaminant in the unsaturated zone is confirmed around 1m/year. With those described conditions and with a decrease in the input at the beginning of 2009, any trend reversal is

predicted by 2015. In the Northern part and Eastern parts of the basin, the trend reversal is predicted later than in the Southern one. These zones are located downstream and receive the contaminated groundwater from the Southern part. The model shows that even in the wells where the nitrate concentrations are nowadays low and largely below the water drinking threshold, a maximum concentration higher than the water drinking limit of 50 mg/l could be reached.

The different assumptions made during the development of the model and, among other, the choice to model the groundwater flow in steady state conditions allow having an efficient model in terms of computation time. For example, the computation time required to run the calibrated model on a PC is only around four hours for more than 100 modelled years.

4.6 Socio-economic analysis

The groundwater model developed in this thesis was used in the framework of the AquaTerra project to perform an economic analysis on the Geer basin case study in collaboration with the socio-economic team of the BRGM. As mentioned previously in Section 4.2, the Hesbaye aquifer was identified as the groundwater body the most affected by agricultural pressures and nitrate in the Walloon region (DGRNE 2005). Moreover, as demonstrated by Batlle-Aguilar *et al.* (2007), nitrate concentrations increase all over the basin. Following the requirements of the WFD, a programme of mitigation measures should be implemented to decrease these pressures and reach a "good chemical status". Potential measures have to be compared and selected according to their cost-effectiveness.

In the framework of the AquaTerra project, an economic analysis was performed (Hérivaux *et al.* 2008), illustrating how results from the groundwater modelling can be useful for socio-economic purposes. The methodology followed for this economical analysis consists in the three following steps (Figure 4.50):

- a cost-effectiveness analysis (CEA) consisting in the design of programmes of measures to reach a defined objective of reduction of nitrate concentration in the infiltrating water at the lower cost;
- a benefit analysis in which the benefits for the society resulting of the mitigation measures are assessed as avoided damages that would occur due to the groundwater nitrate pollution in the coming decades if nothing was done;

- a cost-benefice analysis in which the costs and the benefits of the selected programme of measures are compared.

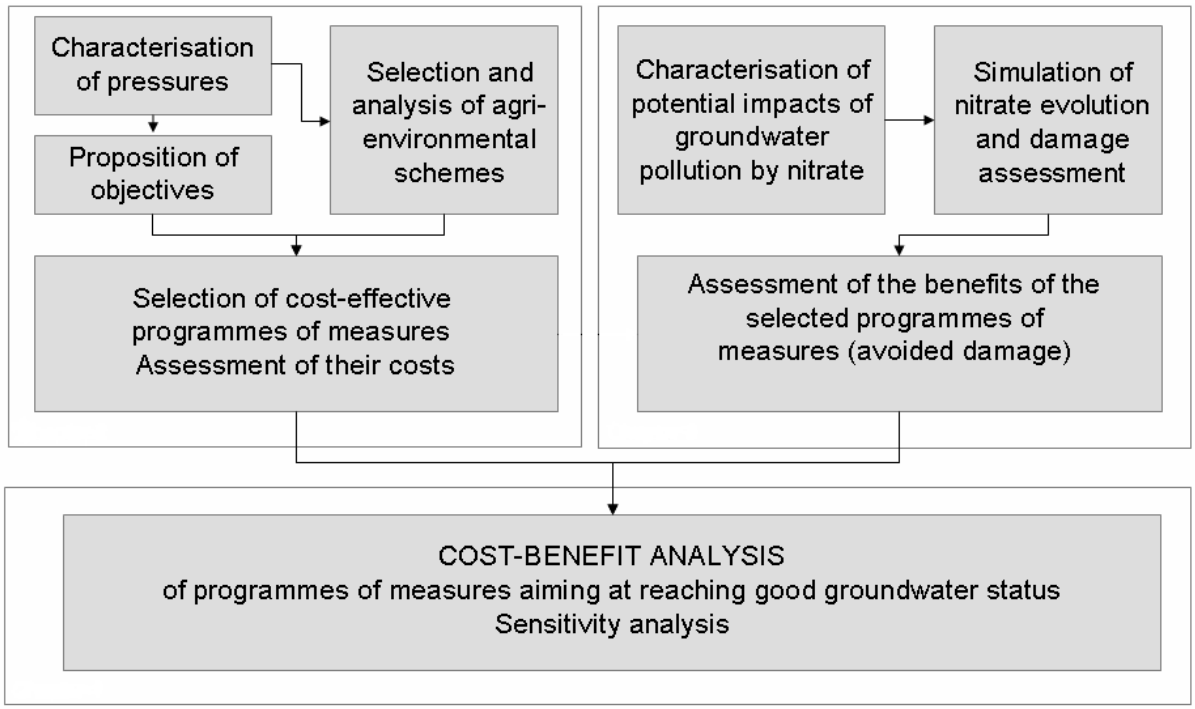

Figure 4.50. Overview of the methodological steps of the socio-economic study in the Geer basin (modified from Hérivaux *et al.* 2008)

4.6.1 Selection of cost-effective programmes of measures

As mentioned previously, mean nitrate concentrations in infiltrating water resulting from agriculture in the Geer basin were estimated to around 67 mg/l. Without any degradation, this mean concentration in the infiltrating water is too high to reach a "good chemical status". In the framework of this economic analysis, three different objectives of decrease of nitrate concentrations in leaching water were considered: (1) objective A: 50 mg/l, (2) objective B: 45 mg/l, (3) objective C: 40 mg/l. All of these scenarios are assumed to enable to reach "good chemical status" in the future but within different laps of time.

To reach these objectives, different measures or agri-environmental schemes[2], that allow reducing the nitrogen load in agriculture have to be considered. In this case study, four agri-environmental schemes were selected:

[2] Agri-environmental scheme were introduced into EU agricultural policy during the late 1980s as an instrument to support specific farming practices that go beyond usual good practices and that help to protect the

- conversion of arable land into grassland;
- conversion from inorganic to organic agriculture;
- implementation of catch crops;
- decrease in nitrogen fertilisation by replacement by crops needing less fertilisers.

The expected decrease in nitrate concentrations in the infiltrating water was estimated for each of these measures and the considered surface where the measures could be implemented where assessed. Then, a cost-effectiveness analysis (CEA) was performed. A CEA consists in organising the selected measures as a function of their capacity to decrease exerted pressures on groundwater at a given cost. Figure 4.51 shows an example of cost-effective combination of four measures A_1 to A_4 with rising cost-effectiveness rates r_1 to r_4 and potential effects from E_1 to E_4. In order to reach objective 1, the CEA would recommend implementing A_1 and A_2 successively. To reach objective 2, the CEA would recommend implementing successively A_1, A_2, A_3 and A_4.

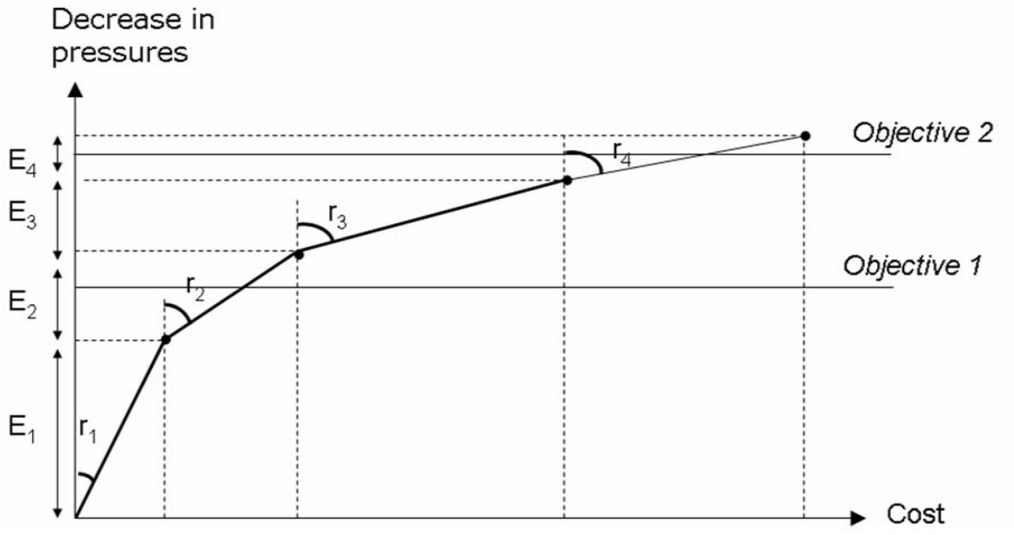

Figure 4.51. Cost-effective combination of measures to reach two levels of objectives (Hérivaux *et al.* 2008)

Using the CEA, the different selected measures for the Geer basin case studies were organised into programmes (called A, B, C hereafter) of measures that allow reaching the different objectives of decrease of nitrate concentrations in the infiltrating water

environment and maintain the countryside. As a compensation, volunteer farmers receive payments that for additional costs and loss of incomes resulting from the adoption of these agri-environmental measures.

4.6.2 Benefits related to the improvement of groundwater quality

Programme of measures selected using the CEA should allow decreasing nitrate concentrations in groundwater. This constitutes a positive economic impact for the drinking water sector (Figure 4.52). The second step of the economic analysis consists in the assessment of these potential economic benefits resulting from the implementation of the different programmes of measures.

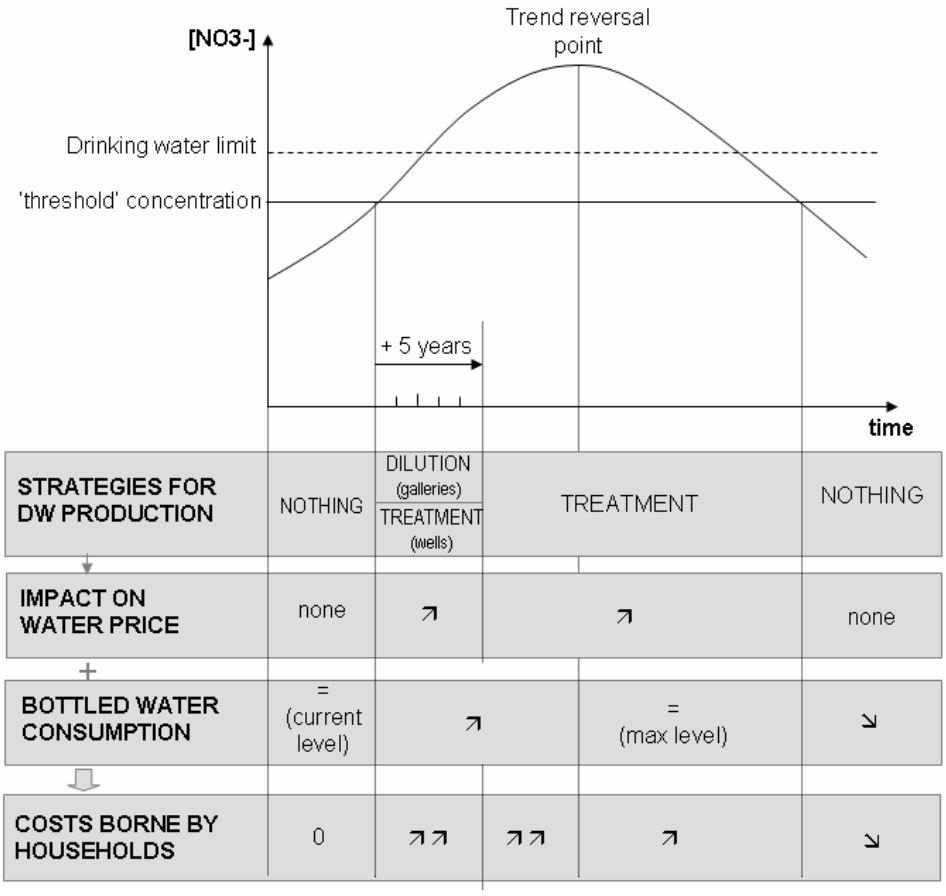

Figure 4.52. Example of potential impacts of groundwater quality variations on the drinking water sector and the price of drinking water (Hérivaux *et al.* 2008).

To assess these benefits, the following methodology is followed:

1. The groundwater abstraction points used for drinking water supply are identified.
2. The evolutions of nitrate concentrations at the groundwater abstraction points are computed with the groundwater flow and solute transport model considering no programmes of mitigation measures (Figure 4.53). The economic damages resulting

from the nitrate contamination were assessed in collaboration with the drinking water supply companies CILE, SWDE and VMW.

3. The implementation of the different programmes A, B and C of measures is analysed. The evolutions of nitrate concentrations in groundwater abstraction points are computed (Figure 4.53) considering the reduced concentrations in the leaching water expected from the different programmes of mitigation measures. The benefits of these programmes were assessed as avoided damage.

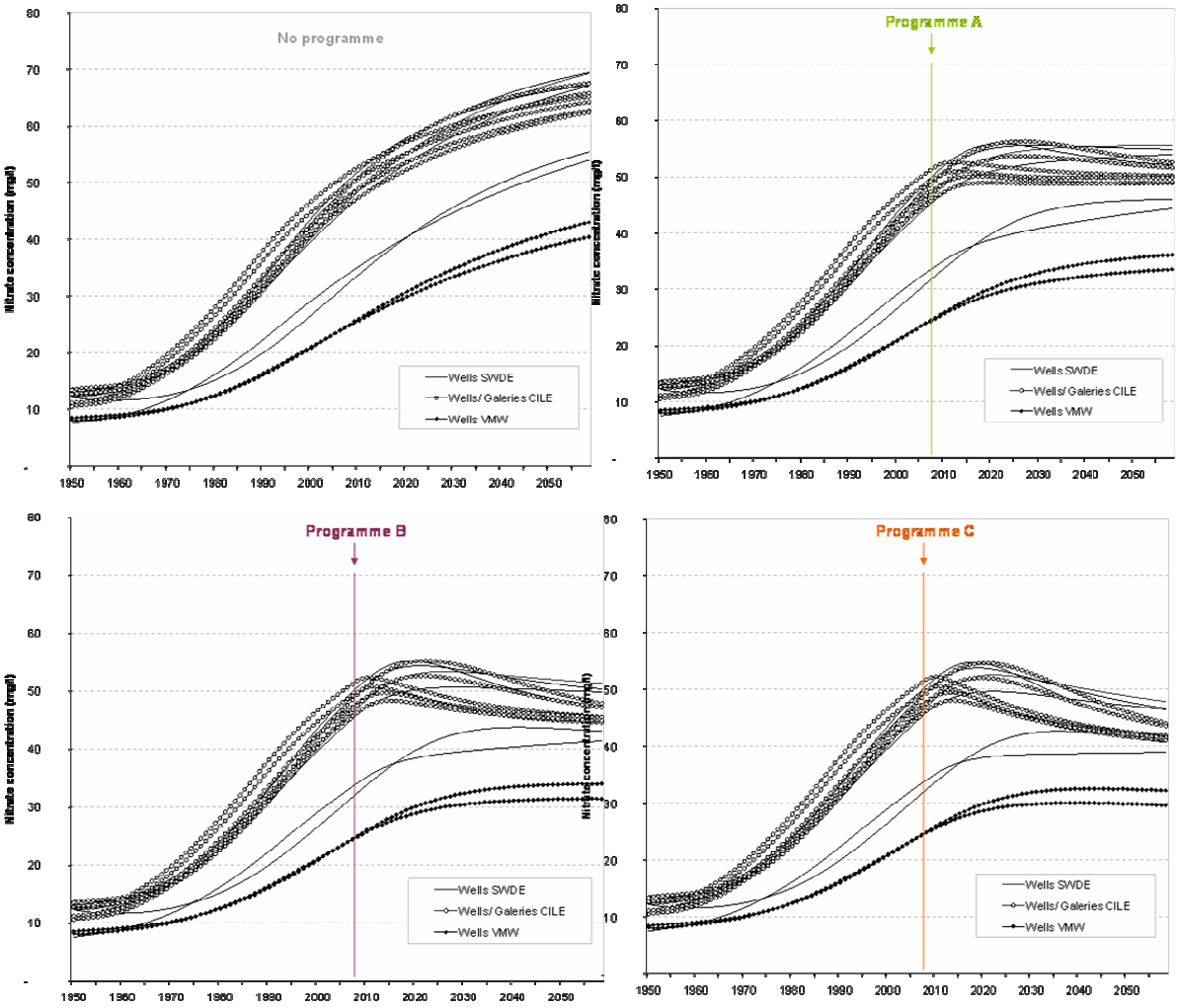

Figure 4.53. Evolution of nitrate concentrations in the abstraction points used for drinking water supply considering no programme or programmes A, B or C of mitigation measures.

4.6.3 Cost-benefit analysis of the selected programmes of measures

The cost-benefit analysis consists in comparing costs and benefits resulting from the implementation of management measures for a given time period. This allows selecting the programme of mitigation measures which provides the more benefits at the lower cost.

4.7 References to chapter 4

AERM (2005). Méthodes et procédures pour l'état des lieux des districts Rhin et Meuse - Sambre, Document de référence, Version finale approuvée par le comité de bassin du 4 février 2005 et approuvée par le préfet coordonnateur de bassin. Etat des lieux des districts Rhin et Meuse - partie française, AERM**:** 162.

Anderson, M. P. and W. W. Woessner (1992). Applied groundwater modeling. Simulation of flow and advective transport. San Diego, California, Academic Press, Inc.

Barrez, F. (2006). Essais de caractérisation hydrochimique verticale de la nappe de la Craie dans le secteur minier Carvin-Douai-Hénin-Beaumont. Laboratoire de Mécanique de Lille. Lille, Université de Lille I.

Batlle-Aguilar, J., P. Orban, A. Dassargues and S. Brouyère (2007). "Identification of groundwater quality trends in a chalk aquifer threatened by intensive agriculture in Belgium." Hydrogeology Journal **15**(8): 1615-1628.

Biver, P. (1993). Etude phénoménologique et numérique de la propagation des polluants miscibles dans un milieu à porosité multiple (Phenomenological and numerical study of miscible contaminant propagation in a multi-porosity medium). PhD thesis. Faculty of Applied Sciences. Liège (Belgium), University of Liège**:** 389.

Broers, H. P. (2004). "The spatial distribution of groundwater age for different geohydrological situations in the Netherlands: implications for groundwater quality monitoring at the regional scale." Journal of Hydrology **299**: 84-106.

Broers, H. P., A. Visser, I. G. Dubus, N. Baran, X. Morvan, M. Normand, A. Gutiérrez, C. Mouvet, J. Batlle Aguilar, S. Brouyère, P. Orban, S. Dautrebande, C. Sohier, M. Korcz, J. Bronder, J. Dlugosz and M. Odrzywolek (2005a). Report with documentation of reconstructed land use around test sites. Deliverable T2.2, AquaTerra (Integrated Project FP6 no. 505428)**:** 64.

Broers, H. P., A. Visser, J.-L. Pinault, D. Guyonnet, I. G. Dubus, N. Baran, A. Gutierrez, C. Mouvet, J. Batlle-Aguilar, P. Orban and S. Brouyère (2005b). Report on extrapolated time trends at test sites, Deliverable T2.4, AquaTerra (Integrated Project FP6 no. 505428)**:** 81.

Brouyère, S. (2001). Etude et modélisation du transport et du piégeage des solutés en milieu souterrain variablement saturé (Study and modelling of transport and retardation of solutes in variably saturated media). Faculty of Applied Sciences. Liège (Belgium), University of Liège**:** 640.

Brouyère, S., G. Carabin and A. Dassargues (2004b). "Climate change impacts on groundwater resources: modelled deficits in a chalky aquifer, Geer basin, Belgium." Hydrogeology Journal **12**: 123-134.

Brouyère, S., H. Corbeanu, M. Dachy, N. Gardin, P. Orban and A. Dassargues (2004c). Projet de recherche PIRENE. Rapport final, DGRNE**:** 105.

Brouyère, S., A. Dassargues and V. Hallet (2004a). "Migration of contaminants through the unsaturated zone overlying the Hesbaye chalky aquifer in Belgium: a field investigation." Journal of Contaminant Hydrology **72**(1-4): 135-164.

Dassargues, A. and A. Monjoie (1993). The chalk in Belgium. The hydrogeology of the chalk of the North-West Europe. R. A. Downing, M. Price and G. P. Jones. Oxford, UK, Oxford University Press**:** Chapter 8: 153 - 269.

Dautrebande, S., A. Dewez, C. Casse and P. Hennebert (1999). Nitrate leaching at the regional scale with EPIC: an implicit example of a hydrotope model concept. Leuven, European Agriculture Engineering Soil and Water Interest Group**:** 765-774.

Dautrebande, S., A. Dewez, V. Hallet, J. Guiot, F. Rouxhet and A. Monjoie (1996). Programme Action Hesbaye. Final report of the EC-Life project**:** 169.

Dautrebande, S. and C. Sohier (2001). Projet de recherche PIRENE, 1er Rapport annuel., University of Gembloux**:** 39.

Dautrebande, S. and C. Sohier (2004). Projet de recherche PIRENE, Rapport final., University of Gembloux**:** 120.

DGRNE (2005). Analyse des pressions anthropiques sur les eaux souterraines. Etat des lieux du District Hydrographique International de la Meuse, Ministère de la Région Wallonne, Direction générale des Ressources naturelles et de l'Environnement, Observatoire des Eaux de Surface, Direction des Eaux de Surface, Direction des Eaux Souterraines**:** 47.

Fretwell, B. A., W. G. Burgess, J. A. Barker and N. L. Jefferies (2005). "Redistribution of contaminants by a fluctuating water table in a micro-porous, double-porosity aquifer: Field observations and model simulations." Journal of Contaminant Hydrology **78**: 27-52.

Gooddy, D. C., W. G. Darling, C. Abesser and D. J. Lapworth (2006). "Using chlorofluorocarbons (CFCs) and sulphur hexafluoride (SF_6) to characterise groundwater movement and residence time in a lowland Chalk catchment." Journal of Hydrology **330**(1-2): 44-52.

Hallberg, K. B. and D. R. Keeney (1993). Nitrate. Regional Ground-Water quality. W. M. Alley. New York, Van Nostrand Reinhold**:** 297-322.

Hallet, V. (1998). Étude de la contamination de la nappe aquifère de Hesbaye par les nitrates: hydrogéologie, hydrochimie et modélisation mathématique des écoulements et du transport en milieu saturé (Contamination of the Hesbaye aquifer by nitrates: hydrogeology, hydrochemistry and mathematical modeling). Faculty of Sciences. Liège (Belgium), University of Liège**:** 361.

Hérivaux, C., P. Orban, J. Batlle-Aguilar, S. Brouyère and P. Goderniaux (2008). Socio-economic analysis integrating soil-water system modelling for the Geer catchment (Meuse, Walloon region) - diffuse nitrate pollution in groundwater, FP6-IP, AquaTerra project (n°505428)**:** 45.

Hodiaumont, A., R. Cantillana and J. M. Compère (1999). "Les eaux souterraines de la CILE : Contexte, captage et qualité." Tribune de l'eau **52**(600-601): 31-50.

IAEA (2002). Use of isotopes for analyses of flow and transport dynamics in groundwater systems, IAEA-UIAGS.

Koh, D.-C., L. N. Plummer, D. K. Solomon, E. Busenberg, Y.-J. Kim and H.-W. Chang (2006). "Application of environmental tracers to mixing, evolution, and nitrate contamination of ground water in Jeju Island, Korea." Journal of Hydrology **327**: 258-275.

Landreau, A., A. Mariotti and B. Simon (1988). "La dénitrification naturelle dans les eaux souterraines." Hydrogéologie **1**: 35-43.

Maloszewski, P. (1994). "Mathematical modelling of tracer experiments in fissured aquifers." Freiburger Schriften zur Hydrologie **2**: 1-107.

Monjoie, A. (1967). Observations nouvelles sur la nappe aquifère dela craie en Hesbaye (Belgique). Mémoires de l'Association Internationale des Hydrogéologues (IAH). Istanboul.

Orban, P., S. Brouyère, H. Corbeanu and A. Dassargues (2005). Large-scale groundwater flow and transport modelling: methodology and application to the Meuse Basin, Belgium. Bringing Groundwater Quality Research to the Watershed Scale, 4th International Groundwater Quality conference, Waterloo, Canada, IAHS.

Orban, P., I. Ruthy and S. Brouyère (2006). Etat quantitatif et qualitatif des eaux souterraines en Région wallonne. Dossier scientifique réalisé dans le cadre de l'élaboration du Rapport analytique 2006-2007 sur l'état de l'environnment wallon. Liège, ULg-FSA-ArGEnCo-Geo³-Hydrogéologie**:** 68p.

Oster, H., C. Sonntag and K. O. Münnich (1996). "Groundwater age dating with chlorofluorocarbons." Water Resources Research **32**(10): 2989-3001.

van Genuchten, M. T. (1980). "A closed-form equation for predicting the hydraulic conductivity of unsaturated soils." Soil Science Society of America Journal **44**: 892-898.

Zoellmann, K., W. Kinzelbach and C. Fulda (2001). "Environmental tracer transport (^3H and SF_6) in the saturated and unsaturated zones and its use in nitrate pollution management." Journal of Hydrology **240**: 187-205.

5 CONCLUSIONS AND PERSPECTIVES

5.1 Main research outcomes

The main goal of this research was to develop a methodology for regional scale solute transport assessment and modelling. Three specific objectives were fixed: (1) to select, acquire and manage appropriate data providing information related to the scale of work; (2) to develop an original flexible numerical approach for regional scale solute transport modelling; and (3) to apply the developed methodology to the modelling of nitrate trends in the Geer basin.

Until now, few methodologies and tools were available to model the groundwater systems and more particularly the fate of diffuse pollution in groundwater at the regional scale. However, the Water Framework Directive requires that Member States manage their water resources within natural boundaries of the hydrological basins, the aquifers or the groundwater bodies. Moreover, good chemical status has to be reached and pollutant upward trends have to be reversed for 2015. Such tools could be of high interest for supporting groundwater managers in charge of the practical implementation of this directive.

The methodology developed in the framework of this thesis is an answer to these requirements. The numerical approach has been tested first on simple cases and compared with analytical solutions. In a second time, an application of the methodology has been developed for the modelling of nitrate trends in the Geer basin. These tests and this application demonstrate that this methodology is efficient and robust. This methodology and results from this work can thus be applicable to other hydrogeological contexts.

5.2 Assessment of groundwater solute transport at the regional scale

Traditional tracer experiments provide information on transport processes representative at the local scale but do not allow assessing solute transport at the regional scale. The interpretation of environmental tracers data could give information more representative at the scale of the groundwater body. Before developing the application of the Geer basin, the available datasets has been completed by two field surveys providing tritium, CFC's and SF_6 data. Two specific objectives were followed with these surveys: (1) to better understand the spatial distribution of the nitrate contamination in the aquifer, (2) to highlight denitrification processes that would eventually occur in some part of the aquifer. If this first objective is

completely accomplished, the second one has not be realised as local contamination of the groundwater by CFC's prevent the interpretation of these data.

5.3 Modelling of groundwater solute transport at large scale

The developed regional scale methodology is based on the use of specific interfaces and of the new flexible, original and physically-based Hybrid Finite Element Mixing Cell (HFEMC) modelling approach. The HFEMC combined in a fully integrated way different mathematical and numerical solutions to groundwater flow and solute transport problems.

The regional scale methodology has been used to develop a 3D spatially-distributed model for nitrate trends assessment and forecasting in the Geer basin. In this application, groundwater flows are modelled using a classical approach based on the Darcy's law combined with a mixing cell approach to simulate the solute transport. The use of the mixing cell concepts do not require to introduce in the model values of hydrodynamic dispersivities that can not be estimated at the regional scale. The mixing cell concept is well adapted to the modelling of diffuse pollution, the source of contaminant is fully dispersed at the top of the model, the dispersion of pollutant in groundwater can be considered as essentially corresponding to the dispersion of the source.

The groundwater solute transport has been calibrated using the new tritium data and the results of a statistical nitrate trend analysis. Even using a simplified and uniform nitrate input, the developed model allows reproducing the observed nitrate trends and their spatial distribution. Nitrate trends have been predicted for different scenarios of nitrate concentrations in the infiltrating water. This possibility of forecasting is, moreover, an advantage over statistical procedure of trend analysis that can not be used for trend prediction.

5.4 Advances in management of the aquifer of the Geer basin

Considering the modelling results, one can conclude that the global inertia of the groundwater quality in the basin is high and the trend reversal will not occur before a long time and certainly not before the 2015 deadline fixed by the Water Framework Directive. Even with an extreme scenario without nitrate in the infiltrating water after 2008, the time needed before a possible trend reversal ranges between 5 to more than 30 years. To reach a good chemical status and groundwater nitrate concentrations below the drinking water limit, nitrate

concentrations in the infiltrating water have to be reduced as soon as possible below 50mg/l and then time up to more than 50 years is needed to reverse upward trend.

The costs and benefits associated to this reduction of nitrate input can be assessed through a socio-economic study as the one developed for the Geer basin in the scope of the FP6-IP AquaTerra project. This study has integrated the results obtained with the model. The evolutions of the nitrate concentrations in groundwater have been computed for different scenarios of management of the use of fertilizers in the basin. The result of this study will allow choosing the best management option in regards of their costs and benefits.

5.5 Perspectives

New regional scale applications using the Hybrid Finite Element are now under development, among other in the framework of the Synclin'Eau project and Interuniversity Attraction Pole TIMOTHY project, in totally different geological and hydogeological contexts. The linear reservoir approaches included in the HFEMC method will be used to model karstic zones. These new applications will allow validating on real regional case studies, these approaches.

The Water Framework Directive requires managing the water resources in an integrated way. Further development of the Geer basin groundwater model could include the coupling with a soil model such as the EPIC model developed by the "Faculté Universitaire des Sciences Agronomiques de Gembloux". Such coupling will allow better representing the nitrate input in the Geer basin and linking directly the agricultural practices and the contamination in groundwater.

The SUFT3D code and the HFEMC approach are now also used for the modelling of groundwater in mined areas. Another perspective, now under development, is the use of the HFEMC approach to model gas in underground reservoirs.

ANNEX
Complement on time evolution of nitrate concentrations of Chapter4

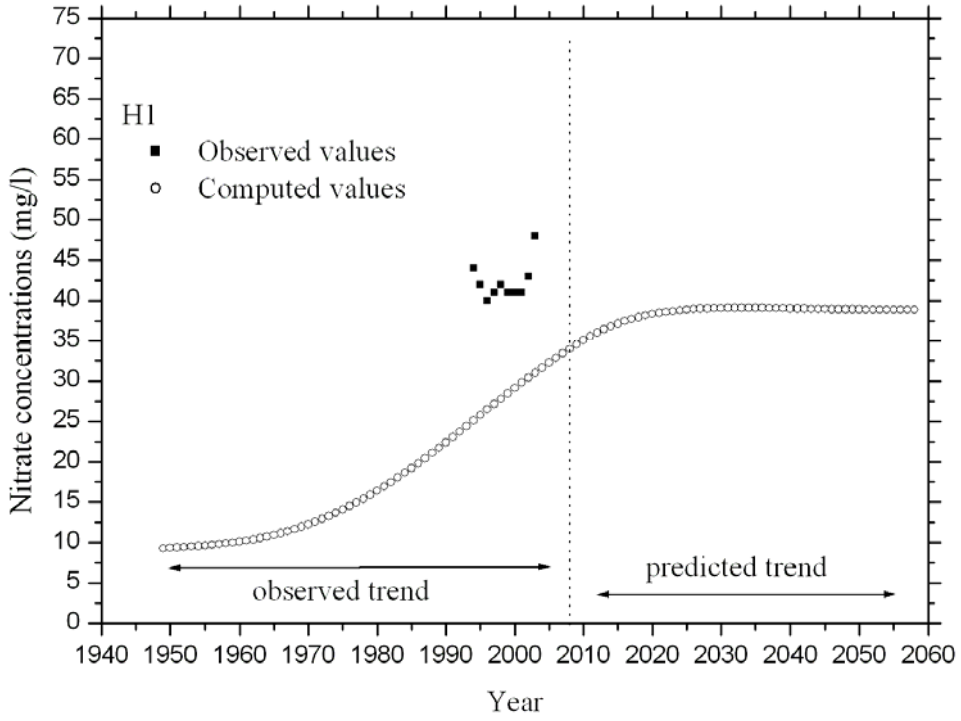

Figure 54. Time evolution of nitrate concentrations in the well H1 computed with scenario 2 described in Section 4.5.4.

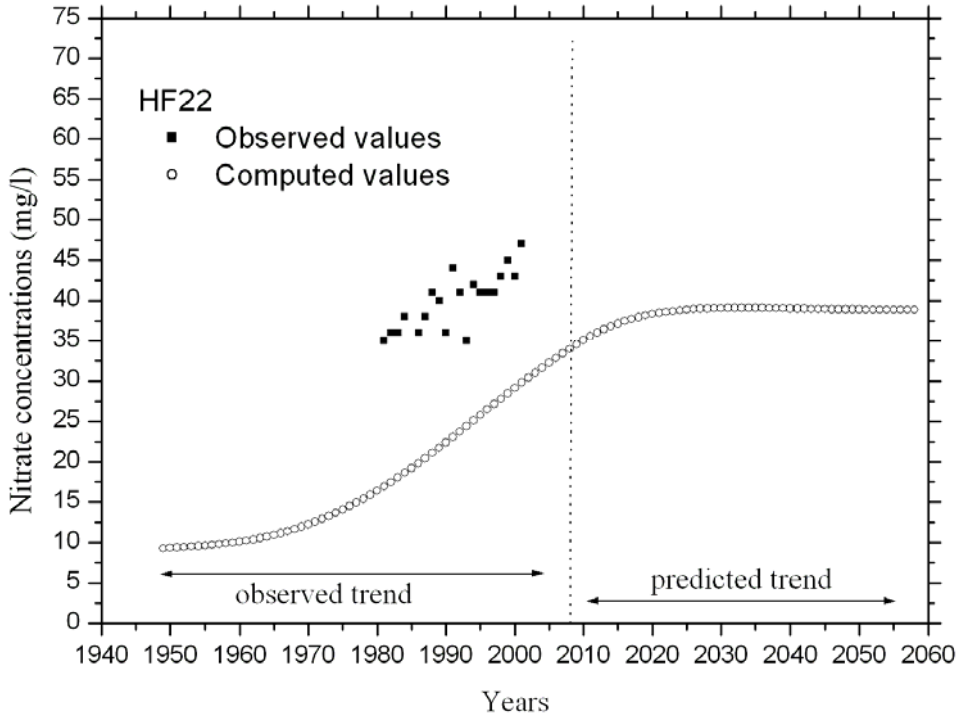

Figure 55. Time evolution of nitrate concentrations in the well HF22 computed with scenario 2 described in Section 4.5.4.

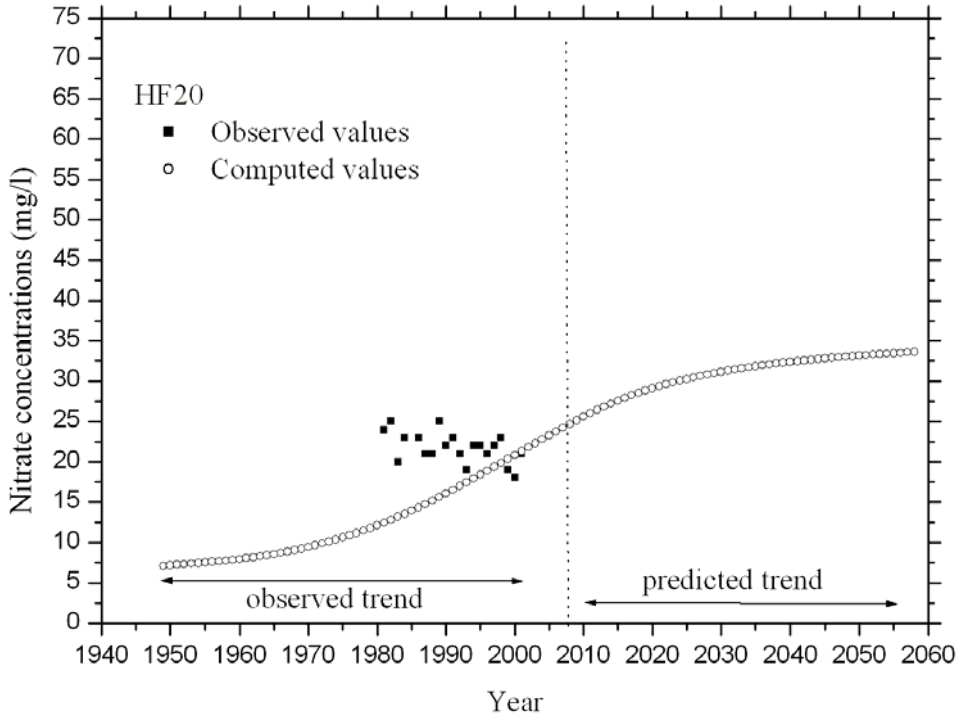

Figure 56. Time evolution of nitrate concentrations in the well HF20 computed with scenario 2 described in Section 4.5.4.

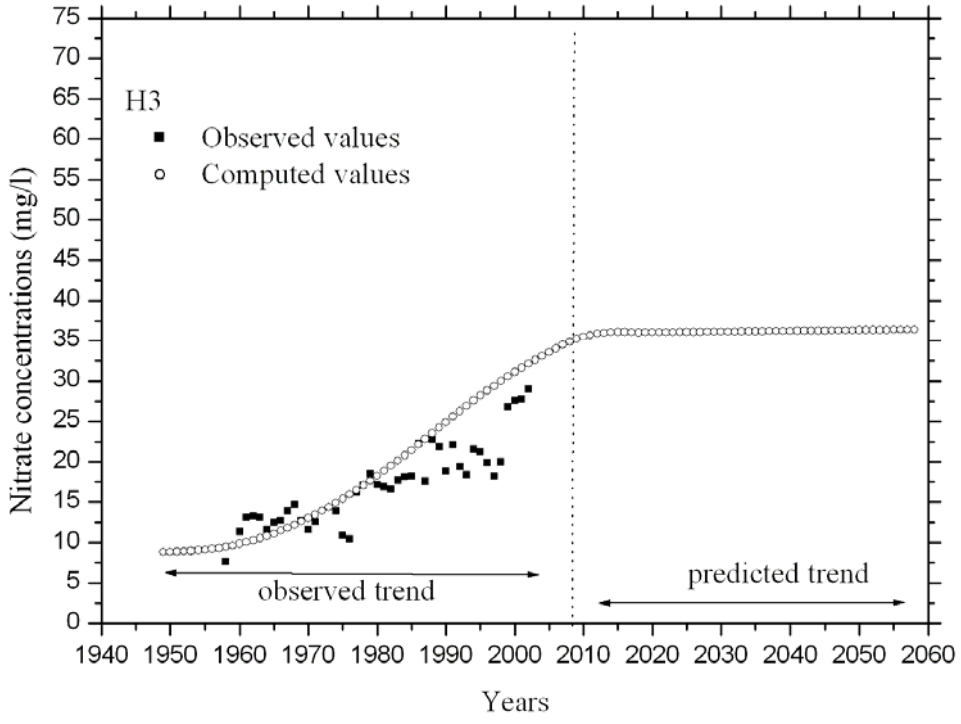

Figure 57. Time evolution of nitrate concentrations in the well H3 computed with scenario 2 described in Section 4.5.4.

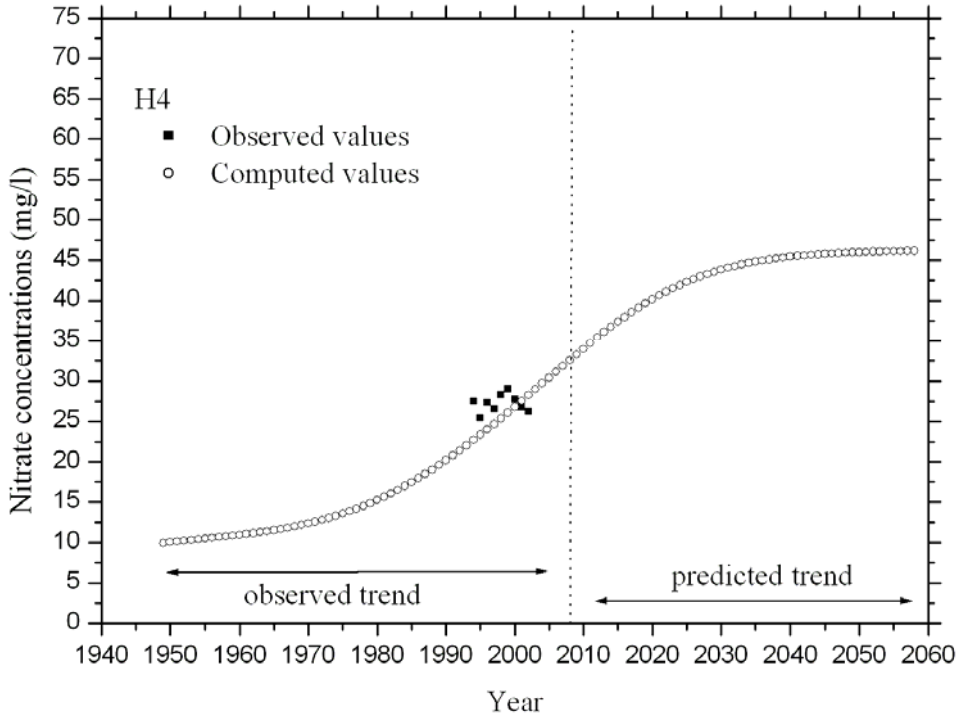

Figure 58. Time evolution of nitrate concentrations in the well H4 computed with scenario 2 described in Section 4.5.4.

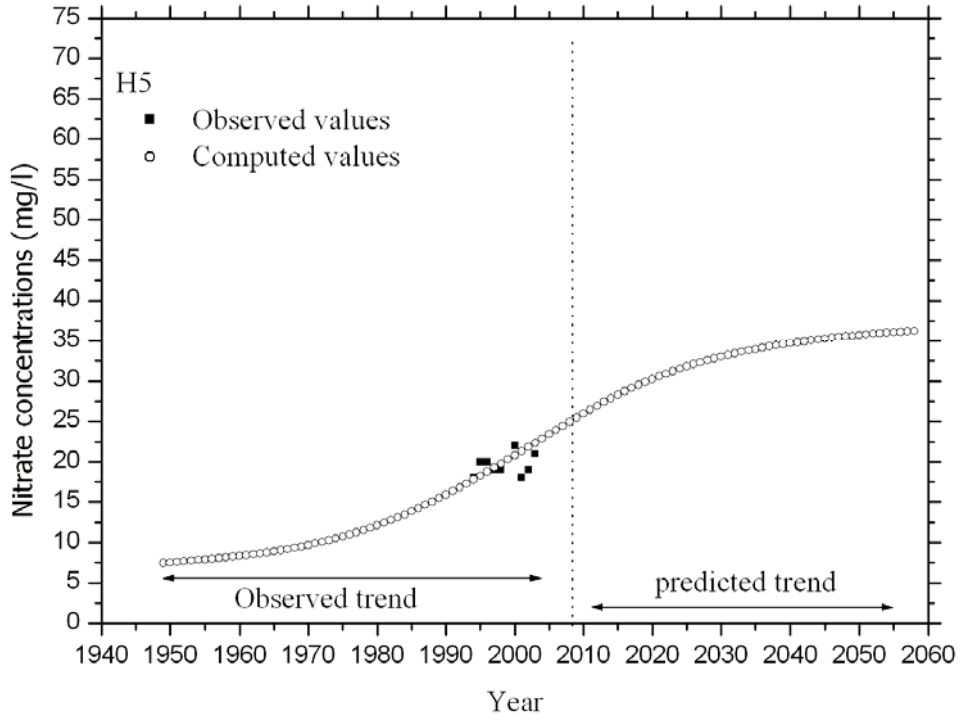

Figure 59. Time evolution of nitrate concentrations in the well H5 computed with scenario 2 described in Section 4.5.4.

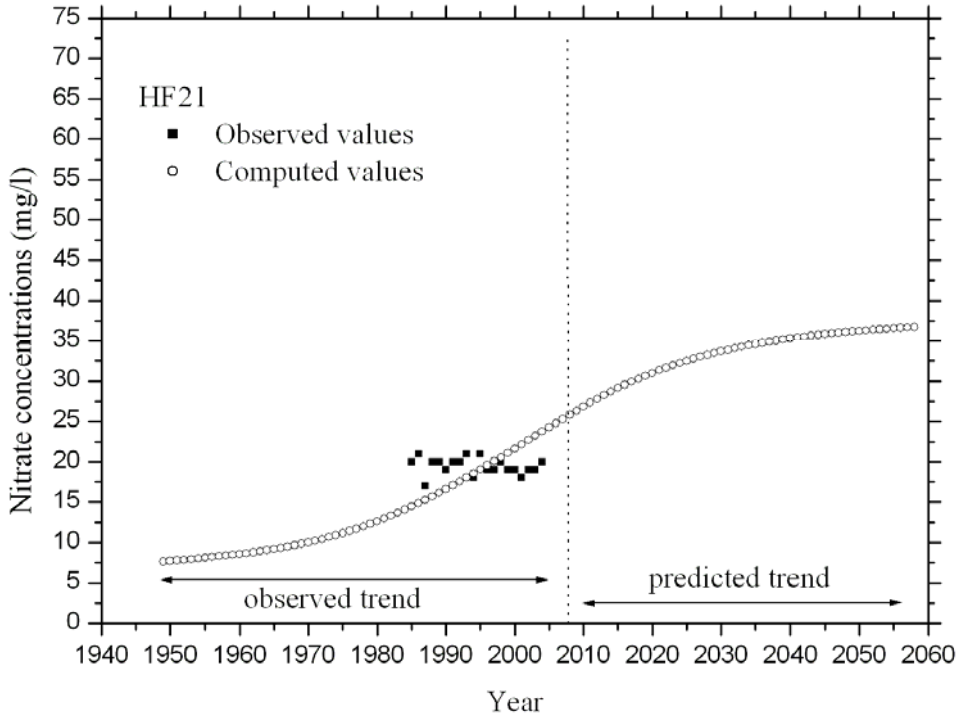

Figure 60. Time evolution of nitrate concentrations in the well HF21 computed with scenario 2 described in Section 4.5.4.

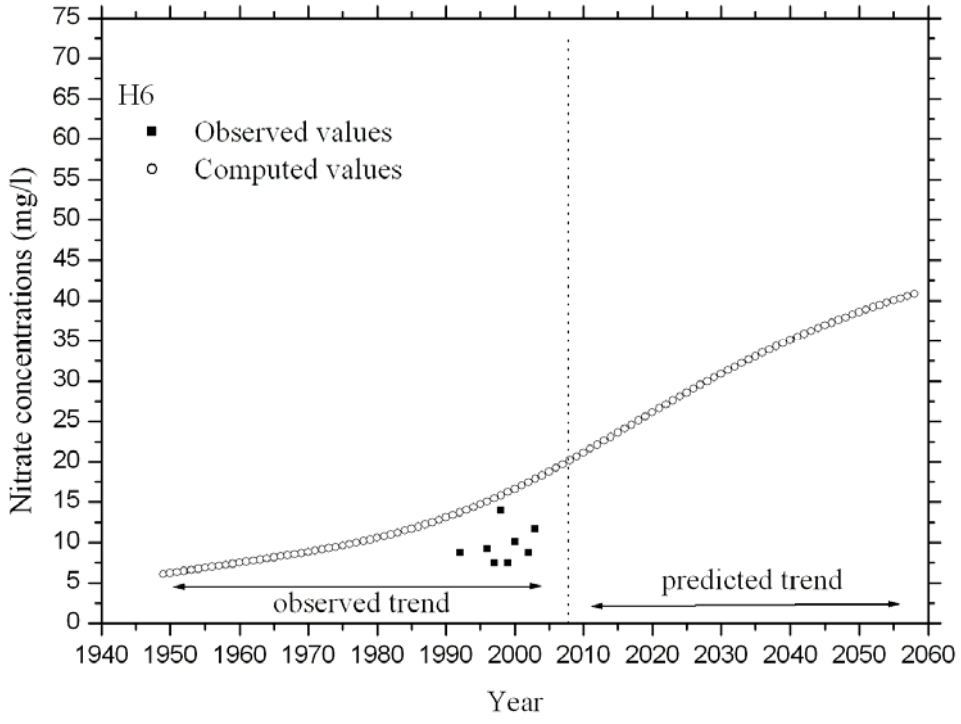

Figure 61. Time evolution of nitrate concentrations in the well H6 computed with scenario 2 described in Section 4.5.4.

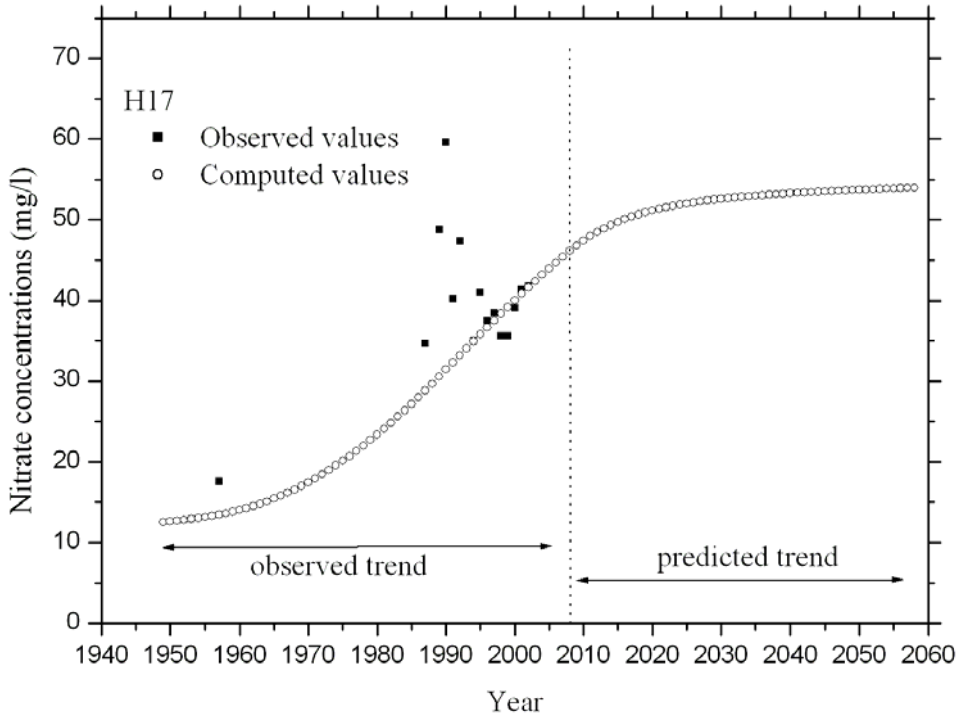

Figure 62. Time evolution of nitrate concentrations in the well H17 computed with scenario 2 described in Section 4.5.4.

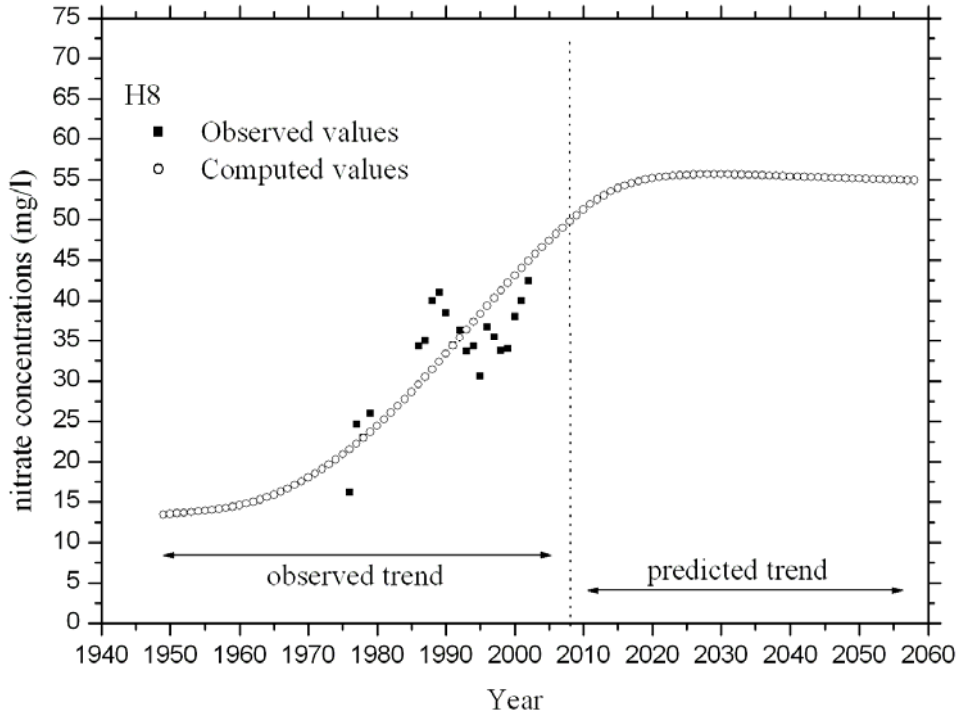

Figure 63. Time evolution of nitrate concentrations in the well H8 computed with scenario 2 described in Section 4.5.4.

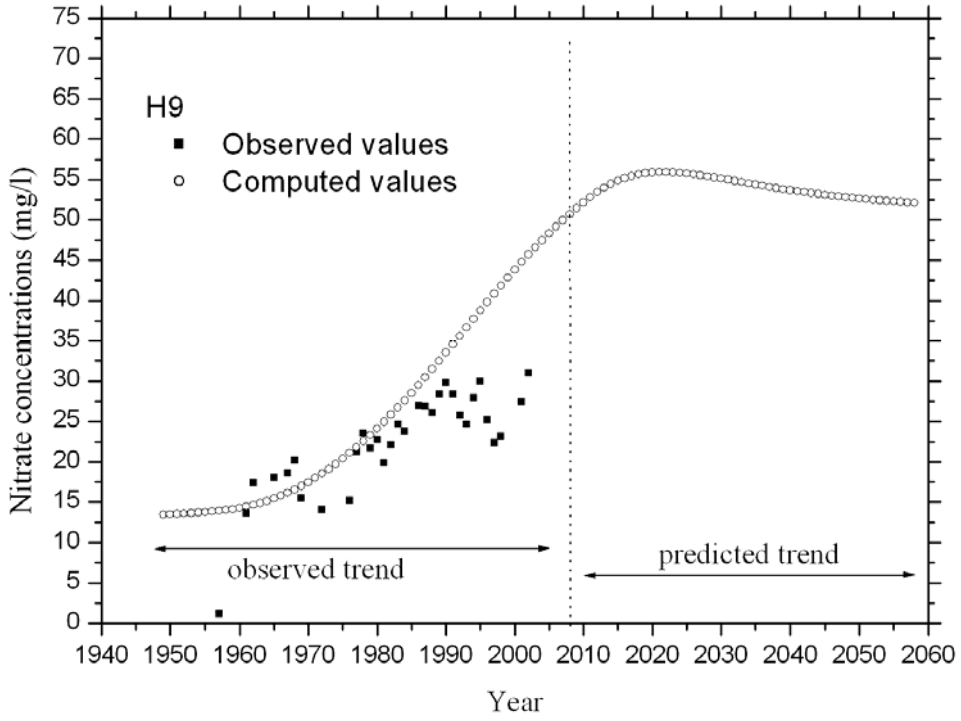

Figure 64. Time evolution of nitrate concentrations in the well H9 computed with scenario 2 described in Section 4.5.4.

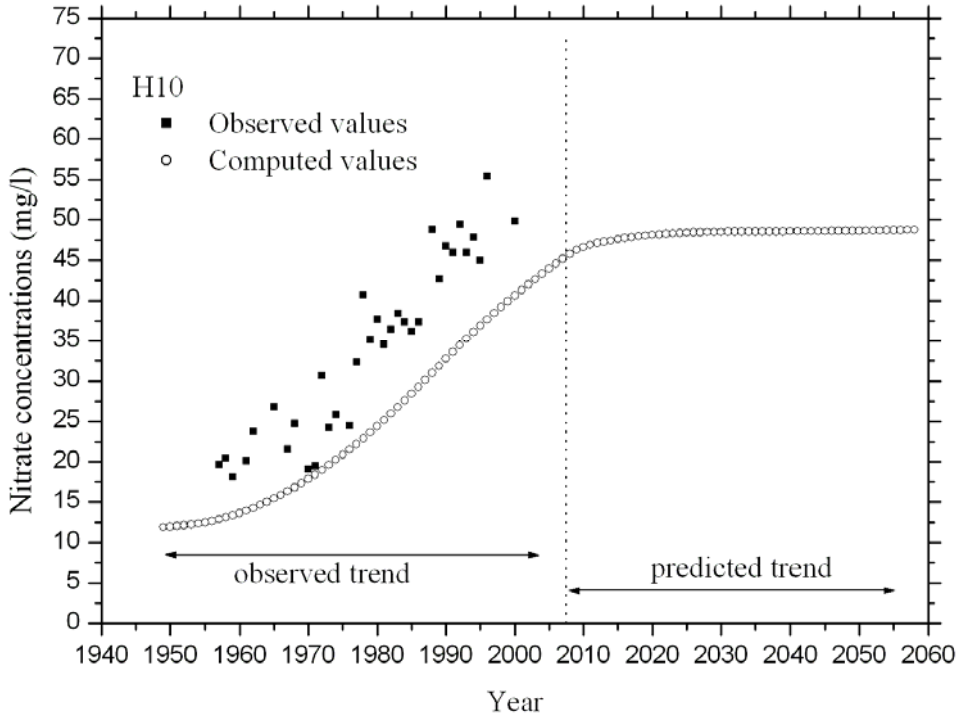

Figure 65. Time evolution of nitrate concentrations in the well H10 computed with scenario 2 described in Section 4.5.4.

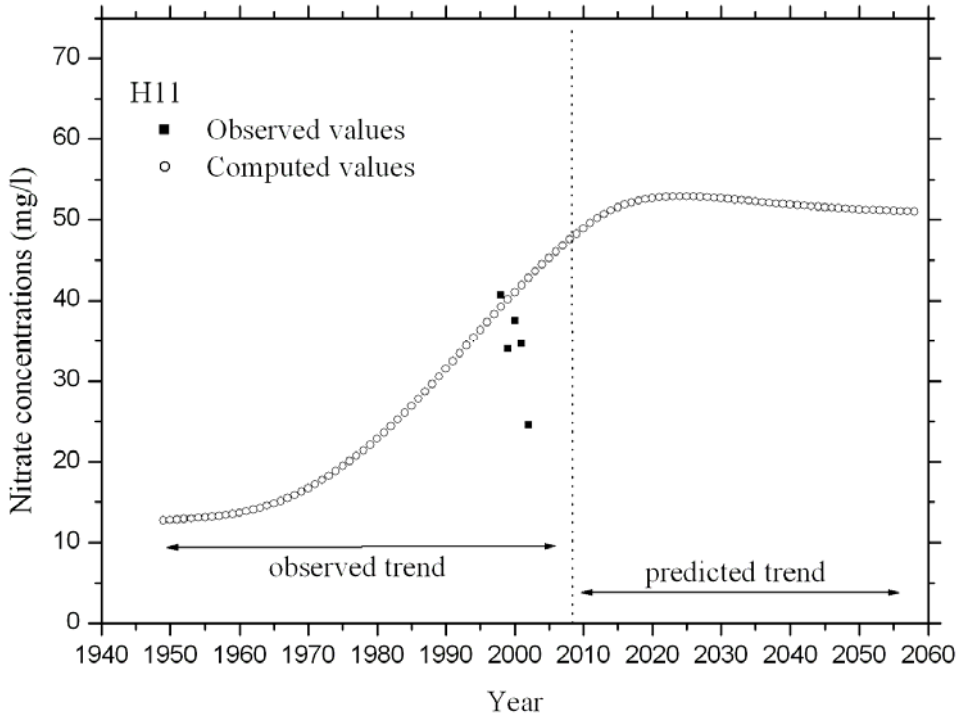

Figure 66. Time evolution of nitrate concentrations in the well H11 computed with scenario 2 described in Section 4.5.4.

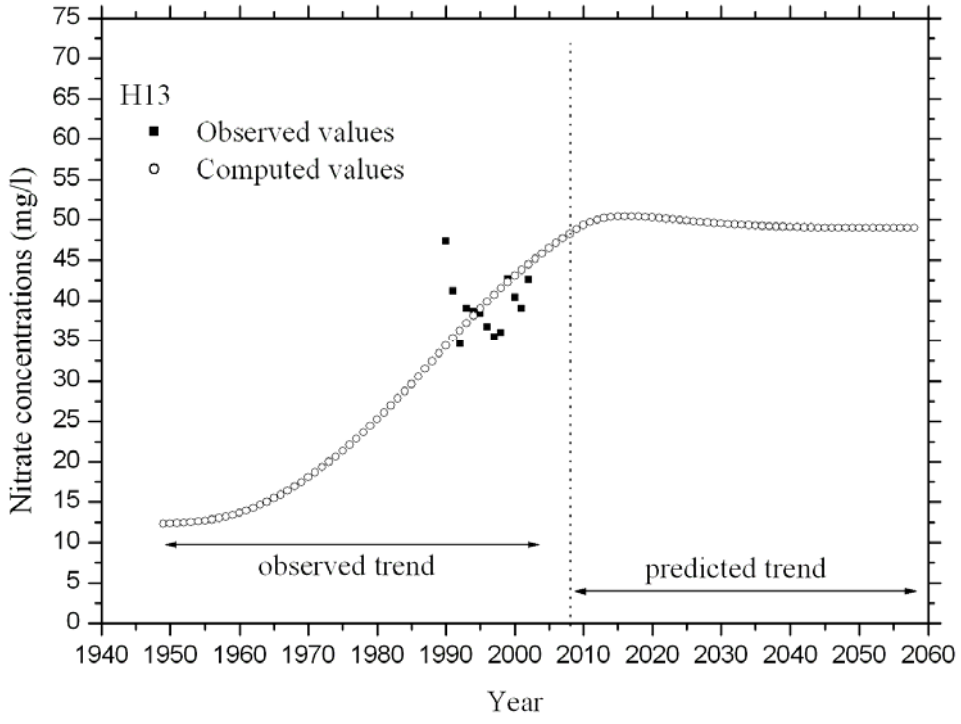

Figure 67. Time evolution of nitrate concentrations in the well H13 computed with scenario 2 described in Section 4.5.4.

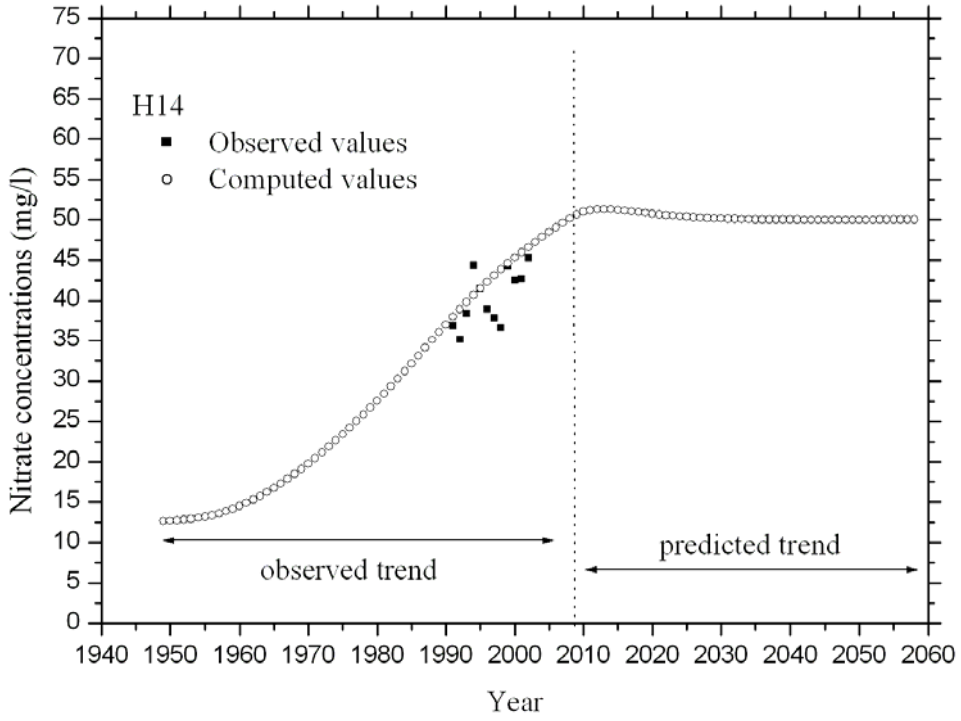

Figure 68. Time evolution of nitrate concentrations in the well H14 computed with scenario 2 described in Section 4.5.4.

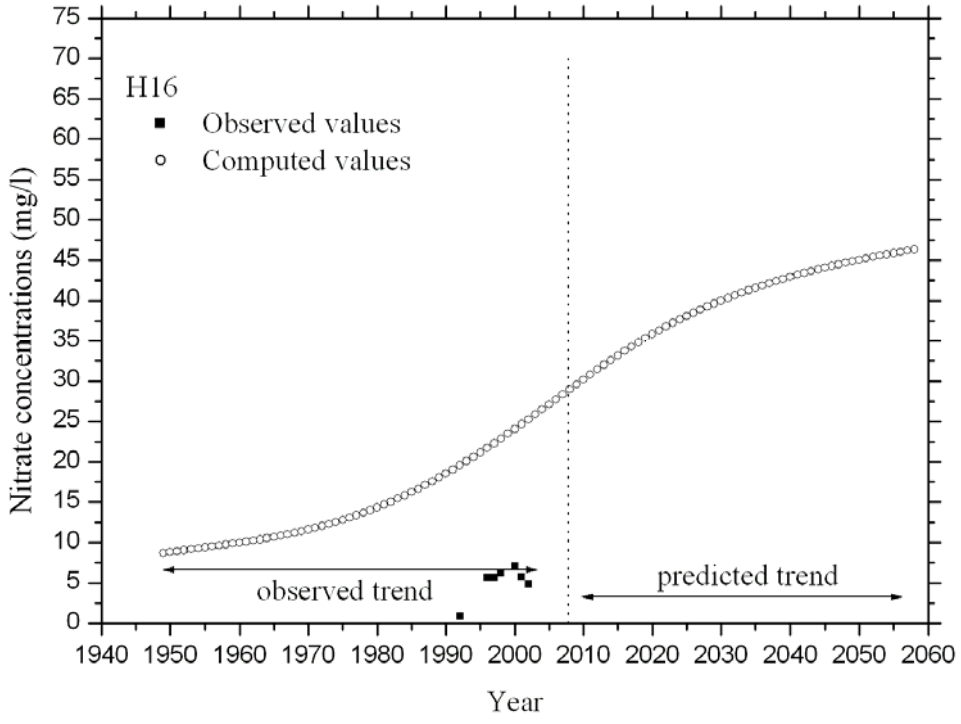

Figure 69. Time evolution of nitrate concentrations in the well H16 computed with scenario 2 described in Section 4.5.4.

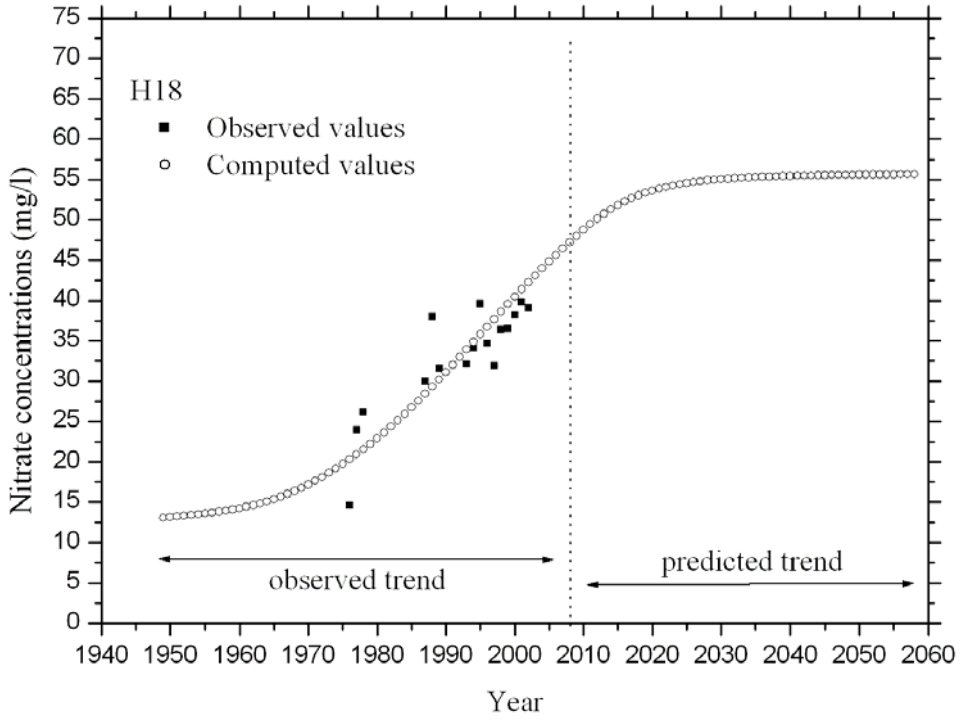

Figure 70. Time evolution of nitrate concentrations in the well H18 computed with scenario 2 described in Section 4.5.4.

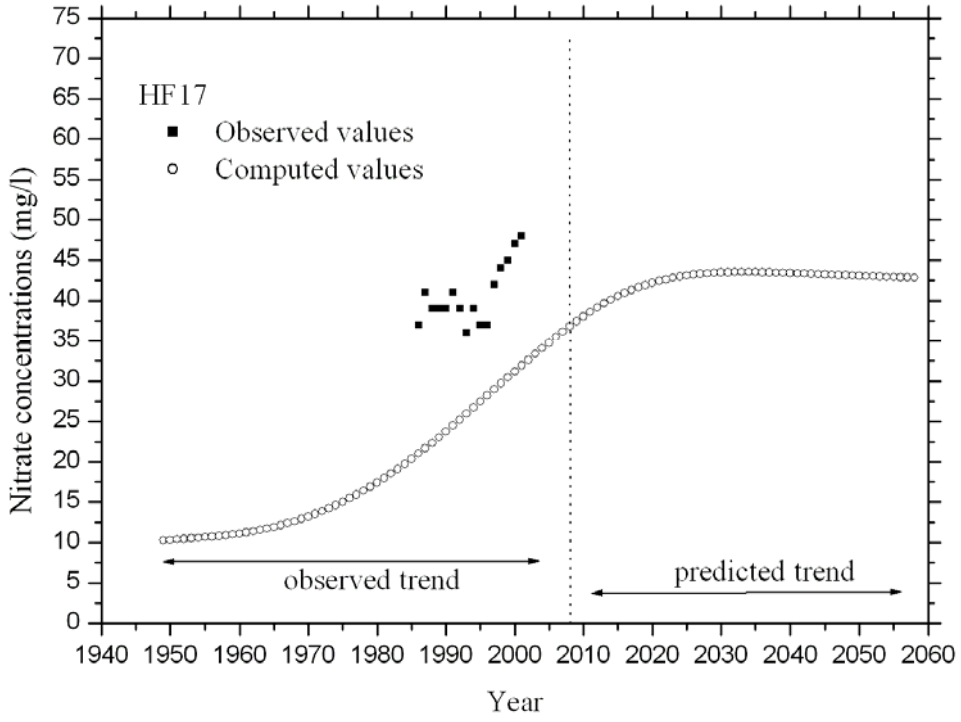

Figure 71. Time evolution of nitrate concentrations in the well HF17 computed with scenario 2 described in Section 4.5.4.

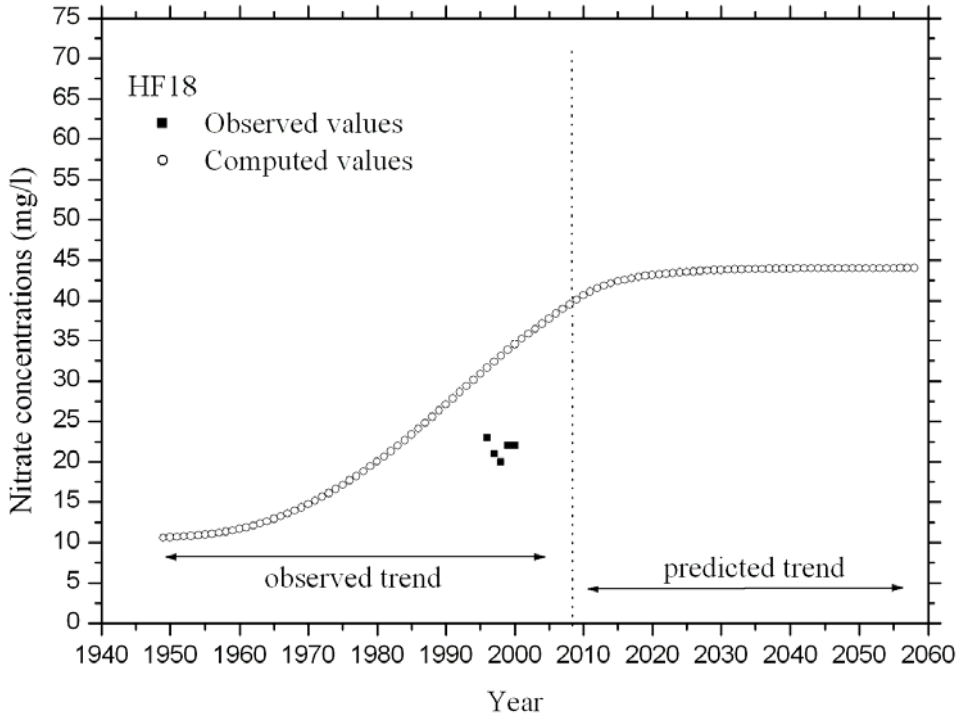

Figure 72. Time evolution of nitrate concentrations in the well HF18 computed with scenario 2 described in Section 4.5.4.

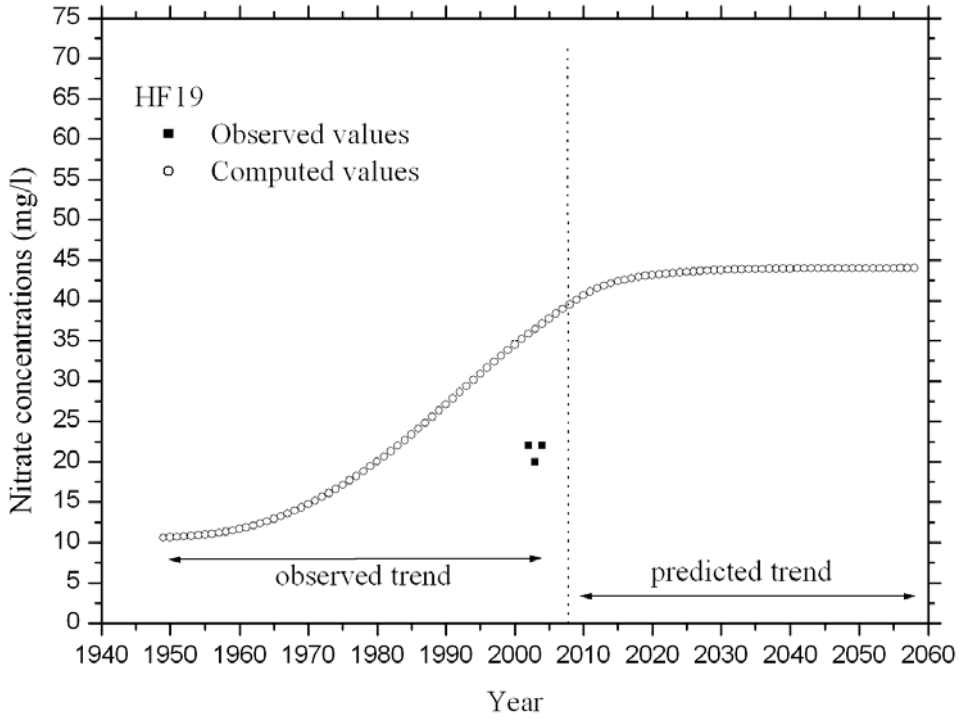

Figure 73. Time evolution of nitrate concentrations in the well HF19 computed with scenario 2 described in Section 4.5.4.

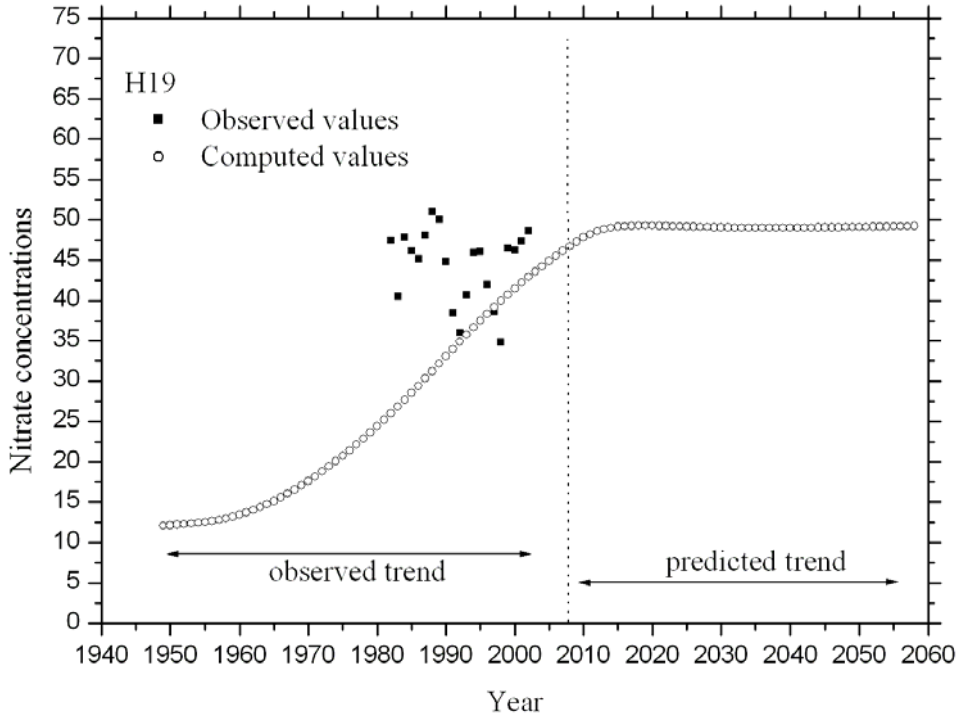

Figure 74. Time evolution of nitrate concentrations for the reservoir of Ans computed with scenario 2 described in Section 4.5.4.

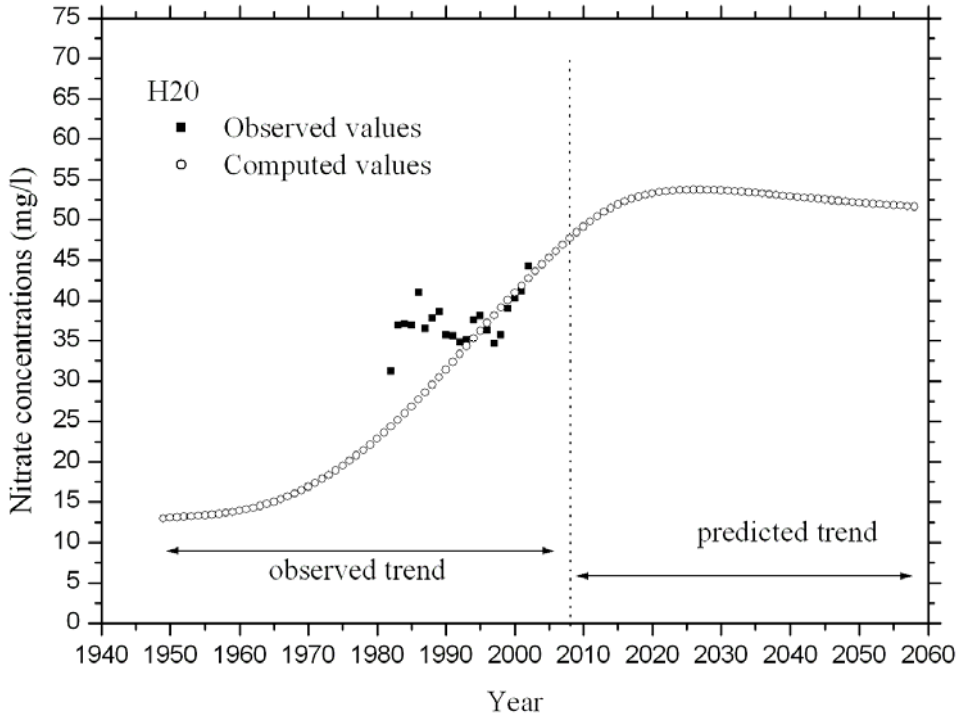

Figure 75. Time evolution of nitrate concentrations for the reservoir of Hollogne computed with scenario 2 described in Section 4.5.4.